design and evaluation of the
gait rehabilitation
robot lopes

jan veneman

DESIGN AND EVALUATION
OF THE
GAIT REHABILITATION ROBOT
LOPES

De beoordelingscommissie is als volgt samengesteld:

Voorzitter en Secretaris (Chairman and Secretary)	
prof.dr. F. Eising	Universiteit Twente
Promotor	
prof.dr. F.C.T. van der Helm	Universiteit Twente
Assistent Promotor (Assistant Promotor)	
Dr.ir. H. van der Kooij	Universiteit Twente
Leden (Members)	
Prof.dr.ing. H. Soemers	Universiteit Twente
Prof.dr. M. IJzerman	Universiteit Twente
Dr. Ir. J. Harlaar	Vrije Universiteit Medisch Centrum
Prof. Dr. A.C.H. Geurts	UMC St. Radboud
Prof. Dr. Ir. D.Lefeber	Vrije Universiteit Brussel
Prof. D.J. Reinkensmeyer PhD.	University of California, Irvine

English title: Design and evaluation of the gait rehabilitation robot LOPES
Nederlandse titel: Ontwerp en evaluatie van de loop revalidatie robot LOPES
Veneman, Jan F.

PhD thesis, University of Twente, Enschede, The Netherlands, November 2007

Cover photography: Arno Stienen, Arthur Aalsma
Printed by: Gildeprint Drukkerijen BV, Enschede, The Netherlands

Design and Evaluation of the Gait Rehabilitation Robot LOPES

Proefschrift

ter verkrijging van
de graad van doctor aan de Universiteit Twente,
op gezag van de rector magnificus,
prof.dr. W.H.M. Zijm
volgens besluit van het College voor Promoties
in het openbaar te verdedigen
op donderdag 6 december 2007 om 13.15 uur

door

Jan Frederik Veneman
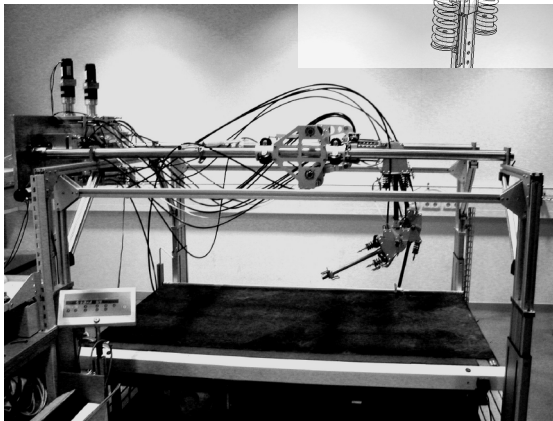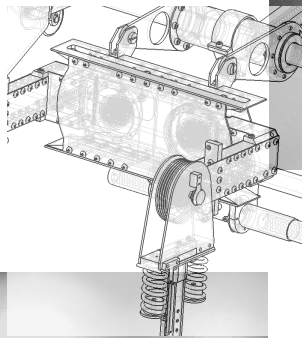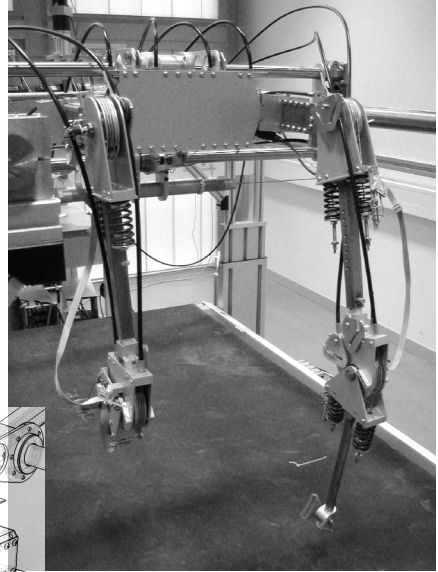
geboren op 1 december 1973
te Tzum (Franekeradeel)

Dit proefschrift is goedgekeurd door:

    Prof.dr. F.C.T. van der Helm (promotor)
    Dr.ir. H. van der Kooij (assistent promotor)

Walking is man's best medicine.
Hippocrates (460 BC - 377 BC)

Summary

The goal of the work presented in this thesis was to realize a robotic device that is able provide suitable gait training to stroke patients.

It is believed that motor training in general, but specifically for stroke patients should be intensive and task-specific in order to reach optimal outcome. Meanwhile, the training of severe stroke patients has proven to be physically very demanding to therapists. For this reason it is believed that robotic aids can be useful alternative for physical therapists to provide gait training. In this research we supposed a training setting in which a therapist is in control of the training, while the robot carries out the physical labor in guiding, assisting and correcting the patient.

We have tried to implement the modern insights in motor training in the robot design. These insights being that for effective motor learning task specificity and self-initiative are essential. We translated this into the demand that the robot should not only allow offering sufficient assistance, but also allow a person to walk near-to-normal on own initiative. In mechatronical terms: the robot should be able to display low apparent impedance. The situations of full robot control, and full human control of walking were entitled a 'robot-in-charge' and a 'patient-in-charge' mode respectively. These functioned as the extremities of the demands we defined for the design.

Based on this we evaluated several actuation principles and robot configurations on their ability to provide both the needed assistance and the desired low impedance. These evaluations resulted in a prototype, presented in chapter six. Chapter two until five and appendix A deal with the mechatronical concepts, while chapter seven and eight deal with the evaluation of walking in the presented prototype.

In chapter 2 we show that free translations of the pelvis are important to allow a normal walking pattern. We showed this by artificially fixating horizontal pelvis translations during treadmill walking. We measured significant changes in several gait characteristics due to this fixation, and linked them to the lack of natural imbalance in standing and walking. This implies that a robot that does rigidly fix these motions during training is affecting the naturalness of walking. How severely this will affect training outcome has to be tested in clinical evaluations, but it made us decide to allow the pelvis translations in our prototype design.

In chapter 3 and 4 we evaluated several actuator types on their ability to provide low impedance. These evaluations were based on the assumptions that a impedance controlled exoskeleton would be used as basic concept. This choice was motivated by the better possibility to implement safety in the design (chapter 6 and appendix A). Important properties on this aspect are the fact that the exoskeleton follows body motions, and that the torque-control is not depending on torque sensors and high-power actuators. To provide low-power, low impedance force sources as actuators we evaluated series elastic actuators, pneumatic cylinders and pneumatic muscles. Qua bandwidth all three appeared to be applicable, we supposed a needed bandwidth in force control of 4Hz for the full torque range and 12Hz for smaller torques. At the same time none appeared optimal, due to problems associated with weight, or typical issues connected to pneumatics, such as complexity of control.

As alternative we designed a Series Elastic Actuator that has the motors removed from the exoskeleton while transmitting mechanical power via Bowden Cables to the actuated

joints (chapter 5). This provided the advantages of Series Elastic force feedback control, combined with a lightweight exoskeleton. The friction introduced with the use of such cables, appeared to be sufficiently compensated for in the feedback control. With optimal cable courses and elastic stiffness we were able to show a resistive torque well below 1Nm during imposed natural motions, combined with a force control bandwidth on the joint of over 20 Hz for lower torques and a peak torque of 50 to 75 Nm.

Based on this kind of actuator a full prototype was designed, as presented in chapter 6. The device, called LOPES – LOwer extremity Powered ExoSkeleton – combines a freely translatable and 2D-actuated pelvis segment with a leg exoskeleton containing three actuated rotational joints; two at the hip, one at the knee. The device is able to assist people with varying measures walking on a treadmill at an arbitrary speed.

To evaluate the design a number of people walking with the LOPES, while their muscle activation patterns and kinematics were measured. This was done to assess the naturalness of walking that would be possible during the 'patient-in-charge' control mode. Natural walking was interpreted as the fact that near-to-normal muscle activation patterns would lead to near-to-normal kinematic gait patterns. We were indeed able to show very little differences between walking with and without the robot. The differences that were found could be associated with the added inertia. Further weight reduction of the robot parts would therefore optimize this outcome.

Additionally we evaluated the effect of the horizontal pelvis translations that were incorporated based on the outcomes of chapter 2. Surprisingly we were not able to show much difference between people walking with or without the possibility of these translations, that is: subjects were still realizing near-to-normal kinematic patterns, with near-to-normal EMG patterns. Still they provide the possibility to include balance training in a training program.

In chapter 9 we state possible technical improvements and the road towards a final product version of the prototype together with possibilities for use in gait research and rehabilitation.

Summarizing, by building a functional prototype we have shown that an exoskeleton device, actuated with compliant actuators based on the principles of series elastic actuation, used as joint torque actuators, together with sufficient degrees of freedom, is able to allow a person to walk normally on own initiative as well as to provide torques with sufficient bandwidth to, according to reasonable supposition, assist and correct during walking. Minimizing disturbances of free walking is likely possible by further weight reduction. How well the device is able to actually assist stroke patients is still to be evaluated by implementing training programs and clinical testing with patients.

Samenvatting

Het doel van het werk dat hier wordt gepresenteerd was het ontwikkelen van een robot die in staat is looptraining te geven die is afgestemd op hersenbloeding patiënten. Het wordt aangenomen dat motor training in het algemeen, maar in het bijzonder voor deze patiëntengroep, intensief en taak-specifiek moet zijn voor een optimaal trainingsresultaat. Tegelijkertijd is gebleken dat het verzorgen van looptraining aan de zwaardere patiënten zeer fysiek belastend is voor fysiotherapeuten. Om deze redenen wordt er aangenomen dat het inzetten van robotische hulpmiddelen een bruikbaar alternatief kan zijn voor therapeuten om een training te verzorgen. In dit onderzoek veronderstellen we een trainings-setting, waarin een therapeut de supervisie op de training heeft, terwijl de robot de fysieke uitvoering van het begeleiden, ondersteunen en corrigeren van de patiënt op zich neemt.

We hebben geprobeerd moderne inzichten in motor training te incorporeren in het ontwerp. Volgens deze inzichten zijn taak specificiteit en eigen initiatief essentieel. We hebben dit vertaald in de eis dat de robot niet alleen voldoende ondersteuning moet kunnen bieden, maar het ook mogelijk zou moeten maken voor een persoon om zo goed als normaal te lopen in het apparaat op eigen inspanning. In mechatronische termen: de robot zal een lage schijnbare mechanische impedantie moeten kunnen weergeven. De situaties van volledige controle bij de robot, en volledige controle bij de mens hebben we respectievelijk de naam 'robot-in-charge' en 'patient-in-charge' gegeven. Dit ware de twee extremen in de eisen die we voor het ontwerp definieerden.

Op deze basis hebben we diverse actuatieprincipes en robot configuraties geëvalueerd op hun geschiktheid om zowel de benodigde ondersteuning als de gewenste lage impedantie te kunnen bieden. Deze evaluaties resulteerden in een prototype, gepresenteerd in hoofdstuk 6, hoofdstuk 2-5 en appendix A behandelen de mechatronische concepten, met name de actuatoren voor de robot. Hoofdstuk 7 en 8 rapporteren de evaluatie van het lopen in het prototype.

In hoofdstuk 2 laten we zien dat de vrije translaties van het bekken belangrijk zijn om een normaal looppatroon te realiseren. We hebben dit laten zien door kunstmatig deze horizontale translaties bij een persoon, lopend op een lopende band, te blokkeren. Hierbij namen we significante veranderingen in uiteenlopende loop-karakteristieken waar, die voor een groot deel te maken hebben met het gebrek aan de natuurlijke imbalans tijdens staan en lopen in de proef conditie. Dit impliceert dat een robot die deze translaties fixeert tijdens de training, de natuurlijkheid van het lopen aan zal tasten. Hoe bezwaarlijk dit is vanuit trainings-oogpunt zal moeten worden getest in klinische evaluaties, maar voor ons was het voldoende reden deze bewegingen in ons ontwerp te realiseren.

In hoofdstuk 3 en 4 hebben we uiteenlopende types actuatoren beoordeeld op hun vermogen om een lage impedantie te realiseren. Deze evaluaties waren gebaseerd op de aanname dat het basis-concept een impedantie-geregeld exoskelet zou zijn. Deze keus werd gemotiveerd door voordelen op het gebied van veiligheid (hoofdstuk 6 en appendix A). Belangrijke aspecten zijn dat een exoskelet lichaamsbewegingen direct volgt en dat de koppel-regeling niet afhankelijk is van stijve krachtsensoren en hoge-vermogens actuatoren. Als opties voor laag-vermogen, lage impedantie krachtsbronnen, evalueerden we serie-elastische actuatoren, pneumatische cilinders en pneumatische spieren. Qua bandbreedte bleken al deze drie principes toepasbaar; we gebruikten de eisen van 4 Hz voor het volle koppelbereik en 12 Hz voor kleinere koppels. Tegelijkertijd bleek geen enkel concept ide-

aal, ten gevolge van problemen gerelateerd aan massa of de typische problemen met pneumatische actuatoren, zoals complexe regelbaarheid.

Als alternatief ontworpen we een serie-elastische actuator waarbij de motoren van het bewegende exoskelet zijn verplaatst naar de vaste wereld, terwijl het vermogen mechanisch wordt overgebracht via bowden-kabels naar de gewrichten (hoofdstuk 5). Dit gaf de voordelen van series-elastische feedback krachtsregeling, in combinatie met een lichtgewicht exoskelet. De wrijving die de kabels met zich meebrengen, bleek in voldoende mate te compenseren in de feedback regeling. Met optimale bowden-kabel standen en een veer met de optimale stijfheid, waren we in staat een weerstand van minder dan 1 Nm te realiseren tijdens extern opgelegde natuurlijke bewegingen, samen met een krachtsbandbreedte van 20 Hz voor lagere koppels en een piekkoppel van 50 tot 75 Nm.

Gebaseerd op deze aandrijving is een volledig prototype ontworpen, gepresenteerd in hoofdstuk 6. Dit apparaat, genaamd LOPES - LOwer extremity Powered ExoSkeleton – combineert een vrij transleerbaar en 2D-aangedreven bekken segment met een been exoskelet voorzien van drie roterende scharnieren, twee op de heup, en een op de knie. Het apparaat is in staat mensen van uiteenlopende proporties te assisteren bij lopen met willekeurige snelheid.

Om het ontwerp te evalueren hebben een aantal mensen met de LOPES gelopen, terwijl hun spieraanspanningspatronen en bewegingen werden gemeten. Dit werd gedaan om te beoordelen hoe natuurlijk het lopen van mensen in het apparaat zou zijn tijdens de 'patient-in-charge' modus. 'Natuurlijk lopen' werd opgevat als dat nagenoeg normale spieraanspanningspatronen zouden leiden tot nagenoeg normale bewegingspatronen. We waren inderdaad in staat aan te tonen dat de verschillen met vrij lopen klein zijn. De verschillen die optreden kunnen worden toegeschreven aan de verhoogde traagheid van de bewegende ledematen. Verdere gewichtsreductie zal daarom het resultaat nog verder kunnen verbeteren.

Aanvullend evalueerden we het effect van de horizontale bekken translaties die waren ingebouwd naar aanleiding van de uitkomsten van hoofdstuk 2. Tot onze verassing waren we niet in staat veel verschil aan te tonen tussen de mensen die met en de mensen die zonder deze vrijheidsgraden liepen; de bewegingen waren nog steeds nagenoeg normaal, evenals de EMG patronen. Het blijft echter staan dat de bekken vrijheidsgraden het mogelijk maken een specifieke training van de balans te realiseren in het apparaat.

In hoofdstuk 9 formuleren we mogelijke technische verbeteringen en de weg naar een uiteindelijk product gebaseerd op het prototype, evenals mogelijkheden voor gebruik in onderzoek en revalidatie.

Samenvattend, door het bouwen van een functioneel prototype hebben we laten zien dat een exoskelet-robot, aangedreven met compliante actuatoren, gebaseerd op het principe van serie-elastische aandrijving die worden gebruikt als koppelbronnen, samen met de gekozen vrijheidsgraden, een persoon toestaat nagenoeg normaal te lopen op eigen inspanning, zowel als dat koppels kunnen worden verschaft bij voldoende bandbreedte om, naar redelijke aanname, assisterende en corrigerende acties tijdens het lopen uit te voeren. Verdere vermindering van de verstoring van vrij lopen is waarschijnlijk mogelijk door verdere gewichtsreductie. Hoe goed het apparaat in staat zal zijn CVA-patiënten werkelijk te assisteren zal moeten blijken uit klinische testen met patiënten na het implementeren van trainingsprogramma's op maat.

Contents

chapter **1**

Introduction

Jan F. Veneman

Abstract

This thesis deals with the design and evaluation of a robotic device for providing gait training to subjects that suffered a stroke, or Cerebro Vascular Accident (CVA).

In this introductory chapter, the topics of gait, gait impairment due to stroke, and gait rehabilitation practise will be introduced. Also the goal and structure of the research will be explicated.

Chapter contents

1. Gait and its importance

Gait can be defined as: 'a particular way of walking, running, or moving along on foot', or shorter 'a manner of walking'. In literature on rehabilitation, gait is usually a synonym for 'walking'. This activity is so familiar, that it may seem excessive to define it in detail.

The activity of walking itself is however way easier than the activity of defining it scientifically as (bio-) mechanical and control process or than the activity of artificially reproducing it in a robot. Almost any human is able to walk, while no robot has yet been constructed that achieves a quality of walking that comes even close to that of a human qua efficiency or stability. Still, observation, quantifying and modeling of human walking and design of walking machines has yielded fruitful insights about the nature of human walking.

A basic insight is that walking is a dynamical process – sometimes described as a constantly prevented falling – in the way that it is not a semi-static motion of the legs, that, would it be stopped, instantly leads to a statically stable standing position. On the contrary, the body centre of mass is periodically brought further forward than the limit of static stability, causing the body to fall forward, and then, by placing a foot forward in time, an actual fall is prevented. This way of moving, uses gravity as main driving force, and therefore is very economic with the use of muscle power.

Except for this forward direction, the body is also sideways instable. In fact it strongly resembles a standing stick, always about to fall. This impels a human to not only constantly prevent a forward fall, but at the same time, using the same two feet, prevent a sideways fall. This has also to be attained by placing the feet in time at position that assures stability. How difficult this combined stability problem is can both be seen from the difficulty children have in learning walking as from the scientific literature on the issue.

As the exact mechanisms in walking are complex and not fully understood, most research literature on walking is limited to the calculation and mutually relating of "gait parameters" such as for example step length, step width, walking velocity, step frequency, and to the observation over a "gait cycle" of averaged kinematics and kinetics, for example motion profiles, calculated torque-profiles in joints and the ground reaction forces. Such information allows identifying and quantifying disorders in walking. A growing amount of effort is put in making robots walk like humans, necessitating a thorough understanding of the process. Phenomenological and statistical descriptions are of course not enough to reproduce the control process.

In the everyday life, walking, or in general 'the ability to move oneself around' is a very important condition for an independent personal functioning, both for private and societal objectives. Loosing this ability severely affects ones functioning and well-being as well as it strongly increases dependency on others. Therefore, usually much personal as well as therapeutic effort is put in recovering gait, in case of disorders. When necessary, assistive aids are introduced, varying from a crutch or an ankle orthosis to a wheelchair. The optimal outcome and the acceptability of aids will depend much on the individual character and circumstances of a patient.

2. Stroke as cause of gait disorders

An important possible cause of gait disorders is a stroke, or a CerebroVascular Accident (CVA, information from (NationalStrokeAssociation 2007)). A stroke occurs when blood supply to a part of the brain gets interrupted. This leads to an ischemic cascade that can damage brain tissue, leading to a possible loss of specific functions. A stroke typically manifests itself with the sudden onset of focal neurological deficits, such as partial loss of movement, sensory deficit, or difficulties with speech. Stroke is the third leading cause of death and leading cause of adult disability in the US and industrialized European nations. The incidence of stroke in the Netherlands is approximately 30.000 per year, and the prevalence is 120.000 patients on a total population of 16.280.000 (Buurke 2005).

Strokes are classified by their cause in two main types: ischemic and hemorrhagic. In ischemic stroke, which occurs in approximately 85-90% of strokes, a blood vessel becomes occluded and the blood supply to part of the brain is totally or partially blocked. Hemorrhagic stroke, or intracranial hemorrhage, occurs in about 10-15% of strokes, when a blood vessel in the brain bursts, spilling blood into the spaces surrounding the brain cells. Hemorrhagic strokes generally carry a greater risk of death and permanent disability than ischemic strokes.

Following stroke, the function and tissue properties of muscles and also their timing characteristics during walking often change dramatically. Damage to cortical or subcortical motor areas may lead to paresis in muscle groups contra-lateral to the lesion, due to the reduced number of active motor units, their reduced firing rates, and their less synchronized firing patterns (Young and Mayer 1982; Gemperline, Allen et al. 1995; Den Otter 2005) A few weeks after stroke, spasticity may evolve as a result of central disinhibition of reflexes which may eventually result in a structural shortening of the involved muscles. These impairments may all affect the temporal layout of muscle activity over the gait cycle (Den Otter 2005).

There is a large variation between patients on the exact consequences of stroke on gait ability. They depend on the size, type and location of the lesion, as well as on the compensatory strategies that are developed by patients to optimize their effective motor functioning (Kwakkel, Kollen et al. 2004). Although several more or less recognizable gait abnormalities occur in stroke patients, it appeared not or hardly possible to categorize them properly and systematically in a way useful for scientific classification or therapy(Den Otter 2005). Nevertheless, on a more general level, several typical defects or adaptations are often seen in the gait of stroke patients, such as:

- Foot drop, which is the inability to prevent the foot from slapping to the ground after landing, because of the inability to pull the foot up (at the right time).
- Hip hiking: an extensive lifting of the pelvis on the side and during the swing of the affected leg. This is apparently a compensatory strategy to assure foot clearance.
- Hip circumduction: swinging the affected leg in an arc to increase ground clearance, rather than straight forwards. This is also a compensatory strategy.
- Asymmetric walking, e.g. leaving the non-paretic behind during walking,in order to prevent a backward fall, this is therefore also a way of coping.

The majority of surviving stroke patients regains their walking ability sooner or later (77% of survivors), but a substantial number (55% of survivors) is left with walking diffi-

culties throughout the sub acute and chronic stages of stroke (Jorgensen, Nakayama et al. 1995).

Recent research on principles of motor recovery has shed some light on what happens during functional recovery (Van Peppen, Hendriks et al. 2007). Stroke patients show abnormalities in gait-related muscle activation patterns. These abnormalities already appear shortly after troke, and do not, or hardly, change during the recovery process. They do apparently not form an impediment for gait recovery. A possible explanation is that the majority of these abnormalities reflect compensatory neuromuscular strategies that are developed early after stroke. Training would then not be unlearning these strategies, but automating and subordinating their use in 'production' of gait.

3. STROKE REHABILITATION, THEORY AND PRACTISE[1]

In literature, two important determinants of a successful training have been identified (Kwakkel, van Peppen et al. 2004; Van Peppen, Hendriks et al. 2007). First, more intensive training in the first six months after the onset of the CVA yields better, or at least faster, recovery of functionality. Second, motor training in general has only task specific effects; there is hardly transfer of skill to not directly trained tasks. Task specificity here, does not just refer to the trained motor-tasks themselves, but also to the context within which these tasks are meaningful.

Other factors that determine effectiveness of motor learning in general are also believed to apply for stroke rehabilitation. Important ones being: challenging a person to seek the limits of his/her abilities, extensive repetition without obstructing the natural variability occurring in motor functions, progressive training of components of a skilled movement and feedback on performance (Dobkin 2004; Teasell, Bitensky et al. 2005; Krakauer and Shadmehr 2006). In the same literature it is also suggested, although not based on hard scientific evidence, that (semi-)automatic actions, like walking, should not be split up in subtasks during training, but should be trained 'unfragmented'.

The ultimate goal of the rehabilitation is to achieve a level of functional independency necessary for returning home and for integrating as fully as possible into community life (Kollen, Kwakkel et al. 2006). In the Netherlands, after a stroke, a patient usually spends up to six weeks in daycare. Patients with motor control problems usually receive an intensive motor training, aiming at a return to the home-situation. After returning home outpatients' treatment is offered as long as improvement occurs.

Clinical gait training consists of an individual mixture of methods and exercises from the therapists' toolbox, determined by the possibilities and character of the patient, the preferences and experience of the therapist and his/her background in education. The lack of basic knowledge about the nature of newly emerging but often pathological co-ordination patterns, led to more than nine different treatment methods that are used in today's clinical practice. Among these, often contradicting, methods, the most well known are: Brunnstrom, Johnstone, Proprioceptive Neuromuscular Facilitation (PNF), Motor Relearning Programme (MRP) and Neuro Developmental Treatment (NDT) (Buurke

---

1   The facts and insights about rehabilitation practise presented in this paragraph were gathered from observation and interviews with therapists at both 't Roessingh R&D, Enschede and the St.Maartenskliniek, Nijmegen.

2005).

Actual gait training is usually preceded by standing- and balance-training. When needed, specific aids are used during the training to guarantee safety, such as parallel bars, a walking stick, a rolling walker, a walker frame or specific orthoses, for example to correct the ankle or suppress spasticity.

The use of treadmills for training is increasing. Treadmill training offers the therapist better opportunities to guide and correct the patient during walking. In a typical setting a therapist is seated beside the impaired leg of a training patient, guiding and correcting leg motions and assuring safety. Sometimes a second or even third therapist is needed to take care of the balance and of the other leg.

A specific form of treadmill training is the Body Weight Supported Treadmill Training (BWSTT) (Barbeau and Visintin 2003; Chen, Patten et al. 2005), where body weight is partly supported by lifting the patient slightly, using a harness and a lifting device (see figure 1.1). This causes a normalization of walking as higher speeds can be applied than a patient can achieve under full weight, which restores the dynamic nature of walking. Another advantage is that training time can be extended as the patient is less loaded. BWSTT also unburdens the therapist as it becomes lighter to correct the patients' motions when weight is supported. It seems especially fit for heavily impaired patients that are not (yet) able to walk over ground.

4. The use of robots for gait rehabilitation

Although the described BWSTT training has shown to be effective (Peurala, Tarkka et al. 2005), the clinical application of this technique is still limited because it is labor intensive and non-ergonomic (Reinkensmeyer, Aoyagi et al. 2006). It is especially labor intensive in case of heavily impaired patients, which still need two or three therapists. Those

Figure 1.1: Body weight supported treadmill training (BWSTT). Picture from: http://depts.washington.edu/rehab/pdfs/sci/sci_update_spri03.pdf

patients would probably profit much from intensive early training. A second limiting factor for optimizing motor training is that the neuroadaptive mechanisms that underlie training are not yet understood. Well-structured and quantified training methods and accurate observation of progress may reveal effects of specific training regimes. For these two reasons, robotic devices are being developed for automating locomotor training in humans. They have the potential to reduce workload on therapists, offer an intensive, reproducible and quantified training and to measure performance of the patient. A well designed robot would therefore extend possibilities of both therapist and researcher.

Commercially available robotic devices for gait training are the Lokomat® (Hocoma AG , Volketswil, Switzerland, figure 1.2) , the Gait Trainer I (GT I, Reha-Stim, Berlin, Germany, figure 1.3) and the AutoAmbulator (HealthSouth, Birmingham, Alabama, USA, figure 1.4) (Reinkensmeyer, Aoyagi et al. 2006).
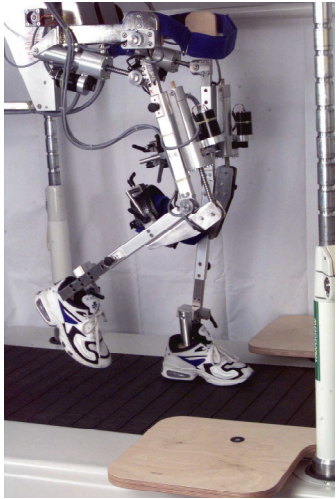
Figure 1.2: Lokomat 4(+1) DoF servo-controlled exoskeleton, with active weigh compensation system

Figure 1.3: Gait Trainer I Predefined footsole-trajectory controller, with passive weigh compensation system

Figure 1.4: AutoAmbulator 4 DoF servo-controlled exoskeleton, with passive weigh compensation system

These devices and the ongoing research in the field will be shortly reviewed here. About the AutoAmbulator regrettably little to nothing has been published scientifically.

The Lokomat (Colombo, Joerg et al. 2000) consists of a BWSTT system combined with a powered exoskeleton (a robotic construction connected in parallel to the patient's legs). Hip and knee flexion and extension are actuated by linear ball screw assemblies driven by DC motors. The feet are prevented from hitting the ground during swing through two passive elastic straps. A limitation of the first versions of the Lokomat was that it was strictly position controlled, so that it was only poorly possible to allow self-initiative during walking. Since the robot was always walking its trajectory regardless of what a patient was doing, a patient was not encouraged to participate actively. Recently implementation of control schemes that facilitate 'human cooperative strategies' or impedance (interactive) control were presented (Riener, Lunenburger et al. 2005). The Lokomat is however not optimally designed to function as a haptic device (Wellner, Guidali et al. 2007). Another limitation is that only sagittal motions of the legs are allowed, while the pelvis of the patient is fixated in the horizontal plane. Actually the only possibility is to enforce gait-like stepping motions upon the legs in the sagittal plane. Differences in EMG patterns during gait, compared to free walking however show that this is different from free walking (Hidler and Wall 2005). The first clinical evaluation of training effects in the position-controlled Lokomat on stroke patients nevertheless shows promising results (Husemann, Muller et al. 2007). Although no difference was found between groups in gain of functional scores, the Lokomat-trained group showed an advantage of robotic training over conventional physiotherapy in improvement of gait abnormality and body tissue composition.

The Gait Trainer I (GT I)(Hesse and Uhlenbrock 2000) consists of actuated foot supporting plates, resembling the well known fitness 'cross-trainers'. The subject's feet are permanently strapped to these plates. The plates are connected to a linkage system and move the feet through a trajectory similar to the foot motion during a healthy reference

gait cycle. The linkages connected to the footplates are driven by a motor that provides a varying level of assistance along its trajectory throughout the gait cycle. The gait-trainer is not an exoskeleton robot, with segments moving in parallel, but a so-called end-effector robot, interacting with only the feet, which can be considered to be the end-effector of the human leg.

A limitation of the GT I, and of end-effector/foot-supporting type gait rehabilitation devices in general, is that the only interaction takes place at the foot sole so that typical poor joint stability of stroke patients cannot be controlled, for example for preventing hyper-extension of the knee. Additionally, the cutaneous input at the foot soles in such a system may be unnatural, which might disturb afferent information needed for walking. For example the typical sudden transition between swing and stance does not appear, because the foot is continuously connected to the footplate. Actually the leg does not make its normal free swing. It is also not possible to deviate from the prescribed trajectory, the only 'choice' for the patient is to either assist or oppose the enforced motion.

The research group that developed the GT I is currently working on fully 'programmable' (haptic) footplates (Schmidt, Sorowka et al. 2003; Schmidt, Werner et al. 2007), which would eventually solve the last two mentioned problems. This force controlled device, called the Haptic Walker, allows the training of arbitrary foot trajectories. This allows to simulate not only walking on plane floor, but also stepping on staircases or any other desired foot trajectory. It would also enable training of other real world walking situations, like for instance walking on rough surfaces or stumbling. Another issue with this kind of devices is the possibly difficult discrimination between a simulated surrounding and the support offered by the device.

However, the current Gait Trainer, which can be considered as a first version of such haptic footplates, already showed clinical success in training of stroke patients (Pohl, Werner et al. 2007): Intensive GT training plus physiotherapy resulted in a significantly better gait ability and daily living competence in sub acute stroke patients compared with

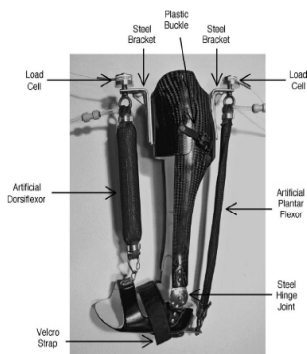**Figure 1.5**: Ankle orthosis, driven with an antagonistic pair of fluidic muscles.

Figure 1.6: Anklebot, driven by a DC motor driven linear traction drives.
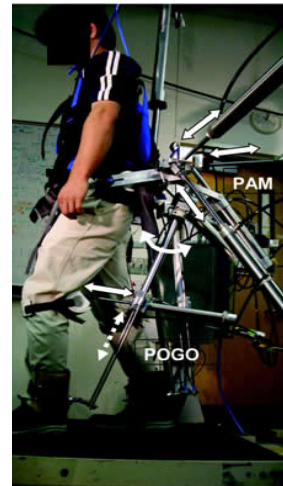
Figure 1.7: POGO Pneumatically Operated Gait Orthosis, driven by pneumatic cylinders.

physiotherapy alone. A still experimental alternative device is the ARTHuR, providing a haptic interface at a person's ankles while walking on a treadmill (Emken, Wynne et al. 2006). Important advantages over the GT I are the natural feedback from the foot soles, as the patient is actually walking on the treadmill and the full flexibility in programming the impedance (stiffness, resistance) of the device.

Another interesting approach is the use of robotic orthoses during walking, as motivated by Ferris (Ferris, Sawicki et al. 2005). As advantage over the aforementioned devices the possible active assistance to the ankle flexion is stressed. It is claimed that using active ankle assistance might cause normalized gait characteristics of SCI patients. Also the possibility of walking over ground, turning and avoiding obstacles is claimed to be possible and advantageous using powered orthoses instead of a fixed or treadmill based set-up. An example is the pneumatic-muscle driven ankle orthosis (figure 1.5) that was constructed and evaluated during walking by Ferris (Ferris, Czerniecki et al. 2005; Ferris, Gordon et al. 2005; Gordon, Sawicki et al. 2006). Some drawbacks are the need to make the ankle orthosis patient-unique fit-to-size and the relative low power and poor controllability of the applied artificial (pneumatic) muscle actuators. Another example of this concept is the Anklebot® (figure 1.6), developed at MIT, a two degrees of freedom powered orthosis to assist ankle movement (Krebs and Hogan 2006). A general problem with powered orthoses is the fact that the actuators have to be carried along with the orthosis by the patient. Usually for power supply a connection to the fixed world remains necessary, or the power source has to be carried around too. Often the use of such orthoses is integrated again in a treadmill- or even exoskeleton- based design; or rather, one can say there is a thin or even no strict line at all between both concepts.

Several groups have recognized the specific importance of pelvic and trunk motions during gait rehabilitation (Donelan, Shipman et al. 2004; Reinkensmeyer, Aoyagi et al. 2004; Peshkin, Brown et al. 2005; Israel, Campbell et al. 2006). Maintaining lateral and sagittal balance are important challenges in walking that probably should not be omitted
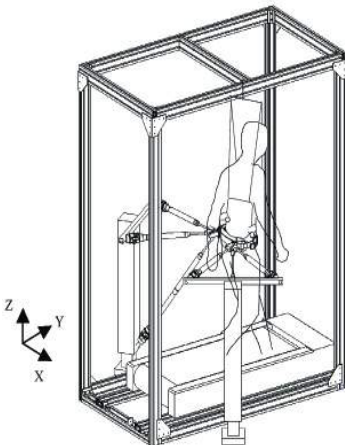

Figure 1.8: PAM
Pelvic Assist Manipulator, pneumatically driven device to assist pelvic motions during treadmill walking
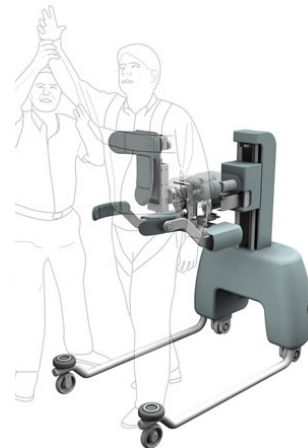

Figure 1.9: KineAssist
Device to assist and offer safety through pelvis motions during over ground walking.

during training by fixating the position of the pelvis too much. For correct load-related afferent input, torques that keep the body upright should be provided via the ground reaction forces and not by external forces at the pelvis or trunk. Some devices have been developed that accommodate and/or control natural pelvic motion, such as the Pelvic Assist Manipulator (PAM, Figure 1.8) (Aoyagi, Ichinose et al. 2005) and the KineAssist (Figure 1.9, Peshkin, Brown et al. 2005). The PAM has recently been extended with a device called the Pneumatically Operated Gait Orthosis, resulting in a device that can also facilitate hip and knee sagittal bending without using an exoskeleton.

5. Blueprint of a new gait training robot

When the described commercial robotic devices of §1.4 for gait training are compared with the training principles of §1.3, it appears that especially the task specificity of the offered training can be improved: the robots possibly restrict too many motions, or hinder self-initiative during walking. An optimal robot would, beside of course the ability to offer the desired support, allow free, unhindered normal walking; at least not disturb the dynamical nature of walking. It should not on before hand 'solve' important challenges such as keeping balance. With such a device the possibility of self-initiative would also be assured. The 'optimal robot' should also allow the development of individual walking strategies, and not only focus on the healthy symmetrical gait.

In the trade-off between a reasonably simple, that is safer and cheaper, device and the possibility of normal free walking a decision hast to be made on the "Degrees of Freedom" the device should allow.

Another important decision is on how these Degrees of Freedom should be controlled. With a regular position control it is possible to enforce motion patterns, but it interferes with developing own walking strategies, free walking, variability and self-initiative. Instead, some form of interaction control is needed. In such a control outline, not the positions but the forces are taken as the base of control, although positions and trajectories can still be used as a higher-level control objective. Interactivity can then for example be realised by adjusting the stiffness, or 'impedance' of this higher level position control (Israel, Campbell et al. 2006). Using force control as basis, many other training and control strategies are possible. This is the subject of the parallel research of Ralf Ekkelenkamp, soon to appear as PhD thesis.

Force control can be realised using high-power actuators together with force-sensors, resulting in a high-performance, so called 'haptic' interface. This is the common industrial approach of interaction control. We however felt that this would be a possibly risky solution, in case of working with human beings in an unstructured setting. We therefore chose for application of 'compliant actuators' to drive the robot, actuators with a limited stiffness, resembling human muscles. Such motors have for common industrial positioning applications a too low performance, but for functioning in unstructured surroundings and for force control in interaction with humans, they appear to be the optimal solution, being especially safe and stable in interaction (Riener, Lunenburger et al. 2004). The use of compliant actuators on all DoFs for example avoids the need to exactly match the motions of the exoskeleton with the motions of the treadmill, something that becomes necessary when a closed kinematical chain is created in a fully position (or admittance) controlled

device (Duschau-Wicke, Zitzewitz et al. 2007). The use of such actuators was a starting point for our design, as will be motivated more extensively in several chapters.

6. Research outline

a. Problem definition

Currently no device is available that is able to automate gait training for CVA patients in a way that well allows unhindered walking as a basis, self-initiative of the patient and natural variability, or that allows the therapist to focus the training interventions on typical disorders of a specific patient. At the same time it is clear that robotic devices are promising for intensifying, optimizing and objectifying gait training.

b. Research goal

The goal of this research is to realize a gait rehabilitation robot that is in better agreement than currently (at the tart of the research, 2002) available robots, with the current insights in proper gait training as described in §1.5 and that can be shortly characterized as a training that is task specific, intensive, variable and challenging to the patient. The device should also allow a therapist or researcher to focus the training on one leg or on subtasks of walking, depending on specific training or research goals, leaving the other leg or subtasks unhindered.

To fulfill this task, a robot should offer a safe training environment, where a patient can walk naturally on own initiative and where desired selective corrective or assistive actions can be set by a therapist and provided by the robot.

c. Approach

Four main research questions are derived from this goal:

a.   *Which degrees of freedom are required to allow a natural walking pattern – or: which degrees of freedom can be blocked without disturbing the natural walking pattern too much?*

b.   *Which mechatronical design concepts are best suited for a robot interacting with a human being for purpose of gait training, concerning basic control outline and actuation principles, considering safety and flexibility in the programming of therapeutic interactions?*

c.   *Which technological design is best suited to implement these degrees of freedom and this mechatronical concept?*

d.   *How well does the prototype satisfy the stated goals?*

The last question can be considered a clinical question that can be only answered by extensive testing with patients. This is true, but beyond the scope of this thesis. The ultimate evaluation test within this thesis will be to assess how well it is possible to walk naturally in the prototype for healthy subjects as ultimate test for providing task specific training. Assuming that the robot is able to provide necessary assistance, this can be considered the minimal demand for a robot according to the stated research goal.

7. Thesis Outline

This thesis reports the design and evaluation of a gait rehabilitation robot. It is however not a design-report, as it is meant as *engineering research*. As such it describes those parts of the design process that are interesting from research viewpoint and yield general knowledge that is interesting qua method or results for other designs. Beside this thesis a second primary result is therefore the gait rehabilitation robot itself.

To address the question on importance of certain degrees of freedom, **chapter 2** contains a research on effects of fixating the pelvis during gait. This question is of importance as for constructional reasons it is the easiest to block these degrees of freedom, as is also done in several existing devices. It might however be possible that this design decision negatively affects training quality. This part of the research was carried out by fixating the pelvis of healthy subjects while letting them walk on a treadmill and then studying changes in several gait parameters. **Chapters 3, 4 and 5** deal with the choice for suitable mechatronical design concepts. The emphasis in these chapters is the choice of actuators for driving the legs in an interactive way (according a kinesthetic interface). To make a proper choice of actuators it is necessary to first determine the overall mechatronical concept of the robot, such as to achieve safe and proper interaction control for rehabilitation purposes. **Chapter 3** addresses the problem generally in a theoretical way, selects impedance control as most suitable basic control outline and assesses experimentally the principal suitability of series elastic actuation and pneumatics for force actuation in impedance control. Chapter 4 and 5 present suitable implementations of these principles. **Chapter 4** describes the modeled and measured performance of pneumatic muscles as force actuators. **Chapter 5** presents a specific design of a series elastic actuator applying Bowden cables for force transmission, which was built and tested.

Based on the latter actuation principle a full prototype was designed. **Chapter 6** presents the final design of the robot prototype, incorporating the gained insights about degrees of freedom and the designed actuator. Applied principles are explained and basic performance is described.

In **chapter 7 and 8** the prototype is analyzed on its ability to allow normal walking in an experimental evaluation. In **chapter 7** walking inside LOPES is compared to free treadmill walking for healthy subjects. For these experiments 15 subjects walked in the robot, while it was controlled to its lowest possible impedance. Changes in walking are studied by EMG measurements on important leg muscles and by changes in several spatio-temporal gait parameters. **Chapter 8** further evaluates the need for the implemented degrees of freedom in the pelvis movements, by fixating the balance related degrees of freedom in the prototype during walking. The same methods as in chapter 7 are applied. **Chapter 9** finally draws general conclusions and looks at the future.

Suggestion for the reader

All chapters of this thesis were written as journal articles, and in several cases seperately published. The text of these publications is largely kept intact here. This implies that especially the introduction of the several chapters may become repetitive. The introductions were however preserved because they have a different accent in different chapters. The reader may however find this repeated information unpleasant, and can skip these intro-

ductory sections by choice. It also implies that the chapters do not have to be read in the same order as placed in this thesis.

8. References

Aoyagi, D., Ichinose, W. E., Harkema, S. J., Reinkensmeyer, D. J. and Bobrow, J. E. 2005. An assistive robotic device that can synchronize to the pelvic motion during human gait training. Paper presented at the 9th International Conference on Rehabilitation Robotics, 2005. ICORR 2005. Chicago.

Barbeau, H. and Visintin, M. 2003. Optimal outcomes obtained with body-weight support combined with treadmill training in stroke subjects. Archives of Physical Medicine and Rehabilitation, 84(10): 1458-1465.

Buurke, J. H. 2005. Walking after stroke Co-ordination patterns & functional recovery , PhD-Thesis, Enschede.

Chen, G., Patten, C., Kothari, D. H. and Zajac, F. E. 2005. Gait deviations associated with post-stroke hemiparesis: improvement during treadmill walking using weight support, speed, support stiffness, and handrail hold. Gait & Posture, 22(1): 57-62.

Colombo, G., Joerg, M., Schreier, R. and Dietz, V. 2000. Treadmill training of paraplegic patients using a robotic orthosis. Journal of Rehabilitation Research and Development, 37(6): 693-700.

Den Otter, A. R. 2005. Gait control after stroke : a neuromuscular approach to functional recovery. PhD-Thesis, Groningen, The Netherlands, .

Dobkin, B. H. 2004. Strategies for stroke rehabilitation. Lancet Neurology, 3(9): 528-536.

Donelan, J. M., Shipman, D. W., Kram, R. and Kuo, A. D. 2004. Mechanical and metabolic requirements for active lateral stabilization in human walking. Journal of Biomechanics, 37(6): 827-835.

Duschau-Wicke, A., Zitzewitz, J. v., Banz, R. and Riener, R. 2007. Iterative learning synchronization of robotic rehabilitation tasks, Paper presented at the 10th International Conference on Rehabilitation Robotics, ICORR 2007. Noordwijk aan Zee.

Emken, J. L., Wynne, J. H., Harkema, S. J. and Reinkensmeyer, D. J. 2006. A robotic device for manipulating human stepping. IEEE Transactions on Robotics, 22(1): 185.

Ferris, D. P., Czerniecki, J. M. and Hannaford, B. 2005. An ankle-foot orthosis powered by artificial pneumatic muscles. Journal of Applied Biomechanics, 21(2): 189-197.

Ferris, D. P., Gordon, K. E., Sawicki, G. S. and Peethambaran, A. 2005. An improved powered ankle-foot orthosis using proportional myoelectric control. Gait & Posture.

Ferris, D. P., Sawicki, G. S. and Domingo, A. R. 2005. Powered lower limb orthoses for gait rehabilitation. Topics in Spinal Cord Injury Rehabilitation, 11(2): 34-49

Gemperline, J. J., Allen, S., Walk, D. and Rymer, W. Z. 1995. Characteristics of motor unit discharge in subjects with hemiparesis. Muscle & nerve, 18(10): 1101-1114.

Gordon, K. E., Sawicki, G. S. and Ferris, D. P. 2006. Mechanical performance of artificial pneumatic muscles to power an ankle-foot orthosis. Journal of Biomechanics, 39(10): 1832-1841.

Hesse, S. and Uhlenbrock, D. 2000. A mechanized gait trainer for restoration of gait. Journal of Rehabilitation Research and Development, 37(6): 701-708.

Hidler, J. M. and Wall, A. E. 2005. Alterations in muscle activation patterns during robotic-assisted walking. Clinical Biomechanics (Bristol, Avon), 20(2): 184-193.

Husemann, B., Muller, F., Krewer, C., Heller, S. and Koenig, E. 2007. Effects of locomotion training with assistance of a robot-driven gait orthosis in hemiparetic patients after stroke: a randomized controlled pilot study. Stroke 38(2): 349-354.

Israel, J. F., Campbell, D. D., Kahn, J. H. and Hornby, T. G. 2006. Metabolic costs and muscle activity patterns during robotic- and therapist-assisted treadmill walking in individuals with incomplete spinal cord injury. Physical therapy 86(11): 1466-1478.

Jorgensen, H. S., Nakayama, H., Raaschou, H. O. and Olsen, T. S. 1995. Recovery of walking function in stroke patients: the Copenhagen Stroke Study. Archives of Physical Medicine and Rehabilitation, 76(1): 27-32.

Kollen, B., Kwakkel, G. and Lindeman, E. 2006. Functional Recovery After Stroke: A Review of Current Developments in Stroke Rehabilitation Research. 1: 75-80.

Krakauer, J. W. and Shadmehr, R. 2006. Consolidation of motor memory. Trends in neurosciences, 29(1): 58-64.

Krebs, H. I. and Hogan, N. 2006. Therapeutic Robotics: A Technology Push. 94(9): 1727-1738.

Kwakkel, G., Kollen, B. and Lindeman, E. 2004a. Understanding the pattern of functional recovery after stroke: facts and theories. Restorative neurology and neuroscience, 22(3-5): 281-299.

Kwakkel, G., van Peppen, R., Wagenaar, R. C., Dauphinee, S. W., Richards, C., Ashburn, A., Miller, K., Lincoln, N., Partridge, C., Wellwood, I. and Langhorne, P. 2004b. Effects of augmented exercise therapy time after stroke - A meta-analysis. Stroke 35(11): 2529-2536.

NationalStrokeAssociation; www.stroke.org.

Peshkin, M., Brown, D. A., Santos-Munne, J. J., Makhlin, A., Lewis, E., Colgate, J. E., Patton, J. and Schwandt, D. 2005. KineAssist: a robotic overground gait and balance training device. Paper presented at the 9th International Conference on Rehabilitation Robotics, 2005. ICORR 2005. Chicago.

Peurala, S. H., Tarkka, I. M., Pitkanen, K. and Sivenius, J. 2005. The effectiveness of body weight-supported gait training and floor walking in patients with chronic stroke. Archives of Physical Medicine and Rehabilitation, 86(8): 1557-1564.

Pohl, M., Werner, C., Holzgraefe, M., Kroczek, G., Mehrholz, J., Wingendorf, I., Hoolig, G., Koch, R. and Hesse, S. 2007. Repetitive locomotor training and physiotherapy improve walking and basic activities of daily living after stroke: a single-blind, randomized multicentre trial (DEutsche GAngtrainerStudie, DEGAS). Clinical Rehabilitation, 21(1): 17-27.

Reinkensmeyer, D., Aoyagi, D., Emken, J., Galvez, J., Ichinose, W., Kerdanyan, G., Nessler, J., Maneekobkunwong, S., Timoszyk, B., Vallance, K., Weber, R., Wynne, J. H., de Leon, R. D., Bobrow, J., Harkema, S. and Edgerton, V. 2004. Robotic Gait Training: Toward More Natural Movements and Optimal Training Algorithms. Paper presented at the 26th Annual International Conference of the IEEE EMBS, San Francisco, CA, USA.

Reinkensmeyer, D. J., Aoyagi, D., Emken, J. L., Galvez, J. A., Ichinose, W., Kerdanyan, G., Maneekobkunwong, S., Minakata, K., Nessler, J. A., Weber, R., Roy, R. R., de Leon, R., Bobrow, J. E., Harkema, S. J. and Edgerton, V. R. 2006. Tools for understanding and optimizing robotic gait training. Journal of Rehabilitation Research and Development, 43(5): 657-670.

Riener, R., Lunenburger, L. and Colombo, G. 2004. Cooperative strategies for robot-aided gait neuro-rehabilitation. Paper presented at the Proceedings of EMBS 2004. 26th Annual International Conference of the IEEE Engineering in Medicine and Biology Society.

Riener, R., Lunenburger, L., Jezernik, S., Anderschitz, M., Colombo, G. and Dietz, V. 2005. Patient-cooperative strategies for robot-aided treadmill training: first experimental results. IEEE Transactions on Neural Systems and Rehabilitation Engineering, 13(3): 380-394.

Schmidt, H., Sorowka, D., Hesse, S. and Bernhardt, R. 2003. [Development of a robotic walking simulator for gait rehabilitation]. Biomedizinische Technik (Berlin) 48(10): 281-286.

Schmidt, H., Werner, C., Bernhardt, R., Hesse, S. and Kruger, J. 2007. Gait rehabilitation machines based on programmable footplates. Journal of Neuroengineering and Rehabilitation, 4: 2.

Teasell, R., Bitensky, J., Salter, K. and Bayona, N. A. 2005. The role of timing and intensity of rehabilitation therapies. Topics in Stroke Rehabilitation, 12(3): 46-57.

Van Peppen, R. P., Hendriks, H. J., Van Meeteren, N. L., Helders, P. J. and Kwakkel, G. 2007. The development of a clinical practice stroke guideline for physiotherapists in The Netherlands: A systematic review of available evidence. Disability and rehabilitation, 29(10): 767-783.

Wellner, M., Guidali, M., Zitzewitz, J. v. and Riener, R. 2007. Using a robotic gait orthosis as haptic display - a perception-based optimization approach, Paper presented at the 10th International Conference on Rehabilitation Robotics ICORR 2007. Noordwijk aan Zee.

Young, J. L. and Mayer, R. F. 1982. Physiological alterations of motor units in hemiplegia. Journal of the neurological sciences, 54(3): 401-412.

chapter 2

Fixating the Pelvis in the Horizontal Plane Affects Gait Characteristics

Jan F. Veneman
Jasper Menger
Edwin H.F. van Asseldonk
Frans C.T. van der Helm
Herman van der Kooij

Abstract

In assistive devices for neuro-rehabilitation, natural human motions are partly restricted by the device. This may affect the normality of walking during training. This research determines effects on gait of fixating the pelvis in the horizontal plane during treadmill walking. Direct effects on the motion of the pelvis and external forces acting on the pelvis were measured. Several gait descriptors (kinematical and force parameters) were defined and measured to indicate changes. We observed the effect of the pelvis fixation on these parameters while varying gait velocity (0.35, 0.60 and 0.90 m/s).

It was shown that the fixation caused a reduction of step width by 33%, and an increase of step length of 15%. Sagittal and axial trunk rotations changed with +68% and -54% respectively. The fixation also changed the effect of speed significantly on most descriptors. It can therefore be concluded that a fixation of the pelvis severely affects gait dynamics and that it should be avoided if natural walking should be possible during training.

Chapter Contents

1. Introduction

In the last decade several gait training robots were developed (Hesse, Schmidt et al. 2003). These devices offer safety and support during gait training. Due to design considerations often concessions are done to the normality of walking during training. A typical limitation that might disturb walking is a fixation of the pelvis translations in the horizontal plane (Colombo, Joerg et al. 2000; Hidler and Wall 2005). Avoiding a fixated pelvis would demand additional degrees of freedom, leading to a mechanically more complex design. Both for designing robotic devices and training practise, it is relevant to know what the effects of such a fixation are.

Literature on pelvis function in gait generally focuses on body-internal pelvis rotations (Inman, Ralston et al. 1981; Perry and Schoneberger 1992). These are however not the focus of this paper. Blocking the pelvis translations in global space comes down to changing body dynamics in both forward and sideways direction. In the sagittal plane it causes the pelvis to move (relatively to the treadmill surface) exactly with the constant velocity of the treadmill, thus opposing the natural fluctuations in velocity and the forward fall that is utilized for propulsion. In the frontal plane the cyclic lateral sway towards the weight-bearing foot is obstructed. In fact the instability of the body is completely omitted, making actions for maintaining the bodies' vertical stance superfluous.

Recently, Israel and colleagues (Israel, Campbell et al. 2006) showed that the metabolic costs during standing with fixated pelvis translations, were significantly smaller than during unassisted standing. They argued that this decrease was caused by a decreased need for muscular work for stabilization in the frontal and sagittal plane as this stability was externally provided by fixation. Donelan (Donelan, Shipman et al. 2004) has empirically shown that an external lateral stabilization in the form of a lateral stiffness at the pelvis pushing the body towards the upright position, strongly decreases the efforts subjects have to put in keeping the body upright, concluded from both metabolic costs and reduction of step width and its variability. The relation between pelvis acceleration patterns in normal walking and gait characteristics as described in (Zijlstra and Hof 2003), also suggests a close relation between pelvis motions and all other aspects of gait. Also the EMG studies of Hidler and colleagues (Hidler and Wall 2005) suggest a large effect of the pelvis fixation in a Lokomat on gait.

The aim of this study is to empirically determine how a pelvis fixation in the horizontal plane affects gait of healthy subjects and to speculate about its relevance for gait rehabilitation practise. Subjects walked on a treadmill with and without pelvis fixation and at three different velocities (0.35, 0.60 and 0.90 m/s), while kinematics of trunk and legs and ground reaction forces were measured.

2. Methods

a. Fixation of the pelvis

The motion constraints to the pelvis as present in the most widely used gait rehabilitation robot, the Lokomat, were taken as starting point (Colombo, Joerg et al. 2000). These constraints also resemble those of the Auto-ambulator robot of HealthSouth. In the com-
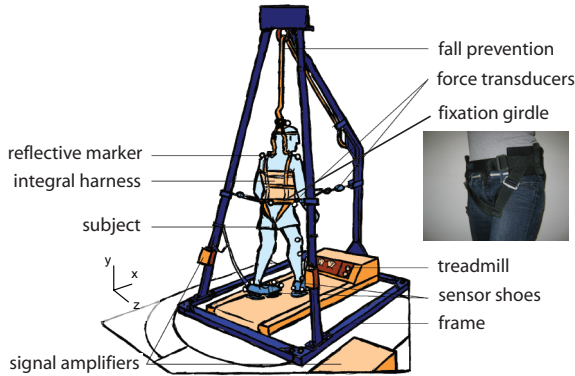
Figure 2.1: Sketch of the experimental setup, mentioning the essential parts. The photograph shows the girdle used for fixating the pelvis.

mercially available versions of the Lokomat, the pelvis of the walking subject is fixed in the horizontal plane. The vertical motion is left free, optionally supported by a body weight support system. The fixation is a result of a lower back cushion, a weight support harness at the trunk and belt connections at the upper legs, which together keep the pelvis in place. Slight rotations of the pelvis are still possible.

In our test setup the pelvic fixation was implemented using of a waist girdle connected to a frame. This girdle was fixed with three horizontal lightweight static ropes, which were brought to tension with screw tensioners. The static tension was about 30 N, high enough to prevent horizontal movement of the pelvis yet still acceptably comfortable. The actual rigidity of the fixation will be shown in the results section. Vertical motion was only restrained by the girdle when deviating too much from the equilibrium position and by the fall prevention system, but unhindered within the common motion range. An impression of the setup is given in figure 2.1. The vertical rope is only for fall prevention and not tensioned during walking.

b. Experimental procedures

Experimental conditions

Measurements were done on eight healthy subjects (all male, age 24.1 ± 4.4 years, length 1.81 ± 0.04 m, weight 72.6 ± 4.2 kg ; mean ±s.d.). All subjects were healthy and exhibited no clinical gait abnormalities. Subjects were asked to walk on the treadmill in 6 different conditions made up of the combinations of: a. free walking vs. walking with pelvic fixation and b. walking with three different prescribed velocities; 'medium' v_1 = 0.90 m/s vs. 'slow' v_2 = 0.60 m/s vs. 'very slow' v_3 = 0.35 m/s. The choice for relatively slow walking is motivated by the common low gait speeds in stroke rehabilitation (Bayat, Barbeau et al. 2005). Every trial consisted of at least ten complete step cycles, and was preceded by a period of at least a minute in which the subject could get accustomed to the situation. During walking full 3D motions and ground reaction forces were measured.

Data collection and analysis

For motion capturing, reflective spherical markers were attached (according to Koopman (Koopman 1989), figure 2.2); for analysis were used, the: lateral malleolus and the anterior superior iliac spine (asi) of both legs, the sacrum and and the left and right acromion. The 'asi' and sacrum markers were not directly attached onto these landmarks during the pelvis-fixed walking, as this was impossible, but on the harness or girdle covering them. This slightly affects the accuracy of the measurement, but was the only available

option.

The foot markers according to Koopman (Koopman 1989) were replaced by the footmarkers already integrated into the instrumented shoes, described below. Three markers were put on the external frame, at the connection points of the fixation ropes, to determine the actual directions of the fixation forces. The movement trajectories of the markers were recorded at a sampling rate of 120 Hz by means of a three-dimensional passive registration system (Vicon Oxford Metrics, Oxford, UK), using six infrared cameras/light sources.

The global coordinate frame was consequently calibrated with one axis aligned with the walking direction, one axis vertical, and the third axis perpendicular to this plane pointing to the right, defined as x, y and z respectively, according ISB standards.

During processing, the signals were digitally filtered using a recursive zero phase-lag second order Butterworth filter of 30 Hz. Gaps of up to 0,3 s in the marker data were filled up by means of spline interpolation.

Figure 2.2: Overview of the placement of the reflective markers for motion capturing. The solid black markers were actually used during analysis. Each shoe had six markers rigidly attached to it; three per force sensor. Three additional markers were put on the frame (frml, frmr, frmf). The markers for the sacrum and both hips were not attached onto bony landmarks as is the custom, but onto the harness as close as possible to those landmarks.

The frame interaction forces were sampled with custom-made 1-D pull force sensors. All frame interaction forces were sampled at 10 kHz without any prior analogue filtering. During the processing they were recursively filtered with a cut-off frequency of 10 Hz. This was followed by resampling to the video frame rate of 120 Hz, and synchronization to the motion data. Finally the static offset was removed from the horizontal force signals. The direction of the interaction forces in the fixation ropes was determined using the positions of the hip (asi) and frame markers in a horizontal plane.

The ground reaction forces were measured using special instrumented shoes. These consist of a pair of adapted orthopaedic sandals of size 43, each equipped with two six degree of freedom sensors (ATI-Mini45-SI-580-20). Orientation of these sensors are measured using sets of three Vicon-markers per sensor. The exact functioning of these shoes and the force measurement routine and their influence on the gait pattern are described in (Veltink, Liedtke et al. 2005; Liedtke, Fokkenrood et al. 2006).

c. Gait descriptors

To describe the changes in walking, specific parameters and characteristics were derived from the marker and force data. The direct effects of the fixation were studied from the pelvis motion, described in three rotations and three translations. This motion was recon-
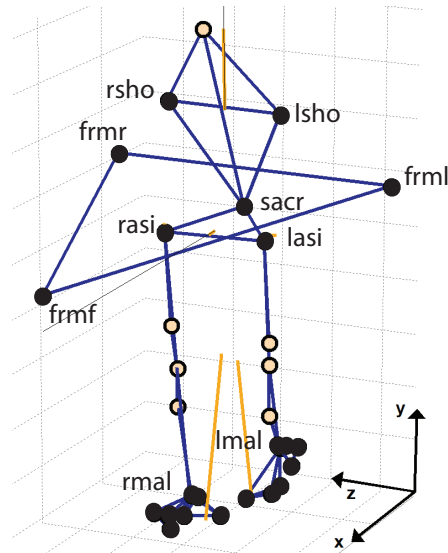
structed from the plane defined by the three pelvis markers; the left and right 'asi' and the sacrum marker. Rotations (3) and translations (3) of this plane are high pass filtered (with a zero-lag 0.7 Hz Butterworth filter) in order to filter out drift. The motion ranges are expressed by the root-mean-squared deviation in the step-average of a trial. This yields information on how rigid the pelvis fixation was. Also the fixation-force profiles per condition, averaged over all steps, averaged over all subjects, and their standard deviation will be shown. Heel strike and toe off times for a foot are found by observing the vertical force signal of that foot.

To further specify the changes in walking several 'gait descriptors' are defined. The first four are standard descriptors; step width, step length, double-stance ratio and step time. The rotation of the trunk is described with two descriptors, as change of trunk motions in the sagittal and frontal plane was very manifest. A last parameter is derived from the ground reaction forces in order to quantify the change in GRF-patterns. The descriptors are defined as:

Step width: the step width W was defined as the average z-distance between the positions of the ankle marker during the double stance phase. The mean of this distance over all double stance phases of one trial was taken as the step width of that trial. The results are normalized with the leg length.

Step length: the step length L was defined as the distance between the positions of the ankle marker at two consecutive foot stance phases, measured along the x-axis. The average of this distance over all steps of one trial and over left and right step length was taken as the step length during that trial. The results are normalized with the leg length.

Double-Stance Ratio (DSR): The double-stance ratio is defined as the duration of the average double stance phase relative to the stride duration, which is defined as the time between one heel contact and the next heel contact of the same foot. The ratio of a certain trial is the average over all strides of that trial.

Step time: The step time is defined as the step length divided by the walking speed. This variable is therefore largely dependent on the step length, and only presented for easier interpretation of the results. It is a well known gait descriptor that can clarify the actual changes in walking.

Trunk sagittal rotation range: The maximum of the range of the global sagittal rotation angle (around the z-axis) of the (thoracolumbar) trunk during the steps of one trial. The segment rotations are supposed to equal the rotations of the plane defined by the three following sensors: left and right acromion and sacrum, projected in the xy-plane.

Trunk axial rotation range: The maximum of the range of the global coronal rotation angle
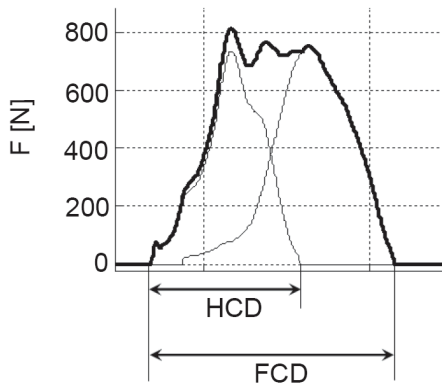

Figure 2.3: The Relative Heel Contact Duration (RHCD) is defined as the ratio of the (Heel Contact Duration) HCD over the (Foot Contact Duration) FCD. These durations were determined from the vertical component of the ground reaction force.

(around the global y-axis) of the (thoracolumbar) trunk during the steps of one trial. The segment rotations are supposed to equal the rotations of the plane defined by the three following sensors: left and right acromion and sacrum, projected in the xz-plane.

Relative Heel Contact Duration (RHCD): The RHCD was defined as the the heel contact duration (HCD) during a foot contact divided by the (total) foot contact duration (FCD), based on the vertical ground reaction force component (see figure 2.3). The average of this factor over all steps of one trial and over left and right stance phases was taken as the RHCD of that trial. The RHCD is defined here to describe changes in the pattern of the vertical ground reaction forces and especially to quantify the changes in the roll-off of the foot.

d. Description of changes

A statistical analysis was carried out to track the significant changes over the population in the described parameters caused by changes in the pelvis fixation condition [on, off] and the walking speed [very slow, slow, medium]. Additionally the changes in mean values as effect of the fixation will be presented to show the actual size of changes, which may be important to judge on the relevance of specific changes.

All statistical tests were done using a multivariate repeated measures General Linear Model (GLM) analysis in SPSS. Post-hoc comparisons were used to further analyse the origin of significant results ($p < 0.05$).

The effect of the fixation on the sacrum marker motion as well as on the gait descriptors was tested using a repeated measures, multifactor ANalysis Of VAriance on every separate degree of freedom. The factors were speed (3 levels) and fixation (2 levels). The results will also be presented graphically.

3. Results

The changes in average ranges of motion of the six degrees of freedom of the pelvis segment are presented in table 2.1.

Table 2.1: The changes in average variation of the motion in the six degrees of freedom of the pelvis segment, expressed as RMS value (absolute and relative) of the deviation from the average of the high-pass filtered values. The significance of the difference is expressed in p-values obtained from an Anova test. The effects of the factor speed on the variations were not significant for any degree of freedom.

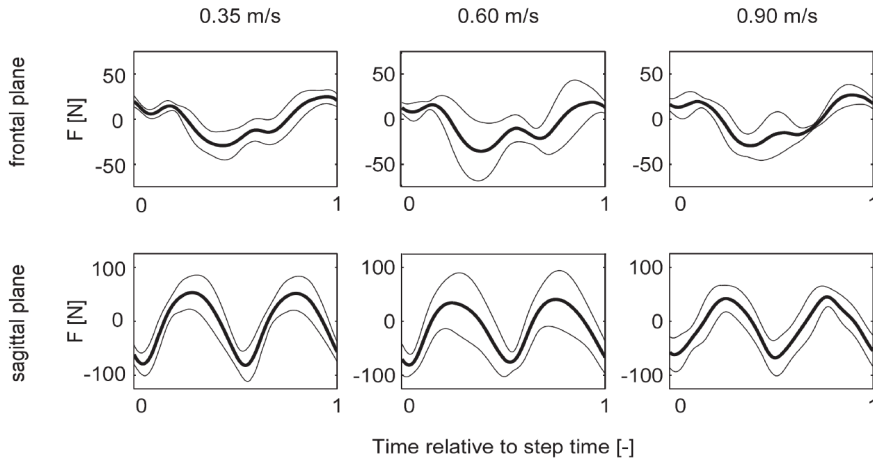| Degree of freedom	Free walking Variation		Fixed pelvis Variation		Significance of difference
	RMS	index	RMS	index	p-value
X translation	11.9 mm	100 %	7.7 mm	64 %	0.045 *
Y translation	14.2 mm	"	12.9 mm	91 %	0.357
Z translation	26.7 mm	"	7.0 mm	26 %	0.000 *
X rotation	12.7 °	"	5.8 °	45 %	0.273
Y rotation	7.9 °	"	5.2 °	66 %	0.060
Z rotation	9.1 °	"	3.4 °	37 %	0.169

Figure 2.4:Average profiles for all conditions of resultant forces on the pelvis imposed by the pelvis fixation. Per subject an average step profile is calculated, which was then averaged over all subjects. The standard deviation of this last averaging is also shown. The horizontal axis contains the normalised step time.

As intended, the translations in the horizontal (xz-) planed were significantly reduced by the fixation girdle. The walking speed had no significant effect on the ranges of motion of the pelvis. The step-average interaction forces averaged over all subjects for the three gait speeds are shown in figure 2.4. These forces appeared to be in counter phase with the forward ground reaction forces; instead of acceleration the body, these forces push the body against the fixation girdle. The standard deviations are reasonably small, indicating consistent patterns over all subjects. Apparently, neither patterns nor amplitudes depend much on walking speed.

The results of the Anova tests on the separate gait descriptors are graphically presented in figure 2.5. In the figures the significance of the fixation factor is shown, effects of the speed factor and the interaction effect of fixation and speed are presented in table 2.2.

Table 2.2: Significance levels of the influence of the factors on the seven gait descriptors.

Gait Descriptor	Fixation	Speed	Interaction FxS
Step width	$p<0.004^*$	$p<0.400$	$p<0.600$
Step length	$p<0.034^*$	$p<<0.001^*$	$p<0.003^*$
Double stance ratio	$p<0.554$	$p<0.001^*$	$p<<0.001^*$
Step time	$p<0.019^*$	$p<<0.001^*$	$p<0.003^*$
Upper body sagittal rotation	$p<0.042^*$	$P<0.037^*$	$p<0.038^*$
Upper body axial rotation	$p<0.001^*$	$p<0.036^*$	$p<0.015^*$
RHCD	$p<0.004^*$	$p<0.837$	$p<0.010^*$

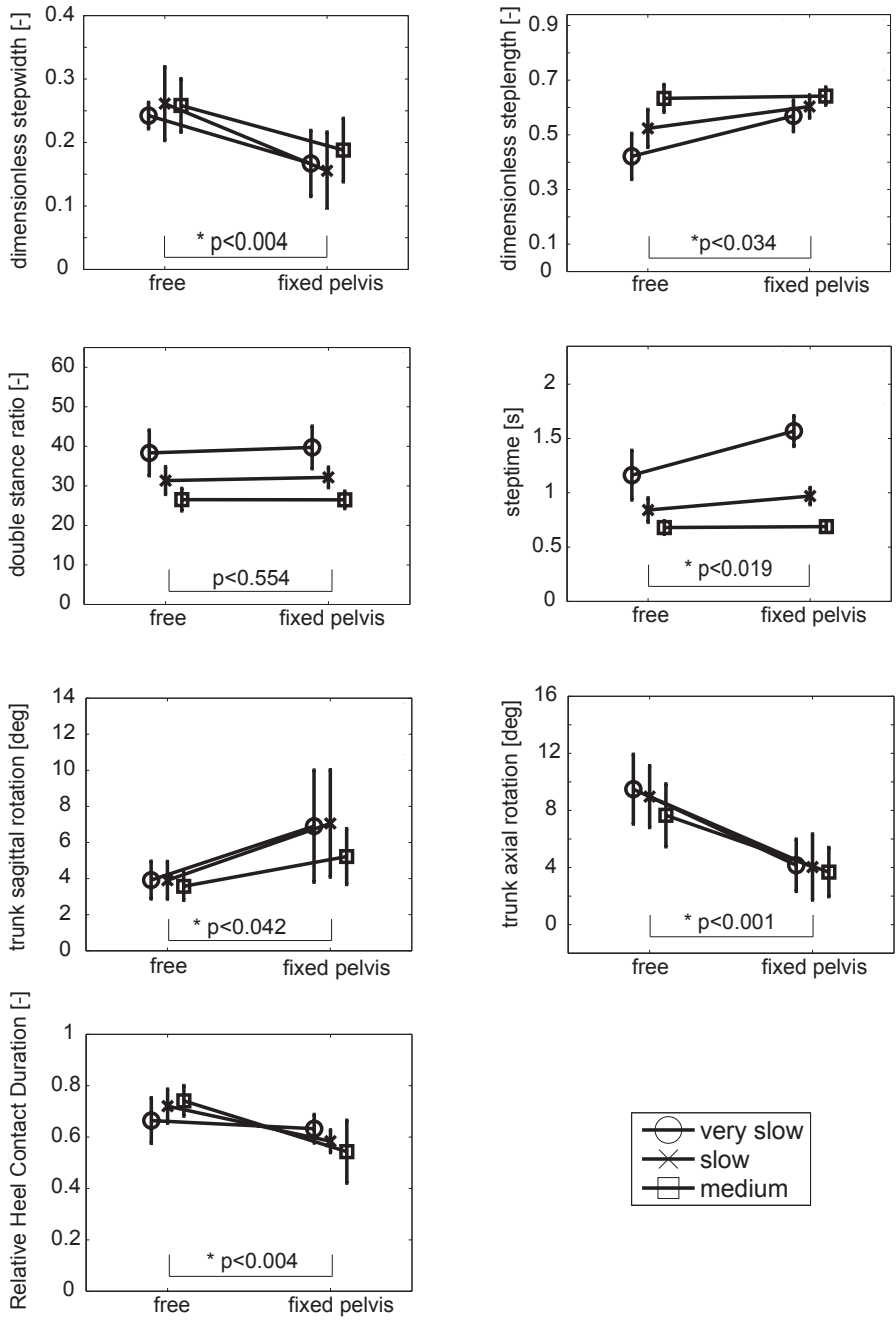**Figure 2.5**: Effect of speed and fixation on the average values of the gait descriptors. Every graph shows one descriptor, the columns show fixed versus free pelvis, the three indicators show the three speeds. The mean values are indicated and the vertical lines show the standard deviations of the averaging. The p-values that are shown are the significance levels of the influence of the factor fixation, regardless of speed.

As can be seen the influence of the fixation is significant on all descriptors except for the double stance ratio. The influence of speed is significant on all descriptors except for step width and RHCD. All descriptors but the step width show an interaction effect. This is most clear for the step length/step time and the RHCD. Step length and step time show a large increase (>40%) with fixation for the slowest speed and a small increase (<1%) with fixation for the highest speed.

The relative change in the descriptors with fixation, averaged over all velocities, is presented in table 2.3. All descriptors that significantly changed with fixation apparently show also a relevant change, never lower than 17% in value. Especially the change of amplitudes of trunk rotations is large in both the sagittal (+68%) and axial (-54%) plane. As noted in the table, about half of the subjects showed exaggerated trunk sway, apparently depending on strategies of coping with the fixation. The mentioned increase of 68% is however the average over all subjects.

Table 2.3: Absolute and relative change in the parameters causes by a fixation of the pelvis. Statistically significant changes ($p < 0.05$) are indicated with an asterisk.

Gait Descriptor	Mean free	Mean fixed pelvis	Relative change
Step width*	0,25	0,17	- 33 %
Step length*	0,52	0,62	+ 19 %
Double stance ratio	32,3	32,5	+ 0 %
Upper body sagittal rotation* [1]	3,80	6,39	+ 68 %
Upper body axial rotation*	8,71	3,96	- 54 %
Step time*	0,90	1,08	+ 20 %
RHCD*	0,71	0,59	- 17 %

[1] A closer look at the sagittal upper body rotation learns that in fact four subjects showed a large increase of this motion, while for the others it stayed the same or even slightly decreased. The first group also showed a slightly larger increase in step length.

4. Discussion

In this section we will discuss the observed differences in walking and their possible clinical implications, especially for the design of training devices.

The fixation of the horizontal motions of the pelvis segment during treadmill walking was shown to significantly change almost all gait descriptors. Also their dependency on speed was significantly changed by the fixation (interaction effect). Considering the size of these changes it can be concluded that the fixation severely affects gait dynamics. The pelvis fixation was shown to cause longer (+19%) and narrower (-33%) steps together with excessive trunk rotations. These spatial changes were accompanied by an increase of the step time and a change of the vertical ground reaction force pattern. Pelvis rotations decreased on average, but not on a significant level.

The reduction of step width (-33%) is in accordance with the findings of Donelan (Donelan, Shipman et al. 2004), as mentioned in the introduction. Because our fixation was much more rigid than Donelan's, an additional reason to diminish step width may

have been that too wide walking would have been uncomfortable due to the fixation rigidity.

The excessive trunk rotations seem to be a strategy (not applied by all subjects) that allows to keep the walking pattern more normal, as the position of the body centre of mass can be adjusted this way to possible leg and centre of pressure motions. This is in accordance with the change in RHCD (ground reaction force patterns).

Clinical relevance

The outcomes suggest that fixating the pelvis translations can help normalizing certain gait parameters during treadmill training. For example if someone walks with too short steps, the fixation could be helpful in increasing step length. This could then be combined with the adaptation of other training parameters such as amount of weight support or speed, as suggested by Chen and colleagues (Chen, Patten et al. 2005). As they already mentioned, it is not yet known what the training effect of such 'artificial' normalization during gait training is on actual ability in over ground walking.

For reaching optimal transfer of trained ability from training situation to free over ground walking, it may rather be more effective to approach the free walking situation as closely as possible during training (Israel, Campbell et al. 2006), without any 'artificial contraints'. This implies that the body dynamics that are important during walking should not be altered too much during training so that natural muscle activation patterns lead to natural gait kinematics, while experiencing the natural sensory feedback. This becomes the more important the more able a patient is to walk on own power.

Apparently the pelvis fixation as artificial constraint alters the dynamics so much that largely different kinematic patterns become optimal or comfortable. This means that the task that is practiced is apparently different from free walking.

Clear examples of such undesired changes are the smaller step width and the exaggerated trunk motions. The smaller step width was argued to be caused by the lack of lateral instability of the body. At the same time training of lateral balance is an important aspect of gait training. Fixating the pelvis omits this aspect of training. Of course for more severe patients this could be beneficial at the onset of training, but it should be a therapeutic choice to omit or provide it. The exaggerated trunk motions indicate that the subjects had to perform additional effort in order the keep walking more or less natural. It is highly questionable if patients will be able to perform these efforts, especially as these additional efforts are ineffective for the task they are learning. Although trunk motions are not always reported in gait research, it is clear that the trunk has an important role in gait, like maintaining the full body balance and increasing efficiency (Perry and Schoneberger 1992), as well as that leg, pelvis and trunk motions are closely interrelated (Bruijn, Meijer et al.,2007).

Returning to the goal of this study, which was to provide information for designing a robotic gait training device, we can conclude that a fixation of the pelvis should be avoided. In the first place several sub-tasks of gait are omitted from the training, such as the need to generate propulsion as well as keeping lateral balance. In the second place important gait characteristics of spontaneous walking of healthy subjects change so much that it is very likely that the training situation is very different from free walking, disturbing the goal of realizing a task-specific and active training. The normalization of certain gait parameters, that could be realized by a fixation, is in case of a training robot not important as a device

will offer other options to alter parameters like step-length, that do not disturb the whole gait function (Van Asseldonk, Ekkelenkamp et al. 2007).

The question how much transfer of skill will appear from training in an artificial training setting to free walking for specific patients can of course not be answered by this kind of research; such questions can only be answered by clinical evaluation of devices with stroke patients.

5. References

Bayat, R., Barbeau, H. and Lamontagne, A. 2005. Speed and temporal-distance adaptations during treadmill and overground walking following stroke. Neurorehabilitation and neural repair, 19(2): 115-124.

Chen, G., Patten, C., Kothari, D. H. and Zajac, F. E. 2005. Gait deviations associated with post-stroke hemiparesis: improvement during treadmill walking using weight support, speed, support stiffness, and handrail hold. Gait & Posture, 22(1): 57-62.

Colombo, G., Joerg, M., Schreier, R. and Dietz, V. 2000. Treadmill training of paraplegic patients using a robotic orthosis. 37(6): 693-700.

Donelan, J. M., Shipman, D. W., Kram, R. and Kuo, A. D. 2004. Mechanical and metabolic requirements for active lateral stabilization in human walking. 37(6): 827-835.

Hesse, S., Schmidt, H., Werner, C. and Bardeleben, A. 2003. Upper and lower extremity robotic devices for rehabilitation and for studying motor control. Current Opinion in Neurology 16(6): 705-710.

Hidler, J. M. and Wall, A. E. 2005. Alterations in muscle activation patterns during robotic-assisted walking. Clinical Biomechanics (Bristol, Avon), 20(2): 184-193.

Inman, V. T., Ralston, H. J., Todd, F. and Lieberman, J. C. 1981. Human Walking. London: Williams&Wilkins.

Israel, J. F., Campbell, D. D., Kahn, J. H. and Hornby, T. G. 2006. Metabolic costs and muscle activity patterns during robotic- and therapist-assisted treadmill walking in individuals with incomplete spinal cord injury. Physical therapy 86(11): 1466-1478.

Koopman, H. F. J. M. 1989. The three-dimensional analysis and prediction of human walking. Ph.D. thesis, University of Twente, The Netherlands, Enschede.

Liedtke, C., Fokkenrood, S. A. W., Menger, J. T., van der Kooij, H. and Veltink, P. H. 2007. Evaluation of instrumented shoes for ambulatory assessment of ground reaction forces. Gait & Posture, 26(1): 39-47

Perry, J. and Schoneberger, B. 1992. Gait analysis : normal and pathological function: Thorofare, NJ : SLACK Incorporated.

Van Asseldonk, E. H. F., Ekkelenkamp, R., Veneman, J. F., Van der Helm, F. C. T. and Van der Kooij, H. 2007. Selective control of a subtask of walking in a robotic gait trainer(LOPES), ICORR 2007. Noordwijk aan Zee.

Veltink, P. H., Liedtke, C. B., Droog, A. and Van der Kooij, H. 2005. Ambulatory measurement of ground reaction forces. IEEE Transactions on Neural Systems and Rehabilitation Engineering, 13: 423-427.

Zijlstra, W. and Hof, A. L. 2003. Assessment of spatio-temporal gait parameters from trunk accelerations during human walking. Gait & Posture, 18(2): 1-10.

chapter 3

Compliant Actuation Principles in Robotic Neurorehabilitation

Jan F. Veneman

Abstract

The LOwer extremity Powered ExoSkeleton (LOPES) robot provides gait training to CVA patients. It is meant as an interactive rehabilitation robot, meaning that it can both follow and move a patient, either compliantly or rigidly. This fact demands for a robot with haptic or kinaesthetic quality. Forces in a gait rehabilitation robot will be considerably higher than in common haptic devices. This results in specific demands to the mechatronical design. A design philosophy for this kind of robot is presented. Impedance control is chosen as basic control strategy for the robot. This choice requires a lightweight construction and actuators that ideally act as pure force sources. This article is specifically about the actuator design within the total mechatronical design philosophy.

An option to realise well controllable, low impedance force sources is the use of intrinsically compliant actuators. Typical examples are the Series Elastic Actuator (SEA), where a spring is used in the output axis, and the Pneumatic Cylinder Actuator (PCA), where the air causes natural compliance.

The basic behaviour of both actuators is modelled. The result is a general compliant actuator model with specific sub-models that is able to describe any compliant actuator, making it possible to compare compliant actuators of different kind for a certain application. For the PCA sub-model this required a feedback linearization of the plant. As saturation is an important issue in (compliant) actuators, it is incorporated in the models. Performance of the actuators is described in terms of force tracking bandwidth and output impedance.

In general it can be concluded that both types of compliant actuator are applicable for an interactive rehabilitation device. The typically designed SEA appeared superior to the PCA, based on performance metrics. Important side factors of the PCA that also favour this judgement are the typical noise, dependency on pressurized air facilities and the complexity of the needed controller, which affects the robustness of the system. Due to the high weight neither one system can be considered truly optimal for use in gait rehabilitation. This would demand for an actuator that combines the advantages of a compliant actuator with a much smaller added weight to the robot.

Chapter Contents

Nomenclature

$A_{1,2}$	[m²]	Cross sectional area of cylinder chamber 1,2 (PCA)
C_{int}	*tf*	Transfer of the internal force controller
F_{act}	[N]	Actual force output
F_{error}	[N]	Error in force tracking
F_{frict}	[N]	Friction force
F_{ref}	[N]	Reference force output
F_{s}	[N]	Spring force
H_{force}	*tf*	Transfer of force tracking
H_{fp}	*tf*	Forward path transfer from control command to force output
H_{frict}	*tf*	Transfer of the friction model
H_{int}	*tf*	Transfer of the actuator-internal motor
c_{m}	[N.s/m]	Motor lumped damping (SEA)
k_{m}	[N/A]	Motor constant (SEA)
K_{s}	[N/m]	Spring-stiffness
l_{cyl}	[m]	Cylinder length (PCA)
P_{err}	[Pa]	Error of pressure tracking
P_{ref}	[Pa]	Reference pressure
$P_{1,2}$	[Pa]	Actual pressure of cylinder chamber 1,2 (PCA)
P_{max}	[W]	Maximal power (SEA)
m_{m}	[kg]	motor mass (SEA)
$u_{control}$	[V]	Control command
$x_{endpoint}$	[m]	Position of the output side of the actuator compliant element
x_{int}	[m]	Internal position of the actuator compliant element
x_{s}	[m]	Actual spring-length
$V_{01,02}$	[m³]	Rest-volume of cylinder chamber 1,2
$V_{1,2}$	[m³]	Volume of cylinder chamber 1,2
$Z_{endpoint}$	*tf*	Mechanical actuator impedance on the output axis
Z_{load}	*tf*	Mechanical impedance of the load
γ	[-]	Ratio of specific heats (PCA)
ω	[Hz]	Frequency
$\sim$		Measured value
$\cdot$		Time derivative

tf indicates a transfer function

1. Introduction

a. Problem introduction and article objective

Robotic neuro-rehabilitation is a specific sub-field of robotics. It concerns robots meant for training motor functions of impaired humans. Several robots have been developed for arm training (Volpe, Ferraro et al. 2002; Hesse, Schmidt et al. 2003) and a limited number for gait training, such as the Lokomat (Colombo, Joerg et al. 2000) and the Gait Trainer (Hesse, Uhlenbrock et al. 2000). (See also chapter one of this thesis)

We are developing a LOwer-extremity Powered ExoSkeleton (LOPES), an advanced gait training robot. The target group consists of people who lost their walking ability due to a stroke. The training is to take place on a treadmill. The robot will replace the therapist in the heavy physical interaction with patients while leaving clinical decisions and other interaction to the therapist. The physical robot interaction mainly intends correction of leg movements in the sagittal direction and assistance in keeping sagittal and lateral balance. Within the LOPES project, it has been decided to realize this by connecting the limbs of the patient to an 'exoskeleton' (Brown, Tsagarakis et al. 2003) so that robot and patient move in parallel (figure 3.1).

The exoskeleton is actuated in order to realize selective supportive actions and preventing fail mechanisms in walking. Typical supportive actions are: assuring enough foot clearance, stabilizing the knee and shifting the weight. The main goal of our robot is to allow the patient walk as independently as possible offering only selective support where needed. This goal puts LOPES apart from the commercially available robots mentioned earlier. Those are either position controlled devices that overrule the patient or support only limited motions due to the limited number of degrees of freedom (Hidler, Nichols et al. 2005). Other groups are also working on related innovations, but little has been published yet (Ferris, Sawicki et al. 2005). Currently new research on the Lokomat is carried out to make it suitable for interaction control (Riener, Lunenburger et al. 2005). The Lokomat was originally constructed as a position controlled device. From the publication it is not clear how well the robot functions in interaction control, whether it for example allows for 'unhindered' walking. Low power, position controlled devices however in general perform poorly in interaction control. Our claim is that this can be improved only by basic mechatronical (re-)design intentionally aiming at an optimal interaction control. This presupposes a clear definition of the goals of interaction control in a rehabilitation robot. Another research on the subject is the development of the HAL (Hybrid Assistive Limb) robot (Lee and Sankai 2005). Although this robot is meant for assistance during all-day life and therefore not straightforwardly suited for rehabilitation, the re-
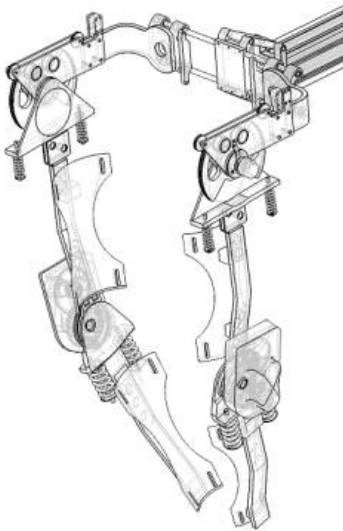

Figure 3.1: impression of a proposed exoskeleton design for the gait rehabilitation robot LOPES.

search recognizes the importance of 'unhindered' walking inside the robot.

In the rest of the introduction we will propose a design philosophy that explicitly reckons with the goal of interaction control. We will then argue that the design or selection of actuators is an important aspect of the mechatronical design. The objective of this article is to facilitate the selection of actuators suitable for the LOPES exoskeleton. This is done by defining the specific application and the corresponding actuator demands. As example two types of compliant actuator, a linear series elastic actuator (SEA) (Pratt, Krupp et al. 2002) and a pneumatic cylinder actuator (PCA) will be considered on their applicability. This process will yield insight in the important consequences of actuator choice on the overall robot behavior.

b. Interactive rehabilitation robots

To define the full range of therapeutic interventions demanded in the LOPES project, two 'extreme' modes of operation can be distinguished. In one extreme mode, referred to as 'robot in charge', the robot enforces a desired walking pattern, with pre-described motion patterns for all joints. In this case the patient can be considered as a passive load from control viewpoint. In the opposite extreme mode, referred to as 'patient in charge' the robot follows motions while hardly hindering the patient. Within these two extreme modes of operation all therapeutic interventions can be defined as specific interaction behavior between robot and human. This operation mode is called 'therapist in charge'.

In the 'robot in charge'-mode it is important that the robot has enough bandwidth and power to achieve the desired positioning performance with the desired stiffness (impedance). In the 'patient in charge'-mode it is important that interaction forces between exoskeleton and human are controlled towards zero; in other words that the *perceived* impedance of the robot is low.

To be able to cover the full range of operation that is defined by those two extreme modes, it is necessary that the involved robot is interactive. It does not suffice for the stated goals if the robot is only able to control position of robot and patient. As several rehabilitation robots are purely position controlled, the specific type considered here will be denoted as: *'interactive neuro-rehabilitation robots'*.

c. Impedance- versus admittance-controlled interactive robots.

Many issues arising in the design of interactive neuro-rehabilitation robots are similar to those appearing in the field of haptic, or more precise: kinaesthetic robotics (Brown, Tsagarakis et al. 2003). The characteristic feature of these robots is the bi-directionality of being able to both 'read from' and 'write to' a human user (Hayward and Astley 1996). Such robots are in general meant to display virtual objects or a virtual environment to a user. This user then can interact with a virtual or distant 'world' in a mechanically realistic way.

In contrast, interactive neuro-rehabilitation robots are meant to operate in between both stated modes of 'robot in charge' and 'patient in charge', acting as a 'robotic therapist'; not to display virtual objects as realistic as possible. Another difference, specific for limb-guiding exoskeletons, is that a kinaesthetic display usually has an end-effector that displays the information at one location on the robot, while an exoskeleton necessarily interacts at several points with human limbs as it is connected in parallel to them. This implies that not only an end-effector force is important, but all 'internal' torques over all actuated joints.
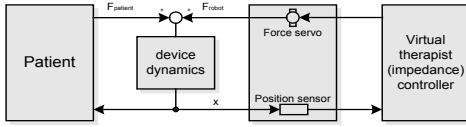
Figure 3.2: basic outline of an impedance-control based rehabilitation robot
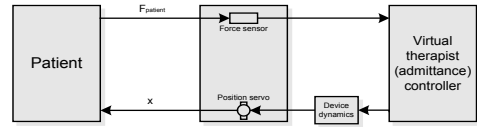
Figure 3.3: basic outline of an admittance-control based rehabilitation robot

This all makes it necessary to select the optimal basic control outline for this kind of robot, as different outlines imply different robot construction and actuator demands.

In general there are two basic ways to realize a kinaesthetic display (Adams and Hannaford 2002); impedance-control-based (figure 3.2), that is 'measure position and display force' and admittance-control-based (figure 3.3), that is 'measure force and display position', although hybrid forms exist. The important difference is that in impedance-control the quality of the display will depend on the accuracy of the position sensors and the bandwidth and accuracy of the force servos, and in case of admittance-control on the accuracy of the force sensors and the bandwidth and accuracy of the position servo. The bandwidth of the mentioned servos will depend on both the robot construction and the actuators. The choice between high performance force servo quality and high performance position servo quality puts specific demands on the robot construction and actuation. This choice has to be made even if a hybrid control architecture with both position and force sensing is used. To make clear what this choice basically is about it can also be presented as the choice between a lightweight (and flexible) uncompensated construction and a rigid (and heavy) controller-compensated (thus actuated with 'high' power) construction.

A fundamental limitation of impedance control is that in each specific controlled degree of freedom (or 'dof') the dynamical behavior of the robot construction in this 'dof' appears in the force transfer ('device dynamics'). It can only be compensated for in case of a proper dynamical predictive model, and proper measurements of position and velocity for stiffness and friction compensation respectively. Mass compensation is possible to a small
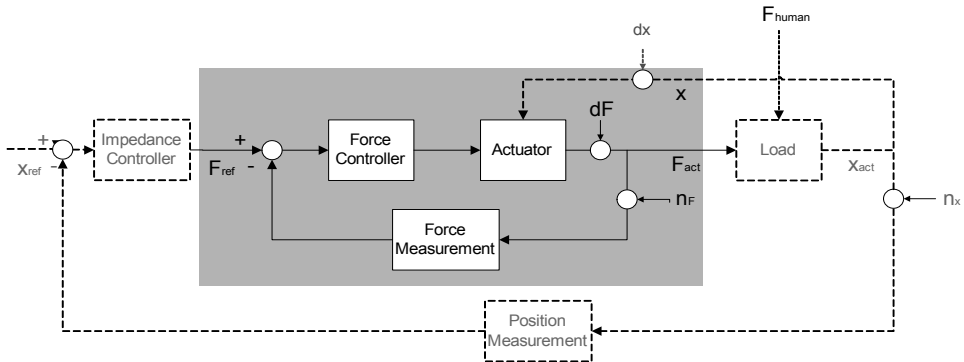
Figure 3.4: Schematic control outline for one degree of freedom. The inner loop (shaded area) assures the actuator to act as a pure force source, and is not necessary if the actuator can be used in open loop force control. The outer loop (impedance controller) sets the force reference based on desired impedance. The load reflects the robot/human-combination dynamics in the considered 'dof'. In case the actuator is compliant the output position directly influences the force output. Symbols: x – position; F – force; dF – external force disturbance; dx – external position disturbance; nF – force sensor noise; nx – position sensor noise; Fhuman – muscle force.

extent only, by adding a force or acceleration feedback loop (resulting in a hybrid control architecture). Best results within an impedance-control architecture are obtained using a lightweight, low friction construction and a low impedance actuator, so that the intrinsic mechanical impedance of the device is kept low. Impedance controlled robots are typically 'low-force' and lack performance in kinaesthetic display of high mass and high stiffness (Linde and Lammertse 2003). This is not essential in gait-rehabilitation as no stiff contacts or large masses have to be displayed, although relatively high forces certainly appear.

An admittance control scheme, on the other hand, demands for a high positioning bandwidth, and therefore for high(-er) power actuators and a rigid construction (Linde and Lammertse 2003). A limitation of admittance control is that the display of low stiffness ('free motion') can become unstable, especially in case of a rather stiff user, because of the high control gains needed in this case. Another limitation is that admittance can only be controlled at the location(-s) of force sensors. The construction will display its (high, thus stiff) intrinsic impedance at other locations, as the interaction behavior there cannot be influenced by the controller without force sensing. This might pose a problem for application in neuro-rehabilitation, because of the possible safety threat (for instance for the therapist). The robot will not react to mechanical interactions that by-pass the force sensors. This is all the more important as with admittance control actuators and construction will be considerably heavier.

Summarizing, compared to general kinesthetic devices less critical stiffness- and mass-display is demanded and movements are relatively slow. An admittance controlled system brings about safety threats due to the higher required actuator power, rigidity and inertia of the robot and is less stable at displaying low stiffness. Considering all this it seems more natural to choose an impedance-control based design strategy for our exoskeleton. An important advantage is also that the programmed dynamical behavior will be available everywhere on the construction, that is, in every actuated degree of freedom.

For the actuators, impedance control implies that they preferably should be perfect force sources, or, realistically, low-impedance, high precision force sources (in contrast with position/velocity sources that would be needed for admittance control). For the construction it means that it should be lightweight, although being able to bear the demanded forces, and containing low friction. Figure 3.4 shows the robot control outline for one 'dof' that suits with these decisions.

d. Actuator demands for an impedance control based interactive neuro-rehabilitation robot

The general demands for the actuation of human limbs within the framework of an impedance controlled exoskeleton, considering two extreme modes of 'robot-in-charge' and 'patient-in-charge' can now be summarized as:

Convenient actuators should:

D1. have enough power and bandwidth to move the concerning limbs up to a certain positioning speed; to be expressed in positioning bandwidth for a specified load, corresponding to the limb dynamics

D2. facilitate an accurate force control; to be expressed in a minimal controllable force step and a force control bandwidth in standstill.

D3. allow for control of a range of impedances in between 'imperceptible' and 'stiff', including impact-proof high frequency impedance; to be expressed in a control-

    lable range of impedances and the intrinsic impedance.
D4. add little mass to the moving construction; to be expressed in the added mass, needed for application.

Demand D1 is common for all regular positioning robots, and is in general the starting point for dimensioning. A difference is that for an interactive rehabilitation robot the demanded positioning bandwidth is relatively low. Demand D2 is essential for any impedance controlled robot, but is not usually emphasized (Robinson 2000). Demand D3 is similar to the impedance- (or Z-) range or Impedance Performance Space (Morrell and Salisbury 1998) as is used as performance metric for kinaesthetic devices. The difference is that here the limits are less critical, as no display of stiff or solid objects is demanded. Demand D4 is especially important in impedance controlled devices, as moving construction mass can only poorly be compensated for.

e. Advantages of compliant actuation in impedance controlled devices with 'high force' demands

As addressed by Robinson (Robinson 2000), commonly used actuators are poor force actuators, even if in many theoretic approaches actuators are supposed to be pure force sources. For small robots common brushless DC motors in combination with cable drives, used in open loop force control usually suffice, as for example used in the WAM-arm (Townsend and Guertin 1999), a haptic device. In general, actuators with high force and high power density typically have high impedance due to necessary power transmission (e.g. geared EM motors) or the nature of the actuator (e.g. hydraulics). These are difficult to use in force control applications.

The solution suggested by Robinson, and several others (Morrell and Salisbury 1998; Robinson 2000; Bicchi, Rizzini et al. 2001; Sugar 2002; Zinn, Roth et al. 2004) is to decouple the dynamics of the actuator and the load, by intentionally placing a compliant element, e.g. a spring, between both. The actuator can then be used in a high gain position control loop, resulting in an accurate control of spring deflection and resulting force, while compensating the internal dynamics of the actuator. The advantage of a compliant element is that it not only filters friction and backlash and other non-idealities in transmission drives from the force output, but also that it absorbs shock loadings from the environment, protecting the transmission.

An alternative way of realizing such a compliant actuator is to use a pneumatic actuator, which is compliant by the nature of air. The most straightforward way is by using a double-acting cylinder, but also an antagonistic pair of fluidic muscles achieves a double acting system (Ferris, Czerniecki et al. 2005) (see also chapter 4 of this thesis). Instead of measuring spring-deflection, pressure measurements can be used as indirect force measurement.

Mechanical compliance in the actuation does not offer its advantages without costs. The lower the stiffness, the lower the frequency with which larger output forces can be modulated. This is caused by saturation effects that limit the maximal achievable acceleration of the motor mass and spring length, or by the limited fluid flows given certain pressures. A limited 'large force bandwidth' decreases in turn the performance in terms of positioning-speed and -accuracy. A careful design and trade-off is needed to suit such actuators for a typical application.

As mentioned by Robinson, it is not yet obvious how to select the proper elastic actua-

tor for a certain application. His general models appeared to be useful for predicting behaviour of a series elastic actuator configuration, but do not clarify what the limitations of several implementations of elastic actuators are. He suggested that important parameters would be the force and power density levels of the specific configuration. To make a proper comparison between series elastic actuators and pneumatic elastic actuators, the latter will have to be described in similar parameters as the first. Once this is achieved the question of the limits and (dis-)advantages of both types of elastic actuation can be addressed.

2. Methods

a. Approach of the compliant actuator modelling and comparison

Both the Series Elastic Actuator (SEA) and the Pneumatic Cylinder Actuator (PCA) will be presented as specific implementations of a general model of a compliant actuator, using only basic system parameters that can be known on beforehand. The outcomes of these models will be compared with measurements, so as to draw conclusions on the predictive value of the models. In the models and measurements the main emphasis is to understand and predict the performance of the force control as stated in demand D2 and D3. To describe the performance on both demands first the force tracking is considered. This will be described by the transfer function $H_{force}(\omega)$, which describes the transfer from the reference force $F_{ref}(\omega)$ to $F_{act}(\omega)$ for a fixed load, that is a load with infinite impedance $Z_{load}(\omega)=\infty$. This transfer corresponds with demand D2. It will depend on signal amplitude in case of non-linearities such as saturation. $H_{force}(\omega)$ is defined as:
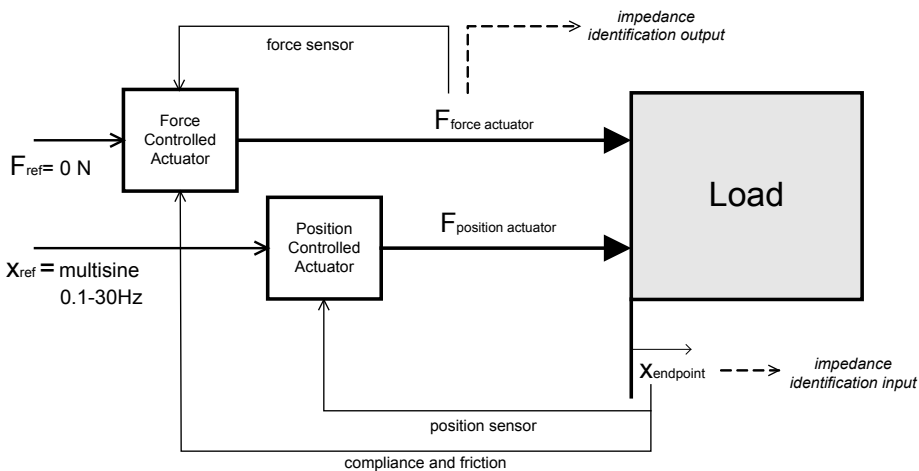

Figure 3.5: Schematic representation of the impedance identification set-up. The force control loop contains the assessed actuator, the force control loop and a position feedback by its intrinsic compliance and friction. The position controller imposes the position perturbations for identification on the output axis of the force actuator (which is also 'the load').

$$H_{\text{force}}(\omega) = \left. \frac{F_{\text{act}}(\omega)}{F_{\text{ref}}(\omega)} \right|_{Z_{\text{load}}(\omega) = \infty} \qquad (3.1)$$

Measurements for determining the force transfer in standstill were carried out on a test set-up (Figure 3.5). The actuator was fixed in a frame, so that the output axis could not move. The output force was measured using a strain gauge based force sensor (ATI-Mini45-SI-580-20). Force tracking transfer functions were identified using a crest-optimized multisine signal, with a frequency content between 0.1 and 30 Hz (or lower in case of saturation problems).

Secondly, the endpoint impedance transfer $Z_{\text{endpoint}}(\omega)$ is considered, which describes the transfer from the endpoint position (-disturbance) $x_{\text{enpoint}}(\omega)$ to the force output $F_{\text{act}}(\omega)$. The impedance can be considered in both the controlled and uncontrolled situation. The impedance in the uncontrolled situation will be referred to as the *intrinsic* impedance of the actuator. These transfers correspond with demand D3. The endpoint impedance is defined as:

$$Z_{\text{endpoint}}(\omega) = \frac{F_{\text{act}}(\omega)}{x_{\text{endpoint}}(\omega)} \qquad (3.2)$$

For determining impedance from measurements, a second (relatively high power) actuator was used to impose position perturbations. Measured position and interaction force between force actuator and perturbed load were used as input and output to identify the impedance transfer. In case of the controlled impedance measurements the feedback control of the test-actuators was done via their internal force measuring principle (spring length or pressure), not via the added force sensor. Impedance transfer functions were identified using a crest-optimized multisine signal, with a frequency content between 0.1 and 10 Hz (or lower in case of saturation problems). Coherence was calculated to check the validity of the identifications and the linearity of the impedance.

Thirdly, the time domain representation of the force response to small motions is also considered. This yields information about the non-linear components of the response, which will be predominantly caused by the output friction of the system.

Finally, based on measurements as well as model-calculations, a discussion will be started on the choice between both actuation types in our specific neuro-rehabilitation robot application.
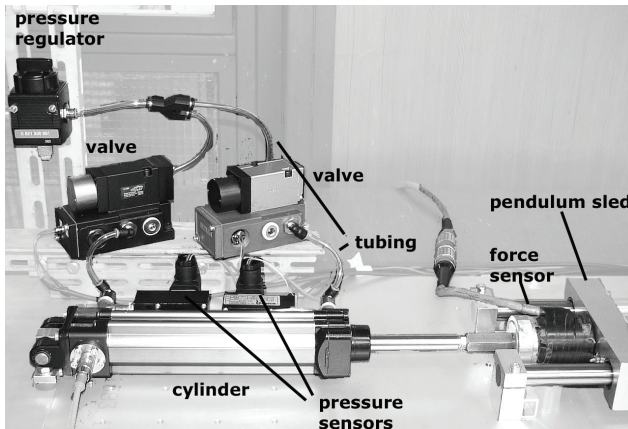

Figure 3.6: Overview of the pneumatic cylinder actuator in the measurement setup.
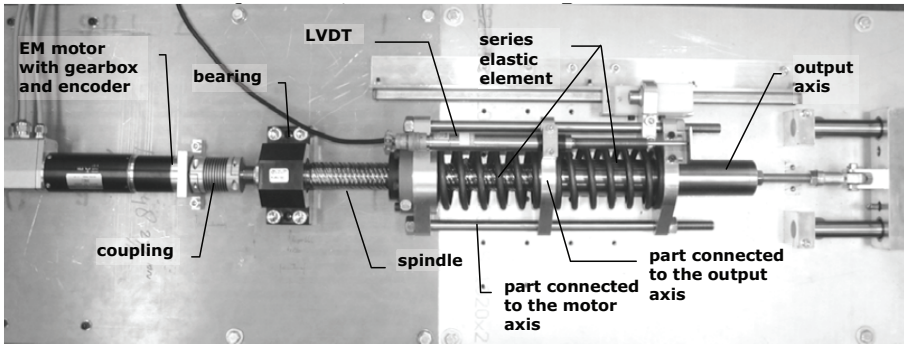
Figure 3.7: overview of the Series Elastic Actuator in the measurement setup.

b. Specifications of the compared actuators

The actuators were designed to meet the demands of actuating the sagittal rotation of the hip of the described gait rehabilitation robot. Sagittal axes are the axes perpendicular to the direction of walking. The parameters mentioned in table 3.1 were used as starting-point.

The nominal values of torque, speed and power were derived from data of healthy human walking (Winter 1990); those are the values appearing in human joints at a normal walking speed. In a rehabilitation setting walking will be slower and supportive corrections may have to be added, so that exact demands may differ from common walking. Furthermore the leg is modeled as a simple pendulum. In addition a pendulum with the same weight and inertia properties was built to evaluate the actuators' performance in the working range. The transmission arm was chosen to be 0.1 m, considering limited design space.

Table 3.1: Design values for hip actuator

Maximum nominal hip torque	55	Nm
Max. force with transmission radius 0.1 m	550	N
Maximum nominal hip speed	2.5	Rad/s
Max. speed with transmission radius 0.1 m	0.25	m/s
Maximum nominal hip power	90	Watt
Hip load moment of inertia (stiff leg)	7.5	kgm^2
Hip mass with transmission radius 0.1 m	750	Kg

Based on these demands both a series elastic actuator and a pneumatic actuator system were assembled. All parameters and transfer functions were transformed to the linear motion domain of the actuator. A force control bandwidth of 4 Hz for large forces (up to 550 N) and a bandwidth of 12 Hz for small forces (below 100 N) were used as target values. These values were based on the maximum voluntary human movement and force frequencies and on frequencies appearing in gait analysis. (see also chapter 4 and 5). This resulted in two actuators setups, a linear series elastic actuator (SEA) presented in Figure 3.7 and Table 3.2, and a double acting pneumatic cylinder actuator (PCA) presented in Figure 3.6 and Table 3.3.

Table 3.2: Selected parts of the SEA.

Component	Supplier/brand	Type number	Remarks
EM Motor	Maxon	EC 45/136209	250 Watt
Encoder	Maxon	HP HEDL 9140	500 counts/turn
Gearbox	Maxon	GP 42 C/203115	i =1/12 [rad/rad]
Coupling	Multicomponents	DKN 100/57	"Metal bellow"
Spindle	SKF	SL 32x40	i =40 [mm/omw]
Bearing block	SKF	PLBU 32	
Springs	Tevema	D14390	30.3 kN/m
Sleeve bearings	SKF	PTFE Composite	2 sizes
Position sensor	Macro Sensors	GHSD 750 series	LVDT

Table 3.3: Selected parts of the pneumatic cylinder actuator

| Component	Supplier/brand	Type number	Remarks
Proportional valves	Positionex	SVP 800	
Valve controller cards	Positionex	ASP 100 analogue motion controller	
Cylinder	Bosch Rexroth	Euromec number 168/40/150	Double acting rod cylinder
Position sensor	Bosch Rexroth	B03084	Intergrated in cilinder
Pressure sensors	Bosch Rexroth	0821100079	
Tubing	Internal diam. Ø 3.2mm, tubes were kept as short as possible, parts of app. 10cm		
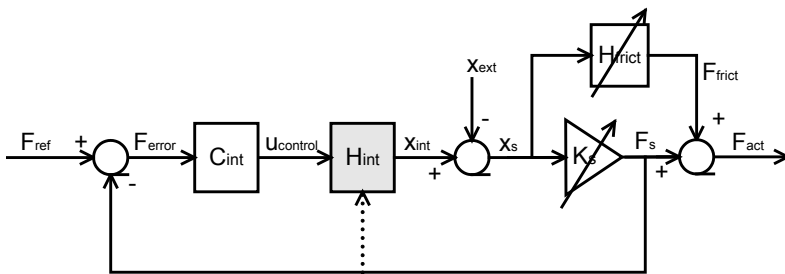
Figure 3.8: General model of a compliant actuator, (fitting in the shaded area of Figure 3.4), consisting of a controlled (with controller C_{int}) *int*ernal position source (H_{int}) a compliant element with (variable) stiffness (K_s) and a (variable) friction model (H_{frict}). These subsystems are possibly nonlinear. The force over the spring element F_s is the actually controlled force, because it is intrinsically measured. In case the real output force F_{act} is measured, this measurement should be used for control, so that also the friction can be compensated. Position variables concerning the elastic element are: x_{int} position of the internal side, x_{ext} position of the external side, x_s length. F_{ref} is the desired reference force, F_{frict} the (external) friction force, whose sign depends on the motion direction.

3. Modeling of the compared actuators

a. General model of a compliant actuator

The first step in comparing compliant actuators is a general model that is detailed and flexible enough to describe the essential behavior of 'any' kind of elastic actuator, in this case both a series elastic actuator based on a brushless DC motor, and a double-acting pneumatic cylinder. The basic element of such an actuator is of course its elastic element or elasticity. Furthermore it should contain an actuator-typical block that describes the part that modulates spring length or force. A last important factor is the friction *after* the elastic element, as this (usually complex) friction can hardly be compensated for by a controller. It appears from the scheme that the actual load influences the force tracking performance, as the external position x_{ext} is an input to the system. With this general model, parts can be modeled as complex as seems necessary, or as complex as availability of system parameters allows for. All parameters should of course be transformed to the output axis domain, to fit in the general model (Figure 3.8). For every kind of compliant actuator the H_{int} forward path (fp) transfer has to be determined. For practical reasons (so that the transfer can be directly measured) the stiffness is included in the measurement. The load impedance is taken infinite (fixed load). The H_{frict} is not included as the linear part of this transfer, the damping, will not be measurable in a practical fixed load test:

$$H_{fp}(\omega, K_s) = \frac{F_{act}}{u_{control}}\bigg|_{Z_{load}=\infty} = H_{int}(\omega)K_s \qquad (3.3)$$

In general the linear force transfer function of this kind of system will be, assumed that the load impedance is infinite (fixed load, x_{ext} constant) and for enhanced clarity neglecting the output friction (which can be considered as a disturbance, mainly depending on the engineering quality of design):

$$H_{force}(\omega, K_s) = \frac{F_{act}}{F_{ref}}\bigg|_{Z_{load}=\infty} = \frac{C_{int}H_{int}(\omega)K_s}{1 + C_{int}H_{int}(\omega)K_s} \qquad (3.4)$$

notice that in general, depending on the actuator, a direct feedback of the spring force into the H_{int} can appear, somewhat complicating this transfer.

The controlled output impedance of this actuator is:

$$Z(\omega, K_s) = \frac{F_{act}}{x_{endpoint}} = \frac{-K_s}{1 + K_s C_{int}H_{int}(\omega)} \qquad (3.5)$$

This already shows that, if the $C_{int}\cdot H_{int}$-gain falls off at higher frequencies, the impedance will become equal to $-K_s$ at those frequencies. It also shows that the output impedance (only) at lower frequencies can be modulated, as the actuator controller C_{int} appears in the impedance transfer function.

H_{int} and H_{frict} will in general not be linear. Saturation effects play an important role in determining the behaviour of elastic actuators. This means that for a prediction of actual performance in a certain operation area, H_{int} should necessarily be accompanied by information on saturation limitations.
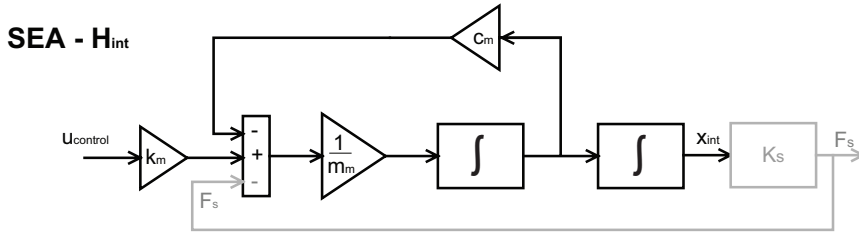
Figure 3.9: H_{int} (see Figure 3.8) for the Series Elastic Actuator, with added K_s. Model of a DC-motor as torque source, including motor inertia and damping. k_m is the motor constant, m_m is the motor inertia, c_m the motor damping, including friction components and back-emf of the motor.

b. Specific model of the Series Elastic Actuator

To fit a series elastic actuator into the model, the appropriate H_{int} and H_{frict} have to be obtained. H_{int} mainly depends on the dynamics of the motor used to drive the actuator, and can be calculated, in case of a brushless DC – driven SEA, with a basic linear motor model, shown in figure 3.9. This model neglects all non-linearities, but this is less important as these will be largely compensated by the feedback spring length control loop. This does not apply for saturation which will be considered separately. Saturation is an actuator inherent limitation that can not be compensated for. The K_s will simply be the physical spring-stiffness. This way all parameters in the H_{int} transfer can be obtained from motor data. For the damping only the back-emf component will be known on beforehand; the damping component of system friction will have to be estimated. During measurements (see results section) a relative damping ratio of about $\zeta \approx 0.5$, slightly underdamped, appeared to be a reasonable first estimate for design purposes. The output friction H_{frict} is difficult to obtain during the design phase. For now it will be neglected in the basic model as it typically is small for a well designed series elastic actuator.

The shown model yields:

$$H_{fp} = \frac{F_s}{u_{control}} = H_{int} \cdot K_s = \frac{k_m K_s}{m_m (j\omega)^2 + c_m j\omega} \tag{3.6}$$

In case of a measurement the feedback loop from F_s would always be included, so this transfer then would be, with no friction model assumed:

$$H_{fp} = \frac{k_m K_s}{m_m (j\omega)^2 + c_m j\omega + K_s} \tag{3.6a}$$

The force tracking (3.7) and impedance (3.8) transfers become:

$$H_{force}(\omega) = \left.\frac{F_{act}}{F_{ref}}\right|_{Z_{load} = \infty} = \frac{C_{int}}{\left(\dfrac{m_m}{k_m K_s}\right)(j\omega)^2 + \left(\dfrac{c_m}{k_m K_s}\right) j\omega + \left(\dfrac{1}{k_m}\right) + C_{int}} \tag{3.7}$$

$$Z(\omega) = \frac{F_{act}}{x_{ext}} = -\frac{m_m (j\omega)^2 + c_m j\omega}{\left(\dfrac{m_m}{K_s}\right)(j\omega)^2 + \left(\dfrac{c_m}{K_s}\right) j\omega + 1 + k_m C_{int}} \tag{3.8}$$
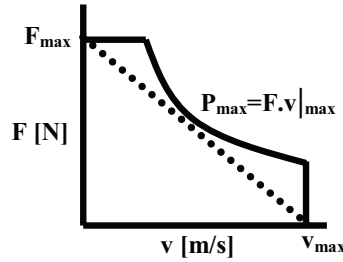
Figure 3.10: Typical saturation characteristic of a brushless DC motor. The solid line is the realistic saturation as usually given in motor specifications; the dotted line is a conservative estimation that suffices in modeling. Limitations are a force (F, or torque) limitation, a power (P) limitation and a velocity (v) limitation. For a series elastic actuator is also possible that these limitations are imposed by other elements in the system: for example a maximum allowable spindle torque or velocity.

Notice that in case of this Series Elastic Actuator the direct feedback of the spring force into the motor is present, shown by the F_s input in Figure 3.9. The basic behaviour is therefore that of a damped second order system.

These transfers would apply for the full range if the actuator was linear. As noted before, saturation will in practise determine much of the behaviour of an elastic actuator in its working range. The saturations to be considered in case of a common DC-motor are in general a velocity limitation, a torque limitation and a power (velocity·torque) limitation; schematically shown for the linear domain in figure 3.10.

These all limit the gain of the internal position controller ($C_{int}H_{int}$). It is also possible to use a conservative simpler model, such as the dotted line of Figure 3.10 (as was done by Richardson, allowing a symbolic expression of expected performance). The data for such a saturation characteristic can also be obtained from the motor data sheet, and can easily be implemented in a model by saturation functions (3.9):

$$d_{linear} \leq d_{saturation} \implies d_{non\text{-}linear} = d_{linear}$$
$$d_{linear} > d_{saturation} \implies d_{non\text{-}linear} = d_{saturation} \quad \text{for any saturated variable d.}$$

(3.9)

c. Specific model of the Pneumatic Cylinder Actuator

For a pneumatic cylinder actuator the story is more complex, because of the fundamental strong nonlinearity of this class of actuators. In a system containing proportional valves, the control input is the valve current, which controls the valve flow area, which depending on actual up- and downstream pressures causes a certain fluid flow (Figure 3.11). The flows determine the pressure changes in the two separate actuator chambers. The pressure
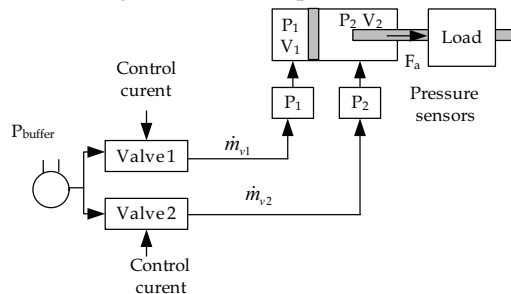

Figure 3.11: general outline of the components of a typical pneumatic cylinder actuator.
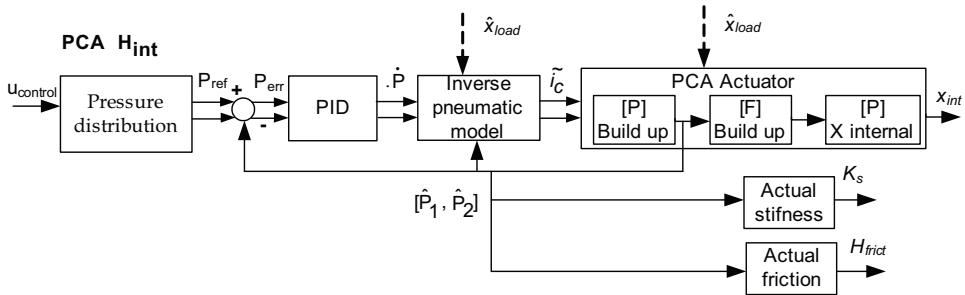
Figure 3.12: H_{int} (see Figure 3.8) for the Pneumatic Cylinder Actuator. The force is indirectly controlled by controlling the actuator pressures corresponding to a control command. The double connecting lines are drawn to show that the system contains two valves to control the air supply to both cylinder chambers independently. The actuator is divided into a pressure build-up part, a force build-up part and a internal x reconstruction part, to clarify the outline of the used model. Symbols indicated with ^ are measured input parameters used in the inverse model. $\tilde{i}_c$ indicates the two valve control currents.

levels and difference together determine force output and stiffness of the cylinder. This results in a relation between the valve current and the chamber pressures that is neither linear nor globally linearisable over the full range of operation.

When a proper model of the actuator system is available, it is possible to add non-linear blocks that mathematically invert the non-linearities of the pneumatic plant, resulting in an approximately linear system (Richer and Hurmuzlu 2000; Richer and Hurmuzlu 2000; Xiang and Wikander 2004), that is a system consisting of actual parts of the plant in combination with their approximate mathematical inverts (Figure 3.12).

These inverts are also non-linear, and typically contain variables like actual pressure and piston position, which therefore need to be measured real-time. After such a linearization, which is a special case of feedback linearization (Slotine and Li 1991), a common linear controller, like a PID, can be used for pressure control. This way the pressure levels can be controlled independently, controlling both the force output and the cylinder stiffness. We used the model descriptions of (Richer and Hurmuzlu 2000), concerning valves, tubing and cylinder chambers, and combined them with an implementation of the block oriented linearization technique as described by (Xiang and Wikander 2004), as he reported best results using pneumatics known to us. This control outline is more detail discussed in the appendix to this chapter. It results in an approximately overall linear plant, outside saturation limits. More details on the model can be found in the appendix at the end of this chapter.

To fit this into the general model the actual stiffness K_s has to be ob-
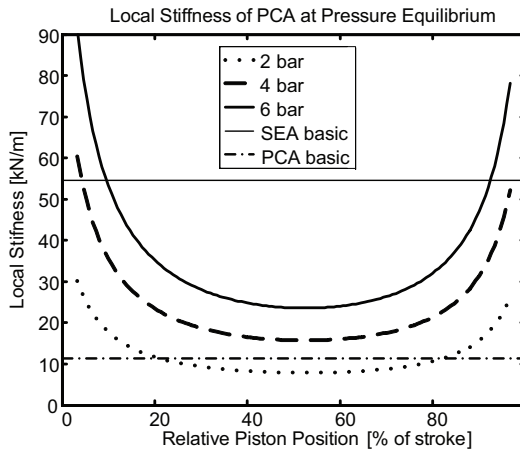

Figure 3.13: Characterisation of stiffness dependency in a pneumatic cylinder, considering the parameters position and equilibrium pressure. The stiffness that is defined to be the 'basic stiffness' is indicated.

tained. It can be estimated with the following equation that depends on several parameters, viz.: the absolute pressures of both cylinder chambers P_1 and P_2, the actual volume of both chambers, as defined by the rest volumes $V_{0,1}$, $V_{0,2}$ and the actual chamber lengths xload (chamber one) and lcyl-xload (chamber two), multiplied with their respective cross sectional areas A_1 and A_2, and the ratio of specific heats, γ.

$$
K_s(P_1, P_2, x_{\text{endpoint}})\Big|_{\gamma, V_{0,1}, V_{0,2}, A_q, A_2, l_{\text{cyl}}} \approx \frac{P_1 \gamma \, A_1^2}{V_1} + \frac{P_2 \gamma \, A_2^2}{V_2} =
$$

$$
\frac{P_1 \gamma \, A_1^2}{V_{0,1} + x_{\text{endpoint}} \cdot A_1} + \frac{P_2 \gamma \, A_2^2}{V_{0,2} + \left(l_{\text{cyl}} - x_{\text{endpoint}}\right) \cdot A_2}
$$

(3.10)

where: $0 < x_{\text{external}} < l_{\text{cyl}}$.

The approximation neglects higher order terms of the Taylor series expansion and the higher order terms in xload, and gives the local linearised semi-static stiffness around the used parameters. It considers the stiffness response an adiabatic process; this also assumes that no air is supplied or exhausted during the relatively fast stiffness response.

For a given cylinder only the pressures (P_1 and P_2) and the piston position (xload) vary. In figure 3.13 this local stiffness is shown as a function of the piston position at several pressure levels; pressure in both chambers is taken equal. In general the equilibrium pressure will be chosen about halfway between buffer and ambient pressure for optimal pressure control bandwidth. Therefore the stiffness at this pressure in middle position can well be defined as 'basic stiffness' of a pneumatic cylinder (dash dotted line).

If this local stiffness is used to define the actual K_s, the actual 'deflection' of this pneumatic spring can be defined as:

$$
x_{\text{int}} = \frac{F_{\text{act}} - F_{\text{frict}}}{K_s} - x_{\text{endpoint}}
$$

(3.11)

The pneumatic system now fits in the general model. And as the system gain of Hint falls off at higher frequencies, also here the impedance will converge to the actual K_s, following equation (3.10).

The transfer functions are hard if not impossible to derive symbolically, but can be described by determining the multisine responses of the system, when it is linearised as described before. Because the block inverts are never exact, in reality open loop responses of the whole system will be hard to obtain, as pressures quickly drift away towards saturation values, e.g. maximal or minimal pressure. Therefore in this case the closed loop pressure transfers per chamber will be shown which underlie the force control loop. These loops contain the model based inverts and should be ideally have a transfer function of 1. This will however only be the case for low frequencies, because of saturation and remaining dynamics in the linearized system.

As the pneumatic system has two inputs, an assumption should be made about the values of both inputs compared to the force controller output. The straightforward assumption would be a symmetrical control, for example (scaled with the difference in cross sectional area):

$$
\frac{\dot{P}_1}{A_1} = -\frac{\dot{P}_2}{A_2} = u_{\text{control}}
$$

(3.12)

To prevent drift of the chamber pressures, it appeared to be better to actually feedback
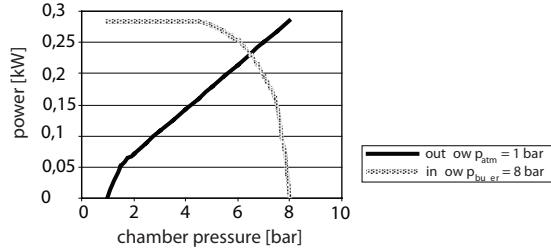
Figure 3.14: Characteristic saturation profile: maximum available power for the mid position of the piston. The actual total maximum power depends on the two actual pressures in both chambers, and is the addition of the both corresponding values in the graph. Also the P_{atm}, the atmospheric pressure end the P_{buffer}, the buffer pressure determine the available power.

control the chamber pressures based on (3.12), by calculating the desired pressures based on the desired $\dot{P}'s$.

For other possibilities for determining reference pressures or pressure change rates, see (Xiang and Wikander 2004).Given such an assumption the transfer functions are defined. Saturation in case of pneumatics is complex, but already incorporated in the non-linear model, because all flow restrictions are part of the fluid flow equations. The force is limited by the maximal force difference between buffer and ambient pressure. The power limit is defined by the expressions for the actual mass flows in the system (figure 3.14). The mass flows are limited by flow areas (valves, connectors) and pressure differences in the system.

Piston friction is a important issue in pneumatics research because it is relatively large, and varying with several parameters, such as position, speed, pressures, temperature and time. It is hard to predict, especially when not all these constituting parameters are measured.

4. Results

The results section contains all measurements and model calculations, needed to check the model validity and to show the performance of both actuation types. The results are presented per actuator.

a. Series Elastic Actuator (SEA)

The validity of the SEA model is checked by comparing the open loop transfer from $u_{control}$ to F_{act} of the actual plant with the model calculation. This is done for small amplitudes to avoid saturation effects. It appears that the basic eigenfrequency of the system agrees well with the model value (figure 3.15), but that damping was quite underestimated. This is due the friction of both spindle and gearbox, which were not known from specifications and therefore not modelled. A relative damping ratio $\zeta \approx 0.5$, that is a slightly underdamped system, appeared a reasonable estimate, and might be generally useable as first estimate for design purposes. For further modelling this assumption for the SEA is used.

Closed loop force tracking
The closed loop force tracking depends on both the system transfer and on the imple-
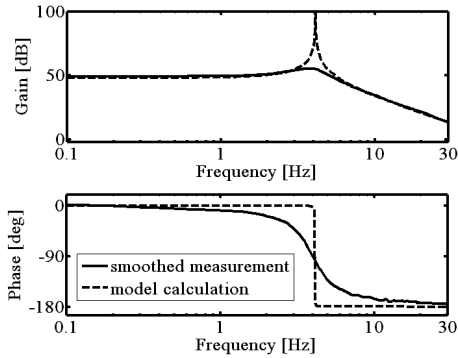
Figure 3.15: SEA – Bode-plots of both the modelled and the measured transfer from $u_{control}$ to F_{act}, in case of a fixed load. The modelled transfer is calculated from known parameters. The measured (estimated) transfer was smoothed by averaging.
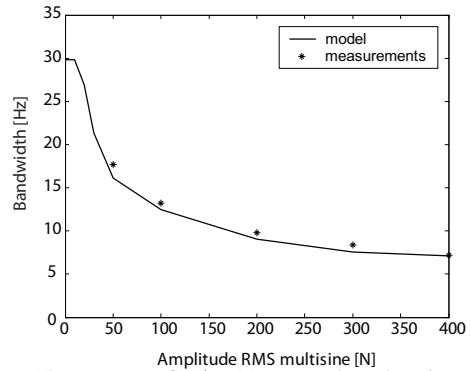

Figure 3.16: SEA – Force tracking bandwidth as function of reference RMS amplitude.

mented controller. In this case a straightforward PID controller tuned with the Ziegler-Nichols method has been implemented.

As saturation plays a role already at very small RMS amplitudes of force, the actual force tracking is compared to force tracking in the model that included the saturation characteristics. The transfer function of the non-linear model is then determined in the same way as in the measurements. The amplitude size is given as RMS value of the multisine reference input. Figure 3.16 shows a good agreement between model and measurements. It also shows that the bandwidth demands, 12 Hz for small forces (below 100 N) and 4 Hz for large forces, are met.

Endpoint impedance

First the intrinsic (uncontrolled) endpoint impedance is described. In case of the SEA there is a difference between smaller and larger amplitude motions. For small amplitudes the spring unit moves, while the motor/spindle unit does not move due its static friction. If this friction limit is just being passed the force response to movements will become very non-linear. The small motion impedance stays below this friction limit. This means that theoretically only K_s and H_{frict} would appear in this transfer. As H_{frict} was not modelled the modelled impedance is simply the spring stiffness response:

$$K_s = 54.54 \cdot 10^3 N / m = 94.7 dB$$

In figure 3.17 this stiffness response and the actually measured small motion impedance are shown. The H_{frict} and especially its non-linear character is best characterized by a time domain plot of the force response to a position sine-
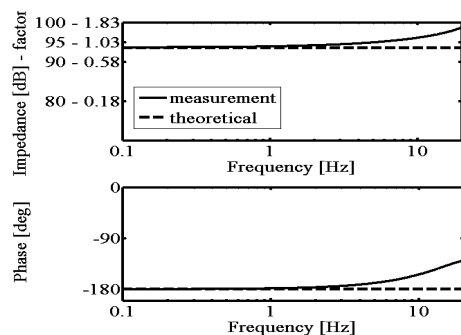

Figure 3.17: SEA – Intrinsic (uncontrolled) impedance response of the SEA. Bode plot of the force response to a small amplitude motion multsine 0.1-20Hz. The dotted line is the pure spring response of the model. The gain is given both in decibels and in factor relative to the basic stiffness.
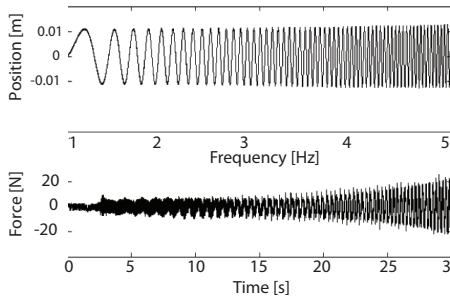
Figure 3.18: SEA – Time domain representation of the force response to externally imposed sine sweep motion profile, ranging from 1 to 5 Hz.
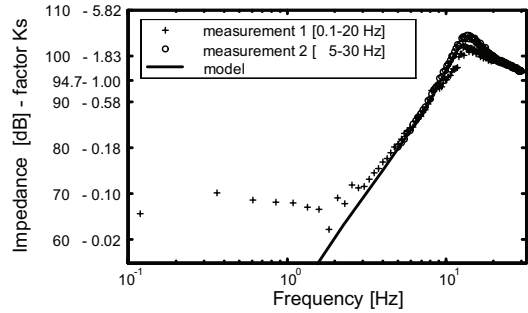

Figure 3.19: SEA – gain of the controlled impedance transfer. For high frequencies the impedance becomes the stiffness of the springs, which is the intrinsic impedance. For low frequencies the model underestimates the impedance/stiffness. This is caused by the coulomb friction component that gives the force response a lower limit. The impedance [N/m] is given in dB and as a factor on the intrinsic stiffness K_s.

sweep. A signal with frequency increasing from 1 to 5 Hz was used. The position signal and the force response are shown in figure 3.18. For motions up to about 3 Hz the force level is about constant, indicating a coulomb friction component. With higher frequencies forces increase, indicating a viscous component. Also slight peaks are visible at reverse of motion, which indicate a slight stiction component.

Controlled impedance

The controlled impedance depends on both system and controller. Here an example is given (using the same controller with reference value F= 0 N), to demonstrate some typical properties (figure 3.19). In general the measurements were well predicted, except for low frequencies. Where the model predicts a further decrease in impedance, the measurement indicates a lower boundary at about 5500 N/m. Further measurements showed that this was actually a lower boundary on the force output, which is caused by the coulomb friction component. Combined with certain motion amplitude, this results in the measured impedance boundary. For high frequencies the impedance approaches the intrinsic value, which is the spring stiffness.

b. Pneumatic Cylinder Actuator (PCA)

For pneumatics the open loop measurement should also be from the control command to the force output. The force output, however, quickly drifts away and saturates, because the model based compensators in the controller are no exact inverts. The mentioned open loop transfer can therefore not be measured. Instead closed loop pressure control transfers are shown. These transfer functions determine what can be achieved in force control. The pressure control transfer depends on the actual chamber volume, on the equilibrium pressure around which the pressure is controlled, and on the reference amplitude. Because of the incorporated feedback loop these transfers do not drift. Original model predictions of these transfers appeared to all overestimate the bandwidth. This was solved by adding additional flow restriction factors, which compensated for non-modelled flow restrictions
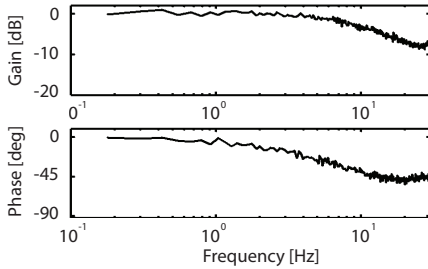
Figure 3.20: PCA – Measured pressure tracking of the controlled PCA for a multisine with RMS amplitude of 1 bar around an equilibrium pressure of 3 bar.
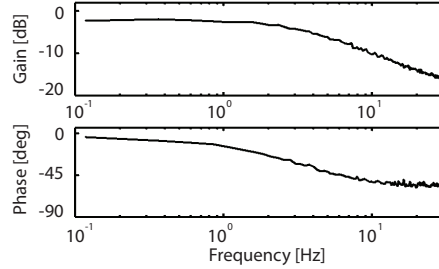
Figure 3.21: PCA – Measured pressure tracking of the controlled PCA for a multisine with RMS amplitude of 2 bar around an equilibrium pressure of 4 bar.

such as outlet dampers, connectors, etc. This way model and measurement behaviour could be matched (i.e. only based on measurements). This obtained 'extended' model was then used for all further modelling.

Figures 3.20 and 3.21 show that using small changes around an equilibrium pressure (chosen in between atmospheric and buffer pressures) achieves a bandwidth of about 10 Hz. If equilibrium pressure and/or amplitude change so that one of these boundaries is approached, pressure control worsens. Realizing a pressure near to a boundary pressure is inevitably slow. This is also the underlying cause for the saturation effects. The overall effect of saturation is shown in figure 3.22, presented as a force bandwidth in case of specific RMS values of the reference input.

It appears that for low forces behaviour is predicted poorly. This is probably due to the heavy influence of friction forces that were only basically modelled. Another possibility is that the pressure measurement is not accurate enough. For larger amplitudes the model appears to give at least a good indication of what the system can achieve.

The force response to a position sine sweep is shown in figure 3.23. For motions up to about 5 Hz the force level is about constant indicating a coulomb friction component. The
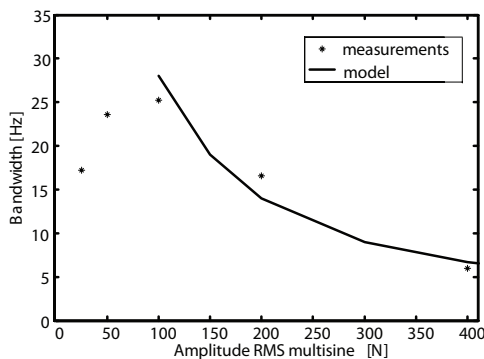
Figure 3.22: PCA – Force tracking bandwidth as function of reference RMS amplitude.
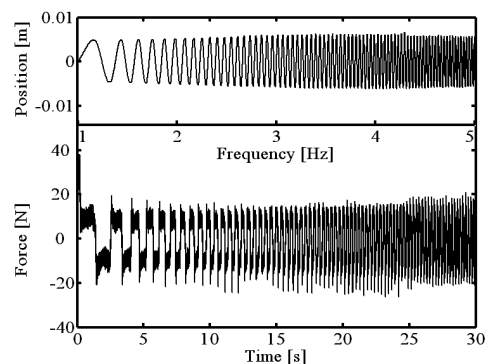
Figure 3.23: PCA – Time domain representation of the force response to externally imposed sine sweep motion profile, ranging from 1 to 5 Hz.
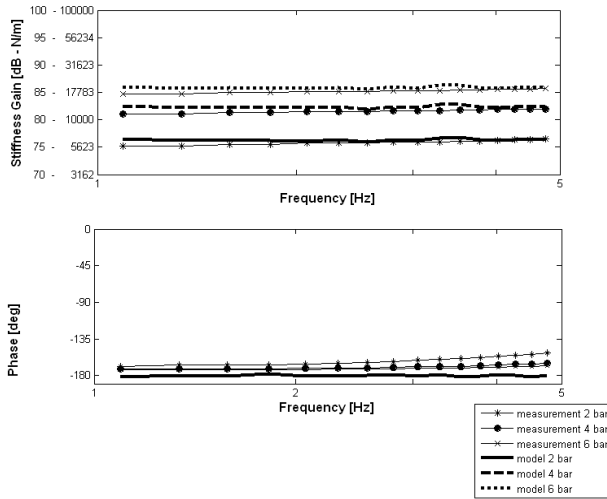
Figure 3.24: PCA – impedance transfer of pneumatic cylinder without controller for several equilibrium pressures. Bode plot of force response to a multisine motion profile 1-5Hz.

force peaks that are visible at reverse of motion indicate stiction, the largest peak is visible at the start of the measurement. Different from the SEA a viscous component is hardly visible at these frequencies, indicating that friction in case of pneumatics is mainly non-linear.

Endpoint impedance

For the pneumatic cylinder larger motion amplitudes had to be used compared to the SEA, as the H_{frict} contains considerable static and non-linear friction. Small motion amplitude measurements would reflect mainly the non-linear friction behaviour (see figure
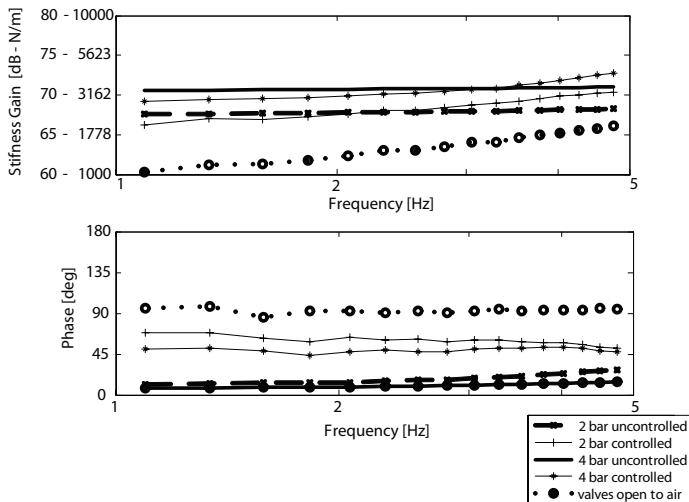
Figure 3.25: PCA – Measurement of controlled impedance of the pneumatic cylinder. Bode plot of the force response to a 1-5Hz multisine motion profile. For comparison the uncontrolled values are added, together with the case in which both valves are switched open to open air.

3.24), and would not be presentable as linear bode plot. This implied that due to limited power of the motor providing position disturbance, impedance measurements had to be limited to lower frequencies only.

Measurements have been carried out at several cylinder pressures, with both chambers of equal pressure. Model predicted values are also given. To show the limits of impedance reduction in the pneumatic cylinder, some controlled (with reference F= 0 N) impedance responses are shown (figure 3.25). It appears that the impedance is hardly reducible compared to uncontrolled situation. The impedance response in case both cylinder chambers are open to the ambient is also shown. This impedance is caused by the friction of the system, together with the resistance to airflow of the air in-/out-lets.

Without any additional force measurement it therefore also indicates the minimally controllable impedance.

5. DISCUSSION

a. Modelling both SEA and PCA as elastic actuators

It was possible to model a series elastic actuator and a pneumatic cylinder actuator within one general framework of compliant actuation. This general model, as presented in Figure 3.8, clearly shows the effect of the intrinsic stiffness (K_s) and controller design on the force tracking bandwidth, and on the controlled and uncontrolled mechanical output impedance. For the comparison of compliant actuators the intrinsic stiffness (K_s) of each specific actuator has to be defined, representing the average stiffness of the actuator during operation. In case of the SEA K_s is the stiffness of the elastic element. In case of the PCA K_s was defined as the stiffness of the cylinder around its equilibrium position, at the pressure halfway in between ambient and buffer pressure, which will be about the average stiffness during operation. We found that saturation behaviour and output friction are very important in modelling elastic actuators as they greatly affect performance.

b. Similarities and differences between SEA and PCA

Depending on its dimensions a PCA can be considered as a realisation of a 'compliant actuator'. Since PCA needs feedback linearization to be controlled properly, it appeared that it was much harder to predict and control a PCA than a SEA. The feedback linearization needs a precise actuator model, which in general will not be available beforehand. Important parameters, temperatures, actual buffer pressure et cetera, were left out of the modelling and will demand extra sensors if actual temperatures and the buffer pressure will be included in the feedback linearization. The PCA saturation behaviour was more complex than for the SEA.

Therefore the design of a PCA demanded much more fine-tuning. The design and prediction of the performance of the SEA can be based on available data-sheet parameters.

The typical spring stiffness of a linear SEA with continuous force output of 500 – 1000N appeared to be limited to the range of 50-300 kN/m, resulting in a large force bandwidth of 4-10 Hz. The stiffness of the elastic element in our design was 54.5 kN/m. In a PCA the intrinsic stiffness is not constant; the range is defined by cylinder dimen-

sions and the actual pressures and stroke position. The range of intrinsic stiffness of the selected cylinder during operation lies in between about 6 and 40 kN/m, depending on the feasible working range (Figure 3.12). The effective stiffness as defined before is 11.3 kN/m. The effective stiffness of a PCA is on average roughly 20% of the designed linear SEA. Choosing the same low stiffness for the elastic element in a SEA would affect the large force bandwidth too much. The minimal stiffness/impedance of a SEA in the controlled situation is typically lower than the achievable stiffness/impedance of a PCA. When a PCA is controlled based on pressure measurements its minimal impedance is determined by both the piston friction and the airflow resistance of the air in- and outlets. These properties depend on the cylinder and might be improvable by redesign, but can hardly be compensated by controller design. In the PCA, flow restrictions (relative small flow areas in cylinder, tubes) appeared to hinder a low-impedance control, i.e. the outflow of the cylinder was mainly determined by these restrictions and not by valve control limitations. It may be possible to re-design a PCA for to minimize the mechanical output impedance. This might however affect system safety, as these small outlets serve as speed limiters. Since the friction is difficult to predict proper impedance control can only be achieved by adding a force sensor to the PCA. Another option would be designing pneumatic cylinders with a very low friction, for example by reducing the sealing and accepting a leak flow between cylinder chambers. Low friction cylinders based on glass are commercially available in small size pneumatics, but to our knowledge not in the sizes needed for gait rehabilitation. Both the SEA and PCA can be designed to achieve a comparable force tracking bandwidth for 'midrange' force amplitudes. For smaller amplitudes the SEA outperforms the PCA in the achievable bandwidth and in accuracy, mainly due the smaller output friction. The force bandwidth for low amplitudes for the SEA was 30Hz and for the PCA about 25Hz. However, the SEA force bandwidth decreased faster with increasing amplitude (compare Figure 3.8 and 3.9). Both actuators appeared to be impact proof due their intrinsic compliant behaviour at higher frequencies. The SEA appeared to be easier and better controllable in an impedance range at low frequencies, due less output friction, and due a more accurate force measuring.

6. Conclusions

The designed SEA was slightly superior to the PCA for the described application in a gait rehabilitation robot, based on performance metrics. Other disadvantages of the PCA are the typical noise, dependency on pressurized air facilities and the complexity of the needed controller, which affects the robustness of the system. The SEA and PCA we evaluated were dimensioned to actuate a gait rehabilitation robot. From the evaluation of both types of actuators it can be concluded that both can be designed to meet power and bandwidth requirements, resulting in actuators of comparable weight and size. However, due the high weight neither one system can be considered truly optimal for use in exoskeleton-type rehabilitation robot. The principles however seem well applicable. To minimize the weight we designed and evaluated a pneumatic muscle based system (chapter 4) and a new Bowden-cable-based series elastic actuation system (see chapter 5), two more exotic types of compliant actuators that add less mass to the moving robot parts.

Appendix: Control of the pneumatic cylinder actuator.

In industry pneumatic cylinders are often applied in so called bang-bang control, applying only a (two-chamber) pressure increase or decrease switching. The natural compliance of air assures stability in contact or impact situations. The only sensors are usually switches to detect end-positions. The use of either position- or force-servo control of cylinders is however increasing. For haptic applications a good force control is explicitly necessary, but also a position control loop can be optimized using a force control inner loop.

Force control in pneumatics can be achieved by applying an external force sensor or through pressure control in combination with a model describing the relationship between the pressures within the actuator and the force output. Pressure control has been implemented in several ways. The most straightforward way is by applying common linear control techniques based on a linearized model around a working point of the plant. The quality of these controllers suffices around the set point, but no guarantees can be given for behaviour or stability of the system for larger working ranges.

Xiang and Wikander (Xiang and Wikander 2004) used a block-oriented approximate feedback linearization for control of a pneumatic cylinder. The physical system was divided in separate blocks; valves, cylinders and tubing. These blocks were then modelled and these models were (dynamically) inverted applying several realtime measurements, so that non-linearities and partly the dynamics of the blocks could be approximately cancelled out. This way the total system was approximately linearised and could be controlled with a straightforward linear controller. The advantage of this method is that it is valid for a large working range. The stability of the controller was also theoretically demonstrated.

We approached the servo-control problem of a double working cylinder from an engineering viewpoint, applying and combining the control approach of Xiang and Wilander (Xiang and Wikander 2004) with the pneumatic plant modelling of Hurmuzlu and Richer (Richer and Hurmuzlu 2000). We were not in the first place interested in developing new controllers or theoretically proving optimality and stability of used controllers, but in determining what would be the limit of performance, using components on the scale that would be needed for gait rehabilitation, for comparison with other actuation principles. In this appendix the pneumatic set-up, the used controller and the model on which it is based, will be described.

a. Model of the PCA

The used set-up is shown in figures 3A.1 and 3A.2. It consists of a double working pneumatic cylinder, two proportional 5/3 valves, connecting tubing, a pressure sensor for each cylinder chamber and a piston position sensor. A force sensor is used to monitor the exerted actuator force. The used parts with their manufacturer and part number are summarised in table 3A.1. This plant was modelled by dividing it into several blocks. The components of this model are shown in Figure 3A.3.
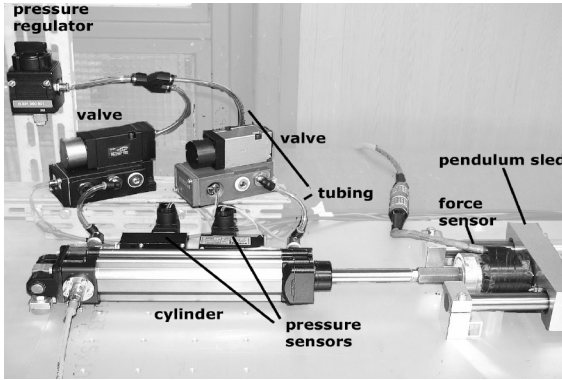
Figure 3A.1: Experimental test-set up for cylinder experiments.

Figure 3A.2: General lay-out of the cylinder set-up. The black lines represent the tubing connecting the different components. A control current determines the valve opening. The valve can either be connected to the buffer (P_{buffer}) or the ambient air. A mass flow ($\dot{m}_{vi}$) is invoked into the actuator volumes (V_i) (through the connecting tubing) due to pressure differences between the actuator volume pressure (P_i) and the pressure supplied to the valves. The pressure build-up inside the actuator volumes results into an actuator force (F_a), which acts on the attached load.
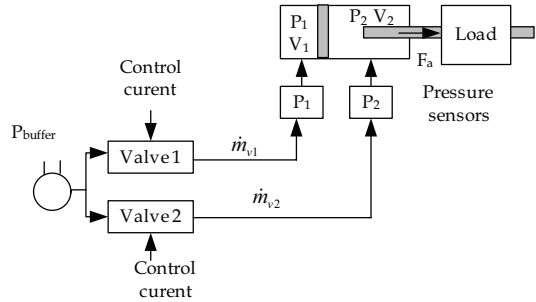
Table 3A.1: Cylinder set-up components

Component	#	Manufacturer	Part number
Proportional valve	2	Positionex	SVP 800
Valve controller card	2	Positionex	ASP 100 analogue
Cylinder	1	Bosch Rexroth	Euromec number 168/40/150
Position sensor	1	Bosch Rexroth	B03084
Pressure sensor	2	Bosch Rexroth	0821100079
Current amplifier	1	Home made	–
Force sensor	1	Home made	Stuurman [1991]
Tubing	2	Internal diameter 3.2 mm	Length 10 cm

Force build-up

The actuator force build-up is linearly dependent on the pressures in both cylinder chambers, on external pressure and on piston friction. This leads to the following expression for the force build-up (eq. 3A.1):

$$F_{cyl}(P_i) = P_1 A_1 - P_2 A_2 - P_{amb} A_r \tag{3A.1}$$

P_1 and P_2 are the pressures inside the first and second cylinder chamber and A_1 and A_2 are the cross sectional areas of both chambers. The third term is the force generated by the ambient pressure acting on the cylinder rod. F_f is the piston friction force.

The friction force was simply modelled using the following expression (actual friction
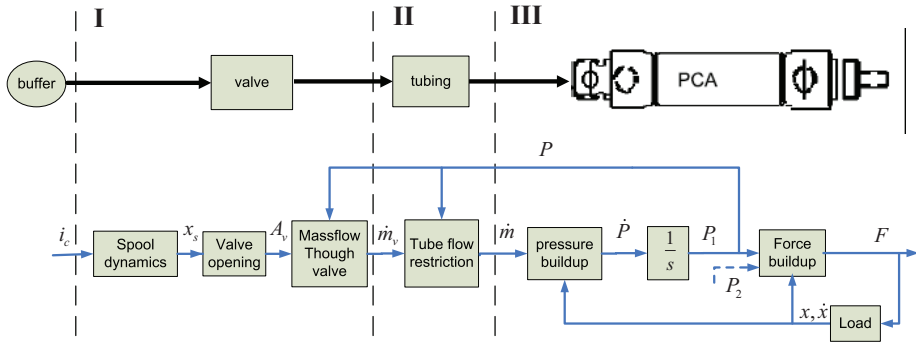
Figure 3A.3: Schematic representation of the total plant and its model from valve input, control current (i_c) to output, force (F). Section I describes the valve mass flow ($\dot{m}_v$) resulting from a control-current (i_c). Section II is the contribution of the tubing, which results into a mass flow into the actuator volume ($\dot{m}$). Finally, section III represents the pressure build-up inside the actuator volume ($\dot{P}$), which is integrated to determine the pressure inside the volume. Pressure in two cylinder (P_1 and P_2) chambers together with a friction model determine the output force (F).

is complexly time and temperature dependent):

$$F_f = \begin{cases} F_{sf} & \text{if } \dot{x}_p = 0 \\ F_{df}.sign(\dot{x}_p) + B_c\dot{x}_p & \text{if } \dot{x}_p \neq 0 \end{cases} \tag{3A.2}$$

where F_{sf} and F_{df} are the static and dynamic Coulomb friction force, B_c the viscous friction coefficient and $\dot{x}_p$ the piston velocity. The empirically determined and used values are shown in table 3A.2.

Table 3A.2: Cylinder friction parameters

Static Coulomb friction	F_{sf}	18.5 N
Dynamic Coulomb friction	F_{df}	13.0 N
Viscous friction	B_c	39 Ns/m

Cylinder chamber

An equation for the pressure build-up inside a cylinder chamber can be derived from the differentiated ideal gas law, assuming constant temperature:

$$\dot{P} = \frac{1}{V_0 + A\left(\frac{1}{2}L_p \pm x_p\right)}\left(RT\dot{m} \pm P\dot{x}_p A\right) \tag{3A.3}$$

V_0 being the rest-volume of the cylinder chamber, L_p the piston length, x_p piston position and A the chamber area, T the temperature and R the gas constant. $\dot{m}$ is the mass flow into the chamber. The + or − signs depends on the direction of the piston motion in the specific cylinder chamber.

Tubing

The tubing between valve and cylinder is modeled as a combined time delay and at-

tenuation:

$$K_t = \begin{cases} 0 & t \leq \tau \\ e^{-\frac{32 \cdot \mu}{D_t^2} \cdot \frac{R \cdot T \cdot L_t}{2 \cdot P_d c}} & t > \tau \end{cases} \quad \text{with a time delay of } \tau = \frac{L_t}{c} \tag{3A.4}$$

Where D_t is the tube diameter, L_t the length of the tube and c the speed of sound in air. The total mass flow through the valve and tubes can then be written as

$$\dot{m} = \dot{m}_v \cdot K_t \tag{3A.5}$$

Where $\dot{m}_v$ is the mass flow through the valve.

Valve

The dominant mass flow restriction is the valve. The mass flow through the valve orifice can be described as:

$$\dot{m} = \begin{cases} A_v C_1 & \frac{P_d}{P_u} \leq c_{cr} \\ A_v C_2 \sqrt{\left(\frac{P_d}{P_u}\right)^2 - \left(\frac{P_d}{P_u}\right)^{\frac{2(k-1)}{k^2}}} & \frac{P_d}{P_u} > c_{cr} \end{cases} \tag{3A.6}$$

$$C_1 = \sqrt{\frac{k}{R}\left(\frac{2}{k+1}\right)^{\frac{k+1}{k-1}}} C_f \frac{P_u}{\sqrt{T}} \quad , \quad c_{cr} = \left(\frac{2}{k+1}\right)^{\frac{k}{k-1}}$$

$$C_2 = \sqrt{\frac{2k}{R(k-1)}} C_f \frac{P_u}{\sqrt{T}} \quad \begin{cases} P_u = P_{buffer} \; ; \; P_d = P \}, \text{if } A_v > 0 \\ \{P_u = P ; P_d = P_{ambient} \}, \text{if } A_v < 0 \end{cases}$$

Where P_u represents the upstream pressure, P_d represents the downstream pressure and P_{buffer} the buffer pressure. While the valve is venting, i.e. A_v is positive, P_u is defined as the chamber pressure and P_d as the ambient pressure. While pressurising the upstream pressure is defined as the buffer pressure and the downstream is the chamber pressure. If the pressure ratio (P_d/P_u) is smaller than the critical flow ratio c_{cr} the flow is 'choked' and dependant only on the upstream pressure, above this ratio the flow is dependant on both up and down stream pressures. The flow coefficient, C_f is empirically determined. The valve opening as function of the spool displacement can be described for the specific type of valve as:

$$A_v = \begin{cases} 0 & |x_s| \leq (p_w - R_h) \\ 2 \cdot n_h \cdot R_h^2 \arctan\left(\sqrt{\frac{R_h - x_t}{R_h + x_t}}\right) - x_t \cdot \sqrt{R_h^2 - x_t^2} & (p_w - R_h) < |x_s| < (p_w + R_h) \\ \pi \cdot n_h \cdot R_h^2 & |x_s| \geq (p_w + R_h) \end{cases} \tag{3A.7a}$$

$$x_t = p_w - x_s \tag{3A.7b}$$

Where R_h is the valve hole radius and n_h is the number of holes in the valve opening, the spool width p_w and the position of the spool x_s. The specified bandwidth of the spool

placement is roughly 100Hz for the valves. This means that for the desired bandwidth of 12 Hz the effects of these dynamics is assumed negligible and has been omitted from the model. p_w Is the spool width. By substituting $x_s = K i_c$ in (7b) we get the relationship between control signal, i_c, and A_v.

b. Inverse model

For control purpose we need to invert the non-linearities as present in the equations 3A.1-7. Measurement of piston position (and velocity) and chamber pressures are used in the linearization. (see figure 3A.4)

Of the described parts an inverse will be determined in order to cancel their non-linear nature. From the inverse of the friction model (2) a reference internal force can be obtained. Symmetry in pressures-change in the chambers, according to $\dfrac{P_1}{A_1} = -\dfrac{P_2}{A_2}$, is used to transform the reference force to a reference pressures. The reference pressures are then controlled in feedback. The details of this pressure feedback control will not be elaborated here.

The desired mass flow is determined based on measurements of the volume and pressure by rewriting (3A.3) as a function of $\dot{m}$. The time delay in (3A.4) has been omitted in the inverse model as this would mean information of future event would be needed. The inverse of (3A.4) now becomes solely a gain factor $1/K_t$. Substituting this in the inverse of (3A.3) the total mass flow becomes:

$$\tilde{\dot{m}}_v = \left[\dot{P}_{ref} \cdot V_{act} + \hat{P} \cdot \dot{V}_{act} \right] \frac{1}{R \cdot T \cdot K_t} \tag{3A.8}$$

The valve opening to achieve this mass flow can be calculated as the inverse of equation (3A.6):
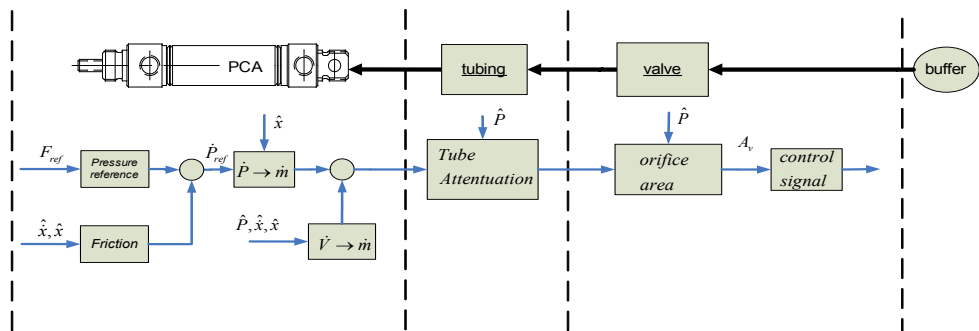
Figure 3A.4: Schematic representation of the invert of the plant presented in figure 3A.3. The symbols indicated with an ^ are real-time measured variables, used in the linearization.
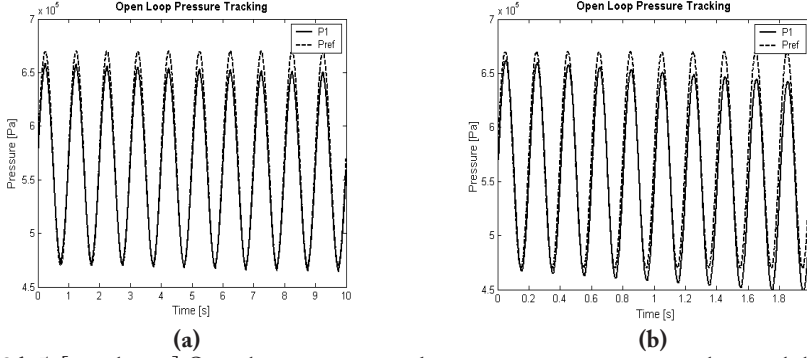
Figure 3A.5: [simulation] Open loop pressure tracking in a constant actuator volume, while using the inverse model, of:
  (a)   1 Hz, 1.10^5 Pa sine wave
  (b)   5 Hz, 1.105 Pa sine wave

$$\tilde{A}_v = \begin{cases} \dfrac{\tilde{m}_v\sqrt{T}}{C_f C_1 P_u} & \dfrac{P_d}{P_u} \le c_{cr} \\[2em] \dfrac{\tilde{m}_v\sqrt{T}}{C_f C_2 P_u}\cdot\dfrac{1}{\left(\dfrac{P_d}{P_u}\right)^{\frac{1}{k}}\sqrt{1-\left(\dfrac{P_d}{P_u}\right)^{\frac{k-1}{k}}}} & \dfrac{P_d}{P_u} > c_{cr} \end{cases} \qquad (3A.9)$$

The control signal i_c can then be expressed as the inverse of (3A.7). The presence of the arctangent function in the algebraic function means that no closed form solution to the inverse of (3A.7a) can be found.

To be able to invert it a polynomial approximation was made and this expression was then inverted. The result is equation (3A.10). Combined with equation (3A.11) an expression for $\tilde{x}_s$ is finally acquired.

$$\begin{aligned} y(\tilde{A}_v) = 10^{-7}\left(\frac{|\tilde{A}_v|}{4R_h^2 n_h}\right)^6 + 13.409\left(\frac{|\tilde{A}_v|}{4R_h^2 n_h}\right)^5 - 26.329\left(\frac{|\tilde{A}_v|}{4R_h^2 n_h}\right)^4 + \\ 19.936\left(\frac{|\tilde{A}_v|}{4R_h^2 n_h}\right)^3 - 7.2452\left(\frac{|\tilde{A}_v|}{4R_h^2 n_h}\right)^2 + 2.22849\left(\frac{|\tilde{A}_v|}{4R_h^2 n_h}\right) + 0.0 \end{aligned} \qquad (3A.10)$$

$$\tilde{x}_s(\tilde{A}_v) = \left((2y-1)R_h + p_w\right).sign(\tilde{A}_v) \qquad (3A.11)$$

This desired spool displacement is then linearly dependent on the control current i_c. In the presented linearization technique it is assumed that the rate of change of the pressure, piston position and piston velocity are significantly slower than the pressure feedback control loop. A quasi static situation for these parameters is thus assumed, the actually measured values are used for linearization. However, actually all these measurement based linearizations constitute non-linear feedback loops with a limited bandwidth. These effects

(a)   **(b)**

Figure 3A.6: [simulation] Effects of variations of the feedback input parameters $\hat{x}$ and $\hat{P}$ on the inverse model output :
(a)   Pressure disturbances, while position is kept constant.
(b)   Position disturbances, while pressure is kept constant.

can be studied from (non-linear) model simulations.

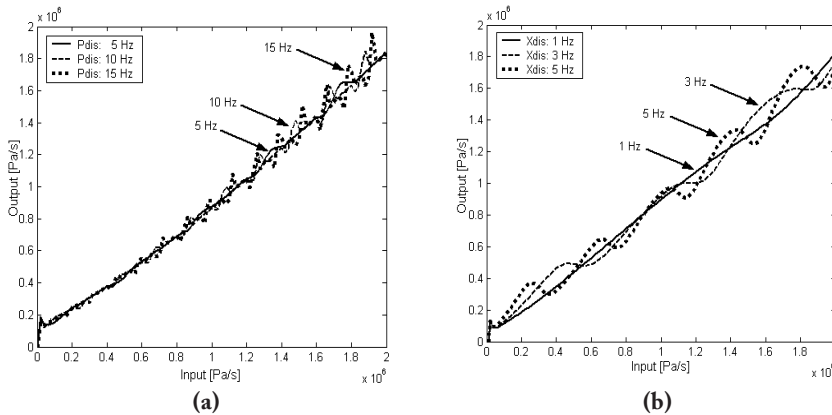In the model, a reference $\tilde{P}$ is the input for the inverse model. The required $\tilde{i}_c$ is then used as the input for the pneumatic plant model. The output is a resulting chamber pressure. For the simulations, the first chamber of the cylinder actuator was used as representative actuator volume. The piston is fixed in its mid-position. This way a constant actuator volume is achieved and the load velocity ($\dot{x}_p$) is equal to zero. In the first simulation a reference pressure is supplied to chamber 1 and the resulting chamber pressure is measured. The result can be found in figure 3A.5.

From the figure can be concluded that the inversion on model level is adequate. The shape of the reference curve can be tracked very well, even for higher frequencies. The output pressure tends to slowly drift away from the reference. This indicates that a (small) error between the normal and inverted model exists. This error is caused by the mismatch between the polynomial approximation of the arctangent function and the arctangent function itself, the neglect of the time delay of the tube flow and the neglect of the dynamics of the relation between x_s and i_c and the tube flow equations cause phase lag and time delays, which also produces errors. Such a small drift will not be a problem once feedback control is applied, given that the time delays remain small (relatively short tubing).

Another simulation, evaluating the sensitivity of the inverse model to variations of its input parameters $\hat{x}_p, \dot{\hat{x}}_p$ and $\hat{P}$ (in reality measured values) was conducted. Sinusoidal pressure changes with amplitude 1.105 Pa and varying frequencies are applied to test the influence of this input parameter. To test the influence of changes in actuator volume, the piston position is varied with sinusoidal position variations with amplitude 30 mm also at varying frequencies. During both simulations, the parameter that is not considered is kept constant. The input of the inverse model ($\tilde{P}$) is a ramp signal.

The output of the pneumatic plant, in this case the rate of pressure change, generated by the input given through the inverse model, is measured. Ideally the output should also be a ramp signal. The results of both experiments can be found in figure 3A.6.

As can be seen in figure 3A.6 (a), the pressure variations do influence the output signal. However at 15 Hz this effect has a maximum 10% deviation of the desired input signal,

this is considered acceptable. In figure 3A.6 (b) can be seen that the influence of the position variations also stays within reasonable boundaries. For the frequency of 1 Hz, the maximum deviation is 2% of the desired signal, for 5 Hz, this number is 5%.

8. References

Adams, R. J. and Hannaford, B. 2002. Control law design for haptic interfaces to virtual reality. IEEE Transactions on Control Systems Technology, 10(1): 3-13.

Bicchi, A., Rizzini, S. L. and Tonietti, G. 2001. Compliant design for intrinsic safety: General issues and preliminary design. Paper presented at the IROS.

Brown, M., Tsagarakis, N. and Caldwell, D. G. 2003. Exoskeletons for human force augmentation. Industrial Robot-an International Journal, 30(6): 592-602.

Colombo, G., Joerg, M., Schreier, R. and Dietz, V. 2000. Treadmill training of paraplegic patients using a robotic orthosis. Journal of Rehabilitation Research and Development, 37(6): 693-700.

Ferris, D. P., Czerniecki, J. M. and Hannaford, B. 2005. An ankle-foot orthosis powered by artificial pneumatic muscles. Journal of Applied Biomechanics, 21(2): 189-197.

Ferris, D. P., Sawicki, G. S. and Domingo, A. R. 2005. Powered lower limb orthoses for gait rehabilitation. Topics in Spinal Cord Injury Rehabilitation, 11(2): 34-49.

Hayward, V. and Astley, O. R. 1996. Performance Measures for Haptic Interfaces. Paper presented at the In Robotics Research: The 7th International Symposium.

Hesse, S., Uhlenbrock, D., Werner, C. and Bardeleben, A. 2000. A mechanized gait trainer for restoring gait in nonambulatory subjects. Archives of Physical Medicine and Rehabilitation, 81(9): 1158-1161.

Hesse, S., Schmidt, H., Werner, C. and Bardeleben, A. 2003. Upper and lower extremity robotic devices for rehabilitation and for studying motor control. Current Opinion in Neurology, 16(6): 705-710.

Hidler, J., Nichols, D., Pelliccio, M. and Brady, K. 2005. Advances in the understanding and treatment of stroke impairment using robotic devices. Topics in Stroke Rehabilitation, 12(2): 22-35.

Lee, S. and Sankai, Y. 2005. Virtual impedance adjustment in unconstrained motion for an exoskeletal robot assisting the lower limb. Advanced Robotics, 19(7): 773-795.

Linde, R. Q. v. d. and Lammertse, P. 2003. Haptic Master - a generic force controlled robot for human interaction. Industrial Robot: An International Journal, 30(6): 515-524.

Morrell, J. B. and Salisbury, J. K. 1998. Parallel-coupled micro-macro actuators. International Journal of Robotics Research, 17(7): 773-791.

Pratt, J., Krupp, B. and Morse, C. 2002. Series elastic actuators for high fidelity force control. Industrial Robot, 29(3): 234-241.

Richer, E. and Hurmuzlu, Y. 2000a. A high performance pneumatic force actuator system: Part I - Nonlinear mathematical model. Journal of Dynamic Systems Measurement and Control-Transactions of the ASME, 122(3): 416-425.

Richer, E. and Hurmuzlu, Y. 2000b. A high performance pneumatic force actuator system: Part II - Nonlinear controller design. Journal of Dynamic Systems Measurement and Control-Transactions of the ASME, 122(3): 426-434.

Riener, R., Lunenburger, L., Jezernik, S., Anderschitz, M., Colombo, G. and Dietz, V. 2005. Patient-cooperative strategies for robot-aided treadmill training: First experimental results. IEEE Transactions on Neural Systems and Rehabilitation Engineering, 13(3): 380-394.

Robinson, D. W. 2000. Design and Analysis of Series Elasticity in Closed-loop Actuator Force Control. Massachusetts Institute of Technology (MIT).

Slotine, J.-J. E. and Li, W. 1991. Applied nonlinear control. l: Englewood Cliffs, N.J. : Prentice Hal.

Sugar, T. G. 2002. A novel selective compliant actuator. Mechatronics, 12: 1157-1171.

Townsend, W. T. and Guertin, J. A. 1999. Teleoperator slave - WAM design methodology. Industrial Robot, 26(3): 167-177.

van der Kooij, H., Veneman, J. and Ekkelenkamp, R. 2006. Compliant actuation of exoskeletons. In A. Lazinica (Ed.), Mobile Robotics – Towards New Applications. Mammendorf, Germany: verlag Rober Mayer-Scholz.

Volpe, B. T., Ferraro, M., Krebs, H. I. and Hogan, N. 2002. Robotics in the rehabilitation treatment of patients with stroke. Current Atherosclerosis Report, 4(4): 270-276.

Winter, D. A. 1990. Biomechanics and Motor Control of Human Movement (2nd ed.). New York: Wiley.

Xiang, F. L. and Wikander, J. 2004. Block-oriented approximate feedback linearization for control of pneumatic actuator system. Control Engineering Practice, 12(4): 387-399.

Zinn, M., Roth, B., Khatib, O. and Salisbury, J. K. 2004. A new actuation approach for human friendly robot design. International Journal of Robotics Research, 23(4-5): 379-398.

chapter 4

Control of a Pneumatic Muscle Using Block Oriented Approximate Feedback Linearization

Ralf Ekkelenkamp
Jan F. Veneman
Bianca Mulder
Peter Veltink
Stefano Stramigioli
Herman van der Kooij

Abstract

Using pneumatic muscle actuators (PMA) as force sources in rehabilitation robotics has often been proposed in literature because of the intrinsic human muscle like behaviour of the PMA. However no extensive evaluations have been performed to determine the exact performance and applicability of these muscles. This article will discuss a novel way of controlling PMA's and will evaluate the viability of PMA muscles in an exoskeleton. Using an inverse blockwise model we were able to control a PMA using a linear controller. We were able to perform a force bandwidth of over 15 Hz in standstill. The PMA with this type of control meets the criteria for use as a force source in lower limb exoskeletons. PMA muscles using the control described in this article appeared to be a viable if not optimal force source for exoskeletons.

Chapter Contents

1. Introduction

Due to aging of the population, growing numbers of people are affected by impairments of their motor system, caused by disorders like stroke. Treatment of stroke patients consists of intensive physical therapy. The treatment time per patient combined with the total number of people suffering from a stroke makes rehabilitation therapy extremely costly. This makes devices that could reduce the costs of therapy attractive to rehabilitation centres. Currently there are robotic rehabilitation devices under development for both the upper and lower extremities (Hidler, Nichols et al. 2005). This paper will discuss the application of a pneumatic muscle in a lower extremity rehabilitation device. The goal of rehabilitation robotics in general is to lighten the load on therapists, decrease costs by enabling therapists to treat several patients simultaneously and reducing the stay in the rehabilitation centres by offering training schemes with high intensity of repetition. Studies (Lotze, Braun et al. 2003; Kaelin-Lang, Sawaki et al. 2005) seem to indicate that the participation of the patient is a important factor in the rehabilitation process. The implication for a gait rehabilitation robot is that this robot should allow for the patient to be able to walk without being constrained by the exoskeleton. Support only needs to be offered in those subtasks that a patient is unable to perform himself. This wide range of interaction behaviour, from free motion to forced motion, would be best controlled using an impedance control scheme (Ekkelenkamp, Veneman et al. 2005). For this type of control scheme good and safe force sources are needed. Pneumatic muscle actuators (PMA) seem to be very appealing for this purpose because of the similarity to human muscles (Ching-Ping and Hannaford 1996; Repperger, Phillips et al. 2005; Repperger, Phillips et al. 2006). However there are some important drawbacks, generally associated with pneumatics such as lack of controllability and the noisy operation of valves. This article proposes a new control design for PMA's and investigates the applicability of a PMA as a possible force actuator for a rehabilitation exoskeleton.

Control of pneumatics

The standard approach to force control of the PMA is through pressure control in combination with a (static) forward model describing the relationship between the pressure within the actuator and the external force applied by the actuator. The pressure control of the PMA has been approached in several ways.

Linearized models of the pneumatic muscle system have been used (Ching-Ping and Hannaford 1996). The quality of these controllers suffices around the set-point at which the system was linearized, but no guarantees can be given for the desired behaviour of the system for the whole contraction ranges of the muscle. Sliding mode controllers have been used to control non-linear pneumatic systems in a robust way and have proven to be adequate for the control of pneumatic cylinders (Richer and Hurmuzlu 2000) for both position and force control. However the nature of the control law implies that chattering will occur around the required sliding surface, leading to noisy operation and a short lifespan of the pneumatic valves. A second drawback is that convergence to the sliding surface is not guaranteed (Edwards and Spurgeon 1998).

Xiang et al. (Xiang and Wikander 2004) used a block-oriented approximate feedback linearization for the control of a pneumatic cylinder. Through the inversion of individual blocks of the system in the feedback loop the system was linearized and could be control-
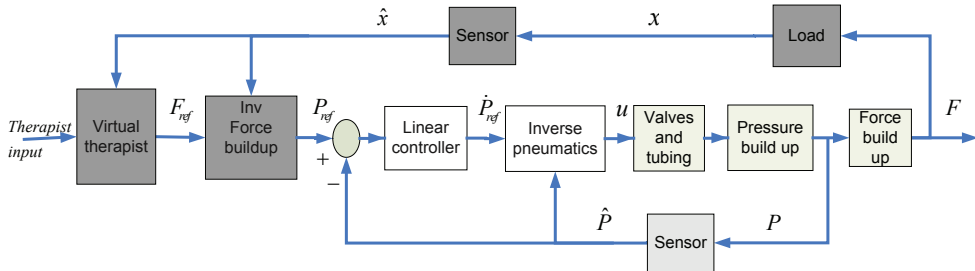
Figure 4.1: Impedance control scheme incorporating the inverse model of the PMA. White blocks denote the pneumatic system and the light grey denote the inverse model discussed in this article. The dark grey blocks compose the outer position loop.

led with a simple linear controller. The advantage of this method over linearizing the system with respect to one set-point is that it is valid for a larger range.

We have chosen to design a controller based on the latter method specifically applied to the PMA. For the implementation of this method a descriptive model is needed. Preliminary measurements have shown that PMA models described in literature are inaccurate or not feasible for the single layered muscle we used. These single layered muscles have a metal mesh integrated into the rubber. The inaccuracy of the current models would not allow the required force bandwidth needed. Many studies on McKibben and other types of pneumatic muscles use a model first proposed by the Bridgestone Company (BridgestoneCompany 1986). Several approaches have been made to improve upon the standard model: Reynolds et al.(Reynolds, Repperger et al. 2003) describe a phenomenological model for the dynamics of a McKibben muscle consisting of a spring, damper and a contractile element. Model parameters were estimated by loading the muscle and then unloading suddenly. This model approached the dynamic situation accurately; no approximation of force bandwidth was given. Davis et al.(Davis, Tsagarakis et al. 2003) used the standard model for the pneumatic muscle and attributed the error between the model and the actual force output to stress in the mesh material. This led to good static tracking of the force. The force bandwidth was measured at 4 Hz for a muscle without filler and a solenoid valve. Furthermore it was shown theoretically that multiple valves and using some material liquid or solid to fill part of the PMA volume increased this value to roughly 10 Hz. However these higher bandwidths were not experimentally verified. Schroder et al. (Schroeder, Erol et al. 2003) used a static fit to the standard Bridgestone model for two muscles in an antagonistic setup. The damping in the muscle was identified around the equilibrium point of the two muscles at different frequencies of position sine waves. The force bandwidth of this setup was estimated around 10 Hz based on the step response of the system. These results were only valid for the linear range of the muscle.

The goal of this paper is to evaluate the viability of a PMA as a force source meeting the requirements for a lower limb exoskeleton. For this purpose a novel linear block oriented feedback linearization controller was designed.

We will first define criteria for the use of a PMA in a lower limb exoskeleton. Secondly we will describe the model blocks of the PMA and the valves and invert this model blockwise. Finally the performance of this model will be judged based on the defined criteria.
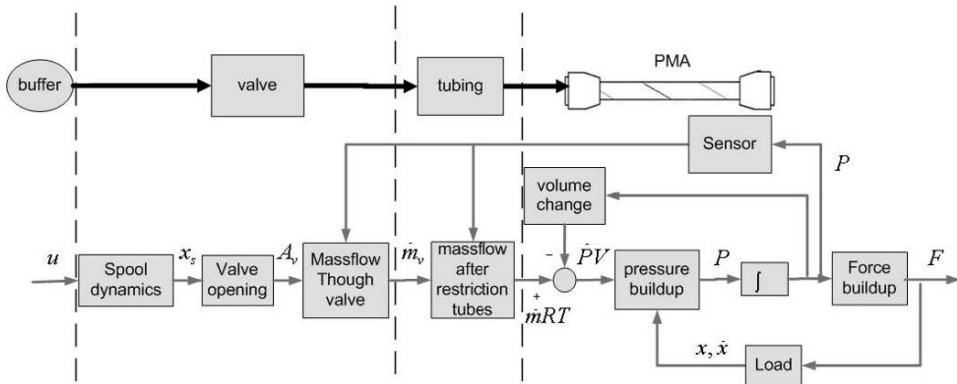
Figure 4.2: Schematic representation of the PMA model. The top schematic diagram shows the physical components of the pneumatic system the lower block diagram shows the blocks used to describe each of these elements.

2.   Methods

In a previous actuator evaluation study we have defined several criteria for the application of force actuators in an exoskeleton used for rehabilitation of the gait functionality (see chapter 5 and appendix A of this thesis). These criteria were based on walking data derived from general motor control properties and specific information of human gait (Winter 1991). These criteria will be mentioned shortly.

a. Criteria

Force bandwidth – According to gait measurements (Winter 1991) the maximum voluntary human movement frequency during walking is 4Hz. 'Fast' movements (>2Hz) are generally coupled with small joint moments and slow movements with relatively high moments. For stroke patients these frequencies are lower but as the goal is to get patients as close to 'normal' walking as possible, we have used normal walking as the criterion. According to Zinn et al. (Zinn, Roth et al. 2004) the bandwidth of the inner control loop of an impedance controller needs to be at least a factor 3 larger than the outer control loop bandwidth, in order to decouple both controllers. This implies that the force bandwidth for small moments (<10Nm) should be around 12 Hz. Larger moments, up to 60Nm need to be exerted with a bandwidth of at least 3 Hz.

Light weight – Due to safety reasons the power of actuators has to be limited. Therefore it is not possible to compensate for the mass of the exoskeleton. For the exoskeleton this means that to make the system dynamically transparent, in order to allow free motion, the apparent mass needs to be kept low.

Safe – The actuator should preferably not be able to exert forces outside the range of motion of the actuated degrees of freedom, in order to take the physical limitations of the patient into account. The actuation should be safe in all cases. This means that the system should be robustly stable in all situations, including impact, when e.g. the exoskeleton hits a solid object.

Compliant – The low weight and safety criteria lead to a compliance criterion. From the safety and weight criteria follows that the actuator power will be limited. This means

that it will not be able to react fast enough to deal with events like impact. In order to be able to deal with impact situations safely the muscle needs to be intrinsically compliant.

Durable – In general the rehabilitation robots will be used in clinical environments. This means that it is unlikely that a technician is available full time. Therefore the mean time between failures should be high.

b. Control system

For safety and stability reasons we have chosen an impedance control scheme. This implies using an inner pressure/force controller and an outer position/impedance controller (see figure 4.1).

The inner loop consists of the physical behaviour of the system and the inverse model combined with a linear controller. The outer loop is the position dependant impedance controller that sets the force reference, and will not be considered in this article. The forward model describes the behaviour of the physical system consisting of the valves, tubes and the actual PMA (white blocks in Figure 4.1). The break-up of these components into blocks is presented in Figure 4.2. The valve is split into 3 parts: the spool dynamics describing the position of the spool as function of the control current, the valve opening as function of the spool position and the mass flow as function of the valve opening. The tubing is modelled as a single block consisting of a delay and an attenuation factor. The PMA model consists of the pressure and force build up loops and a block to describe the effects of a volume change due to lengthening of the muscle.

PMA model

As discussed in the introduction most PMA models use the Bridgestone model as a basis. This model describes the pressure versus force relationship of the pneumatic muscle. Several assumptions have been made in this model: First the PMA is assumed to be cylindrically shaped. Secondly there is no energy dissipation in the muscle either through heat exchange or through friction. This means that the internal work done by the pressure of air on the inside of the PMA is equal to the work done by the force exerted by the PMA (4.1):

$$dW_{in} = (P - P_{amb}) \cdot dV$$
$$dW_{ex} = F \cdot dl$$

(4.1)

With F the force output, P the pressure in the PMA, P_{amb} the ambient pressure, V the inner volume of the PMA. When we assume that $dW_{in} = dW_{ex}$ and substitute the geometric relations, again assuming that the muscle is cylinder-shaped, we obtain the force build up in the PMA (4.2):

$$F_b = -(P - P_{amb}) \frac{(b^2 - 3L^2)}{4\pi n^2}$$

(4.2)

Where b is the thread length of the fibres that form the mesh component of the muscle wall, n is the number of rotations of each fibre around the muscle wall between the two muscle ends and L is the current muscle length.

Substituting the geometric relationship of the PMA, assuming it is cylindrical, into the differentiated standard gas law, we get the pressure build-up equation (4.3):

$$\dot{P} = \frac{d}{dt}\frac{mRT}{V} = \frac{\dot{m}RT}{V} - \frac{P\dot{V}}{V} \quad ,\text{with} \quad V = \frac{L\left(b^2 - L^2\right)}{4\pi\, n^2} \tag{4.3}$$

Where T is the (constant) ambient temperature, V is the actuator volume and $\dot{m}$ is the mass flow into the volume.

The valves

The dominant mass flow restriction is the valve opening. The mass flow through the orifice can be expressed as (4.4):

$$\dot{m} = \begin{cases} A_v C_1 & \frac{P_d}{P_u} \le c_{cr} \\[2ex] A_v C_2 \sqrt{\left(\frac{P_d}{P_u}\right)^2 - \left(\frac{P_d}{P_u}\right)^{\frac{2(k-1)}{k^2}}} & \frac{P_d}{P_u} > c_{cr} \end{cases} \tag{4.4}$$

$$C_1 = \sqrt{\frac{k}{R}\left(\frac{2}{k+1}\right)^{\frac{k+1}{k-1}}} C_f \frac{P_u}{\sqrt{T}} \quad , \quad c_{cr} = \left(\frac{2}{k+1}\right)^{\frac{k}{k-1}}$$

$$C_2 = \sqrt{\frac{2k}{R(k-1)}} C_f \frac{P_u}{\sqrt{T}} \quad \begin{cases} P_u = P_{buffer} \; ; \; P_d = P\}, \text{if } A_v > 0 \\ P_u = P ; P_d = P_{ambient}\}, \text{if } A_v < 0 \end{cases}$$

Where P_u represents the upstream pressure, P_d the downstream pressure and P_{buffer} the buffer pressure. While the valve is venting, i.e. A_v is negative, P_u is the PMA pressure and P_d the ambient pressure. While pressurising, P_u is the buffer pressure and P_d the PMA pressure. If the downstream/upstream pressure ratio is smaller than the critical flow ratio c_{cr} the flow is 'choked' and dependant only on the upstream pressure; above this ratio the flow
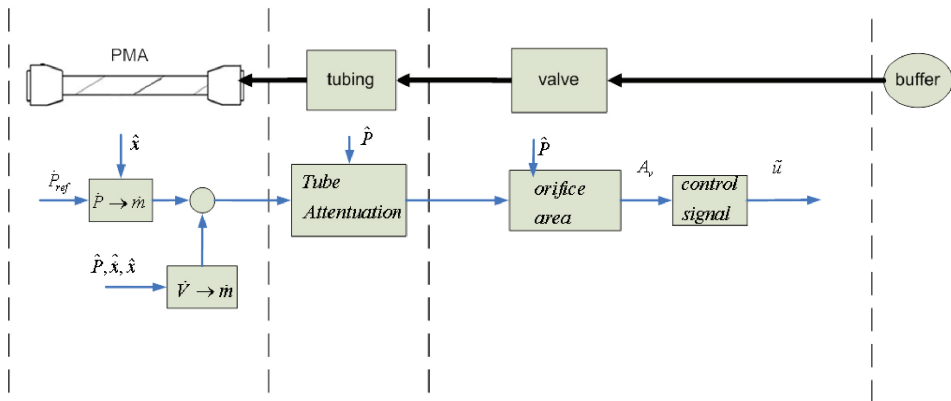

Figure 4.3: Block detailing the inverse model. The top half shows the break up of the system into physical parts and the lower half shows the break up of these components in blocks. The inverse model gives the corresponding control signal to a desired pressure change. ^ indicates real-time measured variables

depends on both up and downstream pressures. The flow coefficient C_f, is a function of the up-and downstream pressure and depends on the geometry of the valve. The exact geometry of the applied valve was not available and therefore this relationship was evaluated experimentally. Based on previous work (Bendov and Salcudean 1995), the shape of the function C_f can be assumed to be:

$$C_f = \left(\left(\frac{P_d}{P_u} \right)^{\frac{1}{k}} \sqrt{1 - \left(\frac{P_d}{P_u} \right)^{\frac{k-1}{k}}} C_1 \right)^q \tag{4.5}$$

Where q is a constant factor dependant on the geometry of the valve. The mass flow has a linear relation with valve opening (A_v). The valve opening of the applied valves, as a function of the spool displacement x, can be given as (4.6)(Richer and Hurmuzlu 2000):

$$A_v = \begin{cases} 0 & |x_s| \le (p_w - R_h) \\ 2 \cdot n_h \cdot R_h^2 \arctan \left(\sqrt{\frac{R_h - x_t}{R_h + x_t}} \right) - x_t \cdot \sqrt{R_h^2 - x_t^2} & (p_w - R_h) < |x_s| < (p_w + R_h) \\ \pi \cdot n_h \cdot R_h^2 & |x_s| \ge (p_w + R_h) \end{cases} \tag{4.6}$$

$$x_t = p_w - x_s$$

Where R_h is the valve hole radius, n_h is the number of holes in the valve opening, p_w the spool width and x_s the position of the spool.

The specified bandwidth of the spool placement is roughly 100Hz for the valves. This means that for the desired bandwidth of 12 Hz the effects of these dynamics is assumed negligible and has been omitted from the model. By substituting $x_s = K \cdot u$, in (4.6) we get the relationship between the control signal u and A_v.

Tubing

Preliminary measurements have shown that the tubes can be modelled as a time delay and attenuation:

$$K_t = \begin{cases} 0 & t \le \tau \\ e^{-\frac{32 \cdot \mu}{D_t^2} \frac{R \cdot T \cdot L_t}{2 \cdot P_d c}} & t > \tau \end{cases} \quad \text{with a time delay of } \tau = \frac{L_t}{c} \tag{4.7}$$

Where D_t is the tube diameter, L_t the length of the tube and c is the speed of sound in air. The total mass flow through the valve and tubes can then be written as $\dot{m} = \dot{m}_v K_t$. Where $\dot{m}_v$ is the mass flow through the valve and K_t the attenuation factor.

c. Inverse Model

This section will describe the theoretical inverse model PMA (see Figure 4.3). The desired mass flow is determined based on the current measurements of the volume and pres-
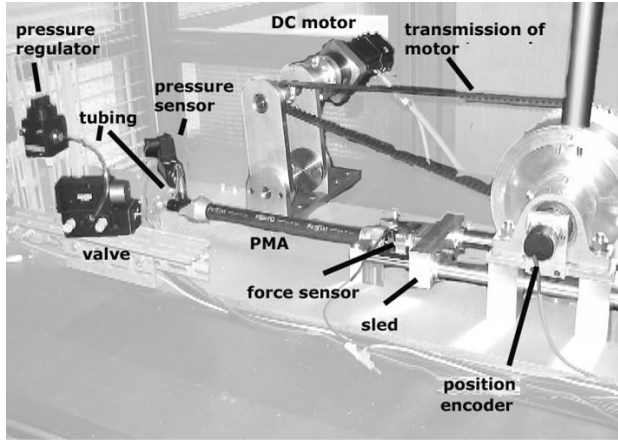
Figure 4.4: Experimental setup: The muscle is connected to the fixed world on one side and connected to a sled on the other. The DC motor controls the position of the sled through a timing belt and cable transmission.

sure by rewriting (4.3) as a function of $\dot{m}$. The time delay in (4.7) has been omitted in the inverse model as this would imply that information of future events would be needed. The inverse of (4.7) now becomes factor K_t. Substituting the inverse of (4.7) in (4.3) the mass flow needed to achieve a certain pressure change, becomes:

$$\tilde{\dot{m}}_v = \left(\dot{P}_{ref} \cdot V_{act} + \hat{P} \cdot \dot{V}_{act} \right) \frac{1}{R \cdot T \cdot K_t} \tag{4.8}$$

The valve opening to achieve this mass flow can be calculated with the inverse of equation (4.4):

$$\tilde{A}_v = \begin{cases} \dfrac{\tilde{\dot{m}}_v \sqrt{T}}{C_f C_1 P_u} & \dfrac{P_d}{P_u} \leq c_{cr} \\[4ex] \dfrac{\tilde{\dot{m}}_v \sqrt{T}}{C_f C_2 P_u} \cdot \dfrac{1}{\left(\dfrac{P_d}{P_u} \right)^{\frac{1}{k}} \sqrt{1 - \left(\dfrac{P_d}{P_u} \right)^{\frac{k-1}{k}}}} & \dfrac{P_d}{P_u} > c_{cr} \end{cases} \tag{4.9}$$

The control signal u can then be expressed as the inverse of (4.6). However, the presence of the arctan function means that no closed form solution to the inverse of (4.6) can be found. An inverse sigmoid function (4.10) was determined as an inverse of (4.6) in the working range:

$$\tilde{u} = 5 \cdot a + \log \left(\frac{b + \tilde{A}_v}{c - \tilde{A}_v} \right) \tag{4.10}$$

The variable is the estimated value for the control signal needed to realize the desired $\dot{P}_{ref}$; a, b and c are constants.
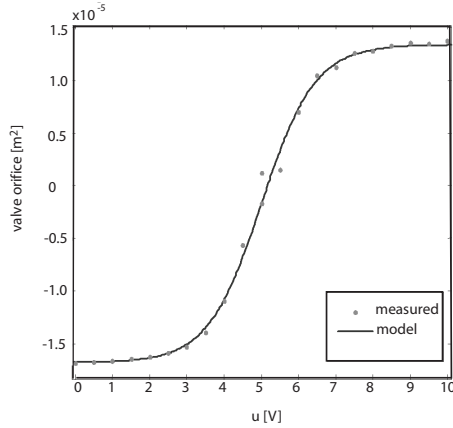
Figure 4.5: Derived orifice area versus control voltage during buffer cylinder pressurization PMA model

d. Identification experiments

The muscle used for this article consists of a rubber hose reinforced with strong fibres; we used the MAS20 PMA from Festo. A large buffer cylinder (10 litres) was used for the identification of the valve characteristics (4.6). In order to characterise the valve opening A_v with respect to the control signal u the filling and venting pressure curves of the buffer cylinder are measured for several static values of u. The minimal discharge time was in the order of 10 sec. meaning the orifice area A_v can be assumed to be constant during these measurements. With this assumption, the value for q in equation (4.5) was estimated by optimization. This optimization was based on half of the measured pressure curves and then tested on the other half. In order to identify the PMA impedance properties we used a setup able to move the endpoint of the muscle along a set trajectory (see Figure 4.4). The length of the muscle could be locked in different positions or controlled using a DC mo-
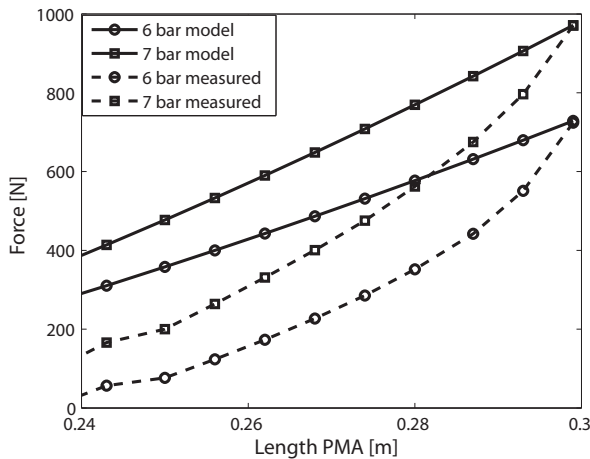
Figure 4.6: Static measurement of the contraction of the muscle versus model predicted muscle force for varying pressures. These measurements show the error between the standard Bridgestone model and the model described in this paper equation(4.13).

tor. The motor is capable of delivering more force than the PMA and has a higher power rating and bandwidth. This means that the DC motor can be considered a velocity source for the impedance measurements. The muscle was extended and released at several pressures and the force/length curves were measured. The muscle length was then varied at different frequencies and pressures to determine the impedance of the muscle.

e. Validation experiments

The transfer function $\frac{u}{\tilde{u}}$ was used to validate the models ability to determine the correct control value. $\tilde{u}$ is the estimated control signal (see Figure 4.3) of the inverse model in series with the physical system. This transfer function shows the ability of the model to predict the correct valve opening to achieve the desired pressure change. As control signal we used a multi-sine with frequencies between 0.1 and 30Hz and a uniform power distribution. Based on the measured pressure, P, and muscle length, L, we determined a predicted control signal $\tilde{u}$ and calculated the transfer function $\frac{u}{\tilde{u}}$ from predicted to actually applied control signal. The force transfer function, $\frac{F}{F_{ref}}$, is used as an overall performance measure of the entire system.

This transfer function was determined using a multi-sine with frequencies between 0.1 and 20 Hz for F_{ref}. The linear controller (see Figure 4.2, in our case a PD controller) used here was tuned using a standard step response method. In both these experiments the muscle was fixed at different lengths within the working range of the model. The force transfer was measured for small and large forces (100N and 500N respectively). These forces, with a suitable transmission ratio, are equivalent to the moments mentioned in the criteria section.

3. RESULTS

a. Identification experiments

The absolute error between forward model and the actual measured charge / discharge pressure curve was less than 2% for the tested curves for all time series given one single value for q and an assumed fixed value for A_v. With the value for q and the discharge curves the relationship between the control voltage u and the orifice area A_v was measured (see Figure 4.5). The error between the measured and the model predicted A_v remains small for the entire range of control values. At the zero mass flow value for u, 5 Volt, there are two values for the valve opening (see Figure 4.5).

This is caused by the difference in leakage between the venting and the pressurizing channels. Based on static measurements with closed valves the relationship between the length, pressure and force were determined (see Figure 4.6). When compared to the standard pneumatic model these measurements vary quite substantially (see Figure 4.6). The error however does not vary with respect to the standard model with different pressures. This would indicate that there is no lengthening of the fibres as presumed for the McKibben muscles in (Davis, Tsagarakis et al. 2003). For the static measurements we did here, there was no noticeable hysteresis for these slow movements.

The error between measurements and the Bridgestone model varied with the length of the muscle, but was independent of the pressure. This discrepancy could be caused by the
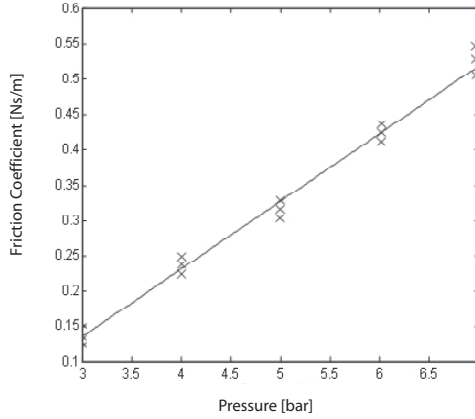
Figure 4.7: Viscous friction coefficient of the PMA for different pressures. For each pressure several different oscillation frequencies were used to determine the friction coefficient C(P) , see equation (4.12).

force needed to deform the rubber or that the geometric assumption of the PMA being a cylinder is incorrect. To compensate for this error we used a 3rd-order polynomial fit of the error as function of the length (4.11).

$$F_c = p_1 L_n^3 + p_2 L_n^2 + p_3 L_n + p_4 \qquad (4.11)$$

The Bridgestone model compensated with (4.11) composes the static part of the Force-Build-up relationship and describes the elastic component of the muscle. However studies have shown that the dynamic damping effect can not be neglected (Davis, Tsagarakis et al. 2003). In order to determine the viscous friction coefficient of the muscle the muscle length was varied slightly using the DC motor. (sine waves with 0.5, 1 and 2 cm amplitudes and frequencies 0.5, 1 and 3 Hz). The muscle was assumed to function as a spring, with a coefficient described by (4.2) and (4.11). The velocity dependant behaviour was modelled as a damper with a constant coefficient for small movement ranges (Schroeder, Erol et al. 2003).

This coefficient was determined to be independent of the actual muscle length and the
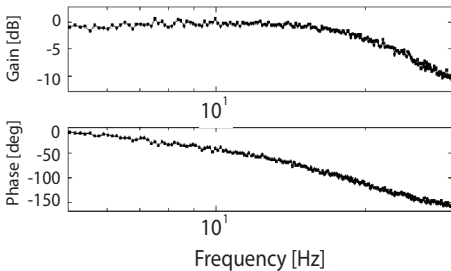
Figure 4.8: Transfer $\frac{u}{u}$ of the inverse model in series with the physical system.
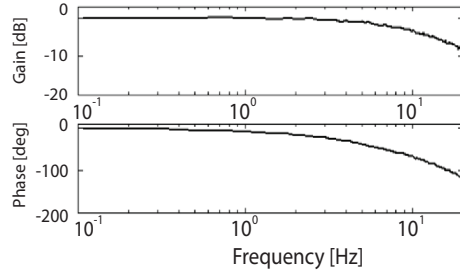
Figure 4.9: Transfer function $\frac{F}{F_{ref}}$ of the complete system determined with a multi-sine reference signal with frequency range 0.1-20 Hz and a uniform power distribution, peak amplitude 100 N.
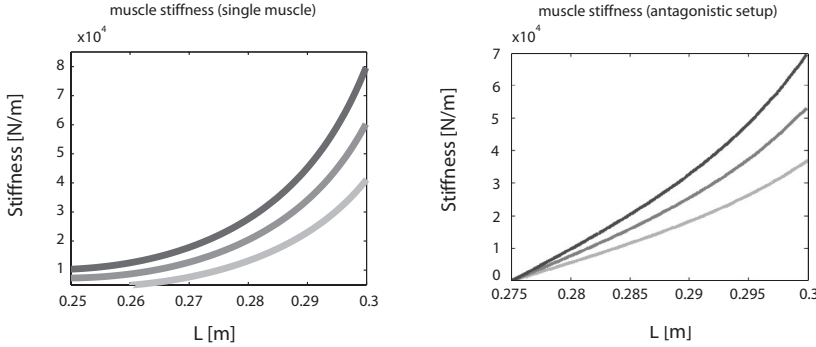
Figure 4.10: Simulated muscle stiffness in antagonistic and single muscle setups based on model predictions. The line represent from top to bottom the impedance (stiffness) at 3, 5 and 7 bar respectively. This pressure range is the optimal working range of the muscle.

frequency, but was dependant on the pressure (see Figure 4.7). The dependence of the friction can be written as:

$$F_d\left(\dot{x},P\right)=C\left(P\right)\dot{x} \quad with: \quad C\left(P\right)=c_1P-c_2 \tag{4.12}$$

The total force build-up of the PMA muscle can now be written as:

$$F = F_b\left(x,P\right)+F_c\left(x\right)+F_d\left(\dot{x},P\right) \tag{4.13}$$

In which F_b is the static force, F_c the compensation for shape change in the rubber and F_d the friction component.

b. Validation of the inverse model

Based on the measured pressure P, and muscle length L, we determined the predicted control signal and then calculated the transfer function $\frac{u}{\hat{u}}$. As can be seen the transfer $\frac{u}{\hat{u}}$ has a 0 dB gain up to the point of saturation, found at roughly15Hz (see Figure 4.8). The phase lag is most likely caused by the impossibility to invert the time delay of the tubing in the inverse model. The coherence of the model shows that the system in combination with the inverted model can be considered linear for the conditions of these experiments. Using a multi-sine with frequencies between 0.1 and 20 Hz as a reference force (F_{ref}) we determined the transfer $\frac{F}{F_{ref}}$ for the entire system (Figure 4.9). For two force amplitudes (100 N and 500 N) the bandwidth was measured to be >15Hz for the small forces and >5 Hz for large forces (500N). To test the assumption of the spring-damper behaviour of the PMA with a constant volume the impedance transfer ($\frac{F}{v}$) was measured of the PMA using a force sensor and an external position disturbance. The impedance of these measurements have been determined and these were described accurately by the model (4.13) (Experimental results not shown here. The model-predicted stiffness can be seen in Figure 4.10).

4. Discussion

a. Evaluation of criteria

Force bandwidth – Bandwidth of the PMA with a fixed length of 30 cm was 15 Hz (100N), which is adequate for the proposed purpose. For large forces (>500N) the bandwidth of the system was still above 4Hz. The bandwidth was largely determined by the limits of the valve opening and the available air flow. The bandwidth can be improved by filling the muscle with a solid or liquid. This reduces the internal volume of the muscle and thus the required airflow without reducing the output force (Davis, Tsagarakis et al. 2003). This could theoretically lead to an increase of the bandwidth by 50% supposing a volume reduction of 60%. The largest restriction of the airflow can be found in the valve. The obvious solution would be to implement a valve with a higher flow rate. Unfortunately because of larger leak flows, between the buffer and the muscle the larger valve is not accurate enough to control small force changes. To solve this problem two or more valves could be used in parallel. This way it would be possible to use one valve to fine-tune the control while a larger valve could be used for the larger mass flows.

The force bandwidth we obtained here is higher than the reported bandwidths found in literature and are adequate for our purposes. Standard EM motors score much higher on the bandwidth scale but are known to be poor force-sources without a force feedback. Also rigidly connecting a DC motor leads to complications when unscheduled stiff interactions occur with the environment.

Weight – The weight to force ratio of the pneumatic muscles by themselves is very high, approximately 3000 N/kg. However the length of tubing between the valve and the muscle must be small to avoid large time delays in the air flow through these tubes. This means that it is not possible to fix the muscle to the exoskeleton and the valve to the fixed world. The force density including the used solenoid valve reduces the ratio to 400 N/kg. To avoid significant pressure drops in the tubing when the valve and the muscle are connected to the frame the tube diameter leading to the frame needs to be adequately large (and thus heavy). The total force to weight ratio now becomes less favourable but is still better than the force to weight ratio of a standard electromotor.

Compliance and safety – The muscle can be considered a linear spring in parallel with a small damper for small position deviations. The compliance of the actuator is between 40-80kN/m. This is in the same order as the series elastic actuator (SEA) designed for the same specifications (see chapter 3). The damping which was found for this type of muscle was considerably lower than the damping found in references (for other muscle types) (Davis, Tsagarakis et al. 2003; Schroeder, Erol et al. 2003). The coulomb friction was negligible and the viscous friction was a factor three times smaller than conventional muscles. This lower damping is due to the fact the applied muscle consists of one layer instead of two moving over each other. It is however not so small that it can be neglected in the inverse model (Figure 4.7). Using the Festo MAS 20 PMA as a variable spring would not be viable for the application in rehabilitation robotics. The intrinsic muscle stiffness is too high and can be modulated by a factor 2 maximum with different pressure values (Figure 4.11). Based on measurements from (Winter 1991) the ranges that would be interesting for rehabilitation robots range from and ideal 0 N/m for allowing free motion to 60 kN/m for position control of human limbs. The use of the variable resistance of the PMA could

be considered for the control of the ankle during foot landing where a high stiffness is required.

Durability – The durability of the PMA is guaranteed for at least 2 million cycles. When the muscles are used in a rehabilitation device in for example a gait trainer it would use approximately 400 cycles per hour of use. We have used the current muscle for an approximate 250000 cycles. This would mean that the expected life of a muscle would be around 5 years. The replacement value of the muscles is therefore very low when compared to other actuation types. However the solenoid valves used in this comparison have a life expectance which is considerably lower. It could be worthwhile to investigate the use of pulse width modulation control using fast switching valves. The life expectancy of these valves is considerably longer at lower cost than the proportional valves we used.

5. CONCLUSIONS

We have shown that the PMA muscle used in this evaluation meets the criteria we defined for the use of an actuation method in a lower limb exoskeleton. Using a block oriented feedback linearization method we have obtained higher bandwidths than reported for similar muscles using innovative control techniques. The actuator matches bandwidth, compliance and safety with many of the commonly used actuator types.

6. REFERENCES

BENDOV, D. and SALCUDEAN, S. E. 1995. A Force-Controlled Pneumatic Actuator. IEEE Transactions on Robotics and Automation, 11(6): 906-911.

BRIDGESTONECOMPANY. 1986. Rubbertuators and applications for robotics, Technical Guide.

CHING-PING, C. and HANNAFORD, B. 1996. Measurement and modeling of McKibben pneumatic artificial muscles. IEEE Transactions on Robotics and Automation,, 12(1): 90-102.

DAVIS, S., TSAGARAKIS, N., CANDERLE, J. and CALDWELL, D. G. 2003. Enhanced modelling and performance in braided pneumatic muscle actuators. International Journal of Robotics Research, 22(3-4): 213-227.

EDWARDS, C. and SPURGEON, S. K. 1998. Sliding mode control, theory and applications. London: Taylor and Francis Ltd.

EKKELENKAMP, R., VENEMAN, J. and VAN DER KOOIJ, H. 2005. LOPES: selective control of gait functions during the gait rehabilitation of CVA patients, Proceedings of ICORR 2005 - IEEE International Conference on Rehabilitation Robotics: 361-364. Chicago.

HIDLER, J., NICHOLS, D., PELLICCIO, M. and BRADY, K. 2005. Advances in the understanding and treatment of stroke impairment using robotic devices. Topics in Stroke Rehabilitation, 12(2): 22-35.

Kaelin-Lang, A., Sawaki, L. and Cohen, L. G. 2005. Role of voluntary drive in encoding an elementary motor memory. Journal of Neurophysiology, 93(2): 1099-1103.

Lotze, M., Braun, C., Birbaumer, N., Anders, S. and Cohen, L. G. 2003. Motor learning elicited by voluntary drive. Brain, 126(Pt 4): 866-872.

Repperger, D. W., Phillips, C. A., Neidhard-Doll, A., Reynolds, D. B. and Berlin, J. 2005. Power/energy metrics for controller evaluation of actuators similar to biological systems. Mechatronics, 15(4): 459-469.

Repperger, D. W., Phillips, C. A., Neidhard-Doll, A., Reynolds, D. B. and Berlin, J. 2006. Actuator design using biomimicry methods and a pneumatic muscle system. Control Engineering Practice, 14(9): 999-1009.

Reynolds, D. B., Repperger, D. W., Phillips, C. A. and Bandry, G. 2003. Modeling the dynamic characteristics of pneumatic muscle. Annals of Biomedical Engineering, 31(3): 310-317.

Richer, E. and Hurmuzlu, Y. 2000a. A high performance pneumatic force actuator system: Part II - Nonlinear controller design. Journal of Dynamic Systems Measurement and Control-Transactions of the ASME, 122(3): 426-434.

Richer, E. and Hurmuzlu, Y. 2000b. A high performance pneumatic force actuator system: Part I - Nonlinear mathematical model. Journal of Dynamic Systems Measurement and Control-Transactions of the ASME, 122(3): 416-425.

Schroeder, J., Erol, D., Kawamura, K. and Dillmann, R. 2003. Dynamic Pneumatic Actuator Model for a Model-Based Torque Controller, IEEE International Symposium on Computational Intelligence in Robotics and Automation (CIRA). Kobe, Japan.

Winter, D. A. 1991. Biomechanics and Motor Control of Human Gait: Normal, Elderly and Pathological. Waterloo: University of Waterloo Press.

Xiang, F. L. and Wikander, J. 2004. Block-oriented approximate feedback linearization for control of pneumatic actuator system. Control Engineering Practice, 12(4): 387-399.

Zinn, M., Roth, B., Khatib, O. and Salisbury, J. K. 2004. A new actuation approach for human friendly robot design. International Journal of Robotics Research, 23(4-5): 379-398.

chapter 5

A Series Elastic- and Bowdencable-based Actuation System for Use as Torque Actuator in Exoskeleton-type Robots

Jan F. Veneman
Ralf Ekkelenkamp
Rik Kruidhof
Frans C.T. van der Helm
Herman van der Kooij

Abstract

Within the context of impedance controlled exoskeletons, common actuators have important drawbacks. Either the actuators are heavy, have a complex structure or are poor torque sources, due to gearing or heavy non-linearity. Considering our application, an impedance controlled gait rehabilitation robot for treadmill-training, we designed an actuation system that might avoid these drawbacks. It combines a lightweight joint and a simple structure with adequate torque source quality. It consists of a servomotor, a flexible Bowden cable transmission, and a force feedback loop based on a series elastic element. A basic model was developed that is shown to describe the basic dynamics of the actuator well enough for design purpose.

Further measurements show that performance is sufficient for use in a gait rehabilitation robot. The demanded force tracking bandwidths were met: 11 Hz bandwidth for the full force range (demanded 4Hz) and 20 Hz bandwidth for smaller force range (demanded 12 Hz). The mechanical output impedance of the actuator could be reduced to hardly perceptible level. Maxima of about 0.7 Nm peaks for 4 Hz imposed motions appeared, corresponding to less than 2.5% of the maximal force output. These peaks were caused by the stick friction in the Bowden cables.

Spring stiffness variation showed that both a too stiff and a too compliant spring can worsen performance. A stiff spring reduces the maximum allowable controller gain. The relatively low control gain then causes a larger effect of stick in the force output, resulting in a less smooth output in general. Low spring stiffness, on the other side, decreases the performance of the system, because saturation will occur sooner.

Chapter Contents

Nomenclature

$c_{b,s,tot}$	Stiffness of, index b – Bowden cable s – SE spring tot – Bowden cable and SE spring together	[N/m]
$F_{a,m}$	Force, index a – at actuator output m – in the motor	[N]
k_m	Motor constant, gain from motor control command to motor force	[N/V]
K_H	Gain of the uncontrolled actuator transfer function	
K_Z	Gain of the uncontrolled output impedance transfer function	
l	Spring-length	[m]
M	Reflected motor mass	[kg]
r	Radius of knee actuator disc	[m]
R	Vector of sampled sine	
T	Torque	[Nm]
u	Control command	[V]
$x_{1,2,3}$	Position, index 1 – on the motor side of the Bowden cable 2 – on the actuator side of the Bowden cable 3 – on the output side of the SE element	[m]
y	Sampled measurement vector	
ω_e	Eigenfrequency	[rad/s]
θ	Angular displacement corresponding to spring length	[rad]
ζ	Damping coefficient	
$\cdot\cdot_l$	Concerning a load	
$\cdot\cdot_{ref}$	Reference value	
$\wedge$	Estimated parameter	

Transfer functions

C	Controller transfer function	
$H_{actuator}$	Transfer function of the uncontrolled actuator, from control command to force output	[N/V]
$H_{closed\ loop}$	Transfer function of the feedback controlled actuator, from reference force to actual force output	
$Z_{actuator}$	Impedance transfer function of the uncontrolled actuator, from external output motion to output force	[N/m]
$Z_{closed\ loop}$	Impedance transfer function of the controlled actuator, from external output motion to output force	[N/m]

1. Introduction

a. Exoskeleton robots

Exoskeletons are a specific type of robots meant for interaction with human limbs. As the name indicates, these robots are basically an actuated skeleton-like external supportive structure. Such robots are usually meant for:

a.   extending or replacing human performance, for example in military equipment (Lemley 2002), or rehabilitation of impaired function (Pratt, Krupp et al. 2004),

b.   interfacing; creating physical contact with an illusionary physical environment or object; these *haptic* devices are usually referred to as kinaesthetic interfaces. Possible applications appear for example in gaming and advanced fitness equipment, or in creating 'telepresence' for dealing with hazardous material or difficult circumstances from a safe distance (Schiele and Visentin 2003).

c.   training human motor skills, for example in the rehabilitation of arm functionality (Tsagarakis and Caldwell 2003) or gait (Colombo, Jorg et al. 2002) after a stroke.

Every typical application brings about specific demands from a mechatronical design viewpoint, on total concept as well as on mechanical design, actuator selection and control outline level. The actuator discussed in this article was designed for use in an exoskeleton for gait training purpose, but might find wider application in other types of exoskeleton robots. First of all the specific application will be described, followed by design, model and performance indication of the actuator.

b. Context: a gait rehabilitation robot

We are developing a LOwer-extremity Powered ExoSkeleton (LOPES) to function as a gait training robot. The target group consists of patients with impaired motor function due to a stroke (CVA). The robot is built for use in training on a treadmill. As a 'robotic therapist' it is meant to make rehabilitation more effective for patients and less demanding for physical therapists. This claim is based on the assumptions that:

-    intensive training improves both neuromuscular function and all day living functionality (Kwakkel, Kollen et al. 2002; Kwakkel, Kollen et al. 2004),

-    a robot does not have to be less effective in training a patient than a therapist (Reinkensmeyer, Emken et al. 2004; Richards, Malouin et al. 2004),

-    a well reproducible and quantifiable training program, as is feasible in robot assisted training, would help to obtain clinical evidence and might improve training quality (Reinkensmeyer, Emken et al. 2004).

The main functionality of LOPES will be replacing the physiotherapists' mechanical interaction with patients, while leaving clinical decisions to the therapists' judgment. The mechanical interaction mainly consists of assistance in leg movements in the forward and sideward direction and in keeping lateral balance.

Within the LOPES project, it has been decided to realize this concept by connecting the limbs of the patient to an 'exoskeleton' so that robot and patient move in parallel, while walking on a treadmill (see Chapter 6). This exoskeleton is actuated in order to realize well-chosen and adaptable supportive actions which prevent fail mechanisms in walk-

ing, e.g. assuring enough foot clearance, stabilizing the knee, shifting the weight in time, et cetera. A general aim is to basically let the patient walk as unhindered as possible, while offering a minimum of necessary support and a safe training environment. Depending on training goals, some form of kinaesthetic environment has to be added. This constitutes the main difference between LOPES and the commercially available gait-trainers. Those are either position controlled devices that overrule the patient and/or allow only limited motions due to a limited number of degrees of freedom, and/or are not fully actuated (Hesse, Schmidt et al. 2003). Position controlled devices omit the training challenges of keeping balance and taking initiative in training. More research groups have recognized this deficiency (Riener, Lunenburger et al. 2005).

In the control design of the exoskeleton in general two 'extreme' ideal modes can be defined, that span the full range of therapeutic interventions demanded in the LOPES project. In one ideal mode, referred to as *'robot in charge'*, the robot should be able to enforce a desired walking pattern, defined by parameters like walking speed and step-length. This can be technically characterized as a high impedance control mode. In the other ideal mode, referred to as *'patient in charge'* the robot should be able to follow the walking patient while hardly hindering him or her. This can be technically characterized as a low impedance control mode. An intelligent controller or intervention by a therapist then can vary the actual robot behaviour between these high and low impedance modes.

c.   Impedance control in rehabilitation robotics

In the 'robot in charge'-mode it is important that the robot has enough bandwidth and power to realize the desired positioning performance with the desired, relatively high, impedance. In the 'patient in charge'-mode it is important that interaction forces between exoskeleton and human are controlled towards zero; in other words that the perceived impedance of the robot is low. In LOPES this will be realized using an impedance controller, as is often applied in kinaesthetic ('force feedback') interfaces (Adams and Hannaford 2002). The schematic outline of this control setup is shown in Figure 5.1.

An impedance control scheme is based on the adage 'measure position and display force'. This implies that the quality of the 'haptic display' depends on the accuracy of the position sensors and the bandwidth and accuracy of the force servos. This 'force-bandwidth' will depend on both the robot construction and the actuators as the quality of the force servo in general depends on these factors.

A fundamental limitation of impedance control is that the impedance of the robot construction in every actuated degree of freedom appears in the force transfer ('device impedance', Figure 5.1). It could only be compensated for in case of a proper dynamical model of
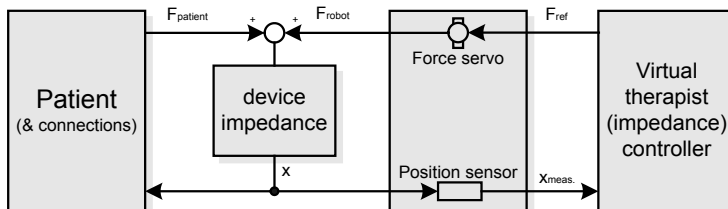

Figure 5.1: Basic outline of an impedance controlled device, applied on robotic therapy. Here the connections between device and patient are taken as a part of the patient impedance, so that the device can be considered rigidly connected to the 'patient'. x Indicates position, F forces.

this impedance, and proper measurements of position and velocity for stiffness (including gravitation) and friction compensation respectively. Mass compensation is only possible with explicit contact-force or acceleration sensing. A solution for this limitation is to use a lightweight, low friction construction and a low impedance actuator, so that the impedance of the device is kept low (Adams and Hannaford 2002). An important additional advantage of a light-weight, low impedance actuated design is its inherent collision safety (Zinn, Roth et al. 2004).

d. Actuator demands in an impedance controlled rehabilitation robot

The stated basic control strategy of impedance control implies specific demands for the actuators in the robot. They should:
- be 'pure' (low impedance) force sources
- add little weight and friction to the moving robot construction in *any* degree of freedom, not only the specific degree of freedom actuated by the considered actuator
- be safe, even in case of failure
- allow fast adjustment to the individual patient's sizes
- be powerful enough for the 'robot in charge' task.

More specific, it is required that the actuators should be able to modulate their output force with 12 Hz for small forces, and 4 Hz for the full force range. Maximum torques differ per joint, and range from 25 to 60 Nm. Joint powers range up to 250 Watt per joint. These numbers were based on study of the human gait cycle and the motion control range of a human therapist. An analysis of a nominal gait cycle (Winter 1991) was studied to obtain maximal needed torques, speeds and powers during walking, and general data on human motor control were studied to estimate maximum expected force-control speed and accuracy of a common therapist.

The resulting actuator bandwidths are typically lower, and the forces typically higher than in the specifications of common kinaesthetic devices which are intended for haptic display of a virtual object, but not to assist humans. Actuators usually selected for kinaesthetic devices are either heavy (like direct drive electro-motors) or poor force actuators (like geared DC motors), or suffer from moderate suitability for a rehabilitation setting due complex non-linear behaviour or lack of safety (like pneumatic muscles or cylinders) (Robinson 2000). The alternative to use spatial transmissions (e.g. cables) generally hinders fast adjustment of the exoskeleton to individual body sizes.

e. Article outline

In this article an actuator will be presented that is feasible for the use in an impedance controlled gait rehabilitation system, facilitating both low and high impedance control modes.

To avoid the mentioned drawbacks of conventional actuator technology a flexible Bowden-cable based transmission is combined with a spring based feedback force control loop. This allows for flexibly detaching the actuator from the robot frame, while achieving appropriate force control performance. The working principle is related to Series Elastic Actuation (SEA) (Robinson 2000). The important difference with standard SEA is the use of a Bowden cable transmission and the detachment of the power source from the robot frame. A fundamental issue therefore is whether this adaptation, which is expected to

worsen performance, still allows sufficient performance of the actuator system.

First the construction of the proposed actuator system will be presented. Secondly a model of the actuator will derived, covering the basic dynamics. Such a model would be useful for scaling this actuator for specific applications. This model will be compared with measurements. Finally the achieved controlled performance will be shown. Performance is defined as force tracking performance for the 'robot in charge' task, and amount of reduction of output impedance for the 'patient in charge' task.

2. Design of a Bowden-cable driven series elastic actuator

The basic idea, in designing the actuator was to detach the actual motor from the robot frame by the use of flexible Bowden cables (Figure 5.2) so that the exoskeleton legs can move unhindered, while little weight is added to the robot construction, compared to the relatively heavy electro motors.

The actuator system is constructed as a rotating joint, which has to function as a torque source. Such joints can be integrated in an exoskeleton (Figure 5.3) as for example hip and knee joints. Both the flexion and the extension (bending and stretching motion) cable are a continuous unit (Figure 5.3, sub 6). This was done for safety reasons. In case a cable breaks, its tension will be lost and no safety threat will occur to due unidirectional forces. This choice implies that the force transfer from the cables to the disc is friction based. The same applies to the cable connecting the springs; to prevent slipping, strips of high friction synthetic material have been fixed on the inside of the disk. Slippage would not affect the force output but could shorten the motion range.

The power transmission from motor to joint is realised by use of so called Bowden-cables. A Bowden-cable is a type of flexible cable used to transmit power by the movement of an inner cable relative to a hollow outer cable, generally a spiral steel wire with a plastic
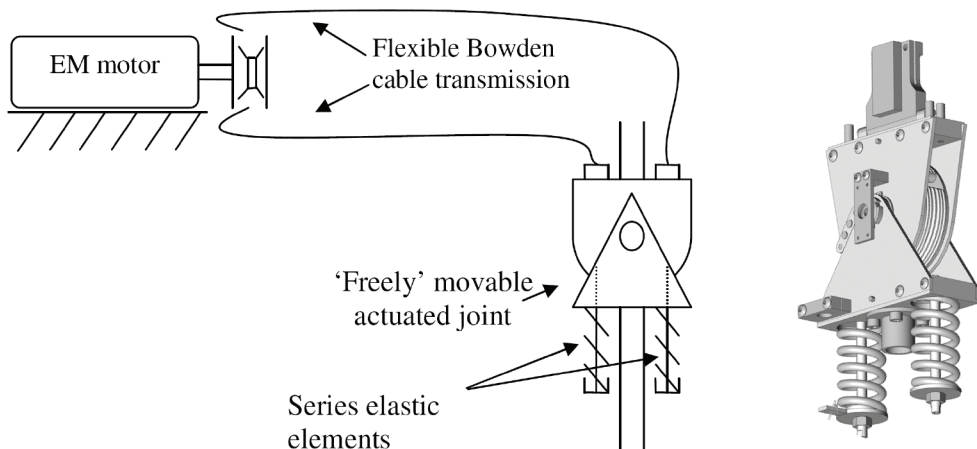

Figure 5.2: Left a global lay-out of the proposed actuator system. The actuated joint can be lightweight as the motor is placed on the fixed world. On the right the final design of the joint alone is shown.
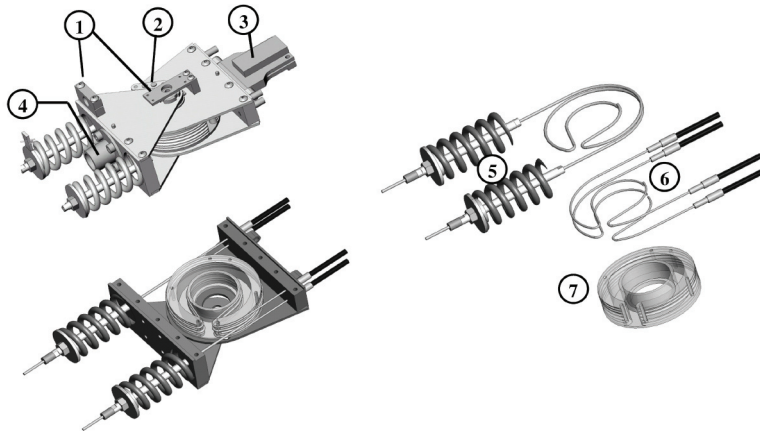
Figure 5.3: The picture shows the actuated joint, the other side (not visible) of the Bowden cables is connected to a second disk driven by a servo motor; the latter side is situated on the fixed world. The cable with the two springs is the connection between the actuated disk and the joint output axis. Numbered parts: 1. sensor mounts, 2. joint end-stop, 3. upper connection side of the joint, 4. lower connection side of the joint, 5. set of two pretensioned compression springs, realizing a rotational spring around the main joint axis; the series elastic element of the actuator, 6. set of two pairs of uninterrupted Bowden cables, connected to the motor, transferring force to the actuator disk via friction. 7. actuator disc; this disc can rotate independently of both connection sides of the joint, or rather, it is connected to them via a force coupling, not an angle coupling.

outer sheath, often containing an inner liner to reduce friction. Because Bowden-cables introduce orientation-, speed- and tension-dependent friction, friction compensation is needed. The angles of the curves in the cable and their radii appear to be the main determinants of the actual friction. Also wear and (pre-)tension of the cables are important factors. Because these parameters are hardly observable and their effects complexly interrelated, it is impossible to compensate the friction properly with feedforward control alone. Acceptable compensation may be achieved by introducing a feedback force control loop. This requires a force measurement located *after* the cable transmission.

We chose to use springs for force measurement. A spring can be considered as a compliant and relatively low-cost force sensor, as its length can be considered proportional with the force. Two compression springs were connected to the actuator disk with a cable so that a torque spring is created in between the actuator disk and the lower segment. The two compression springs are pre-tensioned with the maximally desired force, so that the connecting cable will always be under tension during operation.

The important advantage of a spring is that it allows treating the force control loop as a position control, because the spring length can be considered proportional to the force output. A higher compliance in the force sensor allows for higher control gains in the feedback spring length control loop. This way a better force control performance and actuator impact resistance can be achieved. Adverse effects of for example play and stick in transmissions can also be decreased this way.

The concept is similar to Series Elastic Actuation (SEA), treated extensively in (Robinson 2000). Its theoretical framework has to be only slightly adapted to be applicable on the actuator presented here. The differences with (Robinson 2000) are that we constructed a *rotational* joint instead of a linear (this has been implemented before(Torres-Jara

Table 5.1: stiffness of the different used springs and their resulting angular stiffness around the joint axis

	Catalogue value [kN/m]	Torsion stiffness [Nm/rad]
High Compliance Spring	14.4	63.6
Medium Compliance Spring	35.3	156.0
Low Compliance Spring	89.1	393.6

and Banks 2004), but that design was meant for use in the motor axis), *integrated* the actuator with the robot-joint and added a *Bowden cable* transmission (*common* cable drives have been used with SEA before, for example in the "Spring Turkey"(Pratt, Chew et al. 2001)).

The Bowden cable transmission might negatively influence the bandwidth of the actuator compared to common SEA, as it introduces friction and compliance into the position control loop. On the other hand, it is possible to select a heavier motor, as the motor weight is of no importance in this setting and a larger motor inertia will increase the bandwidth of the actuator, as a smaller gear-ratio, thus a smaller reflected mass can be used (Robinson, Pratt et al. 1999).

Basic design parameters, besides the choice of motor and gearing, are the actuator disk diameter and the stiffness of the springs. The diameter is a compromise between size of the joint versus low tension (thus friction) in the cables. The stiffness is a compromise of a high force control bandwidth versus minimal endpoint impedance combined with optimal non-linear (cable-) friction compensation (Robinson, Pratt et al. 1999).

The proposed actuator was designed and built to function as a knee joint. With this set-up (Figure 5.2), all presented measurements were carried out. It has an approximate peak torque output of 30 Nm. Four Bowden cables of 1.5m each were used. An LVDT sensor was used for spring length measurement. Three different sets of springs were used as series elastic element, as described in Table 5.1.
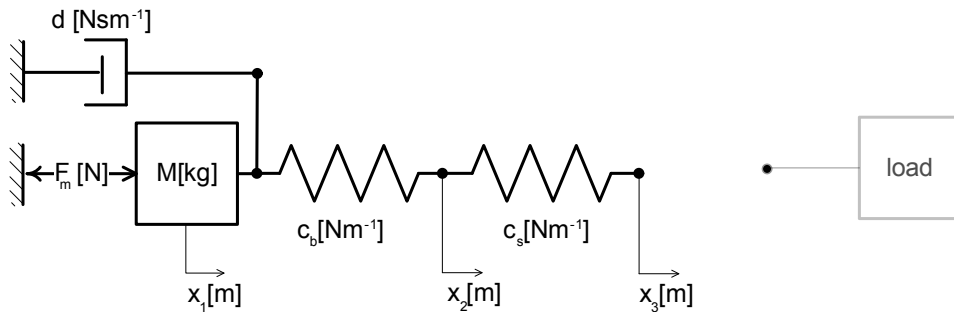
Figure 5.4: Outline of the essential dynamics of the actuator: the Ideal Physical Model (IPM) of the actuator. All degrees of freedom are transferred to the translational domain. F_m is the motor force, x_1 the position of the motor mass, x_2 the position of the actuator disc, which is the disc connecting Bowden cables with series elastic element, x_3 the position of the output axis, which may be connected to a load or to the fixed world, or be left open, in which case basically a very small load mass is connected. The system dynamics are described by the mass M, the stiffness of the Bowden cable cb and the stiffness of the series elastic element cs, and the damping d, and an arbitrary load defined by specific 2nd order dynamics M_l, d_l, c_l.
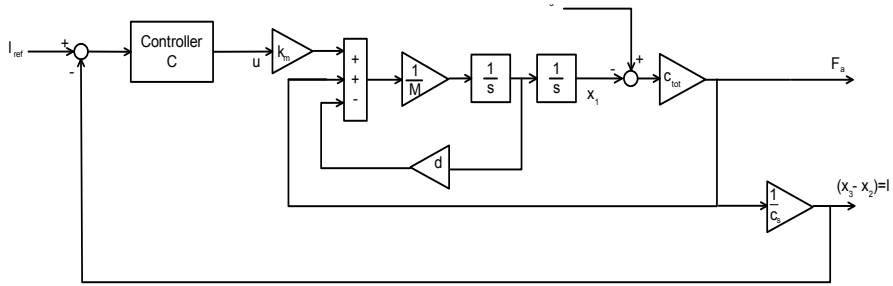
Figure 5.5: Flow scheme of the IPM from Figure 5.5, without load and with an added controller. In this scheme c_{tot} is the resulting stiffness of c_b and c_s, both the outputs F_a, the output force and l, the measured spring length, are defined. k_m is the transfer from control command u to actual motor force F_m and is taken to be a pure gain. l_{ref}, the reference length and l are defined as input and output to show the position control loop. The actuator output force is F_a. Tracking considers the transfer from l_{ref} to the output force or the actual spring length, and output impedance considers the transfer from x_3, the position of the output axis, to the output force.

3. Model of the actuator

a. Linear model

A basic model is assumed to be sufficient to describe the essential linear behaviour of the actuator (Robinson 2000; Sugar 2002). In this section a linear model will be proposed, containing the essential elements of the actuator. Afterwards expected non-linearities and their probable effects will be described. The model is presented as a translational Ideal Physical Model (IPM, Figure 5.4). This means that all parameters and variables were converted to the linear motion of the cables on the joint disc. Conversions from the rotational to the translational domain and vice versa do not affect model behaviour. In addition to the IPM a control scheme is given (Figure 5.5).

The simplest representation of the system is a 2nd order model, obtained when the output axis is fixed, or 4th order obtained when a freely movable load with 2nd order dynamics is added. Basic elements are:

- the inertia M, which is dominated by the motor inertia
- the damping d, which is dominated by the cable friction
- the stiffness c_{tot}, which dominated by the combination of the Bowden cable-stiffness c_b and the series elastic element stiffness c_s, as: $c_{tot} = \dfrac{c_b \cdot c_s}{c_b + c_s}$
- the load, which typically has specific 2nd order dynamics M_l, d_l, c_l.

This implies that in this model the mass/inertia of cables, springs and knee cable disc were neglected. The use of a current/torque-controlled servomotor is presupposed, but not necessary; an alternative would be a voltage/velocity controlled motor. The important transfer functions, which will also be measured and estimated, are:

1. the actuator behaviour, that is the transfer from control command (u) to actual output force (F_a), or possibly spring length (l).
2. the force tracking, that is the transfer from reference force ($l_{ref} \cdot \mathbf{c_s}$) to the actual force ($F_a$), or also from reference spring length (l_{ref}) to actual spring length (l).
3. the output impedance, that is the transfer from external position (x_3) to force output (F_a), or also from external position (x_3) to the actual spring length (l).

Depending on the situation it might be more feasible to use deflection (*l*), forces (*F*), torques (*T*), or disc rotation (*θ*) as in- and output. These conversions are all linear factors, following figure 5.6.
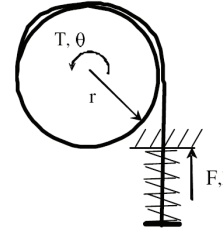
$$F = c_s \cdot l$$
$$T = r \cdot F$$
$$\theta = \frac{l}{r}$$

In case the load has infinite impedance (x3 fixed), the linearised transfer from control command u to output force Fa of the uncontrolled actuator is:

Figure 5.6: conversions as necessary to switch between several in- and out-put definitions. c_S Is the stiffness of the series elastic spring.

$$H_{actuator}\big|_{Z=\infty}(j\omega) = \frac{F_a}{u} = k_m \cdot \frac{\dfrac{c_{tot}}{M}}{(j\omega)^2 + \dfrac{d}{M}(j\omega) + \dfrac{c_{tot}}{M}} = K_H \cdot \frac{\omega_e^2}{(j\omega)^2 + 2\zeta\omega_e(j\omega) + \omega_e^2} \qquad (5.1)$$

, which is similar to a standard damped second order system, as described with the last term of the equation in terms of system gain $(K_H = k_m)$ eigenfrequency (ω_e) and damping ratio(ζ). These three parameters can then be estimated from measurements.

A controller can be added, resulting in a closed loop transfer of:

$$H_{closedloop}\big|_{Z=\infty}(j\omega) = \frac{F_a}{F_{ref}} = \frac{C \cdot H_{actuator}\big|_{Z=\infty}}{1 + C \cdot H_{actuator}\big|_{Z=\infty}} \qquad (5.2)$$

The output impedance, which is the transfer from x_3 to $F\ (=c_s\cdot l)$, is in the uncontrolled (*u*=0) case:

$$Z_{actuator}(j\omega) = \frac{F_a}{x_3} = c_{tot} \cdot \frac{(j\omega)^2 + \dfrac{d}{M}(j\omega)}{(j\omega)^2 + \dfrac{d}{M}(j\omega) + \dfrac{c_{tot}}{M}} = K_Z \cdot \frac{(j\omega)^2 + 2\zeta\omega_e(j\omega)}{(j\omega)^2 + 2\zeta\omega_e(j\omega) + \omega_e^2} \qquad (5.3)$$

Note that both ω_e and ζ are the same as in (5.1), but that K_Z differs from K_H. In case the controller is switched on and $l_{ref} = 0$, the output impedance transfer function becomes:

$$Z_{closedloop}(j\omega) = \frac{F_a}{x_3} = c_{tot} \cdot \frac{(j\omega)^2 + \dfrac{d}{M}(j\omega)}{(j\omega)^2 + \dfrac{d}{M}(j\omega) + \dfrac{c_{tot}}{M} + \dfrac{c_{tot}C}{c_s M}} = \qquad (5.4)$$

$$K_Z \cdot \frac{(j\omega)^2 + 2\zeta\omega_e(j\omega)}{(j\omega)^2 + 2\zeta\omega_e(j\omega) + (1 + C')\cdot\omega_e^2}$$

$$\text{where: } C' = \frac{C}{c_s}.$$

Typical model behaviour

The typical dynamics of the modelled system, as described by the transfer functions (5.1) and (5.3), is given in figure 5.7. As can be read from equation (5.4) the output impedance can be influenced in case of feedback control by changing the controller C. For
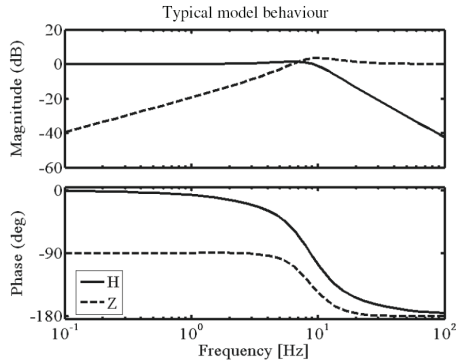
Figure 5.7: Qualitative model behaviour. Bode plots of the uncontrolled actuator transfer H (5.1) and output impedance transfer Z (5.3), both scaled to 0dB gain, and both calculated for the same realistic system. The high frequent gain of the impedance transfer is equal to the stiffness c_{tot}.
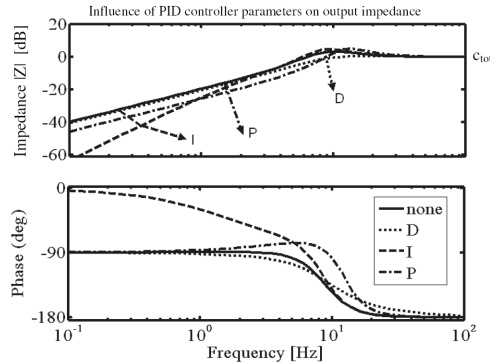
Figure 5.8: Effect of increasing the several terms of the PID controller (*C*) on the output impedance transfer . Changing these terms should of course always consider stability issues. It is clear that at high frequencies the impedance always becomes the same physical parameter c_{tot}. This value has in the plot been scaled to 0 dB.

the case of a PID controller the influence of changing the three basic parameters of a PID controller are given in figure 5.8.

This model can be used to predict the basic dynamics of the system from design parameters. To validate the model, its parameters should be identified from measurements, followed by a comparison of model output with measurements. Identification will be done by Process Model Identification, optimizing the parameters of a chosen transfer function according to measurements, using non-linear least squares minimization, as described in (Ljung 1999; Ljung 2003). All measurements were done at sample rate 5 kHz, and downsampled where needed for proper identification. As input signal a crest optimized multisine signal was used, containing frequencies from 0.1-20Hz or 0.1-30Hz. For reference also higher order fits or other identification methods were performed; this will then be mentioned. To obtain a quality measure for the model fits, the variance-accounted-for factor was chosen, which is defined as:

$$VAF = \left(1 - \frac{var(y - \hat{y})}{var(y)}\right) \cdot 100\% \qquad (5.5)$$

, where y is the measurement output and $\hat{y}$ the output of the model, using the same input. A VAF factor of 100% indicates a perfect fit.

To obtain an overall transfer function of the system, measurements with varying amplitudes were done to obtain an average fit. This identification was done for all three different springs, altering the stiffness of the series elastic element, according to Table 5.1. For comparison the model system eigenfrequency is calculated, as determined by the reflected mass (14 kg) and the series stiffness of the Bowden cable and the SE springs.

b. Expected non-linearities

As mentioned the model is linear. Differences between model predictions and measurements may be expected due the several non-linearities in the actual system. The most important ones are:

- the relation between control command u and the motor force F_m; it is neither a linear nor a pure static relation, as the motor is not an ideal force source (cogging, gearbox play, complex friction) and an electric current control scheme is needed for servo motor torque control, which has its own dynamics, albeit of high frequency compared to the measurements range.
- The real friction is not damping, as the friction of a Bowden cable is complex and depends on many parameters. Also gearbox and other elements contribute to friction.
- The force of the motor, F_m, is limited (at higher velocities depending on the actual $\dot{x}_1$, via a maximal power). This introduces saturation effects in the system. From former studies on SEA it is known that closed loop bandwidth for large forces (large force bandwidth (Robinson 2000)) is determined by saturation and amounts $\sqrt{\frac{C_{tot}}{M}}$, which is also the eigenfrequency of the model transfer of the uncontrolled actuator .

These non-linearities should be kept in mind when identifying parameters, and using the linear model for prediction and design. Most of the described non-linearities are expected to result in an amplitude dependency of the transfer functions. This dependency can be demonstrated by estimating the linear model parameters like before, but for input several constant input signal amplitudes. For every spring three (RMS) amplitudes were measured and fit on the same 2nd order model. A change of cable curvature was carried out to show the effect of a changing friction on the model parameters.

c.   Performance of the actuator

The developed model was mainly meant for design purposes. The performance of the actuator can be considered independently of such model assumptions. In this chapter several issues are considered that determine the feasibility of the actuator for the described application (compare (Hayward and Astley 1996),(Morrell and Salisbury 1998)). Performance depends on many small constructive and sometimes controller decisions, so the outcome should be interpreted as a mere indication of the achievable performance with the presented type of actuation. The joint is as much as possible used in the way it will be used in the final design of the rehabilitation robot.

The performance will be considered in four consecutive issues:

1. Quality of spring based force measurement: how well can the output force or torque be determined by only measuring the deflection of the series elastic element?
2. Bandwidth of force tracking with fixed load: Up to what frequency can the output force of the actuator be modulated using a basic control scheme?
3. Reduction of the output-impedance: how well can the same controller decrease the output impedance of the actuator?
4. Fidelity (or distortion) of force output: how severely is the force output distorted by system non-linearities?

All four issues or measurements will be described shortly below.

For the measurements 2-4 a Bowden cable course has to be defined, as this determines performance. The optimal course of a Bowden cable would be straight, as bending introduces friction and play. A realistic standard situation was defined in which the Bowden

cables are bent over 90° with a radius of 0.8 m. For the sake of conciseness, measurements were only carried out on the medium compliance spring, unless important additional information could be obtained otherwise.

Quality of spring based force measurement

As the springs in the joint are used for force measurement in the control loop, a measurement is done to determine how well the spring-deflection reflects the actual force output. To check this, the joint was fixed on both sides, on one side via a 6D force sensor. From the force sensor measurements the joint torque was calculated and this was compared to the force output based on the spring deflection. As reference input a ramp signal was used. Both signals were filtered at 30 Hz. The low compliance spring was used as worst case example.

Bandwidth of force tracking with fixed load.

To obtain acceptable force tracking a feedback loop is needed. As this article is about the basic outlines of a new type of actuator, only a straightforward controller will be presented. The objectives of the controller design were to improve the extent and accuracy of the force control, to reduce the apparent friction and inertia when back driven, and to reduce the sensitivity to load impedance variations. The force command was interpreted as a desired spring-length, which then was controlled in a feedback loop, resulting in a torque command to the servomotor of the actuator.

A tuned PID controller is the most straightforward choice, and can be designed based on the open loop behaviour of the plant and/or basic tuning rules, like the ultimate cycle method of Ziegler and Nichols. This method has been used to tune a feasible controller.

Due to the amount of noise in the spring length measurement (LVDT), the differential action of the controller introduced a lot of noise into the control command. To prevent this, the encoder measurement of the motor position was used in the differential part of the controller.

This concept of sensing, load position together with actuator velocity, is also generally known to be a workable, conditionally stable concept for 4th order systems(Groenhuis 1991). An alternative would be to design an optimal state space controller based on a measured open loop transfer.

The transfer of the feedback controlled actuator was determined and compared with the uncontrolled actuator. Transfers at force amplitudes of 1, 2, 4 and 8 Nm were measured.

Additional measurements were done with cables bent over 180° with a radius of 0.4 m. Such a configuration should be avoided during operation but illustrates the effect of excessive bending. Force tracking transfer functions were identified using a multisine signal with frequency content between 0.1 and 30Hz. The signal was crest optimized, to prevent appearance of high peaks in the composed signal. The Frequency Response Functions were directly calculated from the output response and this signal, averaged over several frequencies and then checked on validity of estimations calculating the coherence of the result.

Reduction of the output–impedance

In relation to the 'patient in charge'-mode it is interesting to determine how low the impedance of the output axis can be controlled. This is also called the backdriveability of

the device or actuator. The uncontrolled actuator itself is already backdriveable, but still has, depending on the actual configuration, quite high impedance, caused by the large friction of the cables and the reflected mass of the motor. In our case the motor has a relatively low gearing (8:1), so the reflected mass is also low, but in general this might become considerable.

The output-impedance is measured by imposing a position trajectory upon the output axis of the joint, by hand, and then measuring the interaction force between robot and hand. The hand was considered feasible as disturbance source, considered the intended application of the actuator. The spring length was used as force measurement. The transfer from joint angle to actuator torque then is the mentioned impedance. The impedance was measured both in the controlled and uncontrolled situation, to show the improvement obtained by using a force feedback loop. The measurements for the controlled situation were done using the same force control settings as above, while using a zero reference force. It appeared that the power spectrum of the hand-perturbations ranged from about 0.7 to 4 Hz. In addition time domain plots of force response to external motion show implications of non-linear effects, like stick friction.

Force fidelity

As mentioned, one of the effects of non-linearities in a system is distortion of signals: the output signal contains additional frequencies compared to the input signal. Several metrics can be defined to characterize the amount of distortion or its inverse, the fidelity of the system: how undistorted the output signal is compared to the input. The importance of such a metric for actuator comparison was recognized by Morell and Salisbury (Morrell and Salisbury 1998) and by Hayward(Hayward and Astley 1996). To quantify fidelity the following procedure was used (which differs from the method of the mentioned authors):

As input signal a pure sine was used, the output then was measured and scaled to fit the input signal optimally, using an RMS based optimal fit. This way both gain and phase shift are compensated for and solely the remaining (frequency-) distortion can be measured. To quantify the corresponding fidelity, a measure based on the variance-accounted-for factor was used, defined as:

$$fidelity = \left(1 - \frac{\text{var}(y-R)}{\text{var}(y)}\right) \cdot 100\% \tag{5.6}$$

, where y is the vector of the sampled measurement and R the vector of the sampled sine, that was scaled to fit the measurement. Fidelity of 100% indicates a perfectly undistorted sine.

The fidelity of outputs of both the uncontrolled and the controlled actuator were measured as a function of the frequency. In both cases the output torque was tuned to have a peak value of about 2Nm magnitude. In case of the open loop measurement the control command was a sine of a given frequency, which was increased in amplitude until the output showed the desired amplitude. The sampled torque output signal is the vector y. In case of the closed loop measurement, the reference was set to amplitude 2Nm. Again the sampled torque output signal was used as vector y. The measurements were filtered with a 100Hz first order Butterworth filter.

4. Results

a. Feasibility of the Model

Overall linear model

The parameters K, ω_e and ζ, as defined in equation (5.1) were estimated by fitting a general 2nd order model on the measurement data. The coefficients of these fits are shown in Table 5.2. In addition the ω_e, as predicted by the model, according equation (5.1) equal to $\sqrt{\frac{c_{tot}}{M}}$ is given for varying stiffness.

These results are also shown in the bode plots of Figure 5.9. To show how well a 2nd order model fits a measurement, the overall 2nd fit for the low compliance spring was compared with both a 3rd order PMI fit and an optimal order State Space identification (Ljung 1999) (Figure 5.10).

It can be seen that eigenfrequency estimation of the 2nd order fit only is a rough estimate of the actual system. The calculated VAF-factor, according (5.5), was 71% for the 2nd order estimate, and considerably higher for the higher order fits, 85 and 86%. These appeared to be similar for each spring stiffness.

Table 5.2: Parameters of the 2nd order model structure according to (1.1), as identified from measurements for all three sets of springs. Also the model predicted ωe is shown.

SE spring	$\hat{K}_H$	$\hat{\omega}_e$ [rad/s]	$\hat{\zeta}$	Model ω_e
High Compliance Spring	4.3	41	0.67	39
Medium Compliance Spring	5.4	55	0.47	55
Low Compliance Spring	5.4	66	0.40	71
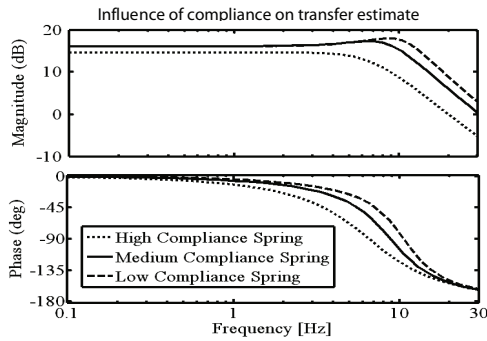
Figure 5.9: Effect of the spring stiffness on the overall uncontrolled actuator transfer functions for overall amplitude (2nd order model measurement fits).
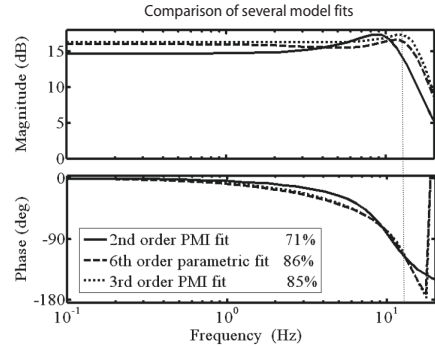
Figure 5.10: Comparison of a fit onto the proposed 2nd order model structure compared to a 3rd order fit and an optimal 6th order parametric fit. VAF-factor for the 2nd order fit is 71%, for the 3rd order fit 85% and for the 6th order 86%. This indicates that a 3rd order model might predict the system behaviour more adequately (Low Compliance Spring)

Table 5.3: Parameters of the 2nd order model structure according to equation (5.1), as identified from measurements with varying amplitudes u for all three sets of springs. All measurements were done with a curvature of 90º over 0.8m, except the last one which was done with a curvature of 180º over 0.4m.

SE spring	RMS u	$\hat{K}_H$	$\hat{\omega}_e$ [rad/s]	$\hat{\zeta}$	VAF
High Compliance Spring	1.0	2.9	35	1.54	70 %
	1.5	4.3	41	0.77	84 %
	2.0	5.0	42	0.56	87 %
	Overall	4.3	41	0.67	77%
Medium Compliance Spring	1.0	5.3	51	0.49	86 %
	1.5	5.2	53	0.51	88 %
	2.0	5.9	55	0.36	91 %
	Overall	5.4	55	0.47	86 %
Low Compliance Spring	1.0	4.2	57	0.64	75 %
	1.5	5.4	65	0.43	82 %
	2.0	5.9	69	0.35	87 %
	Overall	5.4	66	0.40	71 %
Medium Compliance Spring (180º bent)	1.0	2.6	25.9	1.52	53 %
	1.5	2.9	47.9	1.06	67 %

Amplitude dependency

Table 5.3 shows the dependency of estimated model parameters to the amplitude of the input signal. For comparison also the overall estimates for varying amplitudes are shown again. The results are given for all sets of springs, and also for the situation with excessive curvature of the Bowden cables.

In general it appears that the relative contribution of the friction or damping is larger for small command amplitudes, as the identified damping ratio increases. The best iden-

tifications were achieved with the medium compliance spring (VAF 86-91%). The low compliance spring (VAF 71-87%) and the high compliance spring (VAF 70-87%) systems were estimated slightly worse. For high compliance this is due to the fact that the system is identified as more heavily damped. The estimations with the 180º bent cables were poor (VAF 53-67%), due to the heavily increased stick friction in this case.

b. Actuator Performance

Quality of spring based force measurement

A representative measurement (Figure 5.11) shows the force estimate based on the spring deflection compared to the actual torque output, as measured by the force sen-
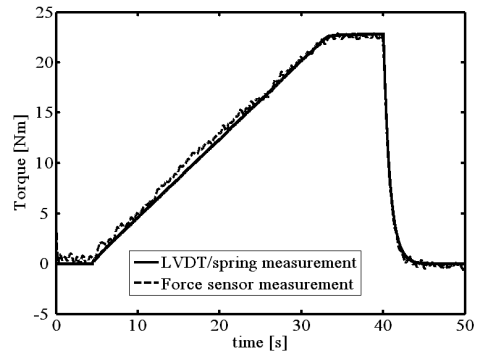

Figure 5.11: Representative comparison of torque determined from an lvdt measurement of spring deflection versus torque determined from a force sensor measurement. The reference for the torque was a ramp signal controlled on the spring measurement. (Low Compliance Spring)
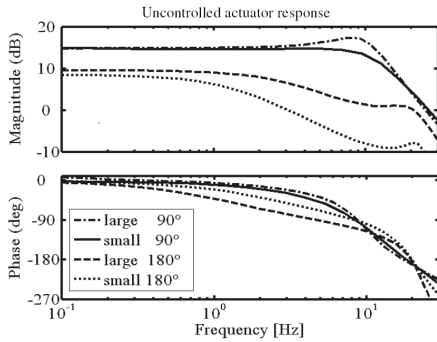
Figure 5.12: Response of the uncontrolled actuator. Bode plot of the transfer from input control command to output joint torque. The RMS amplitude of the input signal [small 1.0 , large 2.0] and the course of the Bowden cables have been varied [90°,180°]. The fits are optimal parametric fits of appropriate order. (Medium Compliance Spring)

sor. The low compliance spring was chosen, as it was the worst case situation.

Bandwidth of force tracking with fixed load.

Before presenting the results of the feedback controlled actuator, the estimates of the uncontrolled actuator transfer, according (5.1), are given in Figure 5.12. The Medium Compliance Spring was used. RMS amplitude of the input signal and the Bowden cable curvature were varied. The effects on these results of varying spring stiffness can be concluded from equation 5.1, Figure 5.1 and Table 5.2.

The bandwidth appears to be about 11 Hz, which is also the large force bandwidth of the system, which is the worst case bandwidth, if only linear model and saturation are considered.

The performance of the feedback controlled actuator with the implemented PID controller is presented in Figure 5.13. The RMS amplitude of the input was varied. It can be seen that the controlled bandwidth of the actuator is over 20 Hz for the measured range of torques in a normal Bowden cable course. For small torques the transfer falls off already at a lower frequency. Closed loop bandwidths for other compliances follow from equation 5.2; by adjusting controller gains the closed loop transfers for any compliance can be adjusted to the same performance as the shown transfer (see also (Robinson 2000)), unless saturation limits are reached.

In case the cable is excessively bent, the effects of friction increase dramatically, as could already be noticed in the uncontrolled actuator bode plot. The controlled actuator bode plot also shows a dramatic decrease of performance (Figure 5.14).

Figure 5.13: Bode plot of the closed loop transfer from reference torque to actual torque. The RMS amplitude of the reference was varied. Here the orientation was 90° with a bending radius of 0.8m. (Medium Compliance Spring)
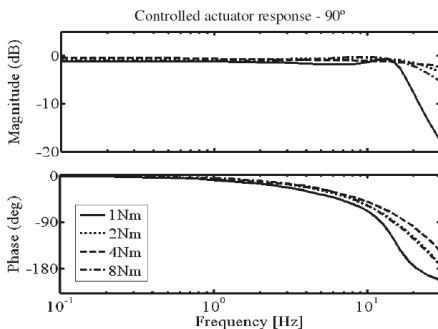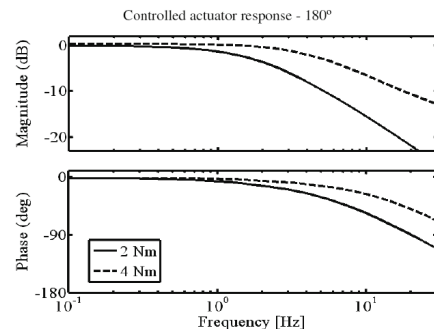

Figure 5.14: Bode plot of the closed loop transfer from reference torque to actual torque. The RMS amplitude of the reference was varied. Here the orientation was 180° with a bending radius of 0.4m (Medium Compliance Spring)

Figure 5.15: Bode plot of the impedance identifications of several measurement-series in both controlled and uncontrolled situations. The input motion disturbance signal was applied by hand. Only the frequency range with appropriate coherence is shown. (Medium Compliance Spring)

Figure 5.16: Typical torque response of the actuator to external motion, while controlled to zero force output. The small peaks are caused by stick, appearing when the motion is reversed. This Figure is also a typical time domain example of the impedance measurements (Medium Compliance Spring).

Reduction of the output-impedance

The reduction of output impedance as achieved by using the PID controller with a zero reference force is presented in a bode plot (Figure 5.15).

From this figure it can be concluded that a reduction of $10 - 13$ dB (factor $3 - 4.6$) of impedance can be realized with feedback control in the frequency range of application. The values of the torques range from negligible up to 0.7 Nm for around 4 Hz motion. The noticeable effects of cable stick forces on the output force are also reduced. The time domain plot (Figure 5.16) shows the small peaks caused by static friction compared to the overall torque response. Tests with a walking subject connected to this joint confirmed that the controlled impedance was low enough to experience unhindered lower leg motion.

Force fidelity

Figure 5.17 shows the closed loop torque-tracking output and its best fit sine at 2Hz, Figure 5.18 for 20Hz. A best fit sine is used instead of the reference sine, as at this point

Figure 5.17: Time domain example. The output for closed loop tracking of a 2Hz sine is shown, together with its best-fit sine. The effects of stick friction are visible. The fidelity for this tracking is 98.7%. This shows how sensitive this metric is. (Low Compliance Spring).

Figure 5.18: The output for closed loop tracking of a 20Hz sine is shown. The fidelity for this tracking is 94.7%. This fidelity is worse due to relatively low frequency disturbances, which are slightly visible in this plot (Low Compliance Spring).
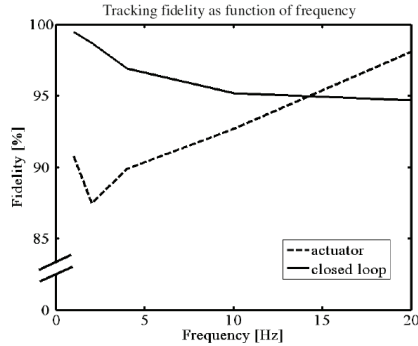
Figure 5.19: Force fidelity of the actuator. The plot shows the fidelity for different signal frequencies, both for the uncontrolled actuator and the closed loop controlled actuator. The measurement was carried out using the low compliance spring which yields the worst fidelity.

solely the distortion of the signal is addressed, not phase shift or amplification. The values for fidelity and distortion according to the given definition show that this quality metric is quite sensitive. One should be careful to qualify seemingly high factors as 'good'.

As was expected, the low compliance spring gave the most distorted force output (comparison between springs is not shown). With this spring the force fidelity of the actuator has been measured. The standard 90º cable courses were applied. In general smaller torques show a decreasing and larger torques an increasing fidelity, outside saturation limits (Figure 5.19).

It is clear that for relatively low frequencies (<15Hz) the controller improves the fidelity of the force output.

5. DISCUSSION

a. Feasibility of the model

Comparing the estimated overall eigen-frequencies with those calculated from design parameters, as presented in Table 5.1, shows that estimation and calculation on this aspect agree quite well (error <10%). The damping coefficients can not be estimated from design parameters due to the complex friction of the Bowden cables. The system can however be expected to be heavily damped.

It was shown that the actual system agrees better with a 3rd order system, increasing the VAF factor from 71% to 85%. This indicates that some important dynamics have been neglected in the model. Most probably the modelling of the Bowden cable as pure spring/da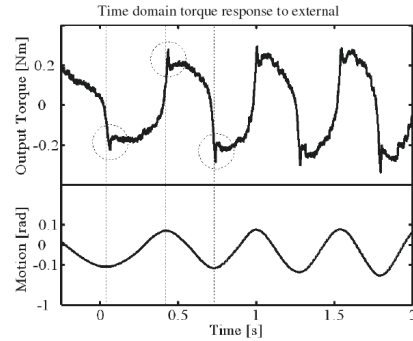mper is too far from reality. The neglected actuator disc inertia is too small to explain this difference. The estimated parameters appear also to depend heavily on the RMS amplitude of the input signal as shown in Table 5.2, indicating amplitude-dependent nonlinearities. Especially for small amplitudes outcomes deviate from the overall estimates and model predictions. This is not too surprising, as especially with low control commands static friction dominates the friction behaviour, resulting in stick-slip, while also the motor torque with low speeds is expected to be less linear related to the control command. This all indicates that for a control design that incorporates the full complexity of system dy-

namics, more than a 2nd order approximation is needed.

b. Actuator performance

Figure 5.10 showed that spring length measurement can be well used as force measurement, as the resulting force estimate only deviates slightly from the reference force sensor measurements for the worst case (low) compliance. Differences are caused by friction in the joint and stretch of the spring cable and the non-ideal physical springs. The cable used for connecting the springs is an order of magnitude 100 stiffer than the medium compliance spring; this will therefore only introduce a slight measurement error.

Using a basic PID controller the actuator was able to achieve force control up to a bandwidth of 20 Hz and an expected large force bandwidth of up to 11 Hz for the full force range. For small torque amplitudes and heavy Bowden cable bending this bandwidth decreased to as low as 2-3 Hz. This could to some extent be compensated for by increasing controller gain, which is possible as long no saturation for the motor is reached. Doing this in practise would demand a good observation of the situation as a return to the standard cable course or normal amplitudes could result easily in instability due to the decrease of physical damping. These problems can partly be avoided by constructing the robot in such a way that cables are never bent excessively. The decrease in bandwidth for (very) small torques is supposed to be an inherent limitation of the system. The extent of this effect depends on the needed (pre-) tension in the cables. Its acceptability depends on the application. Stick-slip compensating control strategies like dither signals, seem to be poorly applicable in Bowden cables. A feasible possibility is perhaps a direct measurement of the friction forces, and incorporating this measurement in the controller.

The output impedance was shown to be considerably reducible by 10-13dB below uncontrolled behaviour. This meant in this application a maximum torque of 0.7 Nm during 4 Hz imposed motion. For gait rehabilitation practice such frequencies are high, and such torques negligible, thus the reduction is acceptable. From the time domain plot it appeared that at every reverse of velocity small torque peaks occur. Their size of about 0.1 Nm is however again negligible for the present application.

Fidelity of the force control appeared to be good – above 95%. Below 15 Hz the feedback controller appeared to reduce distorting effects compared to the fidelity in uncontrolled situation. It is however not fully clear how well the defined metric reflects actually sensed 'smoothness' of force output.

As was shown in Table 5.1 and Table 5.2, the spring stiffness affects all parameters of the system, and therefore will also affect actuator performance. It was shown that a system with stiffer spring has a higher bandwidth in open loop and is relatively less damped than with more compliant springs. A stiffer spring showed worse estimates of the transfer functions, implying more non-linear distortion. This might be explained by the smaller motions of the motor that affect the linearity of the relation between control command and motor torque, or also by the smaller amplitudes of needed spring deflections which increase the effect of play in the transmissions.

Finally, some notes should be made on the stability of the controlled actuator, considering the mentioned non-linearities, especially in the Bowden cable friction. The presence of the compliant element allows for a much higher position control gain, implying a better internal error rejection (Robinson 2000). Furthermore stability can be assured if the controller is tuned to the realistic cable situation with the least friction, so that changing the

situation means increasing friction, which will lower performance but not affect stability, as friction forces always stabilize a system and the possible source of instability could only be overcompensation. This can be concluded considering a Lyapunov-stable linear system; if extra non-linear friction is added, more energy will be dissipated from the system, so that it will stay Lyapunov-stable.

6. Conclusions

A new Bowden-cable-based series elastic actuation system was proposed for use in the exoskeleton-type rehabilitation robot LOPES. A robot joint containing this actuation system was constructed. It was shown that the performance demands of realizing a safe, lightweight, adjustable and powerful torque source were met. A force bandwidth of up to 20 Hz appeared feasible, when extreme cable bending was avoided. Minimal value of the bandwidth appears at higher forces caused by saturation. Maximum bandwidth in this case is the bandwidth of the uncontrolled actuator, about 6-10 Hz. This was considered adequate to control human gait using an impedance controlled exoskeleton. The joint appeared also suitable for low impedance control to facilitate unhindered motion, with maximal torque peaks of 0.7 Nm at 4 Hz motions on a scale of a 30 Nm actuator (less than 2.5%). This implies that a robot using these joints would be able to be used in both a high impedance 'robot-in-charge' as well as in a low impedance 'patient in charge' task for rehabilitation robots, as far as joint and actuator performance are considered.

Beside this typical application in the LOPES project, the principle of actuation could possibly find a wider use in all kinds of exoskeleton-like kinaesthetic interfaces. Of course dimensions should be optimized for every specific application. A basic model appeared convenient for specific design. Of course analyses of interaction with typically expected loads should also be carried out.

The developed actuator system showed that the principle of Series Elastic Actuation can be applied using a heavy friction transmission like Bowden cables. Despite the power loss, the heavy friction does not have to affect performance, because heavier motors can be selected, since they are detached from the actual robot construction. The friction of Bowden cables could well be compensated with high gain feedback control.

A basic second order model was presented and shown to acceptably predict the eigenfrequency of the system as needed for design purposes. For detailed controller design a more accurate fit would be favourable, as there were strong indications of higher (3rd) order dynamics. It was shown that, away from saturation limits, static friction or stick was the most apparent non-linearity in the system. It was also shown that stick hardly distorted the controlled force output at frequencies below 15 Hz.

Spring stiffness variation showed that both a too stiff and a too compliant spring can worsen performance. A stiff spring reduces the maximum allowable controller gain. The relatively low control gain then causes a larger effect of stick in the force output, resulting in a less smooth output in general. A low spring stiffness, on the other side, decreases the bandwidth of the system as demanded displacements, velocities and accelerations increase, which will saturate at a certain level. For every specific application this trade-off has to be made. During design exact required bandwidth or exact amount and implication of stick might not be known. However springs can easily be exchanged; the desired order of mag-

nitude will be known.

It was shown that a standard tuned PID controller suffices to control the actuator accurately supposing normal working conditions (no excessive cable bending, no active/instable loads).

Improvements of the actuator system could be realized in reducing system complexity, size and weight on one side, and controller improvements on the other. The complexity of the system can be slightly reduced by using two (thicker) Bowden cables instead of four. This has been tested and appeared to be equivalent in performance. Also the LVDT sensor has been replaced by a linear slider potentiometer, which is both smaller and cheaper, and also appeared equivalent. Possibly a torsion-spring element could be constructed instead of the two compression springs, which would reduce size and weight. Feasible commercial torsion springs however were not found. The controller outline could be changed to deal better with the specific non-linearities, like the so called 'late motor processing' as described in (Pratt, Willisson et al. 2004), or by using voltage/velocity control instead of current/torque control. Finally, the joint could be redesigned to optimize the cable replacement procedure, and durability tests should be done to determine the needed frequency of cable replacement.

7. References

Adams, R. J. and Hannaford, B. 2002. Control law design for haptic interfaces to virtual reality. IEEE Transactions on Control Systems Technology, 10(1): 3-13.

Colombo, G., Jorg, M. and Jezernik, S. 2002. Automatisiertes Lokomotionstraining auf dem Laufband - Automated Locomotor Training on the Treadmill. Automatisierungstechnik, 50(6): 287-295.

Groenhuis, H. 1991. A design tool for electromechanical servo systems. University of Twente, Enschede.

Hayward, V. and Astley, O. R. 1996. Performance measures for haptic interfaces. Paper presented at the Robotics Research: The 7th International Symposium,.

Hesse, S., Schmidt, H., Werner, C. and Bardeleben, A. 2003. Upper and lower extremity robotic devices for rehabilitation and for studying motor control. Current Opinion in Neurology, 16(6): 705-710.

Kwakkel, G., Kollen, B. J. and Wagenaar, R. C. 2002. Long term effects of intensity of upper and lower limb training after stroke: a randomised trial. Journal of Neurology Neurosurgery and Psychiatry, 72(4): 473-479.

Kwakkel, G., Kollen, B. and Lindeman, E. 2004. Understanding the pattern of functional recovery after stroke: Facts and theories. Restorative Neurology and Neuroscience, 22(3-5): 281-299.

Lemley, B. 2002. Really Special Forces, Discover: 25-26.

Ljung, L. 1999. System Identification - Theory for the User (2nd edition ed.). Upper Saddle River, N.J.: Prentice-Hall.

Ljung, L. 2003. Identification for Control: Simple Process Models. SE-581 83 Linköping, Sweden: Department of Electrical Engineering, Linköping University.

Morrell, J. B. and Salisbury, J. K. 1998. Parallel-coupled micro-macro actuators. International Journal of Robotics Research, 17(7): 773-791.

Pratt, G. A., Willisson, P., Bolton, C. and Hofman, A. 2004. Late Motor Processing in Low-Impedance Robots: Impedance Control of Series-Elastic Actuators. Paper presented at the American Control Conference, ACC'04, Boston, Massachusetts USA.

Pratt, J., Chew, C. M., Torres, A., Dilworth, P. and Pratt, G. 2001. Virtual model control: An intuitive approach for bipedal locomotion. International Journal of Robotics Research, 20(2): 129-143.

Pratt, J. E., Krupp, B. T., Morse, C. J. and Collins, S. H. 2004. The RoboKnee: an exoskeleton for enhancing strength and endurance during walking. Paper presented at the Robotics and Automation, 2004. Proceedings. ICRA '04. 2004 IEEE International Conference on.

Reinkensmeyer, D. J., Emken, J. L. and Cramer, S. C. 2004. Robotics, motor learning, and neurologic recovery. Annual Review of Biomedical Engineering, 6: 497-525.

Richards, C. L., Malouin, F., Bravo, G., Dumas, F. and Wood-Dauphinee, S. 2004. The role of technology in task-oriented training in persons with subacute stroke: A randomized controlled trial. Neurorehabilitation and Neural Repair, 18(4): 199-211.

Riener, R., Lunenburger, L., Jezernik, S., Anderschitz, M., Colombo, G. and Dietz, V. 2005. Patient-cooperative strategies for robot-aided treadmill training: First experimental results. Ieee Transactions on Neural Systems and Rehabilitation Engineering, 13(3): 380-394.

Robinson, D. W., Pratt, J., Paluska, D. J. and Pratt, G. A. 1999. Series Elastic Actuator Development for a Biomimetic Walking Robot. Paper presented at the International Conference on Advanced Intelligent Mechatronics.

Robinson, D. W. 2000. Design and Analysis of Series Elasticity in Closed-loop Actuator Force Control. Massachusetts Institute of Technology (MIT).

Schiele, A. and Visentin, G. 2003. The ESA Human Arm Exoskeleton for Space Robotics Telepresence. Paper presented at the 7th International Symposium on Artificial Intelligence, Robotics and Automation in Space, iSAIRAS, Nara, Japan.

Sugar, T. G. 2002. A novel selective compliant actuator. Mechatronics, 12(9-10): 1157-1171.

Torres-Jara, E. and Banks, J. 2004. A simple and scalable force actuator. Paper presented at the 35th International Symposium on Robotics.

Tsagarakis, N. G. and Caldwell, G. 2003. Development and Control of a 'Soft-Actuated' Exoskeleton for Use in Physiotherapy and Training. Autonomous Robots, 15(1): 21-33.

Winter, D. A. 1991. Biomechanics and Motor Control of Human Gait: Normal, Elderly and Pathological. Waterloo: University of Waterloo Press.

Zinn, M., Roth, B., Khatib, O. and Salisbury, J. K. 2004. A new actuation approach for human friendly robot design. International Journal of Robotics Research, 23(4-5): 379-398.

chapter 6

Design and Evaluation of the LOPES Exoskeleton Robot for Interactive Gait Rehabilitation

Jan F. Veneman
Rik Kruidhof
Edsko E.G.Hekman
Ralf Ekkelenkamp
Edwin H.F. van Asseldonk
Herman van der Kooij

ABSTRACT

This paper introduces a newly developed gait rehabilitation device. The device, called LOPES, combines a freely translatable and 2D-actuated pelvis segment with a leg exoskeleton containing three actuated rotational joints; two at the hip, one at the knee. The joints are impedance controlled to allow bi-directional mechanical interaction between the robot and the training subject.

Evaluation measurements show that the device allows both a 'patient-in-charge' and 'robot-in-charge' mode, in which the robot is controlled either to follow or to guide a patient, respectively. EMG measurements (one subject) on eight important leg muscles, show that free walking in the device strongly resembles free treadmill walking; an indication that the device can offer task-specific gait training. The possibilities and limitations to using the device as gait measurement tool are also shown: at the moment position measurements are not accurate enough for inverse-dynamical gait analysis.

CHAPTER CONTENTS

1. Introduction

A recent development in robotics is the design of robots for the mechanization of physical therapy, usually referred to as robotic (neuro-)rehabilitation or robot-mediated (or -aided) therapy (Lum, Reinkensmeyer et al. 2002; Hesse, Schmidt et al. 2003; Dobkin 2004; Mauritz 2004). These robots replace the physical training effort of a therapist. This may be useful in cases where a therapist's effort is very intensive leading to limitations in availability or even injuries. In the general setting of these robotic systems, a therapist is still responsible for the non-physical interaction and observation of the patient by maintaining a supervisory role of the training, while the robot carries out the actual physical interaction with the patient. Several groups are currently developing robots for 'arm training', as well as for 'gait training', which is the focus of this article.

Current automated gait trainers, such as the Lokomat (Hocoma, AG, Volketswil, Switzerland) (Colombo, Joerg et al. 2000), the pneumatically operated gait orthosis and the pelvic assist manipulator (known as POGO and PAM, respectively; not commercially available) (Reinkensmeyer, Aoyagi et al. 2006), the GaitTrainer (Reha-Stim, Berlin, Germany) (Hesse and Uhlenbrock 2000), the Haptic Walker (not commercially available) (Schmidt, Werner et al. 2007), and the AutoAmbulator (HealthSouth Cooperation), are usually unable to fully adapt their movements to the activity of the patient. Some devices are not able to assist all possible leg movements, but for example only foot movement.

This article describes the design and performance of the gait rehabilitation robot LOPES (LOwer extremity Powered ExoSkeleton). Design-choices will be motivated, the prototype presented and its performance demonstrated.

2. Design Criteria

At the moment, determinants of successful gait training are largely unknown, although intensity (Kwakkel, Wagenaar et al. 1999), self-initiative (Lotze, Braun et al. 2003) and task specificity (Nilsson, Carlsson et al. 2001; Bayona, Bitensky et al. 2005) seem to be important. This is also reflected in current research on robotic neurorehabilitation (Hogan, Krebs et al. 2006; Reinkensmeyer, Aoyagi et al. 2006; Riener, Lunenburger et al. 2006). These facts call for a device that allows near-to-normal free walking and that allows providing a wide range of possible content of training and supportive actions, while safety (for both patient and therapist) is assured at any time.

In order to satisfy these requirements, the robot, in the first place, should allow for a 'patient-in-charge'-mode where healthy subjects are able to walk unconstrained by the device. This concerns the choice of degrees of freedom and the quality of low impedance control. The patient-in-charge mode can be considered as the 'ideal' end situation of training, resembling how a patient would perform outside the device. It assures that foot-sole sensory input (during free walking in the device) will be near to normal. The availability of this mode is important for patients with a non-paretic side, which should not be disturbed during its operation. Secondly, the robot should allow for a 'robot-in-charge'-mode, whereby the robot is able to move a passive subject in a gait-like motion. From design viewpoint, this concerns both torque and speed limitations of the actuation on the actuated degrees of freedom (DoFs). Thus, the robot-in-charge-mode is a position control mode, assuring

that the robot can provide all selective/partial assistance to keep an inactive patient walking. Thirdly, the robot should allow for a 'therapist-in-charge'-mode whereby any required therapeutic interventions can be programmed. Note, that this mode demands the ability of the actuators to act as pure force sources, leading to implementation of the desired impedance patterns. In stark contrast to fully automated gait trainers, the proposed approach allows a therapist to stay in control of the provided therapy and to implement several training strategies.

3. Prototype Design[1]

a. An impedance controlled exoskeleton

Exoskeleton

In order to allow for corrective forces or torques to the legs of a patient, a so-called exoskeleton type robot was designed. The robot moves in parallel to the skeleton of the patient, so that no additional degrees of freedom or motion ranges are needed to follow patient motions. As the exoskeleton-joint-motions of the robot directly correspond with the motions of a patient's joints, it is relatively easy to implement mechanical safety limits to motion- and torque-ranges into the exoskeleton structure. However, a few shortcomings of an exoskeleton include the need to accurately align joints and the need for high torques. The latter may be necessary for interventions that could actually be carried out by smaller end-effector forces.

The exoskeleton as a whole is physically connected to an actuated support located at pelvis height. The virtue of this type of setup allows for weight-compensation of the exoskeleton and for applying external corrective forces to the pelvis of the patient, instead of only muscle-like internal torques at leg level. This simple approach leads to additional possibilities for interventions. Thus, the LOPES robot is a combination of an exoskeleton robot for the legs and an externally supporting end-effector robot for the pelvis.

Impedance controlled

Impedance control, as opposed to admittance control, was selected as a basic interaction control outline for the exoskeleton (see Chapter 3 and 5). Impedance control implies that the interaction control is based on position sensing combined with force actuation (Linde and Lammertse 2003).

While designing the robot, the choice of impedance control implies that the moving parts of the construction must be lightweight and that the actuators are 'pure' force sources. The use of impedance control for an exoskeleton is advocated in chapter 3-5 of this thesis.

Training interventions will be programmed using Virtual Model Control, an implementation of impedance control based on the definition of virtual dynamic components, e.g. virtual springs (Ekkelenkamp, Veneman et al. 2005).

Degrees of Freedom

An optimal set of degrees of freedom was chosen in order to allow for a subject to walk

1. Additional information about the process leading to the design that is presented here can be found in Appendix A.

Table 6.1: actuated, free and blocked degrees of freedom of the LOPES exoskeleton

Degree of Freedom	Human possibility	Robot design		
		Actuated	Free	Blocked
Pelvis to fixed world	3 rotations 3 translations	Left/Right Forwd/backwd	Up/down	All rotations except for play
Hip	3 rotations	Ad-/Abduction Flex-/exten-sion	-	Exo/endo-rotation except for play
Knee	1 rotation (sagittal)	Flex-/exten-sion	Ad-/Abduction[1]	-
Ankle	3 rotations[2]	-	All motions	-

[1] The knee abduction is not a human possibility, but was left free for constructional reasons, to not lead forces through the knee joint.
[2] The ankle is a complex joint, where the axes of motion are not simply the three Euclidian axes.

normally and safely in the device. After studying the literature on gait, and analyzing the experiences with existing devices and tests with the first prototype, a total number of eight actuated degrees of freedom (two for the horizontal pelvis translation and three rotational joints per leg) were considered to be sufficient. One degree of freedom, (the vertical motion of the pelvis) was passively weight compensated by means of an ideal spring-mechanism, and left free to move un-actuated within designed limits. All eight DoFs not only allow the exoskeleton to make a forward stepping motion (as provided by the Lokomat and the AutoAmbulator), but also maintain the fundamental instability of a standing or walking human. As such, balance control still has to be achieved when walking in the device, either by the human or (when necessary) by the robot, and is widely recognized as an important aspect of gait training (Israel, Campbell et al. 2006; Reinkensmeyer, Aoyagi et al. 2006).

Table 6.1 describes which degrees of freedom are possible for a human being, which of these are actuated in the robot, which are left free, and which are blocked. The reason to omit an actuated robotic ankle joint was that it is not necessary to provide an external 'ankle push-off' in the device in order to walk safely. Also, it is possibly painful to apply substantial torque to the feet, at least without using an individually fit-to-size foot-interface. The patient's forward progression can be assured by the treadmill together with the pelvis actuation. For patient safety, the only necessary ankle function is to assure enough foot clearance during swing.

This can be realized with simpler means such as using elastic straps, or a passive orthosis. Of course the robot should allow a recovering patient to generate an ankle push-off during rehabilitation; this not only involves the availability of the natural ankle's DoFs, but also available pelvis translations, so the body can actually be accelerated by a push-off.

In case that an ankle push-off would be externally provided during training, it is important that the device exerts its force through the foot and not directly to the floor as this would affect the sensed ground reaction forces, disturbing the patient's normal afferent input. However, what could be useful for training purposes, is the possibility to provide small torques around the ankle in order to 'suggest' when the patient should 'push-off'.

Table 6.2: Specifications for the actuated degrees of freedom of the LOPES exoskeleton

Degree of freedom	Range of motion	Maximum torque/force	Maximum speed
Hip abduction	+15 ° / -15 °	30 Nm	1 rad/s
Hip flexion	+60 ° / -30 °	65 Nm	2 rad/s
Knee flexion	+ 0 ° / -90 °	65 Nm	5 rad/s
Sideways	+0.30m/-0.30m	250 N	0.5 m/s
For-/back-ward	+0.35m/-0.35m	200 N	0.5 m/s
Up/down	+0.10m/-0.10m	Passively weight compensated	

Devices like the pneumatically driven ankle orthosis (Ferris, Czerniecki et al. 2005) or the Anklebot (Krebs and Hogan 2006) are examples of what is possible. These or similar devices can be added to the LOPES if ankle actuation appears to be crucial from a clinical point of view.

Table 6.2 presents the peak torques and ranges of motion that where chosen as specifications for the actuated degrees of freedom. Torques and forces were chosen based on measured values of joint torques in the 'slow walking cycle' (Winter 1990), and on estimates and measurements of forces that therapists apply during conventional gait training (Galvez, Kerdanyan et al. 2005). The presented torque/speed values are in fact the peak values that appear in the speed-torque curve while walking, where both maxima do not appear at the same time. However, using these values as general demands overestimates the nominal power that is needed. Thus, due to uncertainties in the measured values and the need for an extra margin for safety, the overestimated values are used in the design.

b. Realization of the LOPES prototype

Based on the aforementioned section, we designed an exoskeleton with three rotational joints per leg: two at the hip (abduction-4 and flexion-5) and one at the knee (flexion-6, for numbers see Figure 6.1). The physical hip abduction joint is placed behind the patient, where the position of the hip abduction axis relative to the hip flexion axis is fixed. The position of both abduction axes relative to each other (pelvis width), and the position of the hip axis relative to the knee axis (upper leg length) are adjustable, and are adjusted to suit the dimensions of each patient.

The joints of the robot are actuated with Bowden-cable driven series elastic actuators (see Chapter 5). This concept was chosen in order to implement low weight 'pure' force sources. The concept, construction and functionality of these joints are described extensively in chapter 5. This type of actuator was used for all rotary joints, and the sideways pelvis translation is equipped with a linear version of the same actuation principle. Finally, all forwards and backwards motion is driven by an open-loop force-controllable linear actuator.

The prototype uses Kollmorgen/Danaher AKM22C servomotors, with a maximum speed of 8000 rpm; 567 Watt rated power and a continuous torque of 0.87 Nm and a peak torque of 2.73 Nm. This motor is used in combination with a Neugart Planetary gearheads that reduces speed with a ratio of 64:1. Where, these sets are used for all (6) rotary degrees of freedom. For the sideways motion a Berger Lahr SER3910 is used, with a maximum speed of 6000 rpm, a peak torque of 2.2 Nm and a rated power of 690 Watt. This motor is used in combination with a Neugart Planetary gear head with a reduction of 8:1. For the forward/backward motion a Linmot P01-37x240 linear actuator is used, with a rated
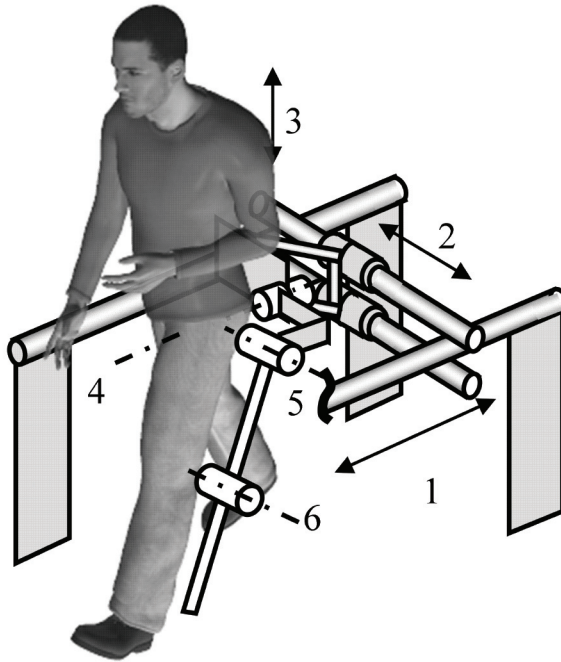
Figure 6.1: Degrees of Freedom of the pelvis and leg segments of the LOPES gait rehabilitation robot: (1) forward linear guide, (2) sideways linear guide, (3) parallelogram for vertical motion, (4) hip frontal rotation, (5) hip sagittal rotation, and (6) knee sagittal rotation. The two horizontal motions (1&2) and the hip frontal rotation (6) are optionally blocked in the experiments. Except for (3) are all mentioned DoFs actuated. (A) indicated the height adjustability of the support frame.

power of 250 Watt and a peak force of 204N. The linear springs applied in the flexion joints (hip and knee) have a stiffness of 35.1 kN/m each; those applied in the hip abduction joints have a stiffness of 57.2 kN/m; and the springs applied for the left right actuation have a stiffness of 3.98 kN/m.

The change in spring length, which is used as force measurement in the actuators, is measured with linear slider potentiometers (where the sliders are connected to a spring). The construction for connecting this exoskeleton to the fixed world consists of (for explanation of the numbers see Figure 6.1):

a)   a height-adjustable frame to match the length of the patient (A), this height is fixed during training, and needs to be adjusted at the beginning of a training session.

b)   two sets of perpendicularly placed parallel bars with carriages for the for-/back-ward (1) and the sideways (2) motion; double bars are used to translate load torques into forces.

c)   a parallelogram with bearings (3) and weight compensation to allow limited vertical motion during operation. The weight compensation is realized with an 'ideal spring' mechanism.

This construction is then placed over a treadmill. The motors that drive the robot joints are placed at the back of the construction, and connected to the robot joints by two

Figure 6.2: Photographic impression of the prototype of LOPES. The two Bowden cables per joint that transmit the power from motors to the robot joints are visible for several joints. The rightmost pictures show how a person is connected to the device. In the left picture, above the back plate, the connector for the cushion is visible
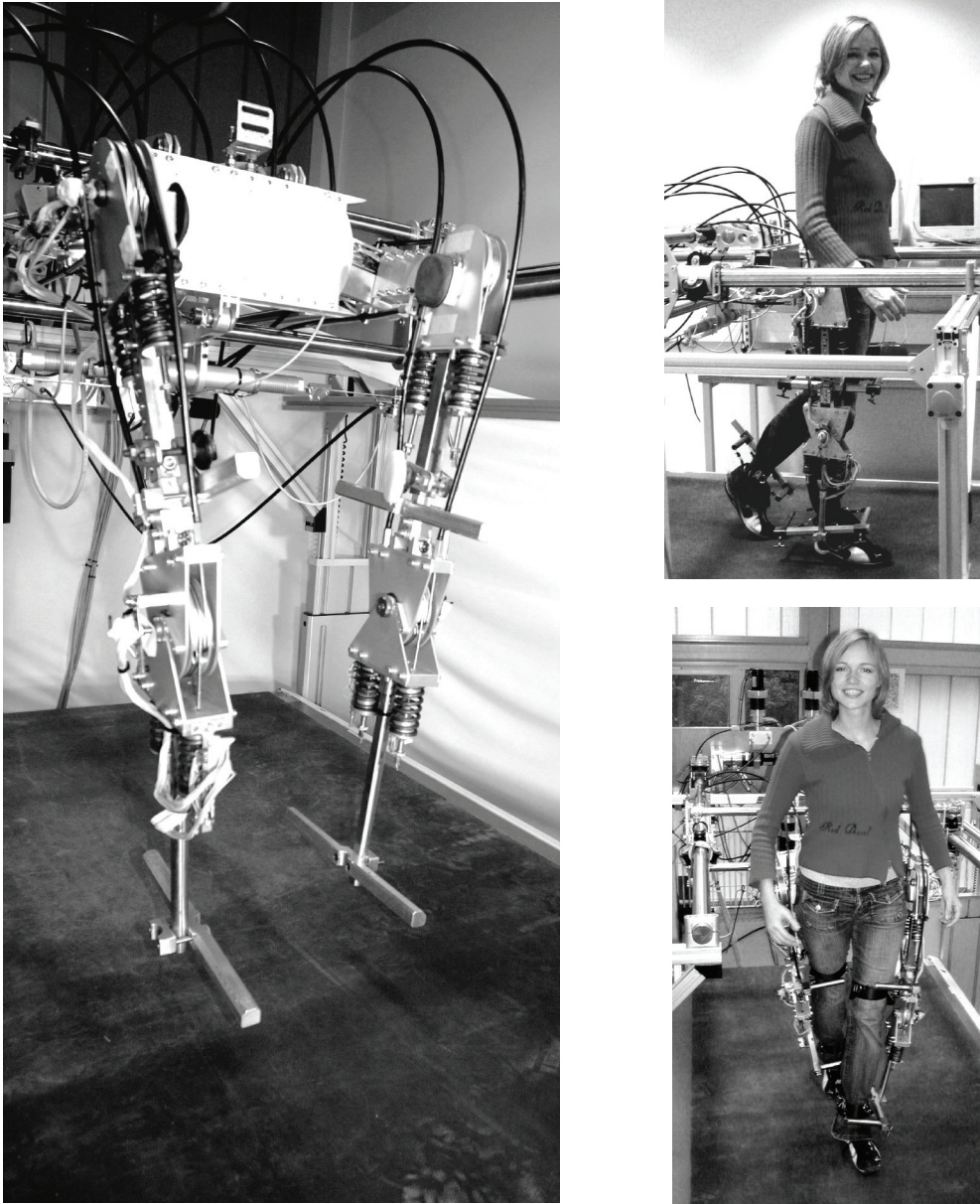
Bowden cables per actuated degree of freedom. A photographic impression of the resulting total construction of the LOPES is shown in Figure 6.2.

4. Evaluation of Performance

a. Evaluation methods

In order to evaluate the performance of the design, and avoid extensive subject or patient tests, several hardware tests were performed based on the demands stated in section II. To prove the functionality of the 'patient-in-charge'-mode, the torque responses to imposed motions were measured. In all cases, the joints were operated in zero-torque control. Firstly, the force response of a single disconnected knee-joint was measured. Secondly, a leg was constructed of two joints, hip and knee, and leg segments. This leg was placed in a test set-up where controlled motions could be imposed at the ankle. The Cartesian impedance at the ankle, the end-effector, was then determined, by measuring the force response to an imposed multisine motion in the range 0.1 – 4 Hz with uniform power distribution. Thirdly, in the full prototype, the peak force responses to hand-imposed motions on all eight degrees of freedom were measured. This last measurement was carried out per separate joint, while fixating the other joints. Motions were exerted by hand, via the force sensor, yielding realistic motion speeds. The motions had a frequency-range of 1-3Hz and an amplitude of about 30 degrees for knee at 1Hz down to 10 degrees at 3 Hz. These values were 20 and 5 degrees respectively for the hip flexion and about 10 and 5 for the hip abduction. Translations showed amplitudes of 10 cm and 2 cm for 1 and 3 Hz respectively. For the measurement of knee and hip flexion torques the sensor was mounted at ankle height, for the measurement of hip abduction at the knee, and for the measurement of the pelvis motions in the middle of the back plate, where during operation the low back cushion is attached (see Figure 6.4). From the force vector, and the known location of the force sensor, the torque around the joint is calculated.

The ultimate test of the 'patient in charge' mode is the comparison between free treadmill walking and walking in the LOPES while controlled to zero impedance. These tests have also been finished, but the findings are too extensive and will be published elsewhere (see chapter 7 of this thesis). Preliminary results of EMG measurements of the activation patterns of eight major leg-muscles of one healthy young (age: 21) female subject at a walking speed 0.75 m/s will be shown. This gives a good indication of changes that appear when walking in the device.

To evaluate the 'robot-in-charge'-mode achievable standstill peak forces on the robot joints are measured. In order to evaluate the 'therapist-in-charge' mode the force bandwidth of the separate robot joints is measured, as this determines the achievable bandwidth of any impedance control. In both cases, all forces are measured with a 6D force sensor (ATI-Mini45-SI-580-20) connected to the robot leg.

Finally, the orientation and position of the leg segments compared to the robot segments are measured as this is important both for accurate control of LOPES and for its use as a measurement/diagnosis device. For the human leg orientation measurements we used a PTI-VZ4000 mocap system from PhoeniX Technologies. This system follows active, uniquely identifiable LEDs in 3D space using a camera bar, where the motion of

both robotic and human limbs (for one leg) are tracked. In order to track the 'human leg', clusters comprised of four markers each are stuck onto the back of both the upper and the lower leg. It was necessary to place the camera on the left behind the subject due to limited visibility of leg markers caused by the mechanical construction.

During walking, the translations of the pelvis and the hip ab-/ad-duction were blocked, so that the walking could be considered purely sagittal - this way the rotation axes could be defined as global stationary axes. Finally, the hip and knee rotation of both human and robot were then tracked during walking and mutually compared. A step-cycle trajectory averaged over fifteen steps, averaged over ten unimpaired subjects (mean age 26) is presented as the result of this measurement. All subjects taking part in measurements provided informed consent prior to measurements.

b. Evaluation Results

Typical values for the resistive torque of the 'Bowden cable-driven series elastic actuators' (Chapter 5) when externally rotated were 0.2 Nm, for 1 Hz imposed rotations to 0.7 Nm peaks, for 4 Hz rotations. (See also chapter 5 of this thesis.) These values were measured while controlling the joint to zero force, and with optimal Bowden cable courses. In this case no additional inertia or weight was added to the joint, so solely the impedance of the actuator system and the friction of the joint were measured, not the inertial properties of the robot segments.

In the test set-up with a leg comprised of a hip and knee joint, an accurate impedance characteristic of the Cartesian impedance at the ankle 'end-effector' was measured (see Figure 6.3). For easier interpretation the zero force / impedance control measurement is accompanied by a measurement where the 1kN/m stiffness is controlled. The Bode diagram shows that in case of the zero impedance control, a damped mass is sensed. With a controlled stiffness, the same mass is sensed at higher frequencies, while a stiffness together with a slight phase shift is measured at lower frequencies. Achievable bandwidths in the final prototype are about 4Hz for the full force range (65 Nm) up to 12 Hz for smaller forces (<10 Nm).

Measuring the 'endpoint' resistive torques in the final prototype yielded the values shown in table 6.3. For interpretation of the difference between the actuator resistive
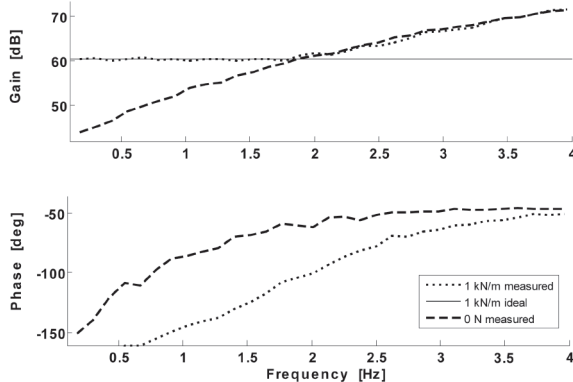

Figure 6.3: Bode diagram of the measured Cartesian impedance at the ankle end effector of a leg with a hip and knee joint. The dB values of the force response to an imposed position multisine are presented. For comparison a controlled stiffness of 1kN/m is shown (ideal and measured). The zero impedance control shows the behavior of a damped mass.

Table 6.3: Measured values for resistive torques to imposed motions and maximally exerted torques on the degrees of freedom of the LOPES exoskeleton.

Degree of Freedom	Actuator Resistive Torque or Force	'Endpoint' Resistive Torque or Force at ~1 Hz	'Endpoint' Resistive Torque or Force at ~3 Hz	Maximum exerted Torque or Force
Knee flexion	< 1 Nm	1.75 Nm	4 Nm	50 Nm*
Hip flexion	< 1 Nm	5 Nm	25 Nm	50 Nm*
Hip abduction	< 1 Nm	5 Nm	12 Nm	30 Nm
Sideways	< 5 N	20 N	30 N	250 N
For-/back-ward	< 10 N	40 N	100 N	250 N

*The peak torques of 50 Nm mentioned for knee and hip flexion were actually measured. Due to the friction based force transmission, higher torques were not feasible yet, as some slip at the joint cable discs appeared. This will be fixed by redesign of the connection of the cables to the joints in such fashion that no slip can occur. The motors provide a continuous torque of max. 65 Nm at the actual joint output axis, with a peak torque of over 100 Nm, for short intervals (<1 second).

Table 6.4: Inertial torques at specific motion profiles (calculated inertial force responses to exerted sinusoid motion).

	Whole leg (hip joint)	Lower leg (knee joint)
1 Hz sine	13 Nm (20 deg)	1.9 Nm (30 deg)
3 Hz sine	29 Nm (5 deg)	5.7 Nm (10 deg)

torque and the 'endpoint' resistive torque the component of this resistance caused by inertia alone are calculated. The results are based on the mass of a leg segment, 3 kg for the lower (including joint) and 6 kg for the whole leg. The centers of gravity are taken at the halfway points in each segment respectively (40 cm from the hip for the whole leg and 17.5 cm from the knee for the lower leg). These values are approximate, as in practice they will change slightly due to the adaptations of segment lengths and connections to the patient. Finally, the masses are taken as point masses and the results of these calculations are shown in table 6.4.

 These values indicate the sizes of inertial torques appearing during walking, and show that the inertia of the construction explains most of the resistive torques that appear when moving the construction.

In order to show the effect of these torques on walking, the integrated EMG patterns of eight major leg muscles are compared for free treadmill walking and walking when connected to the LOPES controlled in zero impedance mode (Figure 6.4). When analyzing Figure 6.4, notice that the difference in patterns is small, especially when timing is considered, and that the Biceps Femoris shows an increase in EMG amplitude. This change takes place in the late swing, and can possibly be attributed to the increased leg mass. Also, the Adductor Longus and the Tibialis Anterior show slight but remarkable changes. The change in adductor activity was accompanied by a smaller step width. The change in Tibialis Anterior can also be explained by the extra mass, together with the need to assure sufficient foot clearance during swing.

The Glutues Medius shows a slight decrease in activity during late stance. This may be attributed to less active push-off, as the progression of the subject is assured by the moving
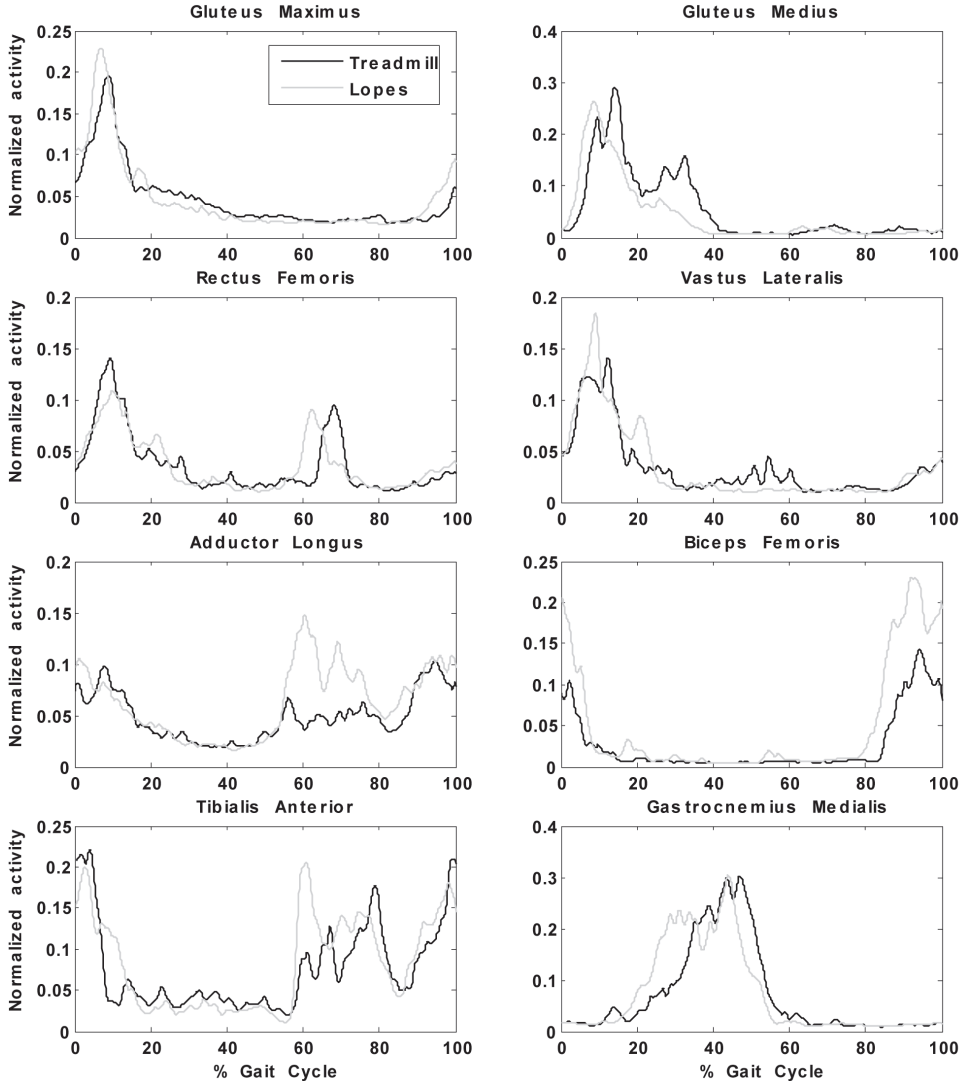
Figure 6.4: Integrated muscle activity for eight major leg muscles in one healthy female subject (age 21). Muscle activation patterns in free treadmill walking are compared to treadmill walking connected to the LOPES in zero impedance control mode ('patient in charge').

treadmill and forces on the pelvis keeping the subject in place.

The peak forces and torques achieved on every DoF are presented in table 6.3, the right column. The bandwidth of feedback force control in the joints alone was measured at 11 Hz for the full force range (there 50 Nm) and 20 Hz for smaller forces (<10 Nm) in an externally fixed joint, for optimal Bowden cable course; see (Chapter 5) for the exact description of measurements and further nuances. Due to suboptimal cable courses in the prototype and of the inertia of the robot segments the bandwidth of resulting force control at the 'end-effector' – the ankle – is lower, down to about 2 Hz for larger forces in the an-
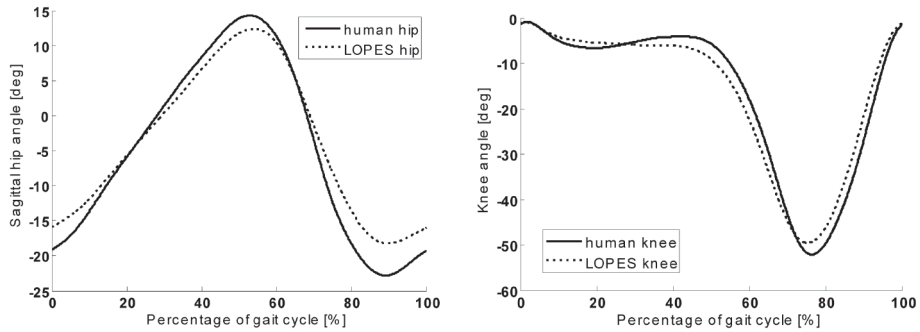
Figure 6.5: Graphs of the sagittal hip and knee angles of both human (position tracking measurement with leg-marker-clusters) and robot (joint angle measurements) for several strides during slow walking (0.75 m/s).

kle in motion, as can be seen in Figure 6.3.

Figure 6.5 shows the sagittal hip angle for one step cycle, averaged over steps and over subjects and the same information for the sagittal knee angle. The bigger differences for the hip angle can be explained by the fact that the cluster marker on the upper leg is positioned on top of the hamstrings, and this appears to cause extra motion (secondary rotations) of the cluster.

However, during certain moments in the gait cycle, the visible differences may therefore be bigger than the actual difference between the segments of robot and human. Visually the robotic upper leg segment hardly deviated from the upper leg orientation. However, the measurements of the angles are not accurate enough in order to perform any inverse-dynamical calculations. They appeared indeed accurate enough for a safe implementations of an impedance controller that interferes with a walking subject (Van Asseldonk, Ekkelenkamp et al. 2007).

5. Discussion

The prototype of LOPES is fully functional. However, for use in clinical research LOPES must be made fully patient safe. This implies, for example, an independent safety circuit that can power the system down in case of any danger and a covering of all possible dangerous moving parts.

The slip that appeared during applying peak torques can be solved by not relying on the friction between cable and disc for force transmission, but by rigidly fixing the cables to this disk. Another design optimization can be made in reducing the weight of the leg parts, as these largely determine the resistive torques while moving the legs. The weight of the legs can be considerably reduced by reducing their dimensions and selecting different materials, and as such are merely a matter of product engineering.

The evaluations showed a decent agreement to the stated demands. Although the resistive torques in the 'patient in charge'- mode may seem considerable, all people that walked in the LOPES robot reported to experience little to no obstruction to normal walking. This is explained by the relatively slow movements that take place and due to

the natural feel of a slight increase of mass. This experience is supported by the EMG measurements, which show only slight differences between walking with and without the LOPES device. Our findings agree with literature on walking with added weight (Noble and Prentice 2006).

The differences in the orientation between the human and the robotic limbs appear to be reasonably small, at least for control purpose. A substantial part of the error in hip angle appeared to be caused by secondary rotations of the marker clusters, caused by deformation of the leg due to muscle contractions. A more critical comparison between orientations is recommended for future work in order to judge on the feasibility of the LOPES robot for inverse-dynamics gait measurements. Current measurements indicate that position/angle measurement of the legs via the robot device is not sufficiently accurate for inverse dynamic calculations.

6. Conclusions

We designed and evaluated a gait rehabilitation robot prototype that functions as a kinaesthetic (mechanically interactive) interface. It is impedance controlled on eight degrees of freedom and capable of a force bandwidth of 4 Hz for large forces up to 12 Hz for smaller forces. Its degrees of freedom allow free leg motions and a free 3D translation of the pelvis, maintaining the fundamental instability of upright standing and walking. The only possibly important motions that are blocked (except for play) are the pelvis rotations.

The robot is an exoskeleton that moves in parallel with the legs of a person walking on a treadmill, at pelvis height flexibly connected to the fixed world. It allows people to walk unhindered in its 'patient in charge'- mode. It also allows enforcing a gait pattern when configured for its 'robot in charge' - mode. The actual use will be in between both modes; in its so called 'therapist in charge'- mode, where selective corrective or supportive torques can be applied to the leg-joints and the pelvis of patients who are walking on their own effort.

Evaluation of the design showed that unhindered walking in the device is very possible, and that any torques/forces needed to impose a gait pattern can be achieved. Also, limb orientations of the robot and the walking subject agree well, sufficient for stable implementation of training and lower level control. Preliminary results of leg muscle EMG measurements show little deviation between treadmill walking and walking with the LOPES exoskeleton. However, any clinical evaluation with patients has yet to be carried out.

## 7. References

Bayona, N. A., Bitensky, J., Salter, K. and Teasell, R. 2005. The role of task-specific training in rehabilitation therapies. Topics in Stroke Rehabilitation, 12(3): 58-65.

Colombo, G., Joerg, M., Schreier, R. and Dietz, V. 2000. Treadmill training of paraplegic patients using a robotic orthosis. Journal of Rehabilitation Research and Development, 37(6): 693-700.

Dobkin, B. H. 2004. Strategies for stroke rehabilitation. Lancet Neurology, 3(9): 528-536.

Ekkelenkamp, R., Veneman, J. and van der Kooij, H. 2005. LOPES: selective control of gait functions during the gait rehabilitation of CVA patients, Proceedings of ICORR 2005 - IEEE International Conference on Rehabilitation Robotics: 361-364. Chicago.

Ferris, D. P., Czerniecki, J. M. and Hannaford, B. 2005. An ankle-foot orthosis powered by artificial pneumatic muscles. Journal of Applied Biomechanics, 21(2): 189-197.

Galvez, J. A., Kerdanyan, G., Maneekobkunwong, S., Weber, R., Scott, M., Harkema, S. J. and Reinkensmeyer, D. J. 2005. Measuring human trainers' skill for the design of better robot control algorithms for gait training after spinal cord injury. Paper presented at the 9th International Conference on Rehabilitation Robotics, 2005. ICORR 2005. .

Hesse, S. and Uhlenbrock, D. 2000. A mechanized gait trainer for restoration of gait. Journal of Rehabilitation Research and Development, 37(6): 701-708.

Hesse, S., Schmidt, H., Werner, C. and Bardeleben, A. 2003. Upper and lower extremity robotic devices for rehabilitation and for studying motor control. Current Opinion in Neurology, 16(6): 705-710.

Hogan, N., Krebs, H. I., Rohrer, B., Palazzolo, J. J., Dipietro, L., Fasoli, S. E., Stein, J., Hughes, R., Frontera, W. R., Lynch, D. and Volpe, B. T. 2006. Motions or muscles? Some behavioral factors underlying robotic assistance of motor recovery. Journal of Rehabilitation Research and Development, 43(5): 605-618.

Israel, J. F., Campbell, D. D., Kahn, J. H. and Hornby, T. G. 2006. Metabolic costs and muscle activity patterns during robotic- and therapist-assisted treadmill walking in individuals with incomplete spinal cord injury. Phys Ther, 86(11): 1466-1478.

Krebs, H. I. and Hogan, N. 2006. Therapeutic Robotics: A Technology Push. Proceedings of the IEEE, 94(9): 1727-1738.

Kwakkel, G., Wagenaar, R. C., Twisk, J. W., Lankhorst, G. J. and Koetsier, J. C. 1999. Intensity of leg and arm training after primary middle-cerebral-artery stroke: a randomised trial. Lancet, 354(9174): 191-196.

Linde, R. Q. v. d. and Lammertse, P. 2003. HapticMaster - a generic force controlled robot for human interaction. Industrial Robot, 30(6): 515-524.

Lotze, M., Braun, C., Birbaumer, N., Anders, S. and Cohen, L. G. 2003. Motor learning elicited by voluntary drive. Brain, 126(Pt 4): 866-872.

Lum, P., Reinkensmeyer, D., Mahoney, R., Rymer, W. Z. and Burgar, C. 2002. Robotic devices for movement therapy after stroke: current status and challenges to clinical acceptance. Topics in Stroke Rehabilitation, 8(4): 40-53.

Mauritz, K. H. 2004. Gait training in hemiparetic stroke patients. Eura Medicophys, 40(3): 165-178.

Nilsson, L., Carlsson, J., Danielsson, A., Fugl-Meyer, A., Hellstrom, K., Kristensen, L., Sjolund, B., Sunnerhagen, K. S. and Grimby, G. 2001. Walking training of patients with hemiparesis at an early stage after stroke: a comparison of walking training on a treadmill with body weight support and walking training on the ground. Clinical Rehabilitation, 15(5): 515-527.

Noble, J. W. and Prentice, S. D. 2006. Adaptation to unilateral change in lower limb mechanical properties during human walking. Experimental Brain Research, 169(4): 482-495.

Reinkensmeyer, D. J., Aoyagi, D., Emken, J. L., Galvez, J. A., Ichinose, W., Kerdanyan, G., Maneekobkunwong, S., Minakata, K., Nessler, J. A., Weber, R., Roy, R. R., de Leon, R., Bobrow, J. E., Harkema, S. J. and Edgerton, V. R. 2006. Tools for understanding and optimizing robotic gait training. Journal of Rehabilitation Research and Development, 43(5): 657-670.

Riener, R., Lunenburger, L. and Colombo, G. 2006. Human-centered robotics applied to gait training and assessment. Journal of Rehabilitation Research and Development, 43(5): 679-694.

Schmidt, H., Werner, C., Bernhardt, R., Hesse, S. and Kruger, J. 2007. Gait rehabilitation machines based on programmable footplates. Journal of Neuroengineering and Rehabilitation, 4: 2.

Van Asseldonk, E. H. F., Ekkelenkamp, R., Veneman, J. F., Van der Helm, F. C. T. and Van der Kooij, H. 2007. Selective control of a subtask of walking in a robotic gait trainer(LOPES). Paper presented at the ICORR'07, 10th International Congres on Rehabilitation Robotics, Noordwijk aan Zee.

Winter, D. A. 1990. Biomechanics and Motor Control of Human Movement (2nd ed.). New York: Wiley.
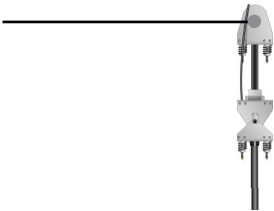
chapter 7

The Effects on Walking of an Impedance Controlled Robotic Gait Trainer

Edwin H.F. van Asseldonk
Jan F. Veneman
Ralf Ekkelenkamp
Jaap H. Buurke
Frans C.T. van der Helm
Herman van der Kooij

Abstract

"Assist As Needed" (AAN) control algorithms promote activity of patients during robotic gait training. Implementing these requires a free walking mode of a device, as unassisted motions should not be hindered. The goal of this study was to assess the naturalness of walking in the free walking mode of the LOPES gait trainer, an 8 DoF lightweight impedance controlled exoskeleton. Kinematics, gait parameters and muscle activity of walking in a free walking mode in the device were compared with those of walking freely on a treadmill. Average values and variability of the spatio-temporal gait variables showed small changes and the kinematics showed a significant and relevant decrease in knee angle range only. Muscles involved in push off showed a small decrease , whereas muscles involved in acceleration and deceleration of the swing leg showed an increase of their activity. Timing of the activity was mainly unaffected. Most of the observed differences could be ascribed to the inertia of the exoskeleton.It is concluded that overall differences appeared small and that the main differences are likely caused by the inertia of the device. Whether further weight reduction is necessary to achieve optimal AAN training needs to be evaluated in patients.

Chapter Contents

1. Introduction

Development of robotic devices for gait rehabilitation of stroke patients is motivated by the need for an intensive training, which has been shown to be the key element in facilitating recovery (Kwakkel, Wagenaar et al. 1997; Kwakkel, van Peppen et al. 2004; Teasell, Bitensky et al. 2005), together with the need for a therapist-friendly training. Now that several robotic devices for gait rehabilitation of stroke patients, i.e. Lokomat (Colombo, Joerg et al. 2000) and Gait Trainer (Hesse, Uhlenbrock et al. 1999), are available on the market (Krebs and Hogan 2006), most research effort is put in determining the effectiveness of these devices (Husemann, Muller et al. 2007; Schmidt, Werner et al. 2007) and in introducing new principles and concepts to extend the possibilities compared to this 'first generation' (Riener, Lunenburger et al. 2005; Agrawal, Banala et al. 2007; Aoyagi, Ichinose et al. 2007; Von Zitzewitz, Bernhardt et al. 2007). These 'first generation' devices are generally characterized by the approach of enforcing gait upon a patient by moving the legs through a predescribed gait pattern. Although this approach might be well suited for severely affected patients and has already been shown to be effective in retraining stroke patients, treatment outcome could be further optimized by increasing the active participation of the patient.

Active patient participation may be realized by increasing motivation (Lunenburger, Colombo et al. 2007) or by necessitating self generated activity. The latter can be achieved by adjusting the robotic assistance to the actual possibilities and actions of the patient, so that the patient only receives 'assist as needed' and performs subtasks where possible on own effort. The potential of an 'Assist As Needed' (AAN) algorithm in promoting recovery, has been shown by Cai and colleagues (Cai, Fong et al. 2006), who taught spinal mice to step with different robotic control strategies. The mice trained with an AAN algorithm showed a larger recovery of stepping ability than mice trained with a fixed trajectory. Recently, an AAN algorithm was implemented in arm training using the MIT-Manus (Ferraro, Palazzolo et al. 2003; Krebs, Palazzolo et al. 2003; Hogan, Krebs et al. 2006). Compared to their previously used strategy of active assistance, this strategy showed a larger decrease in impairments, achieved in 30% less repetitions.

Typical examples of 'Assist As Needed' are: following a patient's movements and only intervening in case of danger, only assisting the affected leg in case of hemiplegia and only assisting pre-selected subtasks of walking for specific training focus. This resembles what a common therapist is doing during gait training. Position controlled devices are not suited to implement such interventions as they largely determine motion patterns. AAN strategies require some kind of interaction control, usually called haptic- or impedance-control(Aoyagi, Ichinose et al. 2007). Impedance control means that the sensed mechanical properties of a device (inertia, friction and stiffness) are freely programmable to desired values, albeit within limits. By adjusting the impedance, the behaviour of an impedance controlled robot can be varied from very stiff to very flexible. A very stiff control mode would then resemble a position control as implemented in existing devices. Next to this, on the other side of the stiffness spectrum, a 'zero impedance' or 'zero-force' mode should be available. Here the subject is able to move freely with minimal resistance of the robot. Any possible intervention during training lies in the large range of possibilities in-between these both extremes. In our project we called these extreme and opposing modes 'robot-in-charge' and 'patient-in-charge' mode of the robot respectively.

The availability of a 'patient-in-charge'-mode is important for two reasons. First, it is the basis for any AAN control or selective control (Van Asseldonk, Ekkelenkamp et al. 2007) algorithm. Only assisting affected functions or subtasks implies that the remaining gait functions should be performed unhindered, or in other words 'no assistance when not needed'. Second, walking in the 'patient-in-charge' mode can be considered the final stage of training, the function the patient is training towards. The better this mode functions, the more the self-initiated walking with the device will resemble walking without the device and the more likely it is that the acquired capabilities will transfer to over ground walking. This also fits in the philosophy that motor training should be task-specific (Dobkin 2004; Van Peppen, Kwakkel et al. 2004; Bayona, Bitensky et al. 2005), meaning that training should consist of a meaningful task and that the task in training should strongly resemble the task that has to be learned.

How well a patient-in-charge-mode can be implemented, largely depends on the mechatronical design of the used device. Not only the quality of impedance control on all actuated joints is important, but also which of the natural human motions (or degrees of freedom, DoFs) are actuated, left free, or restrained in the device. The DoFs of the device determine which motions occurring during normal or impaired free walking will be restrained by de device, and which will be available, although optionally restrained by control of the robot. Consequently, the evaluation of a 'patient in charge' mode reveals at which points the device still influences unrestrained walking. This information is required for a better understanding of the patient's response during training in the device.

No impedance controlled robotic gait training device has yet been evaluated in a patient-in-charge mode. Evaluation of the Lokomat, the device used in most research in the field, has only profoundly been carried out in the position control mode (Hidler, Nichols et al. 2005; Israel, Campbell et al. 2006; Neckel, Wisman et al. 2006; Neckel, Nichols et al. 2007). The Lokomat can also function in a low impedance mode, but only preliminary results have been published (Riener, Lunenburger et al. 2005). As the Lokomat was not designed to function as an impedance controlled device, we developed and built a light weight device called LOPES, LOwer extremity Powered ExoSkeleton (see chapter 6). Apart of being impedance controlled, it differs from the Lokomat in that it has more actuated degrees of freedom. The additional DoFs of the LOPES are pelvis translations in the horizontal plane, and hip ab-/adduction, beside the bacis hip and knee flexion and extension. These additions may be beneficial for training as they allow to leave balance control related tasks to a patient (Israel, Campbell et al. 2006). The importance of adding pelvic motions to gait training, has recently also been pointed out by Aoyagi and Colleagues (Aoyagi, Ichinose et al. 2007) in the design of the PAM gait training device, which specifically focuses on supporting pelvic motions, including rotations, during training..The addition of these DOFs adds an extra dimension to the AAN algorithms, as the added DoFs can by control again be blocked, but can be added by choice of the robot operator when the walking capacity of the patient allows . The number of DoFs is practically limited by complexity and controllability (and therefore safety) of the device.

The goal of the present study is to evaluate the 'patient-in-charge' mode in LOPES, by comparing walking with and without the device. The criteria for evaluation are first of all how close the kinematics and basic gait parameters while walking with the device resemble those in free walking. However, not only the kinematics but also the muscle activity underlying these walking movements should be similar. We quantified the amplitude of the
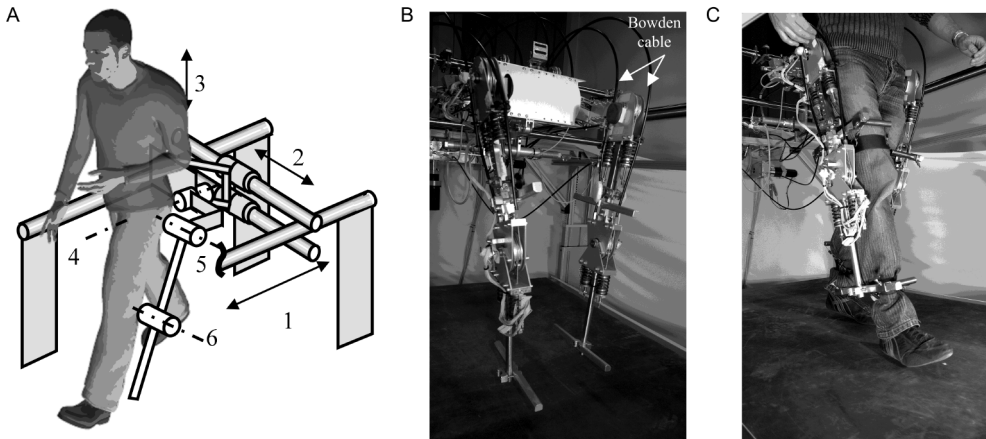
Figure 7.1: A) Schematic overview of the LOPES exoskeleton and its degrees of freedom. The horizontal movements of the pelvis (1 and 2) are actuated, as well as the movements of the leg joints (4, 5 and 6). The vertical movement of the pelvis is unactuated. The three degrees of the not depicted left exoskeleton leg complete the number of degrees of freedom to nine. B) the exoskeleton with its bowden cables to transmit the forces from the motor to the joint. C) Fixation of the subject in the LOPES exoskeleton

muscle activity as this provides an indication of the subject's response to the experienced resistance or restraints. In addition we quantified the timing of the activity, to get a measure of the muscle coordination. Finally, as the neural control of walking is characterized by cycle-to-cycle variation, we also assessed whether walking in the device showed the natural variability.

2. MATERIALS AND METHODS

a. Subjects

Ten healthy young adults (4 male, 6 female), mean age 25,9 years volunteered to be participants for this experiment. All participants provided informed consent before testing began.

b. Experimental apparatus and recordings

Rehabilitation device

For the experiments the prototype of the gait rehabilitation robot LOPES was used. LOPES is an exoskeleton type rehabilitation robot. It is lightweight and actuated by Bowden cable driven series elastic actuators (see chapter 5). It offers 3D translations of the pelvis, where the antero-posterior and medio-lateral motions (1 and 2 in Figure 7.1A) are actuated. Furthermore, it has two actuated rotation axes in the hip joints (4 and 5 in Figure 1A), and actuated knees with one rotation axis (6 in Figure 7.1A) (see chapter 6). The robot is impedance controlled, which implies that the actuators are used as force (torque) sources. This allows implementing both the 'robot-in-charge' mode, that is position control with high impedance, and a 'patient-in-charge' mode, that is zero impedance, in this case

Table 7.1: Approximate inertial characteristics of the robot frame, for reference approximate values for a human person with a body mass of 75 kg.

Segment	Involved DoF	mass / inertia robot	mass / inertia corresponding human body segments
Total robot	Forward/backward	35.0 kg (no rotations)	75 kg (45 kg only trunk)
	Sideways	27.5 kg (no rotations)	75 kg (45 kg only trunk)
Upper leg	Hip Flex/Ext	2.90 kg / 0.0046 kgm2	9.5 kg / 0.15 kgm2
Lower leg	Hip Flex/Ext Knee Flex/Ext	2.25 kg / 0.0012 kgm2	3.5 kg / 0.06 kgm2

synonymous with zero-force control, on each degree of freedom. The latter mode was used in this research to investigate to what degree 'free' walking with the device resembled free walking on a treadmill. The pelvis and the legs of the subject are strapped to the exoskeleton (Figure 7.1B). The inertial characteristics of the robot are presented in table 7.1. These are relevant because the controller is not able to compensate for the inertia of the robotic limbs. The values are compared with the human limbs. It should be noted that the *weight* of the exoskeleton is not sensed by the subject, as it is weight compensated.

Motion capturing

Motions were measured with an PTI Phoenix Visualeyez™ VZ4000 system (PTI Phoenix, Burnaby, BC, Cananda) at a frequency of 60 Hz. Twenty five uniquely identifiable infrared markers were attached to track the motion of the subject's left leg and exoskeleton's left "leg". Motion of the upper leg and lower leg was measured by attaching frames with four infrared markers on the back of the thigh and shank. A frame of four markers was attached to the vertebra prominence, measuring the orientation and position of the trunk. The foot motion was measured by placing markers on the ankle, heel, fifth metatarsophalangeal joint, and dorsum. The motions of the exoskeleton were measured by placing 4 markers on the upper leg and lower leg part of the exoskeleton.

Gait phases were detected with footswitches, taped directly to the subject's heel and fore foot of both feet. The measurement of the footswitches was synchronized with the measurement of the EMGs by sending a pulse at the start and end of each measurement to both systems and aligning these pulses in time.

Muscle activity measurement

During all trials muscle activation patterns were determined by recording bi-polar surface electromyography (EMG) from the gastrocnemius medialis, tibialis anterior, biceps femoris, rectus femoris, adductor longus, vastus lateralis, and gluteus medius and maximus muscles. Skin preparation (shaving of hair, abrading, cleansing with alcohol) and the placement of the disc-shaped (35x26 mm) solid-gel Ag/AgCl-electrodes (type H93SG, Tyco Healthcare / Kendall, Mansfield, USA) in a bipolar configuration (interelectrode distance of 26 mm) were performed according to Seniam guidelines (Hermens, Freriks et al. 1999). For the EMG recordings a compact measurement apparatus (type Porti 16-5, TMS International, Enschede, The Netherlands) was used. The analog signals were not filtered before sampling at 1024 Hz, which was justified by using sigma-delta analog-to-digital

converters with inherent anti aliasing filters. The signals were sent from the portable unit via fibre optics to the computer, where data were stored for further processing.

c. Experimental protocol

The subjects walked freely on the treadmill and while strapped into LOPES, the order of the "type of walking" was randomized between subjects. For each type of walking, the subject walked at 0.5 m/s, 0.75 m/s and 1.25 m/s. The first two velocities were chosen to reflect often reported walking velocities of stroke patients and the latter velocity was chosen to reflect a normal walking velocity. Within each type of walking the order of the velocities was randomized. With each change of walking velocity and/or type of walking the subject was given 3 minutes to get used to the walking condition. Subsequently, data were recorded for approximately 20 steps in total.

Before the subjects could walk with LOPES, the exoskeleton was attached to the subject's leg and pelvis. The subject's joint axes were aligned with the joint axes of the exoskeleton by adjusting the pelvis width of the exoskeleton and the length of exoskeleton linkages. As the exoskeleton did not encompass an ankle joint, the ankle was left free to move.

During this experiment LOPES was controlled to provide minimal resistance during walking. This was implemented by a closed-loop force controller that controlled torques at joint-level to zero. Due to the used control method (See chapter 5 of this thesis) the torques caused by inertia and weight of the exoskeleton remain perceptible for the subject. However, the exoskeleton was designed to have low inertia, which was achieved by placing the actuators away from the moving frame, using flexible Bowden cables to transfer the power from the fixed actuators to the freely moving joints of the exoskeleton (Figure 7.1B). This assures that the disruptive torques remain small, although torques induced by inertia increase with walking speed (see chapter 6 of this thesis), see also again table 7.1.

d. Data Analysis

Joint and segment kinematics

The kinematical data were split into individual stride cycles. The individual marker paths were filtered by the rigid body filter of the PTI software (VZAnalyzer™ V3.50). This filter allows grouping sets of markers in supposed rigid bodies, and uses the motion paths of all markers of the body to reconstruct and filter the motions of the separate markers, mainly based on the impossibility of shape changes and marker jumps. The chosen rigid bodies were: trunk cluster, upper leg cluster, lower leg cluster, foot, robot upper leg and robot lower leg. All positions were expressed in a coordinate system defined by the walking direction (x), the vertical (y) and the axis perpendicular to this plane (z) according to the right hand orientation.

For calculating segment angles, the projections of the orientation vector of the marker-clusters on two global planes (sagittal-xy and frontal-yz) were used. We defined the straight standing posture as zero angle for the different segments. The knee angle was obtained by subtracting the lower leg angle from the upper leg angle. As we did not measure the pelvis angles, we could not calculate the hip angles. However, as the pelvis rotations are relatively small compared to the thigh rotations, the thigh angles reflect the rotations in the hip. To illustrate the average trajectories for each condition, the angles for each cy-
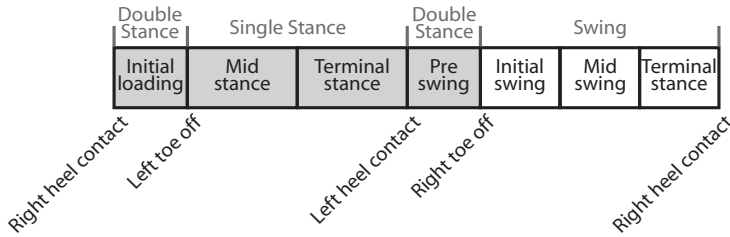
Figure 7.2. Segmentation of the gait cycle into phases for the calculation of the integrated EMG over these phases. For clarity, the standard gait events are indicated with respect to these phases.

cle were time normalized and subsequently averaged over all cycles and ensemble averaged over all subjects.

From the calculated angles, we extracted the angular range of motion of the frontal and sagittal trunk and thigh angle and the sagittal knee angle. The ranges were calculated by subtracting the minimum angle from the maximum angle for each step-cycle.

Gait parameters

We also compared the spatial and temporal gait parameters. From the measured marker positions, we calculated the step width. As only the movements of the left leg were measured, we defined the step width as twice the z-distance between the average position of the left ankle marker during single stance for each cycle and the whole trial average trunk position, obtained from the four trunk markers.

The footswitch data were used to calculate the temporal variables including cycle time (period between two consecutive contacts of the same foot), stance time (period between initial contact and toe-off in the same limb), swing time (period from toe-off to heel contact of the same limb) and double stance ratio (total double stance time divided by the single stance time).

To investigate the within-subject variability, we assessed the standard deviation over the values for the different cycles for each separate condition and subject for the aforementioned spatial and temporal gait parameters.

EMG measurements

All EMG processing was done with custom written software (Roetenberg, Buurke et al. 2003) in Matlab (Nattick, USA). The raw EMG data were band pass filtered at 10-400 Hz with a 2nd order zero lag Butterworth filter and converted to smooth rectified EMG signals (SRE) using a low-pass 2nd order zero lag Butterworth filter at 25 Hz for smoothing. To visually inspect the raw and smooth rectified signals, they were broken up into the individual stride cycles, based on subsequent heel strikes. If one of the muscles contained artifacts (contact artifact, measurement noise) the activity during this cycle was rejected from further analysis. Subsequently, the SRE of each muscle was normalized to its maximal activity over the entire experiment. The mean EMG was calculated from these SRE traces over 7 phases of walking. The values for all the gait cycles for a single condition were averaged to result in one value for each subject, muscle, phase, velocity and type of walking.

The different phases of walking were defined based on the footswitch data of both feet (see Figure 7.2). The double stance phase starting with heel contact of the left leg was defined as initial loading and the second double stance phase was defined as pre swing.

Although loading and swing preparation were not the only ongoing process during the different double stance phases, we decided to call the double stance phases after these processes as these processes were the most dominant ongoing processes during these phases. The single stance phase was split up into two phases of equal length: mid stance and terminal stance and the swing phase was split up into 3 intervals of equal length: initial swing, mid swing and terminal swing.

The smoothed EMG data were used to determine the onset and offset times of the main burst for each muscle. The used algorithm (Roetenberg, Buurke et al. 2003) is based on the approximated generalized likelihood ratio (AGLR) principle described by Staude and Wolf (Staude 2001). This algorithm was used to analyze the smoothed EMG signals of every stride in the gait cycle separately with respect to the on- and off-times of muscle activation. Subsequently, all detected on- and off-times were normalized in time using the stride time starting from the related heel strike.

Statistical Analysis

Linear mixed modelling analyses were applied to explain differences in mean EMG activity over time by the factors type of walking (two-level factor 'type of walking') for each velocity (three-level factor 'velocity') per interval (seven-level factor 'interval'), separately for each muscle. To account for the correlation between the repeated measurements within a subject, in the model different intercepts were assumed for each interval per subject (by including the factor subject and interval as random factors), The factors 'type of walking', 'velocity' and 'interval' were treated as fixed effects. The two-way interactions 'type of walking*velocity', 'type of walking*interval' and 'velocity*interval' and three-way interaction 'type of walking*velocity*interval' were also included. For all significant effects and interactions post-hoc tests (Sidak adjustment) were performed. The level of significance was defined as 5%.

For the onset and offset times of EMG bursts, kinematics and gait parameters a similar mixed model was used without the interval factor, with subject as a random factor, and type of walking and velocity as fixed factors.

3. RESULTS

The naturalness of walking with LOPES was assessed by comparing temporal and spatial gait parameters, movements and muscle activity between LOPES walking and free walking. The results on each of these aspects are presented in the following paragraphs.

Table 7.2: Average values ± standard deviations of the gait parameters for the different types of walking,

Variable	Treadmill walking	LOPES walking
Cycle time	1.427 ± .308 s	1.463 ± .326 s
Double stance ratio	.45 ± .05	.40 ± .06 *
Swing time	.472 ± .082 s	.508 ± .089 * s
Stance time	.955 ± .232 s	.955 ± .246 s
Step width	.328 ± .059 m	.342 ± .053 *m

* significant from treadmill walking with p<.05
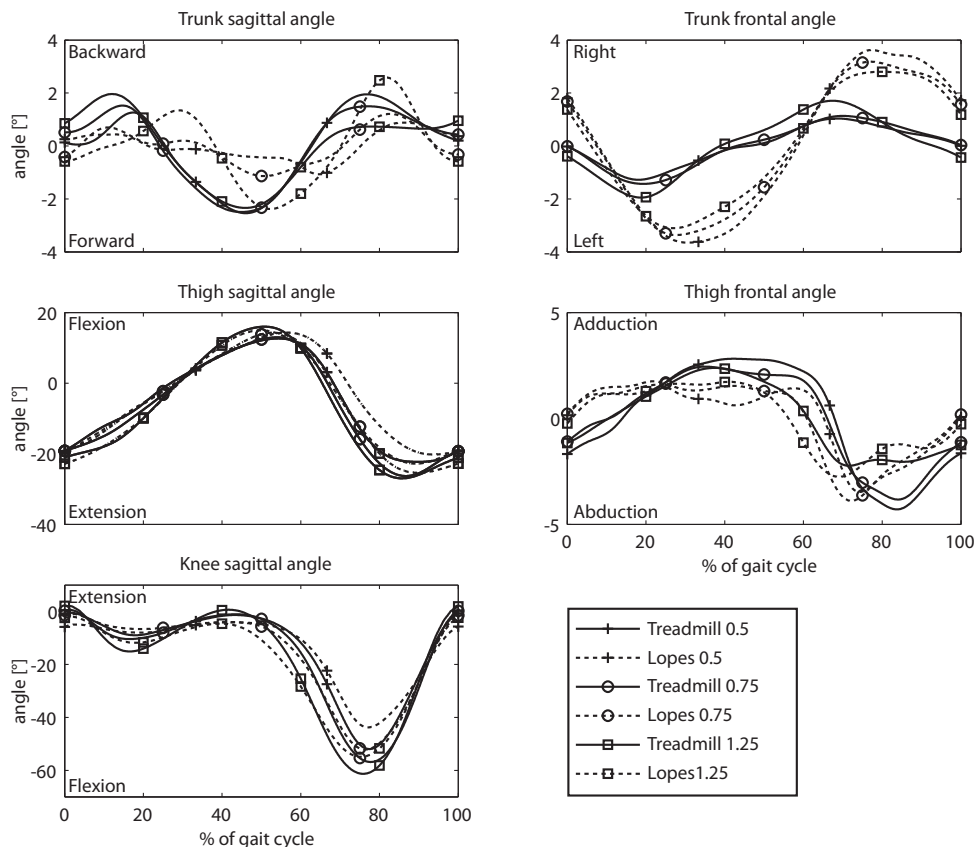
Figure 7.3: The average trajectories of the sagittal and frontal rotations of the trunk (upper panels), of the upper leg (middle panels) and the sagittal angle of the knee (lower panel) for all conditions, averaged over all subjects.

a. Gait parameters and kinematics

The basic gait parameters showed some significant changes while walking in LOPES compared to treadmill walking (see Table 7.2). The cycle time and total stance time did not show a significant change, whereas the swing time showed a significant increase. The absence of a change in cycle time implied that also the step length did not change as these

Table 7.3: Average angle ranges ± standard deviations for the different types of walking

Variable	Treadmill walking	LOPES walking
Sagittal trunk angle	2.0 ± 1.1 °	2.1 ± 1.2 °
Frontal trunk angle	1.7 ± 1.0 °	2.7 ± 1.4 ° *
Sagittal thigh angle	42.9 ± 10.8 °	39.0 ± 9.9 ° *
Frontal thigh angle	8.9 ± 3.4	7.9 ± 3.0*
Sagittal knee	66.0 ± 10.9 °	54.1 ± 8.7 ° *

* significant from treadmill walking with $p < .05$

Table 7.4: Within subject variability (± standard deviations) for all subjects for the temporal and special gait parameters.

Variable	Treadmill walking	LOPES walking
St Dev Cycle time	.031 ± .020 s	.034 ± .023 s
St Dev Double stance ratio	.028 ± .017	.033 ± .020
St Dev Swing Time	.032 ± .015 s	.035 ± .027 s
St Dev Stance Time	.018 ± .008 s	.018 ± .011 s
St Dev Step width	.023 ± .006	.027 ± .010 *

measures are directly related when walking with imposed velocities. The increase in swing time was accompanied by an increase in single stance time, which led to a significant decrease in Double stance ratio (p<.001). The step width showed a small (0.014 m) but significant (p=.011) increase in LOPES walking compared to treadmill walking.

The changes in gait parameters were accompanied by changes of the segment/joint kinematics. Figure 7.3 illustrates the ensemble average over all subjects for the rotations in trunk, thigh and knee. The sagittal knee and thigh rotations and the frontal thigh rotation showed similar patterns in LOPES walking and treadmill walking. Still, the range of motion for the knee (p<.001), sagittal (p=.005) and frontal (p=.040) thigh movements were significantly smaller in LOPES walking compared to treadmill walking (see Table 7.3). The general trajectories of the trunk diverge considerably more between the different modes of walking. For the frontal trunk rotation, this was accompanied by significant (p<.001) change of the range of motion. During LOPES walking subjects demonstrated an increased frontal trunk rotation.

Within-subject variability

In order to assess, whether walking in LOPES influenced the amount of within-subject variability, the standard deviation of the values of the different cycles were calculated for each subject and condition and compared between conditions. The within subject variability for the cycle time, stance time, swing time and double stance ratio did not show any significant difference (see Table 7.4). The variability in the step width was significantly (p=.032) larger in LOPES walking compared to treadmill walking, although the absolute difference was small (0.004 m).

None of the gait parameters or kinematic parameters showed an interaction effect between type of walking and velocity.

b. Muscle activity

An evaluation of the movements does not suffice in determining whether unhindered walking is possible in the LOPES device, as subjects could have produced the same movements at the cost of different muscle activity in coping with the device. Therefore we also evaluated the muscle activity in timing and in amplitude.

Onset and offset times of burst

The onset and offset times of the main bursts reflect the timing of muscle activity (see Figure 7.4). For the rectus femoris, we only used the burst during stance-to-swing transition, as this burst reflects the activity of the rectus femoris and is not caused by cross talk from the vastus lateralis and vastus intermedius as is the case with the often reported burst during initial contact (Nene, Byrne et al. 2004). The occurrence of the burst in rec-
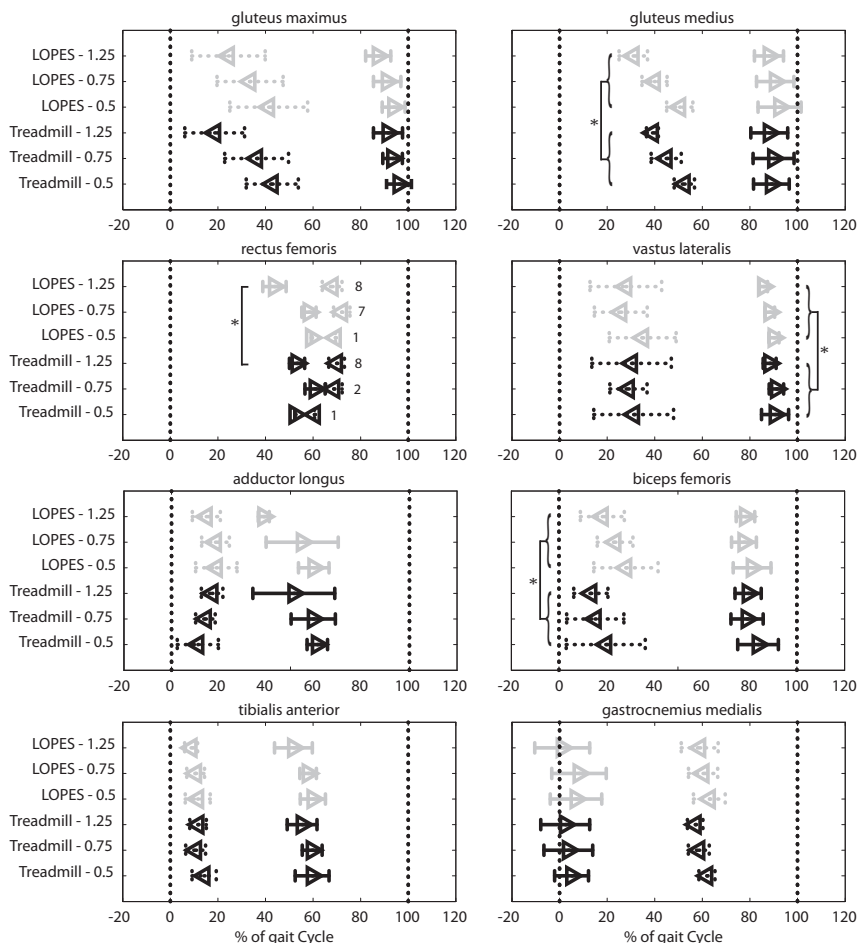
Figure 7.4: Mean and standard deviation of the onset and offset time of the main burst for each muscle. On the left side the conditions are indicated. The grey symbols indicate the different LOPES conditions and the black symbols the different treadmill conditions. The ▶ symbol indicates the onset of the burst and the ◀ symbol indicates the offset of a burst. The numbers in the rectus femoris panel specify the number of subjects who showed a burst in that condition. Significant differences are indicated with a *.

tus femoris was strongly dependent on the walking velocity. For the lowest velocity only one subject in each condition showed the burst (see numbers in the rectus femoris panel of Figure 7.4). The absence of a burst in the other subjects indicated that this muscle was not active for these subjects. Although these unbalanced numbers obstruct the performance of statistical analysis, the inequality in subjects showing the burst could be considered as a measure of the difference in treadmill and LOPES walking. Furthermore, these difference in burst occurrence will also be reflected in differences in mean integrated activity. For the highest velocity, only two subjects did not show a burst, the remaining subjects showed a significant earlier onset in LOPES than in treadmill walking (43.8 % vs. 53.3 % walking, p<0.001), whereas the offset did not change significantly. Apart of the changes in rectus
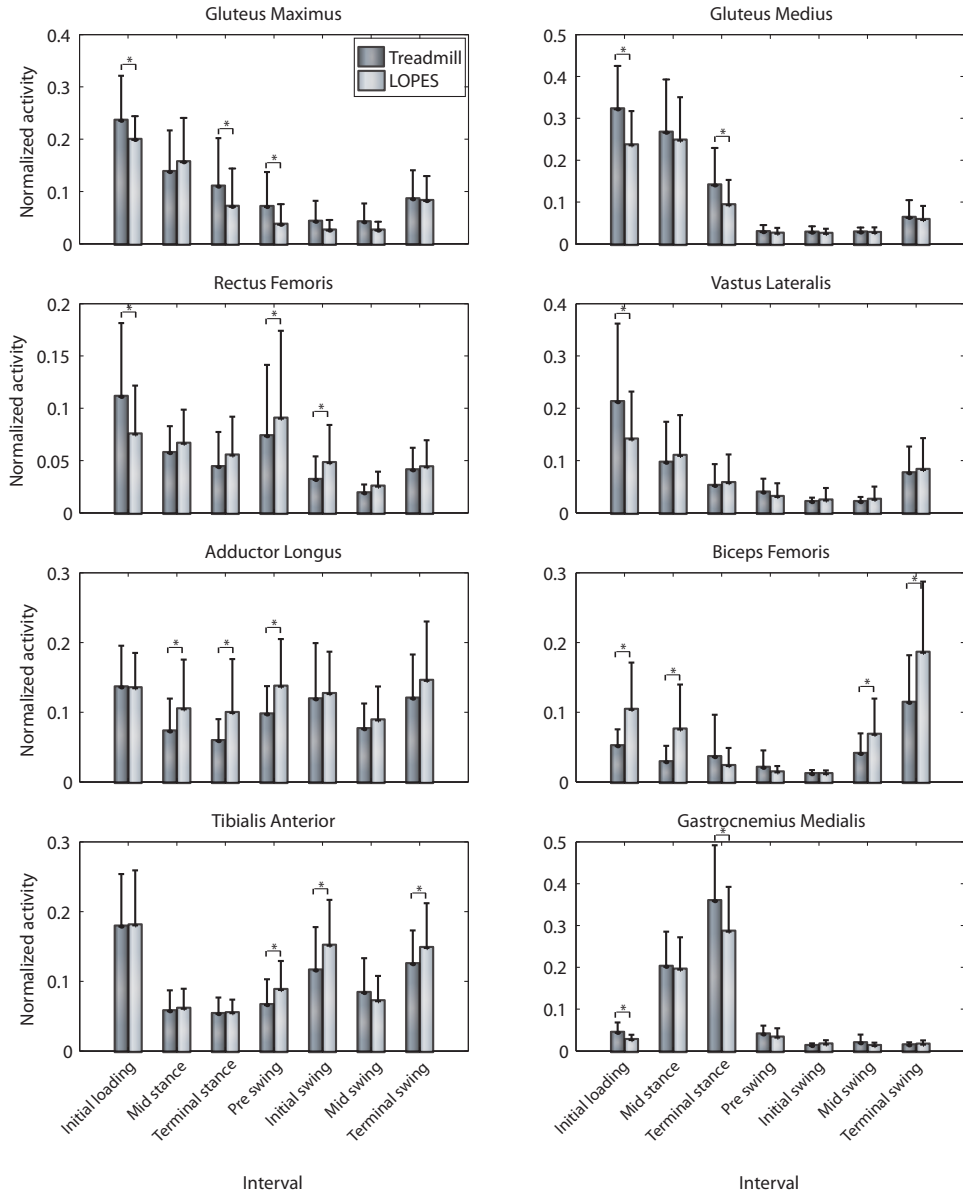
Figure 7.5. Mean normalized integrated activity for each muscle over the different phases for LOPES walking and treadmill walking.

remoris, three significant changes were observed in the timing of the burst of the other muscles. The onset occurred significantly earlier in LOPES walking compared to treadmill walking for the vastus lateralis (88.0 % vs. 90.0 %, p=0.031). The burst of the gluteus medius ended significantly earlier in LOPES walking compared to treadmill walking (40.5 % vs. 45.4 %, p<0.001) whereas the biceps femoris showed a delay offset while walking in LOPES (16.1 % vs 23.4 %, p=0.024). None of the muscles showed an interaction effect

Table 7.5: Significance levels for the main effect of type of walking and all interaction effects containing type of walking for the comparison of the mean normalized EMG activity.

	Type of walking	Type of walking x Interval	Type of walking x Velocity	Type of walking x Interval x Velocity
Gluteus maximus	<.001	.012		
Gluteus medius	<.001	<.001		
Rectus femoris		<.001		
Vastus Lateralis		<.001		.001
Tibialis anterior	.001	.001		
Biceps femoris	<.001	<.001		
Adductor Longus	<.001		.006	
Gastrocnemius Medialis	<.001	<.001		

Table 7.6: The p-values for comparison of the mean normalized EMG of LOPES walking and treadmill walking for the different muscle and for the different phases.

	Gl Ma	Gl me	RF	VL	TA	BF	AL	Ga Me
initial loading	.004	<.001	<.001	<.001		<.001		.049
mid stance						<.001	.012	
terminal stance	.002	<.001					.002	<.001
pre swing	.007		.012		.009		.002	
initial swing			.017		<.001			
mid swing						.002		
terminal swing					.005	<.001		

between velocity and condition.

Mean integrated activity

Although all muscles showed approximately the same pattern during LOPES walking and treadmill walking (*this can be imagined by connecting the different bars with lines in Figure 7.5*), they all showed a significant difference in the integrated activity for at least one phase (an overview can be found in Table 7.5). The hip extensors (gluteus medius and gluteus maximus) showed a decrease of their activity while walking in LOPES (significant type of walking effect, see Table 7.6). The difference was dependent on the interval. During the start and the end of the stance phase, the mean activity was significantly lower, while in the other intervals there was no significant difference. For the knee extensors (vastus lateralis and rectus femoris) the overall activity did not differ significantly. Still, for the rectus femoris the activity was higher during the transition from stance to swing. In addition, during the initial loading the activity of both muscles was lower in LOPES. However, using needle electrodes Nene and colleagues (Nene, Byrne et al. 2004) showed that the activity of the rectus femoris during initial loading and the single stance was the consequence of cross talk from the vastus lateralis and vastus intermedius. The significant 3rd order type of walking x interval x velocity interaction for the vastus lateralis indicated that the difference in type of walking during initial loading was dependent on velocity. For the middle and high velocity, the difference was significant. The bi-articular biceps femo-

ris showed an increase of its activity for LOPES. This difference was dependent on the interval, only the intervals from mid swing to mid stance were higher. Exact during these intervals the main burst of the biceps femoris occurred. The adductor longus was the only muscle that showed an interaction between type of walking and velocity. For the highest velocity the activity was significantly higher in LOPES walking, while for the middle and lowest velocity the difference was not significant. The lower leg muscles both showed a type of walking effect and an interaction effect between type of walking and interval. They showed their most prominent differences during the transition from stance to swing. The gastrocnemius had a smaller activity during terminal stance in LOPES walking than in treadmill walking, whereas the tibialis anterior showed an increased activity during pre swing and initial swing while walking in LOPES.

4. Discussion

In the introduction we argued that a proper functioning of a 'patient-in-charge' or 'zero force' mode, that is walking in a gait training device with minimal resistance, is important for the implementation of interactive training according to the principles of 'Assist As Needed'. Proper functioning means that for a person walking with the device, near-to-normal muscle activation patterns would lead to near-to-normal gait kinematics.

The results showed that walking in a zero impedance controlled gait training device differed on various aspects from walking without the device. The observed variability was at least as large as during normal walking and in case of the step width variability it was even significantly larger. Still, the observed change was only 0.004 m. Also on other gait and kinematic parameters the observed significant changes were small compared to the limits of measurement and calculation accuracy. The significant changes in joint angle ranges were smaller than 3° (except from the knee angle), whereas 5° is a common reported value of kinematic error due to soft tissue artefacts (Leardini, Chiari et al. 2005; Cereatti, Della Croce et al. 2006). Also the observed difference in swing time of 0.02 s was small compared to the accuracy in determining contact phases from heel switch data as reported in literature (Hausdorff, Ladin et al. 1995) . In essence, the walking pattern with the device was similar to the walking pattern without the device, except from the knee movement. These changes were accompanied by significant changes in the muscle activity.

In the next paragraphs, we will first discuss these differences, identify possible sources and elaborate upon the significance of these findings for implementation of AAN algorithms, before we go into the clinical relevance of the findings.

a. Sources of observed differences

Pelvis motion
The amplitude of the muscle activity did show several differences, especially for the Biceps Femoris and the Adductor Longus. The increased activity of the Adductor Longus and the frontal trunk rotation, might have their origin in the resistance of the device to lateral movements of the pelvis. Although the controller was set to regulate the sideward forces on the exoskeleton to zero, it did not compensate for the inertia of the exoskeleton and some remaining friction. Less pelvis motion would theoretically lead to less lateral centre of mass excursion.

The increase of activity of the Adductor Longus during stance may be caused by increased effort needed to still push the total body centre of mass to above the weight bearing stance leg. The decrease in lateral pelvis motion is compensated for by an increased frontal trunk rotation. The need to do this is amplified by the increase in step width, which was probably caused by experienced 'danger' of walking narrow, because of the connective constructional parts at the left and right leg.

The aforementioned changes might have been aggravated by restraining the pelvic rotation, though the pelvic rotations during normal walking are generally rather small (see for example chapter 2) and the fixation of the subject into device might have allowed some movement (which we didn't measure). A similar study using the PAM (Aoyagi, Ichinose et al. 2007), which allows pelvic rotation could further clarify the importance of pelvic rotations in gait training.

Inertia of the exeskeleton

The increased activity of the biceps femoris during mid swing and terminal swing can be explained by the increased inertia of the swing leg when wearing the LOPES exoskeleton. This increase was described in the methods section. Inverse dynamic calculations showed that the maximum interaction torque between exoskeleton and leg for the lower leg amounts to 3, 4 and 5 Nm for the three speeds, and for the upper leg to 7, 13 and 20 Nm. Especially for faster walking these maximum torques become considerable. The swing phase of walking is normally a largely pendulum like movement driven by the rectus femoris, which is decelerated by the activity of the biceps femoris and semitendinosus. When the exoskeleton is attached to the leg, not only the mass of the leg has to be decelerated but also the mass of the exoskeleton leg. These results are in agreement with a study investigating the effect of an additional mass to the lower leg (Noble and Prentice 2006) . Adding a 2 kg weight to the left lower leg resulted in an increase of the hip extensor torque and an increase of the knee flexor torque at the end of the swing phase. Both of these torques can be generated by the bi-articular Biceps femoris. In addition, they showed that initial swing was characterized by an increase of the hip flexion torque and knee extension torque. These results correspond to the increased rectus femoris activity during pre-swing and initial swing. Noble and Prentice also found a decrease of maximum knee flexion during swing and an increase of the ankle dorsiflexion, corresponding to the decrease of the maximal knee angle range and the increase of the tibialis anterior activity during the pre swing and initial swing phase. Finally in the study of Noble and Prentice and in other studies (Skinner and Barrack 1990) the addition of weight has shown to increase the swing time, which is also agreement with the present study. Apparently, wearing an exoskeleton is much like adding mass to your lower legs. This stresses the need for impedance controlled exoskeletons to be designed as light weight as possible and also indicates a point of further improvement in LOPES.

In general, the observed changes in muscle activity during the stance phase while walking in LOPES showed lower EMG activity compared to free walking. The gluteus maximus, gluteus medius and gastrocnemius medialis all showed a decrease in activity during initial loading and terminal stance. The gluteus maximus and gastrocnemius medialis have shown to play an important role in forward progression during mid stance and terminal stance, respectively (Neptune, Kautz et al. 2001; Gottschall and Kram 2003; Neptune,

Zajac et al. 2004). The drop of their activity indicates a decrease of push off force. Apparently, the contribution of the muscles to the acceleration of the Center of Mass (CoM) had decreased, which could be the result of an overall decrease of the amplitude of the fluctuations in the acceleration and deceleration of the CoM through continuously opposing forces like friction (in the linear guide) and inertia of the exoskeleton. During the experiments, we indeed observed relatively small movements of the pelvis while walking in Lopes, compared to free walking (chapter 8). However the experimental setup did not allow measurement of the pelvis position in both conditions, so we were not able to directly compare them.

Apart of the changes in integrated activity of the muscles, some muscles also showed changes in timing of their activity. Changes in timing, indicate that a different coordination is required for walking in the device. The observed changes were in some cases so small that it could be questioned whether the changes were also relevant. Based on results of Perry (Perry 1992), Buurke (Buurke 2005) argued that a change in timing between conditions should be at least 5% to be relevant. The changes in gluteus medialis and vastus lateralis were smaller than 5 %, 4.9 % and 2 % respectively, and consequently were considered irrelevant. The rectus femoris showed a significant and relevant earlier onset in LOPES walking (9.5 %) and the biceps femoris showed a delayed offset (7.3 %) Both of these changes could be attributed to the increased inertia of the swing leg, when the exoskeleton is attached to it. The earlier onset of the rectus femoris indicated an earlier force build up for the initiation of the swing phase, while the delayed offset of the biceps femoris could have indicated an increase of time to decelerate the swing leg.

Comparison with other studies

Some other studies also compared the activation patterns while walking with a robotic device with the patterns outside the device (Aoyagi, Ichinose et al. 2007; Schmidt, Volkmar et al. 2007). However, most of these studies restricted their analysis to a qualitative comparison and did not perform a detailed quantitative analysis as was done in this study. Only Hidler and Wall (Hidler and Wall 2005) performed a similar detailed analysis when they assessed the alterations in muscle activation patterns of subjects that walked in the position controlled Lokomat compared to free treadmill walking. The muscle activity in their study not only differed during the main burst but also outside these bursts. Especially, the rectus femoris, adductor longus, biceps femoris, vastus lateralis and gluteus maximus showed clear increases of muscle activity during periods in which the muscle was normally silent. This would probably have resulted in significant changes in the timing of these muscles, however data about the timing were not provided in this study. In total, Hidler and Wall found 32 significant differences with free treadmill walking, compared to 21 in the present study. However there were some differences in the conditions and especially the analysis which could hinder a direct comparison of both studies. If we would analyse our data in a similar way as they did, only considerng comparable walking velocities, use predefined intervals instead of intervals based on detected contacts and use a repeated measures ANOVA, we would only have observed 11 significant differences.

Although these results do indicate that the muscle activation patterns were closer to normal while walking in a zero impedance controlled device compared to walking in a position controlled device, one should be aware that the comparison of EMG patterns is quite cumbersome in a position controlled device. Despite that the the position control is

not ultimately stiff and that the patient fixation in the device will allow some movement, the generated muscle activity will only minorly influence the resulting motions, in other words, different activation pattern would result in approximately the same motion pattern. One is therefore measuring two aspects at the same time: how well a person is actively walking according to the device trajectories (which could also have been passively followed), ánd how natural these trajectories are. This combination makes outcomes hard to interpret. Of course, for healthy subjects, it will feel more natural to walk according to the device instead of working against it (Aoyagi, Ichinose et al. 2007).

Another aspect that complicates a direct comparison with the mentioned study is the difference in DoFs between the Lokomat and LOPES. Recently, we have shown (chapter 8) that the additional DoFs of LOPES (pelvis translations and hip abduction) had only small effects on the results as presented in the current study, especially on the EMG results. Most clear effect of blocking of these DoFs was increased rotations of the trunk around all axes. The larger resemblance of EMG patterns in LOPES walking with free walking compared to Lokomat and free walking, should therefore be mainly contributed to the zero impedance control that replaced the joint-trajectory (position) control.

Implications for assist as needed

An analysis like the one performed in this study can provide important considerations regarding the implementation of assist as needed. Walking with the device in a mode where no assistance is offered, is not exactly the same as free walking. This may be of importance in deciding on training interventions.

For example, when we will not provide assistance in knee flexion, the patient will in fact have to generate more activity than normal to overcome the resistance in swinging the leg. Therefore, no assistance in knee flexion should only be provided to those patients that are very well able to swing their leg, or a no-assistance situation should be simulated by offering a little assistance to compensate for the noticed deviations. Without this, prolonged exposure to this resistance as during training, could in fact lead to an exaggerated knee flexion while walking without the device.

The results also indicated that there was still some resistance in the horizontal pelvis motions. These degrees of freedom in the pelvis are essential in balance control during gait. Israel and colleagues (Israel, Campbell et al. 2006) showed that the metabolic costs during standing in the Lokomat were significantly smaller as during unassisted standing. They argued that this decrease was caused by a decreased need for muscular work for stabilization in the frontal and sagittal plane as the lateral and sagittal stability were provided by the horizontal pelvis fixation in the Lokomat. As stroke patients have a decreased lateral stability, training of the stability should be a crucial element in their gait training. The observed remaining resistance in the pelvis degrees of freedom of LOPES also contributes in stabilizing the body. This stabilization might be beneficial early after stroke, when this assistance in balance control might be seriously needed. However, it is an undesirable effect when the subject needs to be encouraged to recover his balance control during gait through progressively decreasing the amount of provided assistance. Either improvements in the design or controller based compensation can be used to simulate a no-assistance situation.

b. Clinical relevance

This study showed that healthy people walking with LOPES show walking patterns closely resembling those of walking without the device. It can be hypothesized that this implies that the device has the potency to deliver task specific training, because task-specificity can be interpreted as: walking during training similar to natural walking. In the sense that the dynamics of walking in training remain largely unaffected, so that natural muscle activation patterns lead to natural gait kinematics, while experiencing the natural sensory feedback. In a device with too large imperfections (considerable friction or inertia, or constrained movements), a patient would learn to generate activity that leads to completely different motions when walking without the device; the learned activation pattern would not be appropriate for walking over ground. As mentioned before, the patient-in-charge mode reflects the end stage of training as here (ideally) no assistive forces are applied by the robot that interfere with the patients' self-generated forces. Based on the results of this study in healthy subjects we can conclude that LOPES seems to have a good potential to provide a task specific training. It is however not known how close to normal walking during training should be in order to consider the training as sufficiently task-specific. This is an important issue, that can be resolved only with realizing actual training sessions with patients.

As LOPES is going to be used to retrain stroke patients, we need to assess in future research whether LOPES also minimally affects the typical walking pattern of stroke patients. Due to their impairments, the walking pattern of stroke patients clearly differs from healthy subjects on several aspects (Chen et al., 2005; Den Otter et al., 2006; Olney and Richards, 1996). This places additional demands on the degrees of freedom of the LOPES exoskeleton. For example, a large group of stroke patients shows an increased abduction during the swing phase (Kim and Eng, 2004). This increased abduction is part of a hip circumduction strategy which also involves pelvic rotation and which enables patients with a hyper extended knee at push off, to achieve enough toe clearance during swing. Although the amount of pelvic rotation is limited in the device, by utilizing the hip abduction/adduction degree of the exoskeleton, stroke patients could possibly perform these movements in LOPES and consequently would make the movement in LOPES that they usually make without the device. This is especially important as most stroke patients develop their own optimal way of walking during training, which is not necessarily the healthy symmetrical way of walking (Buurke 2005).

By using impedance controlled robotic devices with sufficient degrees of freedom such as LOPES, or a combination of the PAM and POGO (Aoyagi, Ichinose et al. 2007), compensatory strategies can be allowed to occur and could even be trained. However, for training of these strategies a joint based control in which "normal" reference trajectories are used, will not suffice. A possible solution is to use a teach and replay approach (Aoyagi, Ichinose et al. 2007). Fundamental to this approach is that subject specific trajectories are defined by recording a reference trajectory, while the device functions in a patient-in-charge mode and a therapist assists the movement. Another solution is to implement a specific assist as needed algorithm that selectively controls subtasks of walking (Ekkelenkamp, Veltink et al. 2007; Van Asseldonk, Ekkelenkamp et al. 2007). In this kind of control, walking is subdivided in subtasks (like foot clearance, lateral balance control, weight support) that all have to be accomplished successfully to progress without falling.

The performance on each of the subtasks can be evaluated and regulated separately. The patient can use different strategies to accomplish a certain subtask, i.e. the patient can use a hip circumduction strategy instead of the regular knee flexion to get enough foot clearance. When the therapist believes that the prognostics for regaining knee flexion are not very good, he can decide to provide the patient with support to learn a hip circumduction strategy. This means that training with selective control does not necessarily have to result in a symmetrical walking pattern, but can be aimed to achieve the most functional walking pattern for this particular patient. We believe that by allowing or even facilitating alternative movement strategies the efficacy of robotic devices could possibly be further improved. At least it will provide valuable information in the ongoing debate (Kwakkel, Kollen et al. 2004) about whether during recovery in stroke patients the emphasis should be placed on restoring the original movement strategies (restitution) or on achieving the best functional recovery possibly with the use of compensatory strategies (Kwakkel, Kollen et al. 2007).

5. Conclusion

Evaluating the LOPES in a 'patient-in-charge' or 'zero-force' mode showed that healthy subjects walking with the device show several differences in both activation patterns and kinematics.

The changes that were found could likely largely be contributed to the inertia of the device which cannot be compensated for in the current implementation. It is therefore important to further minimize weight, or to compensate controller-based for the undesired effects of the inertia. Compared to a related study the differences were however both few, and small. Cycle-to-cycle variation while walking with the device was comparable to free walking variability. These results can largely be addressed to the proper working of an impedance-control mode, much more than to the additional pelvis degrees of freedom of the LOPES.

Together this shows that the LOPES, or more generally, an impedance controlled device with sufficiently low realizable impedance is a promising approach for providing gait training that would fit in a progressive training regime that is task specific and following an 'Assist-As-Needed' approach. How 'natural' walking with such a device should be, to offer a sufficiently task specific training that teaches skills transferable to free walking, remains a question open to research. The next step is to evaluate the device with stroke patients, first in the same zero-force mode and subsequently extending this to a full training.

6. Acknowledgement

7. References

Agrawal, S. K., Banala, S. K., Fattah, A., Sangwan, V., Krishnamoorthy, V., Scholz, J. R. and Hsu, W. L. 2007. Assessment of motion of a swing leg and gait rehabilitation with a gravity balancing exoskeleton. IEEE Transactions on Neural Systems and Rehabilitation Engineering **15**(3): 410-420.

Aoyagi, D., Ichinose, W. E., Harkema, S. J., Reinkensmeyer, D. J. and Bobrow, J. E. 2007. A robot and control algorithm that can synchronously assist in naturalistic motion during body-weight-supported gait training following neurologic injury. IEEE Transactions on Neural Systems and Rehabilitation Engineering **15**(3): 387-400.

Bayona, N. A., Bitensky, J., Salter, K. and Teasell, R. 2005. The role of task-specific training in rehabilitation therapies. Topics in Stroke Rehabilitation **12**(3): 58-65.

Buurke, J. H. 2005. Walking after stroke Co-ordination patterns & functional recovery, PhD-thesis, Enschede.

Cai, L. L., Fong, A. J., Otoshi, C. K., Liang, Y., Burdick, J. W., Roy, R. R. and Edgerton, V. R. 2006. Implications of assist-as-needed robotic step training after a complete spinal cord injury on intrinsic strategies of motor learning. The Journal of Neuroscience **26**(41): 10564-10568.

Cereatti, A., Della Croce, U. and Cappozzo, A. 2006. Reconstruction of skeletal movement using skin markers: comparative assessment of bone pose estimators. Journal of Neuroengineering and Rehabilitation **3**: 7.

Chen, G., Patten, C., Kothari, D. H. and Zajac, F. E. 2005. Gait differences between individuals with post-stroke hemiparesis and non-disabled controls at matched speeds. Gait & Posture, **22**(1): 51-56.

Colombo, G., Joerg, M., Schreier, R. and Dietz, V. 2000. Treadmill training of paraplegic patients using a robotic orthosis. Journal of Rehabilitation Research and Development **37**(6): 693-700.

Den Otter, A. R., Geurts, A. C., Mulder, T. and Duysens, J. 2006. Abnormalities in the temporal patterning of lower extremity muscle activity in hemiparetic gait. Gait & Posture.

Dobkin, B. H. 2004. Strategies for stroke rehabilitation. Lancet Neurology, **3**(9): 528-536.

Ekkelenkamp, R., Veltink, P. H., Stramigioli, S. and van der Kooij, H. 2007. Evaluation of a VMC for the selective support of gait functions using an exoskeleton. Proceedings of ICORR 2007 - IEEE International Conference on Rehabilitation Robotics, Noordwijk.

Ferraro, M., Palazzolo, J. J., Krol, J., Krebs, H. I., Hogan, N. and Volpe, B. T. 2003. Robot-aided sensorimotor arm training improves outcome in patients with chronic stroke. Neurology, **61**(11): 1604-1607.

Gottschall, J. S. and Kram, R. 2003. Energy cost and muscular activity required for propulsion during walking. Journal of Applied Physiology **94**(5): 1766-1772.

Hausdorff, J. M., Ladin, Z. and Wei, J. Y. 1995. Footswitch system for measurement of the temporal parameters of gait. Journal of biomechanics **28**(3): 347-51.

Hermens, H. J., Freriks, B., Merletti, R., Stegeman, D., Blok, J., Rau, G., Disselhorst-Klug, C. and Hägg, G. 1999. European Recommendations for Surface ElectroMyoGraphy Enschede, The Netherlands: Roessingh Research and Development.

Hesse, S., Uhlenbrock, D. and Sarkodie-Gyan, T. 1999. Gait pattern of severely disabled hemiparetic subjects on a new controlled gait trainer as compared to assisted treadmill walking with partial body weight support. Clinical Rehabilitation **13**(5): 401-10.

Hidler, J., Nichols, D., Pelliccio, M. and Brady, K. 2005. Advances in the understanding and treatment of stroke impairment using robotic devices. Topics in Stroke Rehabilitation **12**(2): 22-35.

Hidler, J. M. and Wall, A. E. 2005. Alterations in muscle activation patterns during robotic-assisted walking. Clinical Biomechanics (Bristol, Avon) **20**(2): 184-93.

Hogan, N., Krebs, H. I., Rohrer, B., Palazzolo, J. J., Dipietro, L., Fasoli, S. E., Stein, J., Hughes, R., Frontera, W. R., Lynch, D. and Volpe, B. T. 2006. Motions or muscles? Some behavioral factors underlying robotic assistance of motor recovery. Journal of Rehabilitation Research and Development **43**(5): 605-18.

Husemann, B., Muller, F., Krewer, C., Heller, S. and Koenig, E. 2007. Effects of locomotion training with assistance of a robot-driven gait orthosis in hemiparetic patients after stroke: a randomized controlled pilot study. Stroke, **38**(2): 349-354.

Israel, J. F., Campbell, D. D., Kahn, J. H. and Hornby, T. G. 2006. Metabolic costs and muscle activity patterns during robotic- and therapist-assisted treadmill walking in individuals with incomplete spinal cord injury. Physical therapy **86**(11): 1466-78.

Krebs, H. I., Palazzolo, J. J., Dipietro, L., Volpe, B. T. and Hogan, N. 2003. Rehabilitation robotics: Performance-based progressive robot-assisted therapy. Autonomous Robots, **15**(1): 7-20.

Krebs, H. I. and Hogan, N. 2006. Therapeutic Robotics: A Technology Push. Proceedings of the IEEE, **94**(9): 1727-1738.

Kim, C. M. and Eng, J. J. 2004. Magnitude and pattern of 3D kinematic and kinetic gait profiles in persons with stroke: relationship to walking speed. Gait & Posture, **20**(2): 140-146.

Kwakkel, G., Wagenaar, R. C., Koelman, T. W., Lankhorst, G. J. and Koetsier, J. C. 1997. Effects of intensity of rehabilitation after stroke. A research synthesis. Stroke, **28**(8): 1550-1556.

Kwakkel, G., Kollen, B. and Lindeman, E. 2004a. Understanding the pattern of functional recovery after stroke: facts and theories. Restorative neurology and neuroscience **22**(3-5): 281-99.

Kwakkel, G., van Peppen, R., Wagenaar, R. C., Wood Dauphinee, S., Richards, C., Ashburn, A., Miller, K., Lincoln, N., Partridge, C., Wellwood, I. and Langhorne, P. 2004b. Effects of augmented exercise therapy time after stroke: a meta-analysis. Stroke, **35**(11): 2529-2539.

Kwakkel, G., Kollen, B. J. and Krebs, H. I. 2007. Effects of Robot-Assisted Therapy on Upper Limb Recovery After Stroke: A Systematic Review. Neurorehabilitation and Neural Repair.

Leardini, A., Chiari, L., Della Croce, U. and Cappozzo, A. 2005. Human movement analysis using stereophotogrammetry. Part 3. Soft tissue artifact assessment and compensation. Gait and Posture, **21**(2): 212-225.

Lunenburger, L., Colombo, G. and Riener, R. 2007. Biofeedback for robotic gait rehabilitation. Journal of Neuroengineering and Rehabilitation **4**(1): 1.

Neckel, N., Wisman, W. and Hidler, J. 2006. Limb Alignment and Kinematics Inside a Lokomat Robotic Orthosis. Paper presented at the Proceedings of EMBS 2006. 28th Annual International Conference of the IEEE Engineering in Medicine and Biology Society.

Neckel, N. D., Nichols, D. and Hidler, J. M. 2007. Joint moments exhibited by chronic stroke subjects while walking with a prescribed physiological gait pattern, Proceedings of ICORR 2007 - IEEE International Conference on Rehabilitation Robotics. Noordwijk, The Netherlands.

Nene, A., Byrne, C. and Hermens, H. 2004. Is rectus femoris really a part of quadriceps?: Assessment of rectus femoris function during gait in able-bodied adults. Gait and Posture, **20**(1): 1-13.

Neptune, R. R., Kautz, S. A. and Zajac, F. E. 2001. Contributions of the individual ankle plantar flexors to support, forward progression and swing initiation during walking. Journal of Biomechanics **34**(11): 1387-98.

Neptune, R. R., Zajac, F. E. and Kautz, S. A. 2004. Muscle force redistributes segmental power for body progression during walking. Gait and Posture, **19**(2): 194-205.

Noble, J. W. and Prentice, S. D. 2006. Adaptation to unilateral change in lower limb mechanical properties during human walking. Experimental Brain Research **169**(4): 482-95.

Perry, J. 1992. Gait Analysis. Ontario: Slack Inc.

Riener, R., Lunenburger, L., Jezernik, S., Anderschitz, M., Colombo, G. and Dietz, V. 2005. Patient-cooperative strategies for robot-aided treadmill training: first experimental results. IEEE Transactions on Neural Systems and Rehabilitation Engineering **13**(3): 380-394.

Roetenberg, D., Buurke, J. H., Veltink, P. H., Forner Cordero, A. and Hermens, H. J. 2003. Surface electromyography analysis for variable gait. Gait and Posture, **18**(2): 109-117.

Schmidt, H., Volkmar, M., Werner, C., Helmich, I., Piorko, F., Krüger, J. and Hesse, S. 2007a. Muscle activation patterns of healthy subjects during floor walking and stair climbing on an end-effector-based gait rehabilitation robot. Proceedings of ICORR 2007 - IEEE International Conference on Rehabilitation Robotics, Noordwijk.

Schmidt, H., Werner, C., Bernhardt, R., Hesse, S. and Kruger, J. 2007b. Gait rehabilitation machines based on programmable footplates. Journal of Neuroengineering and Rehabilitation **4**: 2.

Skinner, H. B. and Barrack, R. L. 1990. Ankle weighting effect on gait in able-bodied adults. Archives of Physical Medicine and Rehabilitation **71**(2): 112-5.

Staude, G. H. 2001. Precise onset detection of human motor responses using a whitening filter and the log-likelihood-ratio test. IEEE Transactions on Biomedical Engineering **48**(11): 1292-1305.

Teasell, R., Bitensky, J., Salter, K. and Bayona, N. A. 2005. The role of timing and intensity of rehabilitation therapies. Topics in Stroke Rehabilitation **12**(3): 46-57.

Van Asseldonk, E. H. F., Ekkelenkamp, R., Veneman, J. F., van der Helm, F. C. T. and van der Kooij, H. 2007. Selective control of a subtask of walking in a robotic gait trainer(LOPES). Proceedings of ICORR 2007 - IEEE International Conference on Rehabilitation Robotics, Noordwijk.

Van Peppen, R. P., Kwakkel, G., Wood-Dauphinee, S., Hendriks, H. J., Van der Wees, P. J. and Dekker, J. 2004. The impact of physical therapy on functional outcomes after stroke: what's the evidence? Clinical Rehabilitation **18**(8): 833-62.

Von Zitzewitz, J., Bernhardt, M. and Riener, R. 2007. A novel method for automatic treadmill speed adaptation. IEEE Transactions on Neural Systems and Rehabilitation Engineering **15**(3): 401-409.

chapter 8

The Effect on Walking of Balance-Related Degrees of Freedom in a Robotic Gait Training Device

Jan F. Veneman
Edwin H.F. van Asseldonk
Ralf Ekkelenkamp
Frans C.T. van der Helm
Herman van der Kooij

Abstract

In the design of exoskeletons for gait rehabilitation, the choice of degrees of freedom (DoFs) is one of the main issues. The goal of this research is to evaluate the effect of availability of additional DoFs related to balance-keeping on the normality of walking. These additional DoFs are the horizontal translations of the pelvis and the ab-/adduction of the hip. Measurements on the gait of ten healthy subjects showed that kinematics and muscle activation patterns (EMG) differ only slightly when these DoFs are blocked (and only the sagittal joint rotations are available), in the impedance-controlled LOPES exoskeleton. This shows that omitting the additional DoFs allows walking with close-to-normal motor control, and also that effects of waking in this robot per se overshadow the additional effects of the mentioned DoFs. All subjects however reported a more difficult and uncomfortable walking when the horizontal pelvis motions were blocked. An additional motivation for keeping the DoFs despite these results is that they allow implementation of balance training.

Chapter Contents

1. Introduction

In rehabilitation of stroke patients growing emphasis is put on the importance of task specific and intensive training (Dobkin 2004; Bayona, Bitensky et al. 2005). A task specific training is a training in which a subject is performing a functional and meaningful task. An important factor for successful task specific training is that the motor control during training should strongly resemble the motor control for the trained function when it is performed in 'real life'.

This state of affairs should be kept in mind when designing devices for automated gait training. It can be translated into the demand that the device should allow normal walking, *upon* which interventions can be added, exactly like what therapists are doing nowadays during for example (Body Weight Supported) Treadmill Training(Israel, Campbell et al. 2006). The degree to which normal walking in a device is possible, can be considered an important criterion for evaluating assistive devices for gait rehabilitation. Such an evaluation can in the first instance be carried out with healthy subjects, as they are perfectly able to perform normal walking.

Devices that are currently commercially available usually allow neither motion of the pelvis in the horizontal plane nor frontal hip rotations, but focus on the forward (sagittal) stepping motion. In for example the Lokomat (Hocoma Medical Engineering Inc.), the legs are supported in the sagittal direction by a rigid, usually position controlled, 'exoskeleton'. The blocking of the pelvis implies that the common instability that is present during free human walking, is absent when walking in the device and that the problem of balance keeping is omitted. The complex task of walking is reduced to the 'subtask' of timed stepping. Although such training may be still beneficial for patients, it is an open research question if including the balance task in training may or may not increase training effect (Israel, Campbell et al. 2006).

Hidler (Hidler and Wall 2005) showed that walking in a position controlled Lokomat altered EMG patterns of healthy subjects compared to free treadmill walking. From his research it could not be concluded to which extent the changes could be adressed to the fixation of the pelvis, to the position control of the legs, to the lack of possibility of hip-abduction or to walking in an exoskeleton per se. In chapter 2 of this thesis we showed that a fixation of pelvis translations in the horizontal plane alone, severely alters the gait kinematics of healthy subjects. This restriction caused changes in the speed to steplength relationship, in the stepwidth and in trunk rotations.

Based on such information we constructed an exoskeleton-type gait training device that does not block pelvis translations during walking. It controls the legs with impedance control, offering a minimal resistance ('patient in charge') mode. The used device, LOPES, is described in chapter 6 of this thesis. In chapter 7 we showed that walking in this exoskeleton hardly changes EMG patterns (compared to the findings of Hidler(Hidler and Wall 2005)) or gait kinematics.

Although this indicates that LOPES is hardly interfering with the natural gait of healthy subjects, and consequently allows task specific natural training, the question remains whether this can be specifically adressed to the impedance control mode or to the additional degrees of freedom of the device.

In this paper we evaluate whether blocking the degrees of freedom that facilitate the horizontal translations of the pelvis, negatively influences the normality of walking in the

LOPES device. The same is done for an additional blocking of the abduction possibility of the hip. The normality of walking is assessed by measuring both EMG and kinematics and comparing them for walking with and without the mentioned DoFs available. Measurements are carried out on healthy subjects.

For observing changes in walking, several methods can be used. Tempo-spatial step parameters give a good overall indication of walking. More precise information can be obtained from specific joint trajectories, although these show more inter-personal and step-to-step variations and are more difficult to compare statistically. EMG activation patterns, finally, show differences in muscle control patterns. This is important additional information because the same resulting walking pattern can be obtained using different control patterns in combination with differences in the external forces that act on the walking subject. In other words a subject can answer to constraints both with altering the motion pattern, possibly with the same activation patterns, as well as by altering muscle forces to keep the same motion pattern as much as possible or with a combination of both options.

2. Equipment and Methods

a. Subjects

Ten healthy young adults (4 male, 6 female), mean age 25,9 years volunteered to be participants for this experiment. All participants provided informed consent before testing began.

b. LOPES gait rehabilitation robot

For a detailed description of the LOPES robot see chapter 6 of this thesis. The degrees of freedom of the pelvis segment in the horizontal frame were blocked by obstructing the linear guides in both directions (Figure 8.1). The frontal hip rotations were blocked by physically obstructing the hip abduction joint (Figure 8.1, sub 4).

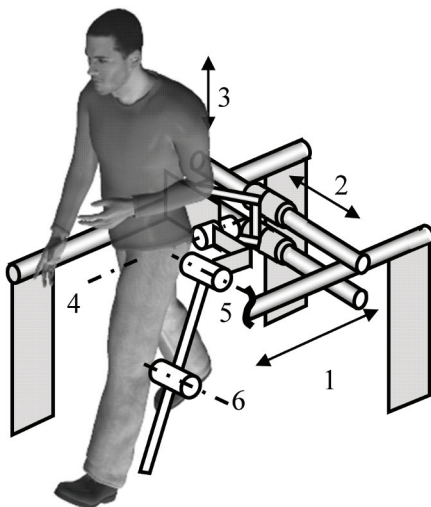During the experiments LOPES was controlled to provide minimal resistance during

Figure 8.1: Degrees of Freedom of the pelvis and leg segments of the LOPES gait rehabilitation robot: (1) forward linear guide, (2) sideways linear guide, (3) parallelogram for vertical motion, (4) hip frontal rotation, (5) hip sagittal rotation, and (6) knee sagittal rotation. The two horizontal motions (1&2) and the hip frontal rotation (6) are optionally blocked in the experiments. Except for (3) are all mentioned DoFs actuated.

Figure 8.2: Fully equipped test subject. The left leg carries the position tracking markers, the right leg the EMG electrodes. The subject is not yet connected to the LOPES robot

walking. This was implemented by a closed loop force controller, which controlled torques at all joints to zero. This way it was possible to nearly compensate for friction and gravity forces, resulting in torques below 1 Nm on joint level. It was not possible to compensate for the inertia of the exoskeleton. However, the exoskeleton was designed to have low inertia, which was achieved by removing the actuators from the exoskeleton and using flexible Bowden cables to transfer the forces from the actuators placed on the fixed world to the joints of the exoskeleton and using mainly aluminum as material.

c. Motion Capturing

Motions were measured with a PTI Phoenix Visualeyez™ VZ4000 system (PTI Phoenix, Burnaby, BC, Cananda) measuring at a frequency of 60 Hz. The system's resolution is 0.015mm and the accuracy 0.65 mm 3D combined, at 1.2m distance. Twenty five uniquely identifiable infrared markers were attached to track the motion of both the subject's and the exoskeleton's left "leg". Those markers are tracked in 3D-space by a camera bar.

The motions of the upper leg and lower leg were measured by attaching a small frame with four markers on the back of the thigh and shank. A frame of four markers was attached to the vertebra prominens, measuring the orientation and position of the trunk. The foot motion was measured by placing markers on the ankle, heel, fifth metatarsophalangeal joint, and dorsum. The motions of the exoskeleton were measured by placing four markers on both the upper leg and the lower leg part of the exoskeleton. One marker was attached to the pelvis-part of the exoskeleton. Gait phases were detected with footswitches, taped directly to the subject's heel and fore foot of both feet.

d. Muscle activity measurement

During all trials surface EMGs were recorded from the most important muscles on the right leg. The eight measured muscles were gastrocnemius medialis, tibialis anterior, biceps

femoris, rectus femoris, adductor longus, vastus lateralis, and gluteus medius and maximus muscles using a Porti EMG system (TMS international, Enschede, The Netherlands). The analog signals were not filtered before sampling at 1024 Hz, which was justified by using sigma-delta analog-to-digital converters with inherent anti aliasing filters.

The signals were sent from the portable unit via fibre optics to the computer, where data were stored for further processing. Skin preparation and the placement of the electrodes in a bipolar configuration were performed according to Seniam guidelines (Hermens, Freriks et al. 1999). A reference electrode was placed on the medial malleolus. Only the right leg was instrumented with EMG electrodes since all subjects walked healthy and symmetrically (Figure 8.2).

e. Experimental protocol

The subjects walked strapped into LOPES, with (condition LOPES Free-LF) freely movable pelvis and hip rotations, with (condition LOPES Pelvis Constraint-LPC) blocked horizontal pelvis motions and with (condition LOPES Pelvis and Abduction Constraint-LPAC) blocked horizontal pelvis motion together with blocked frontal hip rotations. The order of these three conditions was randomly selected. For each condition, the subjects walked at 0.5 m/s, 0.75 m/s and 1.25 m/s. The first two velocities were chosen to represent often reported walking velocities of stroke patients during rehabilitation and the latter velocity was chosen to represent a normal walking velocity. Within each type of walking the order of the velocities was randomized. With each change of walking velocity and/or type of walking the subject was given 3 minutes to acclimate to the walking condition. Subsequently, data were recorded for approximately 20 steps in total.

For all experimental conditions the exoskeleton had to be attached to the subject's legs and pelvis. Special care was taken to align the subject's joint axes with the joint axes of the exoskeleton. The distance between left and right hip and the distance between hip and knee joint was individually adjusted prior to walking for every subject. As the exoskeleton does not contain ankle joints, the subject's ankles were left free to move.

f. Implementation of constraints

The blocking of the additional degrees of freedom was carried out by physically blocking them as described above. In case of the pelvis translations this meant placing physical end-stops on the parallel slider bars. The frontal rotations of the hip were obstructed by blocking the joints.

It is however not a matter of simply allowing versus blocking the degrees of freedom of the human being. While allowing the motions the inertia and friction of the moving parts remain, partly hindering free motion. While blocking the motions some flexibility of the construction still allows some motion, neither is the connection of the legs to the exoskeleton fully rigid. To quantify the difference between the free and the blocked state of the three degrees of freedom the actual motion is measured. For measuring the pelvis translations a marker was connected to the robot part of the frame. For evaluating the frontal hip rotations four markers were attached to the upper leg segment of the exoskeleton. This way of measuring does not take into account the flexibility of the connection between robot and human. The motivation for this is that this flexibility will always be available in the device. The measurement is presented as the three average pelvis translation trajectories during one step. The steps measured during the trials for every condition were averaged

over all steps and subsequently over all subjects. The significance of reduction of motions is tested by comparing the ranges of the translations in the horizontal plane and the frontal hip rotations with an ANOVA test.

3. Data Analysis

a. EMG Measurements

The footswitch data of both feet were used to define the different phases of gait. These phases were defined with respect to the leg of which the muscle activity was measured. The gait cycle was divided in seven phases (see figure 7.2). The first double stance phase was defined as initial loading (1), the subsequent single stance phase was split up into to phases of equal length: mid stance (2) and terminal stance (3), the second double stance phase was called pre swing (4). The swing phase was split up into three intervals of equal length: initial swing (5), mid swing (6) and terminal swing (7). This numbering will be used in the figures and analysis

All EMG processing was done with custom written software (Roetenberg, Buurke et al. 2003) in Matlab (Nattick, USA). The raw EMG data were band pass filtered at 10-400 Hz with a 2nd order zero lag Butterworth filter and converted to smooth rectified EMG signals (SRE) using a low-pass 2nd order zero lag Butterworth filter at 25 Hz for smoothing. The smooth rectified EMG (SRE) signals were broken up into the individual stride cycles, based on subsequent heel strikes. The SRE data were visually inspected for every separate gait cycle. If one of the muscles contained artifacts (contact artifact, measurement noise) the activity during this cycle was rejected from further analysis. Subsequently the SRE of each muscle was normalized to its maximal activity over all conditions. The mean EMG was calculated from these SRE traces over the previously defined seven phases of walking. The values for all the gait cycles for a single condition were averaged to result in one value for each subject, muscle, velocity and experimental condition.

The smoothed EMG data were used to determine the start and stop times of the main burst for each muscle. The used objective algorithm (Roetenberg, Buurke et al. 2003) is based on the approximated generalized likelihood ratio (AGLR) principle described by Staude and Wolf (Staude 2001). This algorithm was used to analyze the smoothed EMG signals of every stride in the gait cycle separately with respect to the on- and off-times of muscle activation. Subsequently, all detected on- and off-times were normalized in time using the stride time starting from the related heel strike.

b. Movement Analysis

The kinematical data were also split into individual stride cycles. The individual marker paths were filtered by the rigid body filter of the PTI software. This filter allows grouping sets of markers in supposed rigid bodies, and uses the motion paths of all markers of the body to reconstruct and filter the motions of the separate markers, mainly based on the impossibility of shape changes and marker jumps. The default filter settings of the software were used. The chosen rigid bodies were: trunk cluster, upper leg cluster, lower leg cluster, foot, robot upper leg and robot lower leg. All positions were expressed in a coordinate system defined by the walking direction (x), the vertical (z) and the axis perpendicular
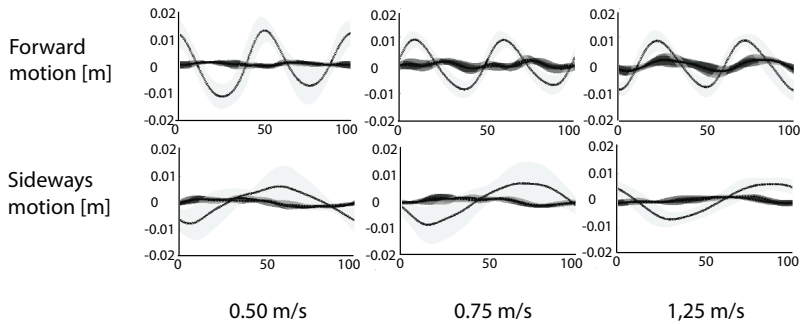
Forward motion [m]		
Sideways motion [m]		
0.50 m/s	0.75 m/s	1,25 m/s

Figure 8.3: The pelvis marker trajectories (forward and sideways direction) for all conditions, averaged over all subjects and within a subject over all steps and the standard deviations plotted as shaded areas. The line with the light standard deviation shading is the condition LF. The conditions LPC and LPAC are dark and nearly coincide. The reduction between LF and LPC &LPAC is clearly visible.

to this plane (y) according the right hand orientation. For calculating angles the projections of the markers in the xz-plane (side view) were used. Per rigid body an average vector was defined of which the angle with the x axis in this plane was calculated. This way angle ranges of and between rigid bodies were calculated. For the trunk cluster segment this procedure was followed for all three planes (xy, xz and yz). Zero angles were obtained from a standstill reference measurement. For the step-averaged trunk angle trajectories the RMS difference between the several conditions was calculated to indicate the amount of change. Parameters are determined for every individual step-cycle and averaged over the steps ignoring the two extreme values.

4. Results

a. Conditions

The reduction of motion range between condition LF on one side and condition LPC and LPAC on the other (Figure 8.3), is clearly significant for all three gait speeds ($p < 0.005$ for all comparisons) indicating that the blocking of the pelvis segment functioned well, although it should be noted that the motions of the pelvis in free walking are remarkably higher than what is measured here, in LF. In previous experiments the motions of a sacrum marker where measured to be about 8-10 times larger than the motion measured here in the LOPES-free walking condition. This is described in chapter 2 and chapter 7 respec-
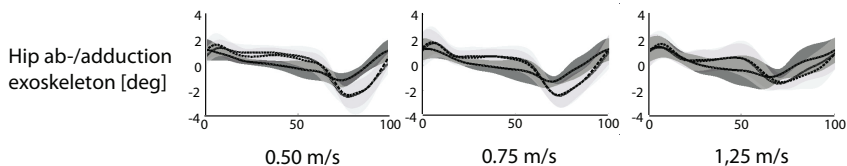

Hip ab-/adduction exoskeleton [deg]		
0.50 m/s	0.75 m/s	1,25 m/s

Figure 8.4: The trajectories of the frontal rotations of the upper leg segment of the exoskeleton for all conditions, averaged over all subjects and within a subject over all steps. The standard deviations are plotted as shaded areas. The line with the dark standard deviation shading is the condition LPAC. The conditions LF and LPC are lighter and nearly coincide. The reduction between LF&LPC and LPAC is clearly visible, though small.

Table 8.1: Average values of spatio-temporal gait parameters

variable	Reference Free walking	LF	LPC	LPAC
Step length	0.616 m	0.610 m	0.627 m	0.615 m
Step width	0.255 m	0.238 m	0.236 m	0.237 m
Swing time	0.500 s	0.523 s	0.546 s*	0.538 s
Stance time	0.900 s	0.912 s	0.970 s	0.948 s
Upper leg rotation range	42.8°	37.0°	38.0°	36.4°
Knee rotation range	63.4°	53.1°	55.9°	55.3°

* significant difference p<0.05

tively.

The same kind of evaluation was carried out for the constraining of the hip ab-adduction (Figure 8.4). The line with the dark standard deviation band (in all three pictures the line with the smallest amplitude) is the rotation trajectory for condition LPAC, and is clearly reduced in motion range compared to the lines for the other conditions that almost mutually coincide, LF and LPC. The significance of the reduction of the range of this rotation trajectory was p<0.009 for the reduction between condition LF and LPAC as well as between condition LPC and LPAC. The reduction is quite small in range, about 1.8 degree, down to 0.7 degree for the highest speed.

b. Kinematics

The most important characteristic parameters are shown in table 8.1. As can be seen LPC and LPAC differ little to nothing compared to the walking of condition LF. For reference the measured values for walking without exoskeleton are shown.
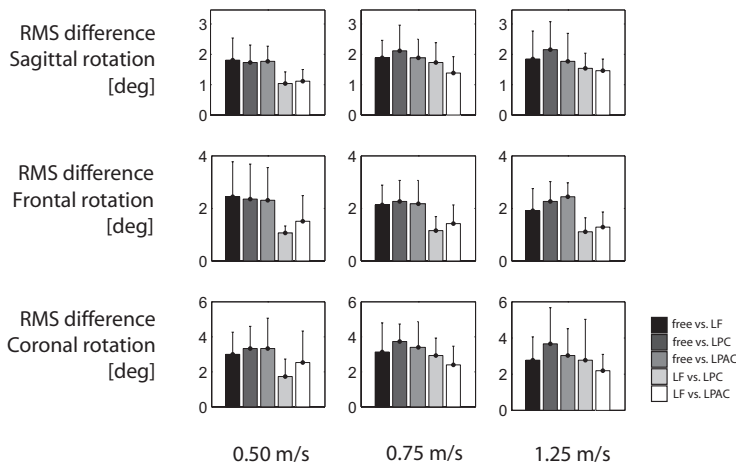

Figure 8.5: The changes in trunk rotations around the three axes, measured in RMS deviation over the averaged step trajectory. Trajectories are compared with the trajectory of free treadmill walking (first three bars) these changes appear comparable in size for all three conditions LF, LPC and LPAC. The last two bars show that there are also considerable differences between the LF condition on one hand and the LPC and the LPAC conditions on the other.
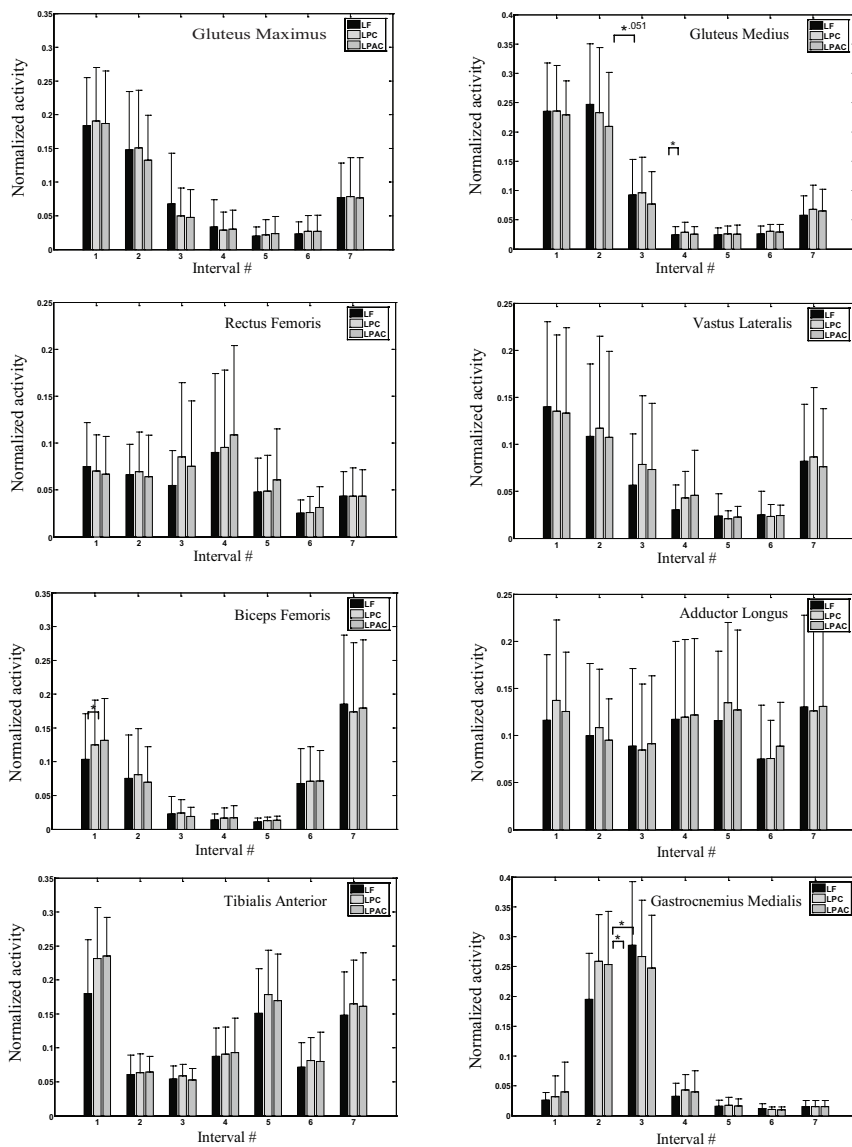
Figure 8.6: Normalized, integrated EMG activity over the defined intervals of the averaged step. Very few significant changes appear between conditions, and those that appear are small in size. In the Gastrocnemius Medialis the peak slightly advances in time.

As during the experiment increased, apparently rather forced sway of the upper body was experienced by several subjects, the overall values for change of upper body rotations are also reported (Figure 8.5). The RMS deviation from free walking appeared comparable for all three conditions, while there were also differences between LF on one side and LPC & LPAC on the other.

c. EMG

The EMG measurements (Figure 8.6) show little mutual differences between the three conditions. As can be seen from the figure, significant but small differences appear in the Gluteus Medius, interval 2 and 3, where condition three differs slightly.

The Biceps Femoris shows a small change in the first interval between LF and LPC. The change in the Gastrocnemius Medialis was the clearest of all and actually showed an advancing of the peak activation during stance or push-off.

d. Subjective perceptions

All subjects reported that walking with a fixated pelvis segment in LPC and LPAC, especially in the forward/backward direction, hindered walking. Although the reduction from free walking to walking in the freely movable exoskeleton (LF), reduced ranges of motion much more than the additional blocking of DoFs (LPC and LPAC) this last reduction was experienced as much more inconvenient. The additional blocking of the hip ab-adduction in LPAC was reported to be hardly sensible.

5. DISCUSSION

It is remarkable that despite the lack of clear differences in parameters and EMG between the conditions, all test subjects reported the walking with allowed pelvis motions (LF) to be more comfortable than walking with blocked motions (LPC & LPAC). The cause of the small difference between conditions are most likely that even in condition LF, the mass and friction of the construction still limit and counteract the intended motions of the walking subject, reducing the pelvis range of motion already with 80-90% compared to free treadmill walking. Although the weight is compensated for, the inertia of about 20-30 kg is sensed by the subject; this mass is mainly located in the carriage/pelvis segment located behind the subject. Although the motions in this direction are actuated in the LOPES robot, the inertia in these DoFs is not compensated for. Active inertia compensation, certainly possible for slow motions, would address this effectively.

The reason that subjects experience walking with this added inertia as much more comfortable compared to a fully blocked pelvis may be that they can adapt to this new dynamics, and incorporate it in their motion control. When the pelvis motions however are fully blocked, this may be too much of a limitation; the trajectories are as good as prescribed and no variability is possible. This is a rigid obstruction appearing every time that a slight deviation is made by the subject, and this may be experienced as very uncomfortable. The subjects possibly adapt their trunk motions to deal with the lack of pelvis motions, to keep their centre of mass approximately above their feet during the gait cycle, and to deal with the reaction forces of the muscles that move the upper leg. Unfortunately the activation patterns of the muscles controlling the trunk motions were not measured, and are also very

difficult to measure.

The only clear change in the EMG patters of the leg muscles is the change in pattern for the Gastrocnemius. This change is probably related to the push-off, as it appears in the mid stance / terminal stance; what actually happens is that the peak activation takes place earlier in the gait cycle. A change in push-off is most likely directly related to the blocking of the pelvis, which makes a forward acceleration of the body CoM impossible. A regular push-off would result in reactive forces at the pelvis connection; to avoid this, an earlier, more upwardly aimed push-off might be applied.

It is remarkable that none of the subjects showed a more 'passive' motion control during stance in the LPC and LPAC. This could be expected because the fixed pelvis and the moving treadmill together make push off superfluous, although the body weight of course still has to be supported by the leg muscles. It remains an open question how naturally more passive patients react to such altered circumstances. In their case also additional weight support will be offered. For them there might be little incentive to use their own muscles, if no contribution to progression is demanded.

It is also remarkable that these measurements seem to contradict (both for LF as for LPC and LPAC conditions) our earlier research in chapter 2 on the subject of pelvis fixation, where blocking of the pelvis caused considerable changes in gait characteristics. Differences were that in that research slower gait speeds were used ($0.35 - 0.90$ m/s against $0.50 - 1.25$ m/s) and that no exoskeleton was connected to the legs. It seems like the exoskeleton "filters out" some of the effects of a pelvis fixation alone, but this still needs a more detailed research and satisfactory explanation.

The presented measurements seem to indicate that the pelvis translations and hip abduction DoFs do not add much to the normality of walking, especially when compared to the small but more substantial differences between free treadmill walking and walking in LOPES without additional constraints (LF). Even if a more detailed (statistical) analysis may make subtle changes visible, it is clear that these changes will be small.

However, when the experience of the test subjects is considered, these DoFs do add something to the experience of free walking. The differences are apparently very subtle in measurements, but easier to sense for subjects, who may have to work harder or focus better to maintain their "normal" walking pattern.

Another important motivation for keeping the additional DoFs despite the presented results is that they allow specific training on balance, for example by offering disturbances or interventions at the horizontal pelvis translation DoFs, challenging the subjects in balance control. In the end clinical research on training effectivity will have to judge on the true benefit or irrelevance of these DoFs (Israel, Campbell et al. 2006).

6. Conclusion

All in all it can be concluded that differences in parameters and EMG between unconstrained walking and walking with a constrained pelvis or frontal hip rotation seem very small, certainly when compared to the differences between free walking and unconstrained walking in LOPES. This contradicts, to some extent, expectations about the importance of availability of pelvis motions for normal walking. To put it more clearly, the additional effects of blocking these motions could not well be separated from the effects of walk-

ing in the LOPES per se, in these measurements. Earlier measurements in which solely a 'weightless' pelvis fixation was applied, showed important changes in gait kinematics. In a full actuated exoskeleton apparently several interacting mechanisms play a role.

The measurements however demonstrate that the use of lightweight impedance controlled leg segments in the exoskeleton adds more to the normality of walking in the device than leaving the pelvis motions free. These conclusion would most probably be different if the inertia in these additional DoFs could also be kept small, or if the inertia would be actively compensated for, by applying the right sensing, actuation and control.

Despite this, with the available LOPES robot, the test-subjects repeatedly noticed a decrease of walking comfort when blocking the pelvis motions. Therefore, and because of the additional options for balance training, these DoFs may still be advantageous in a gait training devices.

7. References

Bayona, N. A., Bitensky, J., Salter, K. and Teasell, R. 2005. The role of task-specific training in rehabilitation therapies. Topics in Stroke Rehabilitation, 12(3): 58-65.

Dobkin, B. H. 2004. Strategies for stroke rehabilitation. Lancet Neurology, 3(9): 528-536.

Hermens, H. J., Freriks, B., Merletti, R., Stegeman, D., Blok, J., Rau, G., Disselhorst-Klug, C. and Hägg, G. 1999. European Recommendations for Surface ElectroMyoGraphy Enschede, The Netherlands: Roessingh Research and Development.

Hidler, J. M. and Wall, A. E. 2005. Alterations in muscle activation patterns during robotic-assisted walking. Clinical Biomechanics (Bristol, Avon), 20(2): 184-193.

Hocoma Medical Engineering Inc. Lokomat, www.lokomat.com. Zurich, Switzerland.

Israel, J. F., Campbell, D. D., Kahn, J. H. and Hornby, T. G. 2006. Metabolic Costs and Muscle Activity Patterns During Robotic- and Therapist-Assisted Treadmill Walking in Individuals With Incomplete Spinal Cord Injury. Physical Therapy, 86(11): 1466-1478.

Roetenberg, D., Buurke, J. H., Veltink, P. H., Forner Cordero, A. and Hermens, H. J. 2003. Surface electromyography analysis for variable gait. Gait and Posture, 18(2): 109-117.

Staude, G. H. 2001. Precise onset detection of human motor responses using a whitening filter and the log-likelihood-ratio test. IEEE Transactions on Biomedical Engineering 48(11): 1292-1305.

chapter 9

Conclusions and Final Remarks

Jan F. Veneman

Abstract

In this concluding chapter an overview is presented of the most important conclusions, of unanswered questions and undecided discussions that remain after this research project.

Chapter Contents

1. Introduction

In this thesis the design and evaluation of the robotic gait trainer LOPES (Figure 9.1) were described. Here an overview will be presented of the most important conclusions, of unanswered questions and undecided discussions that remain after this research project.

The design process was aimed at a device that would allow a training that is task specific, intensive, variable and challenging to the patient. Main emphasis in the design process was put on selecting a mechatronical concept for the robot, on selecting or designing optimal actuators in this concept and on selecting the needed possible motion freedom.

To summarize the result: we designed a freely translatable support located behind the pelvis, connected to two impedance controlled exoskeleton legs. The exoskeleton is driven with joint actuators, that have the motor detached from the moving leg parts by use of a Bowden cable transmission. The robot has in total nine actuated degrees of freedom, six internal rotations: left and right knee and hip flexion, left and right hip abduction; and three external translations: pelvis left right translation and pelvis forward backward translation. The vertical translation of the pelvis is weight compensated but not actively actuated.

LOPES was evaluated mainly by determining how well it is possible to walk naturally in it, in its so called 'patient-in-charge', 'zero-force' or 'zero-impedance' mode. This mode reflects the final stage of training, the outcome patients are training 'towards' and as such a measure for the task specificity of training in the device.

In the beginning of training patients are supposedly heavily supported, and the robot is operated close to position control, in a so called 'robot-in-charge' mode. During training
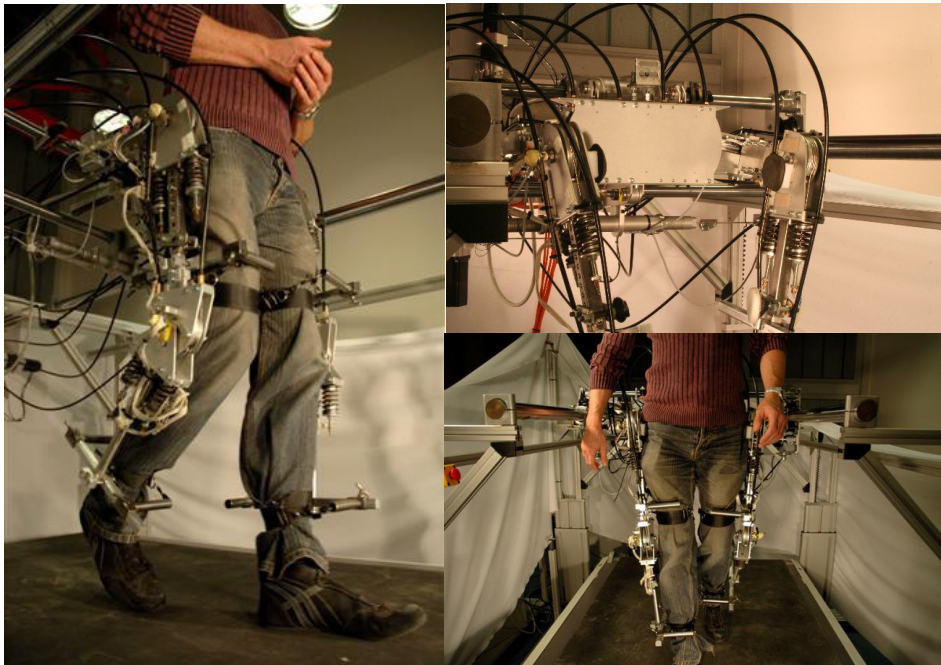

Figure 9.1: photographic impression of the LOPES gait rehabilitation device

this support can be gradually and selectively reduced to no assistance at all. During such selective control, unsupported 'aspects' of walking should be carried out by the patient, and minimally disturbed by the robot while other aspects are performed by the robot.

In chapter 7, walking in the LOPES was judged to be natural, by showing that near-to-normal muscle activation patterns led to near-to-normal kinematics for healthy subject walking on own power within the LOPES. The robot did also hardly affect the normal variability in walking. The main conclusion of the evaluation is therefore that the principles applied in the robot design are suitable for use in a gait rehabilitation robot that is in better agreement with current insights in rehabilitation of stroke patients.

2. Research questions.

Following the four research questions the results of research will be discussed in some more detail.

a. Which degrees of freedom are required to allow a natural walking pattern?

It was obvious that the sagittal rotations of hip and knee are essential for making steps and thus for walking; any available device allows these motions. Special attention was paid in this research to the importance of the pelvis motions, especially to the translations in the horizontal plane. Introducing these translations necessarily had to be accompanied with the possibility of hip abduction, as without these sideways translations of the pelvis would still be impossible.

The pelvis translations are blocked in for example the Lokomat and the AutoAmbulator. In chapter 2 we concluded from measurements that walking without horizontal motions of the pelvis severely alters the characteristics of walking during a certain speed, for example step length and step width. Changes were significant and clear already in a group of 8 healthy subjects. The changes indicated that fundamental properties of walking were altered by the pelvis fixation. We argued that this was mainly because of the fact that due to the fixation no stabilizing actions of the muscles are necessary to maintain a stable upright position during walking. This study was done to make decisions in the design process and made us decide the horizontal pelvis translations should be available in a gait training device.

It was therefore surprising that, when we repeated a similar experiment within the LOPES these changes in gait characteristics were hardly observed. The latter experiment was carried out by explicitly blocking the pelvis translations when walking in the LOPES, as described in chapter 8. In fact few differences were found between walking in LOPES with all degrees of freedom available (chapter 7) and walking in LOPES with blocked pelvis motions (chapter 8).

Comparing the pelvis fixation of chapter 2 with the LOPES-pelvis fixation of chapter 8, only the increased sway and rotation of the trunk appeared clearly in both experiments. Apparently the connection of the legs to an exoskeleton prevented changes in step length, step width and consequently EMG from emerging. It can be supposed that LOPES complicated the optimal walking within the constraints of chapter 2, so that for example a larger step length was prevented by the increased inertia of the legs and the smaller step width was prevented by the leg connections in LOPES, that make narrow walking uneasy.

Such hypotheses should be tested by walking in the LOPES device *with* fixated pelvis, but *without* leg segments.

It seems clear that walking in the LOPES comes closer to normal walking, even when the pelvis is fixed, than walking with a fixated pelvis alone. However, even though the effect of the free moving pelvis on walking seems to be less than could be expected based on the experiments, it is still beneficial to have these motion freedoms in order to provide balance-training during gait training, for example by offering small disturbances.

b. Which mechatronical design concepts are best suited for an interactive gait rehabilitation robot?

As basic control outline we selected impedance control, combining a lightweight construction with joint actuators used as torque sources. Within this concept both the actuator power and the construction stiffness and weight can be kept relatively low, supposedly lower than in a comparable admittance-control-based design. Important additional advantages of impedance control are that, in case of impacts, in case of velocity deviation between exoskeleton and treadmill, and in case of zero force control, it is relatively easy to keep the robot stable. This because no high gain position control loop is necessary as in admittance controlled devices. These aspects are beneficial for the patient safety during use.

Using an impedance-control-based design for relatively high forces implied that the construction became relatively heavy. This brought about considerable uncompensated inertia and lower bandwidth for an impedance controlled device, resulting in force errors during operation. We stated that such a concession could be acceptable in case of a gait rehabilitation device (chapter 3), because in this case it is not needed to display high or very accurate stiffness or other haptic information.

From chapter 8 we can conclude that the choice of impedance control appeared suitable: the zero-torque control was shown to very well allow free walking in the device, one of the basic demands for proper functioning as interactive rehabilitation device. A further reduction of weight could even improve this performance. This would also improve the force output and enlarge the possible force or impedance control bandwidth. Weight-reduction may be possible by using advanced materials like composites.

To realize proper force sources on the exoskeleton DoFs, we chose to use compliant actuators. Compliant actuators have a relatively low internal stiffness compared to common EM-motors. This implies that these actuators are easier to control stably during interaction with an unstructured environment. In case of the Series Elastic Actuator (SEA, an EM motor placed in series with an elastic element or spring) an additional advantage is that the EM motor can be used optimally in position control mode, controlling the spring length, hence the force output, resulting in a 'clean' force output. We showed that qua performance a SEA as well as a pneumatic cylinder or a pneumatic muscle could be used as adequate actuator for interaction with humans for rehabilitation purposes. We selected the SEA as most adequate concept, mainly due to several additional disadvantages of the other actuators, that originated from the use of pressurized air, such as noise, temperature dependency, control complexity and danger in case of wear.

As the first version of the SEA was too heavy we removed the actuators from the exoskeleton to the global frame, and introduced a Bowden Cable transmission from motors to joints. The elastic elements remained at the joints, allowing for feedback force control. Despite the non-linear and poorly predictable friction of the cables, including stick-slip we

managed to realize proper force control in the prototype, able to control the joint torques during normal operation (30Nm) at 8Hz. This was sufficient to implement the kind of interactive controllers that we want to use for programming the robot.

Although the Bowden cable transmission is quite troublesome from practical engineering viewpoint, as it wears, and replacement is yet difficult and there are many cables, it is not so easy to realize a comparable alternative. Optimization of the cable courses, lubrication, use of cable liners, replaceability of cables and connection of the cables to the discs will probably lead to a reliable application.

c. Which technological design is best suited to implement these degrees of freedom and this mechatronical concept?

The resulting technological design was described above in this chapter, and more detailed in chapter 6. The presented design is in agreement with the answer to both aforementioned questions. Actually the answers to those questions were already formulated with the concept of a joint actuated exoskeleton together with a pelvis support in mind. Such 'feedback' loops are unavoidable in a design process. It is therefore difficult to defend that the presented design is the optimal solution, but the evaluations show that it is at least a suitable implementations of the principles stated before.

Of course we also have considered alternative basic concepts. Although not described in this thesis, we studied several constructions that would realize the mentioned DoFs together with force actuation. An interesting solution was the use of cable transmissions that could drive limb segments independently, using one transmission system to rotate the lower leg, one to rotate the upper leg and so on, turning the patient into a kind of 'string puppet'.

A wire based transmission was developed that allowed free translations, but transmitted nbg nfcrotations or torques (de With 2003). The system appeared realizable in 2D, but very hard to implement in 3D. Also safety seemed hard to assure with a complex wire based system. A comparable system is built under the name String-man (Surdilovic, Bernhardt et al. 2004; Surdilovic, Zhang et al. 2007). A very important advantage of an exoskeleton based system is that the motions and torques in the robot are always directly related to those of the human. This makes it simpler to implement safety observation systems.

For the prototype we put most constructional effort in designing the Bowden-cable driven joints and in realizing the desired degrees of freedom in the pelvis and hip-segment in a compact and lightweight, yet sufficiently stiff fashion. Additional effort should be put in reducing the weight of the moving parts of the construction, in the facilitating fast replacement of cables and in the reduction of the complexity of certain parts to reduce production costs. These aspects will be elaborated in the future directions.

d. How well does the prototype satisfy the stated goals?

Chapter 6, 7 and 8 evaluated the design, with as most important conclusions that the current design allowed near to normal walking (chapter 7), and that the horizontal pelvis translations appeared less important than expected (chapter 8) for normal walking. This was already discussed early in this chapter.

For evaluation of the possibility to walk normally with the LOPES robot, kinematics, gait parameters and muscle activity of walking with a zero-force controlled LOPES were

compared with those of walking freely on a treadmill. Average values and variability of the spatio-temporal gait variables showed either no or minor changes and the kinematics only showed a significant and relevant decrease in knee angle range in LOPES walking. Muscles involved in push off showed a small decrease when walking in LOPES, whereas muscles involved in acceleration and deceleration of the swing leg showed an increase of their activity. Timing of the activity was mainly unaffected. Most of the observed differences could be ascribed to the inertia of the exoskeleton.

3. Future directions

a. Short term developments.

From engineering viewpoint the prototype presented in this thesis was a proof of principle: it met the design criteria and showed that the chosen solutions are adequate. Current effort is put in implementing high-level control algorithms (the control layer above the already implemented force control that sets the force references) to provide actual training or at least interventions in walking of both healthy walkers and stroke subjects. This work is carried out in a parallel research and is based on application of so called Virtual Model Control (Pratt 1995). The control is based on defining virtual components that lead to forces at a certain time and a certain place during the walking cycle. If well defined, such components, for example virtual springs or virtual dampers, can be translated into joint torques. At the moment a controller is implemented that can increase foot clearance during swing, leaving the rest of the gait cycle unaffected (Ekkelenkamp, Veltink et al. 2007; Van Asseldonk, Ekkelenkamp et al. 2007). Similar controllers can be implemented for several partial tasks of walking, such as balance keeping, weight bearing and step length. This type of control avoids defining trajectories relative to time, leaving a relative freedom to the patient to develop his or her own walking pattern, in collaboration with the device.

b. Possible technological improvements.

In the current prototype many technological improvements are possible within the concept. Several may even appear necessary in case of extensive tests with patients, or production. Important aspects are: weight reduction, design for easy production and assembly, more elegant guiding of springs, size of the sensors, ease of adaptation to individual measures, ease of cable replacement, possibility to precisely adjust pretension in the cables and ease of getting a patient in the device. These aspects are not so interesting from research and development viewpoint, but very important for practical use.

There are also some basic extensions on a more conceptual level that may be worth considering. First, it may appear important to offer an active actuation of the ankle joint, although we argued in chapter 6 that this may be less important than might seem on first sight. As it is quite difficult to apply substantial forces on a foot, it may be an option to use functional electro stimulation (FES) in combination with the robot to normalize walking at a certain stage of training. With FES a more or less natural push-off as well as foot clearance during swing can be generated (Daly, Roenigk et al. 2006). It is however not clear how useful this will be from training viewpoint. Possibly this kind of training is only useful for patients that will remain walking with FES.

Second, to ease the patient-installation procedure, it may be convenient to use a construction that can automatically align the axes of rotation of the exoskeleton and of the human body. If the axes of the exoskeleton and the human are not well aligned, secondary forces and motions between robot and limbs, which can be very uncomfortable. Therefore it is very important to use well coinciding rotation axes. An example of how this can be realized is given in the design of the Dampace (Stienen, Hekman et al. 2007), a project focusing on arm rehabilitation. The dampace arm exoskeleton applies an elbow joint that has no fixed rotation axis, but is able to apply a pure torque between upper and lower arm. The mechanism used there would have to be adapted for in the LOPES exoskeleton, as the forces are considerably higher, and the Dampace construction cannot deal with the two limbs placed in one line in a vertical position. With such joints less attention has to be paid to well aligning hip and knee axes of the robot with the human axes, which would considerably speed up the installation procedure.

Third, the Bowden cables in the control loop are somewhat troublesome, both for reasons of wear and for reasons of control performance. Although we considered flexible hydraulic transmissions before and concluded they were less feasible, additional design efforts may result in a flexible transmission that is more optimal than the current cables. Possbile options that have been considered and may still be applicable are the use of hydraulics, the use of bars or a more advanced use of Bowden cables. The hydraulics necessarily are micro hydraulics and most probably specific valves have to be designed. As alternative for flexible cables the use of parallel bars was also considered. To realize sufficient flexibility of the transmission these have to consist of several links. The friction of Bowden cables can possibly be lowered by partly using the cables without outer cable, and only use Bowden cables at the parts that have to change orientation during operation. For all these solutions, that are only mentioned very shortly here, it counts that a lot of engineering effort and testing has to be invested to realize a well functioning alternative. Friction, or lack of flexibility of the transmission are the problems that will have to be dealt with in any possible solution.

Finally a lot of effort has to be put in designing the higher-level control layer that allows a therapist to influence the robot behavior, or the researcher to design his or her experiments, without knowing all lower level details of the system. Also the possibility to feedback the gait process to the patient, therapist or researcher, by showing forces, torques, motions or training goals has to be implemented. An even more advanced feature is to link gaming elements or virtual environments to the motions of the robot (Luenenburger, Wellner et al. 2007).

c. Use of the device in gait training or gait research

Considering the functioning of the device in practice, that is in rehabilitation or in gait research, I will conclude with some remarks.

The concept of the LOPES device offers a lot of possibilities for objective measurements during training. Motions and interaction torques between robot and human can be recorded. Both the actions of the robot and the performance of the human can be well measured. Also specific impairments that result in specific torques on joints could well be quantified, both statically as dynamically, such as synergies in muscle contractions, spasticity and rigidity.

Another new aspect is the interactivity of the robot which allows the patient to influence and vary his own walking during training. This aspect may appear important in train-

ing and has to be implemented in the design of training programs. The role of the therapist in the future rehabilitation setting is to observe the gait of the patient and to select which partial subtasks should be assisted by the robot, or left to the patient, and to which extent. This boils down to shaping the training, based on a set of possibilities offered by a control interface. Other roles are of course motivating the patient and assuring safety.

The current prototype, with some additional safety covers, is a fully functional prototype that allows testing with CVA patients. After the control and software safety measures are well implemented, the question can be addressed what "works well" for patients. Extensive testing with patients will undoubtedly result in information for further technical adaptations and improvements.

A very extensive field of research lies ahead on what defines optimal gait training for CVA patients. Should a patient be guided towards "the right way" of walking, or should errors be emphasized by amplifying them? Should the patient develop his own optimal way of walking, or should symmetry be stressed? Is focus on limited subtasks of walking effective? Is it effective to disturb balance during training? How important is motivation in training and how can motivation be extended by implementing for example a virtual reality or gaming interface? These are only a few questions which may be addressed using the LOPES as a research device.

Probably the device has also potential outside the field of gait rehabilitation for stroke patients. People that need to rehabilitate due to other impairments may well benefit by the device, although probably need other training options and therapist interfaces.

The LOPES and its successors can also appear the basic of fascinating future developments where fitness, virtual reality based gaming and motor learning are combined into some futuristic form of sport.

4. References

Daly, J. J., Roenigk, K., Holcomb, J., Rogers, J. M., Butler, K., Gansen, J., McCabe, J., Fredrickson, E., Marsolais, E. B. and Ruff, R. L. 2006. A randomized controlled trial of functional neuromuscular stimulation in chronic stroke subjects. Stroke, 37(1): 172-178.

de With, G. J. 2003. Design of a gravity compensation system for the gait rehabilitation robot LOPES. Unpublished Masters thesis, University of Twente, Enschede.

Ekkelenkamp, R., Veltink, P. H., Stramigioli, S. and van der Kooij, H. 2007. Evaluation of a VMC for the selective support of gait functions using an exoskeleton. Paper presented at the Proceedings of ICORR 2007 - IEEE International Conference on Rehabilitation Robotics, Noordwijk.

Luenenburger, L., Wellner, M., Banz, R., Colombo, G. and Riener, R. 2007. Combining Immersive Virtual Environments with Robot-Aided Gait Training. Paper presented at the International Conference on Robotics Rehabilitation 2007, Noordwijk aan Zee, the Netherlands.

Pratt, J. E. 1995. Virtual model control of a biped walking robot. PhD Thesis, MIT, Cambridge.

Stienen, A. H. A., Hekman, E. E. G., Helm, F. C. T. V. d., Prange, G. B., Jannink, M. J. A., Aalsma, A. M. M. and Kooij, H. V. d. 2007. Dampace: dynamic force-coordination trainer for the upper extremities. Paper presented at the International Conference on Rehabilitation Robotics (ICORR) 2007, Noordwijk aan Zee.

Surdilovic, D., Bernhardt, R., Schmidt, T. and Zhang, J. Y. 2004. STRING-MAN: A novel wire robot for gait rehabilitation. Advances in Rehabilitation Robotics, 306: 413-424.

Surdilovic, D., Zhang, J. and Bernhardt, R. 2007. STRING-MAN: Wire-robot technology for safe, flexible and human-friendly gait rehabilitation. Paper presented at the 10th International Conference on Rehabilitation Robotics (ICORR), Noordwijk aan Zee, the Netherlands.

Van Asseldonk, E. H. F., Ekkelenkamp, R., Veneman, J. F., van der Helm, F. C. T. and van der Kooij, H. 2007. Selective control of a subtask of walking in a robotic gait trainer(LOPES). Paper presented at the Proceedings of ICORR 2007 - IEEE International Conference on Rehabilitation Robotics. , Noordwijk.

Appendix A: Backgrounds on the design of LOPES

This appendix gives additional information on the origin of design requirements for the gait rehabilitation robot. The first part is about the degrees of freedom important in walking, and the second more specifically about the quantative and qualitative actuator demands.

a. Degrees of Freedom

For describing the human gait cycle, the lower human body can be described with 6 joints: two hip joints; two knee joints and two ankle joints and 7 segments: the pelvis; two upper legs; two lower legs and two feet. The segments are connected at the joints, that link the segments. The connections in the joints are not rigid connections, with a fixed rotation axis, they rather can move at least a little bit in every direction. The large rotations of the joints are (Perry 1992):
- Hip flexion and extension.
- Knee flexion.
- Ankle dorsiflexion and plantar flexion.

Combining this with important training goals for CVA patients, such as:
- minimizing hip abduction during swing phase,
- controlling cadence,
- foot clearance,
- stabilizing knee in heel-down,
- controlling knee flexion during swing phase,
- hip abduction control,
- correct positioning of the COM/COP (Centre of Mass, Centre of Pressure)
- improving the timing,
- improving muscle strength,
- correct leg placement for balance,
- hip flexion at the start of the swing phase,

we concluded the need for especially:
- Actuation of the hip: flexion, extension and ab/-adduction
- Actuation of the knee: flexion, extension
- Actuation of the body Centre of Mass in the horizontal plane, translations of the pelvis.
- Possibility of ankle motions (but not actuated).

For the patient not to be hindered by the robot, the smaller additional motions of the segments should not be constrained. In rigid constructions, two rotating components that are connected need to be aligned to prevent unwanted forces. This could pose a significant problem in designing a gait rehabilitation robot. However, the muscles and skin of the leg are not rigidly connected to the skeleton. This makes the problem much simpler. Because the skin can move with respect to the skeleton, it can compensate for misalignments of the robot's joints with the patient's joints. This means that the axes of the robot's joints can translate with respect to the patient's without introducing large extra forces.

Since the pelvis is very near to the COM of the patient, all translations concerning the body of the patient are assumed to apply here. The resulting needed DoF's are depicted in Figure A.1, in the caption an explanation is offered.
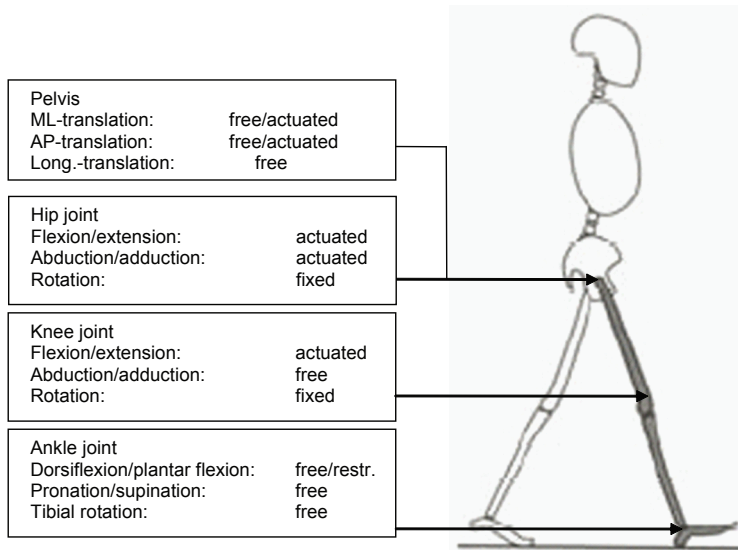
```
Pelvis
ML-translation:          free/actuated
AP-translation:          free/actuated
Long.-translation:           free
```

```
Hip joint
Flexion/extension:               actuated
Abduction/adduction:             actuated
Rotation:                        fixed
```

```
Knee joint
Flexion/extension:               actuated
Abduction/adduction:             free
Rotation:                        fixed
```

```
Ankle joint
Dorsiflexion/plantar flexion:    free/restr.
Pronation/supination:            free
Tibial rotation:                 free
```

Figure A.1: Desired degrees of Freedom of a gait rehabilitation robot.
Pelvis: For the pelvis (and the COM) the anterior-posterior (forward/backward) and longitudinal (up/down) translations have to be free and are only limited by the dimensions of the treadmill used. The medial-lateral translation (left/right) is either free or actuated, depending on whether the abduction in the hip can be comfortably actuated, both can be used to shift the COM.
Hipjoints:The flexion/extension and abduction/adduction are to be actuated for the rehabilitation goals. The endorotation / exorotation has to be fixed to ensure alignment of the knee joints.
Kneejoints: As discussed for the knee joints, flexion/extension is actuated for rehabilitation goals. Rotation of the knee-part of the orthosis must be restrained to prevent misalignment of the knee and the abduction/adduction is free to make sure the actuation of the hip abduction/adduction only moves the upper leg. All translations are defined by the movements of the hip.
Anklejoints: The ankle joint will not be actuated, but the dorsiflexion/plantar flexion might have to be restrained for some patients to ensure foot clearance and proper heel down. To ensure a realistic ground reaction force, the pronation/supination has to be unrestricted. The foot has to be possibily restrained to block hip endorotation / exorotation to ensure alignment at the knee.

b. Actuation demands

First the human gait cycle is described, from which the general demands like range of motion, power, force, velocity and acceleration can be derived. Subsequently additional (actuator) design requirements are discussed, like safety, smoothness and adaptability are discussed

To quantify the load demands for the joint actuators in LOPES, an overview of joint angles and powers during slow walking is given. Using data from gait measurements to dimension the actuators, assumes that the robot's task is to execute the muscle task. This is therefore only an indication for the possible operative demands on the robot.

This overview is based on a set of regularly used data of normal human gait collected and well documented by (Winter 1991). The data of slow walking (1m/s) have been chosen because most of the post stroke patients have a lot of difficulties walking and their training will be at low walking speeds. Average gait speed of hemiparetic patients typically
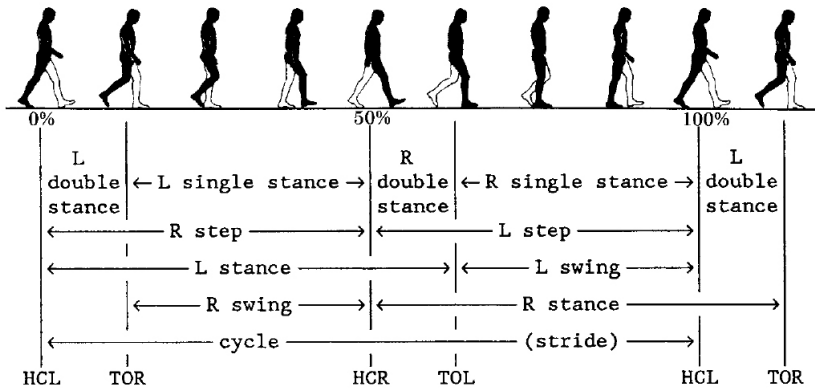
Figure A.2: Description of the human gait cycle.

varies from 0.25 to 0.65 m/s, so Winter's 1 m/s is probably a good indication of a final training speed. The data merely gives an indication of the load demands as it is averaged over multiple steps and multiple persons and the actual values show a large deviation. Note that this data is normalised to bodyweight. For a better understanding of Winter's data a short description of the gait cycle is given first.

(Koopman, 1989) gave the following description of normal walking. All step parameters are determined by the points of heel contact (HC) and toe-off (TO) for the left and right foot. When a walking cycle is started with left heel contact (HCL), it is followed by toe-off right (TOR), right heel contact (HCR) and left toe-off (TOL). A cycle is completed with HCL again (see figure A.2). These points divide the walking cycle in four different phases. The stance phase of the left leg is from HCL to TOL and the swing phase (or stance phase of the right leg) is from TOL to HCL. During one cycle there are two double stance phases, when both feet are on the floor. The left double stance phase is from HCL to TOR. The left step is usually defined from HCR to HCL. One stride consists of two steps.

The sagittal joint rotations for slow walking at each point of time of the walking cycle from Winter are given in figure A.3. The range of both robot and actuators should be such
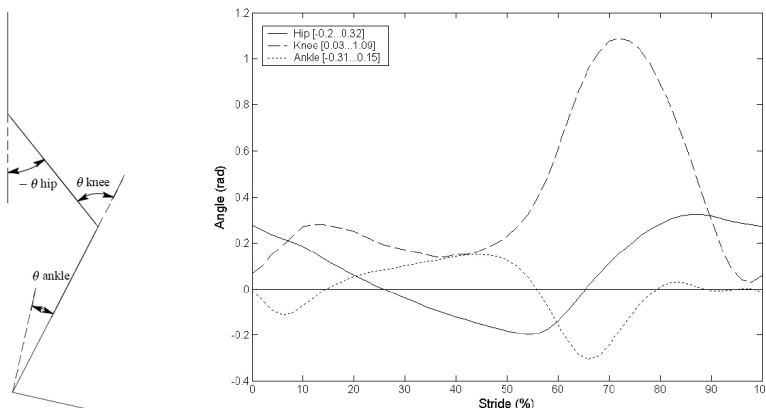

Figure A.3: Joint angle trajectories during slow walking according to Winter (Winter 1991). Left a definition of joint angles.
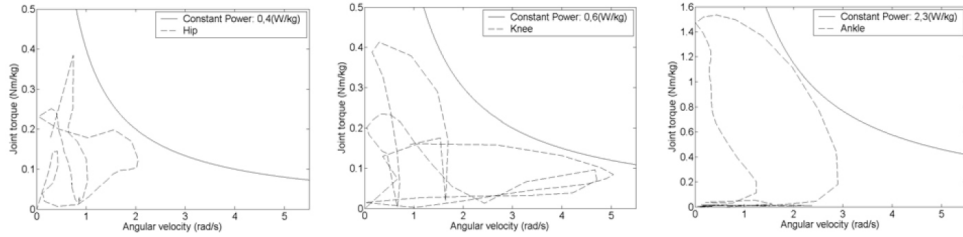
Figure A.4: Speed-Torque curves for the human hip, knee and ankle joint during slow walking, transformed to one quadrant; during walking joints of course operate in all four quadrants. Also the maxium power curves are given.

that at least all joint rotations can be made.

Besides the joint angles it is important to know which powers are required to drive each joint or segment. Figure A.4 shows the absolute torque-speed curves for hip, knee and ankle joints. To indicate the magnitude of the maximum required power of each joint, a certain constant power is plotted in the same figure. Important for the understanding is to realise that these torque-speed curves are plotted in one absolute quadrant, while the actual operating area is distributed over all four quadrants. Power is defined as the product of speed and torque. Not only the maximum of this product is an important parameter, the maximum of both torques and velocities and their time derivatives can also be decisive factors in choosing actuators or actuator parts. Therefore the courses of torques and velocities will be more thoroughly investigated.

Because it is not possible to measure torques in human joints directly, they are derived using inverse dynamic models and the measured information about joint angles and ground reaction forces. The joint torques can be interpreted as the net result of all muscular, ligament and friction forces acting on the joint. Hip, knee and ankle torques during one gait cycle are plotted in figure A.5. The given torques consist of dynamic torques, needed to accelerate the limbs, and static torques, needed to compensate gravity. When LOPES has to actuate a fully passive person, the actuators have to generate the same torques on the joints to induce a correct gait pattern. As can be seen, the maximum ankle torque is by far the highest of the three joints. This maximum appears during toe-off, when the centre of mass is lifted up and brought forward, the so called push-off.
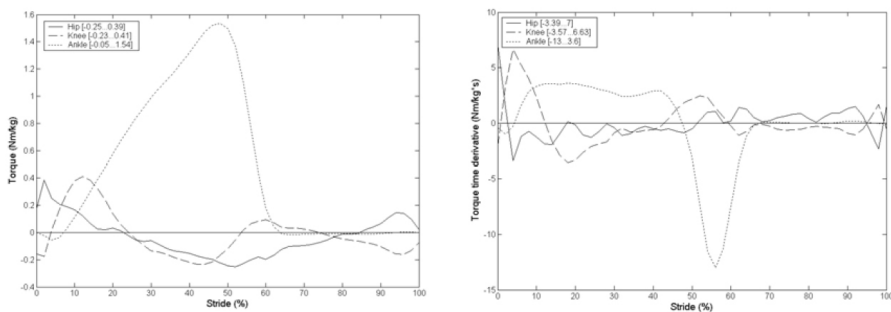

Figure A.5: On the left the joint torques during slow walking, on the right their derivatives.

Typical demands for a person of 90 kg are give in the table below.

	Hip	Knee	Ankle
max. actuator stroke	29.8 [°] (0.52 [rad])	60.7 [°] (1.06 [rad])	26.4 [°] (0.46 [rad])
max. actuator torque	57.6 [Nm]	57.6 [Nm]	143.1 [Nm]
max. actuator power	36 [W]	54 [W]	207 [W]

The last important gait characteristic is the course of the joint angular velocity and its time derivative, the accelerations of the joints. Because the limbs have to move with the same speeds as during natural gait and actuators have to induce these movements, they at least must be able to match these speeds and accelerations, figure A.6.

Except as needed accelerations the demands can also be formulated as a needed dynamic bandwidth of the robot and its actuators. According the measurements (Winter 1990) the maximum voluntary human movement frequency during walking is 4Hz. 'Fast' movements (>2Hz) are generally coupled with small joint moments and slow movements with relatively high moments. For stroke patients these frequencies are lower but as the goal is to get patients as close to 'normal' walking as possible, we have used normal walking as the criterion. According to Zinn et al. (Zinn, Roth et al. 2004) the bandwidth of the inner control loop of an impedance controller needs to be at least a factor 3 larger than the outer control loop bandwidth, in order to decouple both controllers. This implies that the force bandwidth for small moments (<10Nm) should be around 12 Hz. Larger moments, up to 60Nm need to be exerted with a bandwidth of at least 3 Hz.

In addition to this overview of the gait cycle data, which is used as a basic demand for selecting and dimensioning actuators, criteria that define the suitability for interaction with humans in general and specifically for rehabilitation are formulated. Because the interaction between robot and human here is similar to the interaction in haptics, the criteria formulated for haptics can be used, although they will have to be rephrased for the case of rehabilitation robotics and actuation.

Safety

Safety is the first concern in robots that, like LOPES, are meant to interact with humans. Not only the safety of the patient should be regarded, but also the safety of the surroundings, in the first place of the therapist, that is likely to assist in the LOPES training.
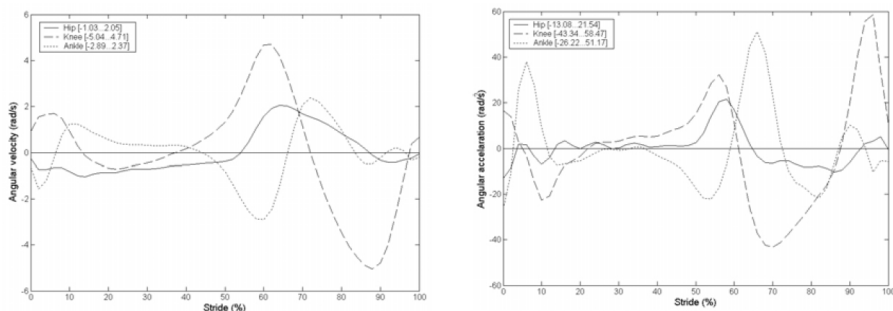

Figure A.6: On the left the joint velocities during slow walking, on the right their derivatives.

Safety of the patient basically comes down to prevent the occurrence of too high forces or torques on the limbs during training. As the admissible forces depend on the gait-state this will be mainly a control concern, but where possible forces should be limited in the hardware too. This means for example the controller should be robustly stable in the interaction, or that the actuation of the robot never should get 'stuck', in other words always be 'backdriveable', both in the controlled situation as intrinsically. This also facilitates the possibility for the patient and the therapist to overrule the actions of the robot to a certain degree. Safety for the surroundings (the therapist), as far as the actuation is concerned, consists of avoiding the danger of impacts. This danger of impacts is directly dependent on the moving inertia of the robot. Therefore, in case actuators would constitute a substantial part of the moving mass of the robot this would demand for a minimal actuator mass. This will be the case when the actuators are placed on the exoskeleton. Concluding, the two important qualities that are usefull for defining safety are:
- lightweight
- backdriveability

Smoothness

A second basic concern in physical human-robot interaction is the comfort or 'gentleness'. The main contribution of the actuation to this might be the smoothness of the induced force patterns. Smoothness can be defined as the lack of undesired, but perceptible variations in force or torque while moving.

In literature concerning haptics, smoothness has been defined in several ways, usually based on minimising the jerk, the third time derivative of the position [32]. Usually in haptics smoothness is considered as the smoothness of a certain trajectory. However, for comparing actuators, notjust the smoothness of a certain trajectory should be quantified, but also the achievable smoothness using a certain actuator. For example in electricmotors, "torque ripple" or "cogging" can appear. Friction and backlash can also produce a lack of smoothness by exciting stick slip vibrations. It will be more sensible to compare the lowest achievable controlled smoothness, for example by determining the smallest force step, or time derivative of force that can be reached.

Adaptability

A third basic concern, specific for LOPES, is its quality as rehabilitation device that will be determined by the ability to adapt the robot behavior to the actual needs of the patient. The basic idea of LOPES is to support the patients only there where needed, while the patient walks as much as possible on own initiative. Such adaptive assistance involves that the robot should act in between two extreme tasks. The first is forcing the patient to walk according a prescribed gait pattern, requiring the actuator to act as a pure force source. The second is following the patient without much interaction forces, requiring the actuators to behave backdriveable. In between these two tasks the rate of support must be freely adjustable. Concluding, the two actuator qualities that will be used for defining the adaptability are:
- backdriveability
- force source quality
The first criterion was already mentioned in relation to safety.

Installation dimensions

The size and weight of the actuator are a consideration. This will especially be a concern when the actuators are placed on the exoskeleton. When this is the case, minimal actuator mass and volume are demanded. This is both a safety- and a control concern. A high moving inertia of the robot imposes high forces when an impact might occur, which could be dangerous to the patient. It also poses higher demands on the control effort needed. Another option is to place the actuators elsewhere (not on the exoskeleton) and use some kind of transmission to transport the actuator force. In this case, special care has to be taken to minimise the adverse effects of the used transmission.

REFERENCES

Koopman, H. F. J. M. 1989. The three-dimensional analysis and prediction of human walking. Ph.D. thesis, University of Twente, The Netherlands, Enschede.

Perry, J. and Schoneberger, B. 1992. Gait analysis : normal and pathological function: Thorofare, NJ : SLACK Incorporated.

Winter, D. A. 1990. Biomechanics and Motor Control of Human Movement (2nd ed.). New York: Wiley.

Winter, D. A. 1991. Biomechanics and Motor Control of Human Gait: Normal, Elderly and Pathological. Waterloo: University of Waterloo Press.

Dankwoord

*Een goed reiziger heeft geen vaste plannen
en is niet van plan om aan te komen.....*

Zo aan het eind (hoewel, voor de lezer waarschijnlijk aan het begin), als het werk er op zit, is het de natuurlijke plaats om bedankjes uit te delen.

Het eind! Daarom bedank ik allereerst de hemel, de goede geesten, en alles wat verder aan het welslagen van het leven meewerkt, dat dit traject van promoveren, dat soms wel eindeloos leek, dan toch aan zijn eind is gekomen! Hoewel het dus allemaal enigszins lang geduurd heeft, was het tegelijkertijd een leuke en leerzame tijd, die ook zeker niet eenzaam was, wat je wel eens hoort over promotie trajecten. Ik wil dan ook een aantal mensen hartelijk bedanken voor de inhoudelijke steun onderweg, en hun bijdrage aan het realiseren van dit proefschrift.

Met name wil ik noemen: Frans van der Helm, 'mijn' professor, altijd gewapend met een nuchtere en scherpe blik, goede adviezen en vertrouwen in mijn werk, Herman van der Kooij, dagelijkse begeleider, 'aanstichter' van heel het LOPES project, man van vele ideeën (soms wel erg veel), werkend en begeleidend zoals hij hardloopt, soms vooruit 'sleurend', soms wat 'hangend' op adem komend; niettemin altijd betrokken en motiverend (weliswaar op zijn geheel eigen wijze), kortom een grote drijvende kracht achter het werk dat in dit proefschrift is gepresenteerd. Bedankt! En niet in de laatste plaats voor deze zinvolle besteding van mijn vrije tijd gedurende het afgelopen jaar.

Vervolgens mijn collegae LOPES promovendi. Allereerst Jan-Tom Bellos, die mij overhaalde samen op dit project te solliciteren, ondanks dat dat destijds meer bij mijn interesse en motivatie dan bij mijn afstudeerrichting aansloot en ik nog wel wat twijfels had. Ik heb uiteindelijk zeker geen spijt gehad van deze beslissing, bedankt dus voor dat duwtje, ook al ging jij zelf al snel weer een andere kant op! Natuurlijk in het bijzonder de mannen die het vier(+) jaar met mij hebben weten uit te houden, op kantoor ('de Gouden Kooij'), en in voortdurende samenwerking, Edwin van Asseldonk (eindelijk kun je bij het raam zitten en kun je je PSV (PFV?)-autootjes in het volle licht kwijt & nee, je krijgt geen iPod van me) en Ralf Ekkelenkamp (jij hebt mij een aantal regeltechnische begrippen ingeprent, zoals 'resonantie' en 'eigenfrequentie' alsmede het belang van het minteken in de regeltechniek). Onze samenwerking is wat mij betreft altijd heel plezierig en productief verlopen. Ook los van de inhoud waren jullie plezierige collega's (collega's *plus*). Jullie gaan de kroon op dit traject zetten als mijn paranimfen! Alvast bedankt! Op deze plaats wil ik ook Heike Valery nog noemen, die als collega promovendus uit München enkele nuttige en enthousiaste bijdragen aan het LOPES project heeft geleverd. Ook met jou was het plezierig samenwerken! Als je verder gaat met LOPES: houd hem alstjeblieft heel!

Een avondlijke fotosessie waarop alle laatstgenoemden aanwezig waren, heeft geleid tot de foto's die nu op de omslag zijn te bewonderen, en waarop jullie jezelf terug kunnen vinden. Ook de ogen achter de camera, Arno Stienen en Arthur Aalsma, bedankt voor de mooie foto's - ik kom er wel erg voordelig op uit al zeg ik het zelf.

In de loop van de tijd hebben een heel aantal studenten (deels) onder mijn begeleiding hun bachelor of afstudeerwerk in het project gestoken. Ik was dan wel jullie begeleider, maar heb tegelijkertijd zelf heel veel aan jullie werk gehad, wat ook wel blijkt uit jullie mede-auteurschap aan enkele artikelen in dit proefschrift. Ik noem in willekeurige volgorde: Jelmer Edens, Govert-Jan de With, Marieke de Bruin, Remke Burie, Bianca Mulder, Stijn Chapelle, Jasper Menger, Rik Kruidhof, Marieke van Gemert en Karin Gorter. Jullie bijdragen hebben veel geholpen bij het slagen van de LOPES.

Dan wil ik 'onze' gebruikerscommissie (de klankbord-groep) graag bedanken voor de goede adviezen en kritische blik die wij van hen gedurende dit project hebben mogen ontvangen;

met naam noem ik alleen de meer direct bij LOPES betrokkenen Stefano Stramigioli en Peter Veltink, die met name in het begin mij goed op weg hebben geholpen, en Jaap Buurke, die heeft meegewerkt aan een aantal subject metingen.

Last but not least de mannen van de techniek, Edsko Hekman, als ervaren ontwerper die ieder idee wist aan te scherpen, Theo Krone en later Gert-Jan Nevenzel als technische ondersteuners, ik weet dat jullie wel eens, om het zachtjes uit te drukken, meer dan genoeg van LOPES hadden, maar daarom des te meer bedankt dat jullie het LOPES project in meer letterlijke zin draaiende hebben weten te houden. Ook bedank ik Hayo Okkinga van Roessingh Revalidatie Techniek BV, die ons met advies en materiaal enkele keren heeft geholpen om de bevestiging van de robot aan de 'patiënt' wat minder pijnlijk uit te voeren.

Een stapje verder van de inhoud, maar niettemin onderdeel van 'het werk', de mede AIO's, en de 'vaste staf' van Biomedische Werktuigbouwkunde, een aantal collega's van BSS en de grote schare afstudeerders en bachelor studenten die door de jaren langs zijn gekomen: ik vond het altijd een heel aangename werk-omgeving, ik denk aan de koffiepauzes, uitstapjes, activiteiten, verjaardagen, het squashen en natuurlijk met name ook het voetballen in het vermaarde Bio-Ballen team, met als hoogtepunten het winnen van het UT-kring kersttoernooi en natuurlijk mijn benoeming als captain. Hoewel jullie zeer moeilijk te coachen zijn, zijn de prestaties uitstekend!

Vervolgens bedank ik (nogmaals) Jaap Buurke, die mij voor een klein half jaar bij RRD aan een interessant project heeft laten deelnemen, en Theo van der Meer, die mij aansluitend aannam om aan twee nieuwe ontwikkelingen in het onderwijs te werken, op een geheel ander maar niet minder interessant gebied (duurzame energie). Behalve dat deze werkzaamheden mij de kans gaven mijn promotie-werk in goede orde af te maken, was het allemaal ook zeer leerzaam en aangenaam.

Nog een stap verder van de inhoud komen de mensen uit mijn persoonlijke leven, die ook ieder op hun manier indirect bij de totstandkoming van dit werk hebben mee of tegen gewerkt (dat is meestal moeilijk uit te maken), en die natuurlijk niet in de eerste plaats op dit promotiegebeuren zijn betrokken. In het bijzonder wil ik als groep de (oud) mede-bewoners van de Patio 20 vermelden, het studentenhuis waar ik al lange tijd woon, en waar ik van broekje ben opgeklommen tot iets benoemd met vleiende titels als 'opa' en 'fossiel'. Ondanks het toch wel toenemende verschil in leeftijd, heb ik me altijd goed bij jullie thuis gevoeld en op deze manier ben ik natuurlijk ook zo jong gebleven. Toch komt mijn al jaren aangekondigde vertrek wel dichterbij…langzaam maar zeker. Van jullie wil ik in het speciaal Christina noemen, die met een paar deskundige tips het ontwerp van mijn omslag naar een hoger plan heeft weten te tillen (zo is het beter, toch?) – bedankt!

Tenslotte, hoewel het eigenlijk voor mijn gevoel niet bij het werk hoort, maar omdat het toch al weinig wordt gezegd, Heit, Mem, Hillie, Johan (de 'familie Veneman'), letterlijk en figuurlijk meestal op afstand (of op nog meer afstand), bedankt dat jullie er zijn, en mij waar nodig hebben gesteund.

En dan, echt aan het eind gekomen, wil ik alle vrouwen bedanken die niet mijn vriendin zijn geworden, zodat ik me nu ook niet aan hen(jullie) hoef te verontschuldigen voor diverse vormen van verwaarlozing, noch mijn hoofd hoef te breken over de vraag of het nu eigenlijk wel past om je 'levensgezel' via een boekje als dit te bedanken.

Maar goed – sa as wy in it Frysk sizze soene: 't praat wurdt hurd minder ('het niveau daalt') – tot zover – alle genoemden en bedoelden, hopelijk tot ziens, maar in ieder geval het allerbeste toegewenst!

Tijd om een bladzijde om te slaan….

Jan Veneman, Oktober 2007, Enschede

Curriculum Vitae Academica

Jan Frederik Veneman was born december 1st 1973 in Tzum, Franekeradeel, The Netherlands

1992-1998	Bachelor and Master Mechanical Engineering University of Twente, Enschede Specialization: thermal engineering Graduation project on cleaning of emission gases with a combined centrifugal filter and reactor
1998-2001	Master Philosophy of Science, Technology and Society University of Twente, Enschede Specialization: systematic philosophy Graduation project on the political influence on, and the political impact of technological developments
2002-2006	PhD student at the University of Twente Biomechanical Engineering, this thesis
2006	Roessingh Research and Development Research on the possible use of pelvis accelerometers for gait diagnostics
2007-	Programme Developer for a new master course Sustainable Energy Technology at the 3TU, The Cooperation of Delft, Eindhoven and Twente Universities of Technology